The Selective Oxidation of Bio-derived Platform Chemicals over Supported Gold Catalysts

Mark Douthwaite

January 2016

Thesis submitted in accordance with the requirements of Cardiff University for the degree of Doctor of Philosophy

Abstract

A fundamental limitation effecting the exploitation of bio-fuels is that they are not currently economically competitive with conventional fossil fuels. The development of novel chemical processes to convert bi-products from these reactions into high value chemicals could be one method to reduce the economic deficit between these two industries. Glycerol and furfural are produced as bi-products in the production of 1st and 2nd generation bio-fuels. This thesis explores the potential of using supported Au catalysts for the oxidation of these bio-derived compounds for the synthesis of high value chemicals.

The reaction conditions were found to significantly affect the product distribution and the reaction rate for the aerobic, liquid phase oxidation of glycerol over a $AuPt/TiO_2$ catalyst. Mechanistic studies suggested that glyceric acid and tartronic acid are primary products in this reaction. This study also implied that C-C scission leading to the unfavourable formation of C_1 and C_2 products occurred from glyceraldehyde, dihydroxyacetone and glyceric acid. Au nanoparticles supported on hydrophobic supports were found reduce C-C scission, and the incorporation of Pd and Pt to a Au/BN catalyst was found to further increase desirable C_3 selectivity. Additional work confirmed that the in-situ formation of H_2O_2 was primarily responsible for C-C cleavages, which led to the postulation that Dakin oxidation was the mechanistic process by which it proceeds. Supported trimetallic AuPdPt nanoparticles were found to be active for the oxidation of glycerol under base free conditions. The catalyst was found to significantly influence the activity of these particles.

It was determined that a Au/TiO_2 catalyst could selectively oxidise furfural to produce reasonable yields of furoic Acid. Polymerisation of the substrate was found to inhibit catalytic performance which was suggested to be a result of the polymers binding irreversibly to the catalyst. Optimisation of the catalyst and experimental procedure was found to reduce this unfavourable polymerisation, which led to the production of furoic acid yields in excess of 89 % using a $AuPd/Mg(OH)_2$ catalyst. Further tests indicated that the size of the metal nanoparticles and the Au:Pd ratio significantly affected catalytic performance for this reaction. Mechanistic studies identified the presence of three reactions; the direct oxidation of furfural, the oxidative dehydrogenation of furfuryl alcohol and the Cannizzaro reaction. A kinetic study allowed for the determination of the activation energies corresponding to each of these pathways, which ultimately highlighted the potential of using a catalyst for this reaction on an industrial scale.

Glossary

βHA	β-hydroxy pyruvic acid
CMB / C.M.B.	Carbon mass balance
DAD	Diode array detector
DFT	Density functional theory
DHA	Dihydroxy acetone
E_a	Activation Energy
EDX	Energy-dispersive X-ray spectroscopy
FA	Furoic acid
FDCA	2, 5-Furandicarboxyllic acid
FF	Furfural
FOH	Furfural alcohol
FOA	Formic acid
FWHM	Full width half maximum
GA	Glyceric acid
GLA	Glycolic acid
GLAD	Glyceraldehyde
HAADF	High-angle annular dark-field imaging
HMF	5-Hydroxymethyl-2-furfural
HPA	Heteropolyacid
HPLC	High performance liquid chromatography
HT	Hydrotalcite
IMP-CON	Conventional impregnation
IMP-MOD	Modified impregnation
KE	Kinetic energy
LA	Lactic acid
MA	Mesoxalic acid
MEA	Maleic acid

MP-AES	Microwave plasma atomic emission spectroscopy
OA	Oxalic acid
PET	Polyethylene terephthalate
PSD	Particle size distribution
PVA	Polyvinyl alcohol
RDS	Rate determining step
RID	Refractive index detector
SA	Succinic acid
SOL-CON	Conventional sol-immobilisation
TA	Tartronic acid
TEM	Transmission electron microscopy
TPA	Terephthalic acid
TOF	Turnover frequency
TS-1	Titanosilicate zeolite
XPS	X-ray photoelectron spectroscopy
XRD	X-ray diffraction

Table of Contents

Chapter 1

Introduction

1.1. A Background in Catalysis

Over the last century, industrial science has flourished. Scientific developments have enabled the scientific community to produce new and innovative materials that have shaped the face of the modern world. Historically, the objectives of industrial science were to satisfy the growing thirst of consumers and as a consequence, very little attention was given to the impact of these practices on the environment. The emphasis of modern science is to satisfy the needs of consumers through methods which are sustainable and economical. Catalysis is a key field in the development and maintenance of such an infrastructure. Without effective catalysts, the manufacture of many materials, pharmaceuticals and foodstuffs would not be possible[1].

The development of the principles of green chemistry has now placed emphasis on the formation of chemical products and processes, that reduces or eliminates the generation and application of hazardous chemicals[2]. A dramatic progression in catalysis science in recent years is considered to have and remains to play a pivotal role in this ethical transformation[3]. Today, catalysts act as a lynchpin in some of the biggest industries in existence[4-6] and it is believed that over 90 % of all industrial processes in the chemical industry currently employ catalysts. Although the progress made is encouraging, it is clear that with the increasing influence of climate change and ongoing damage to and extinction of ecosystems, further development is required[7].

By definition, a catalyst increases the rate of a reaction as it approaches equilibrium by offering an alternative reaction pathway. This is not always the case however, as enzymes are often used to stabilise transition states in bio-catalytic processes. It is important to note that the catalyst is unchanged as a result of this process, which as a consequence, allows for its continuous participation in a given reaction.

Catalysts can be divided into two fundamental groups determined by the phase of the catalyst and reagent. Catalysts are considered to be homogeneous in nature when the catalyst and reagents are in the same phase. In contrary, catalysts are considered to be heterogeneous in nature when the catalyst and reagent exist in different phases. Within these two groups further methods of classification exist. For instance, photocatalysis is a relatively new concept and relies on the activation of a catalyst through the application of light. This type of catalysis is displaying excellent potential for the production of hydrogen through water splitting[8], as well as the decomposition of pollutants in waste streams[9]. In addition, the design and synthesis of new enzymes for participation in chemical reactions is fast becoming a suitable method for industrial application[10].

Homogeneous catalysts can provide an excellent degree of atom efficiency and reaction selectivity. Typically, these catalysts consist of ligand bound metal centres with a specific co-ordination number. The metal oxidation state and the stereoelectronic properties of the ligands are fundamental factors which must be considered during the synthesis of these catalysts. It is the ability of a rationally designed catalytic complex to control these parameters which gives the required site specificity to achieve exceptional product selectivity. Catalysts of this nature have proven to be applicable for a range of industrial applications such as hydroformylation[11], hydrogenation[12] and hydrosilylation[13] along with many more. In addition, the ubiquitous application of Pd complexes for C-C cross coupling reactions was recognised when Heck, Negishi and Suzuki were awarded the 2010 Nobel Prize for chemistry[14]. Despite the clear merits associated with this type of catalysis, it is not yet considered economically viable for the majority of industrial processes. This is due to numerous factors including product extraction together with financial and time cost associated with the synthesis of these materials. That said, recent innovations in the heterogenisation of homogeneous catalysts and the application of biphasic reaction systems is paving the way for further industrial application[15].

Heterogeneous catalysts are predominantly solid materials, used to catalyse reagents in the gas or liquid phase. The difference in phases between the catalyst and reagents means that the post reaction extraction of the product(s) is far easier, which is beneficial from an industrial perspective. Typically, these catalysts consist of either a metal oxide or mixed metal oxides[16, 17]. The performance of these catalysts can be enhanced by the deposition of additional nanoparticles[18], promoters[19] or combinations of both[20]. Single site catalysis is more difficult to control in this field, which can ultimately lead to poorer reaction

selectivity than that observed with homogeneous catalysts. Despite this, the favoured industrial viability of these catalysts has allowed for the incorporation of heterogeneous catalysis in numerous major industrial processes including the direct synthesis of NH_3 from H_2 and N_2[21], the oxidation of SO_2 to SO_3[22], steam reforming[23], oil cracking and reforming[24] as well as many more. The complexity and ambiguity of the mechanistic processes surrounding heterogeneous catalysis means that there is room for development in this field.

1.2. The Kinetics and Thermodynamics of Catalytic Systems

Figure 1.1 illustrates how a catalyst can offer an additional pathway from reactant to product with a reduced activation energy.
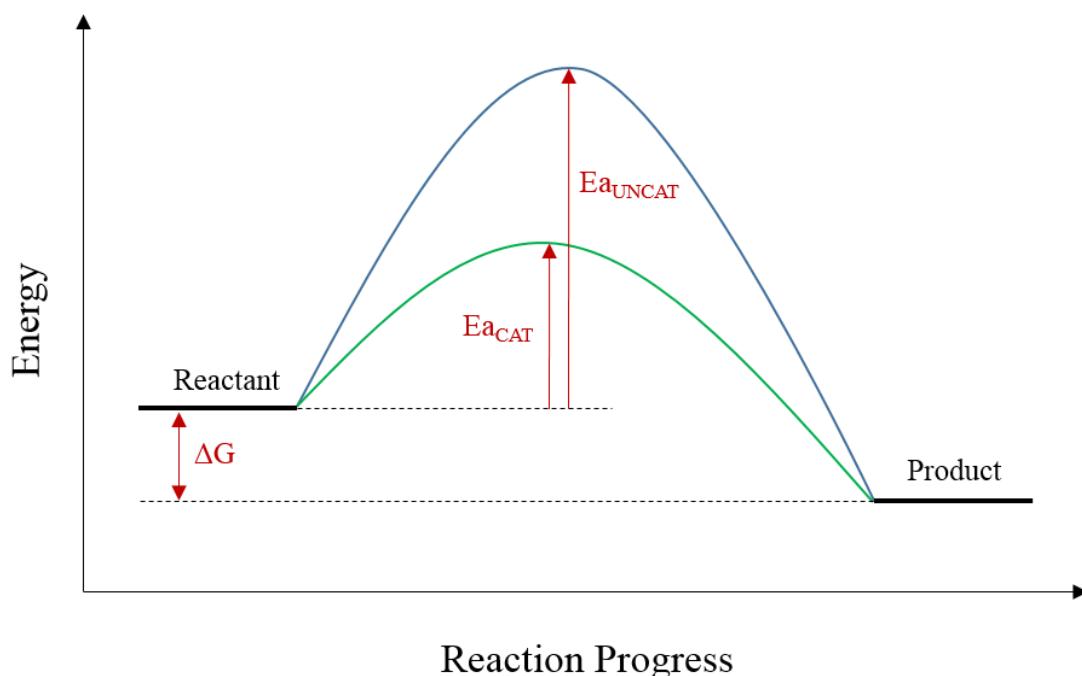
Figure 1.1. An energy level diagram of a reaction which compares the activation energies of a catalysed (Ea_{CAT}) and un-catalysed (Ea_{UNCAT}) reaction pathway.

It is important to note that the addition of a catalyst to any given reaction does not change the free energy of the system, as it has no effect on the energy of the reactant(s) and product(s). Equally, the laws of thermodynamics suggest that a catalyst can have no effect on the position of the equilibrium. For this to be true, with any given system in equilibrium, a catalyst must promote the forward and backward reactions equally. Thus, catalysts only affect the kinetics of a system, not the thermodynamics. As highlighted in Figure 1.1, a

catalyst can provide a reduced activation barrier for a reactant to proceed over. Although this appears to be fairly straightforward in Figure 1.1, in reality it is far more complex. The activation barrier represented by Ea_{CAT} would actually consist of numerous other activation barriers, representative of the different intermediate states formed in the catalytic mechanisms. For instance, in heterogeneous catalysis, these intermediate states could represent physical obstacles such as the adsorption and desorption of species to and from the catalysts surface. They could also be representative of chemical features such as bond formation or destruction.

Derivation of the kinetics associated with a chemical reaction can help gain a further understanding of a reaction's surface mechanism. Determining the rate dependencies of certain stages of the mechanism can assist in the optimisation of the reaction conditions, reactor and catalyst design. In turn, the optimisation of these variables could allow for significant enhancements in the process development. Consider a unimolecular decomposition reaction - the reaction would occur in three fundamental stages and by monitoring the rate of each stage, it would be possible to identify the rate determining step (RDS). Let's assume that a kinetic study is conducted and the RDS was found to be the initial adsorption of the substrate – through the modification of the catalyst it would be possible to increase the sticking probability of the substrate which in turn would increase the rate of this specific step and perhaps increase the rate of the overall reaction.

In reality, most reactions are bimolecular in nature and the rate can be effected by many different variables such as the adsorption of multiple reactants, possible bond decomposition(s) / formation(s), surface diffusions of molecular species and of course product desorption. Additional concerns such as catalyst poisoning adds a further degree of complexity to the system making kinetic modelling extremely difficult. For instance, let us consider the oxidation of CO to CO_2 over a supported Au catalyst.

$$CO + \tfrac{1}{2}\,O_2 \quad \rightarrow \quad CO_2$$

Scheme 1.1. Stoichiometric equation for the oxidation of CO to CO_2

Initially, this transformation appears to be very straightforward, yet theories regarding the catalytic mechanism have expanded decades[25-27]. It is incredibly difficult to model the

kinetics of a heterogeneously catalysed reaction as the complete control of every variable is required.

For more complicated reaction systems involving multiple reaction pathways, kinetic modelling becomes even more difficult. In this situation, it is worth applying kinetics to a sequence of steps. For instance, rather than applying kinetics to the adsorption, transformation and desorption, it is worth looking at the kinetics of the transformation from substrate to product as a whole. This at the very least gives an efficient method of comparing catalysts. Information regarding the stoichiometry of each reactant is also derivable using this method. The rate constants, reaction orders and reaction rate can be combined in one mathematical expression, as shown in equation 1.1.

$$K = k.\,cat.\,[A]^a[B]^b[C]^c$$

Equation 1.1. Rate equation for the catalysed reaction between A, B and C. K – Rate of reaction, k – rate constant, cat – catalyst (constant), indices a, b and c represent the orders of reaction with respect to the concentrations of A, B and C

The orders of reaction with respect to A, B and B can easily be determined by monitoring the reaction rate with respect to the concentration of each reactant. These reaction orders can also give valuable information regarding the quantity of each required for one mechanistic transition. For example, in a reaction where two molecules of NaOH are required in order to convert one molecule of substrate to the desired product, the order of reaction with respect to the concentration of NaOH would be 2. The rate of the reaction (K) can be determined simply using the initial rate method. A rearrangement of the equation would subsequently allow for the derivation of the rate constant, k. If this process is repeated at multiple temperatures it is possible to derive the activation energy (Ea) by using the Arrhenius equation (equation 1.2).

$$k = Ae^{\frac{-Ea}{RT}}$$

Equation 1.2. Arrhenius equation used to derive the activation energy (Ea) of a chemical reaction. k – rate constant, A - pre-exponential factor, R – gas constant, K – temperature in Kelvin

1.3. A Brief History in Catalysis

Perhaps the first catalytic process to be used by man, albeit unknowingly, was the fermentation of sugar to form alcohol. It wasn't until the late seventeen hundreds that scientists began to realise that it was possible for reactants to demonstrate non-stoichiometric behaviour in reactions. Homogeneously catalysed reactions were first to be considered, when questions were raised regarding the role of H_2O in the oxidation of CO to CO_2[28] and the role of dilute acids in the hydrolysis of starch[29]. The first known observation of heterogeneous catalysis was determined when Sir Humphrey Davy recorded that combustible gases could react violently in the presence of O_2 and heated platinum[30]. This led a host of studies exploring the role of platinum metal in other chemical transformations[30-33]. The sudden boom in new innovative methods for the synthesis of chemicals caught the attention of Berzelius, who classified these non-stoichiometric reactants as catalysts[30, 34].

The industrial revolution led to an exponential increase in population size and industrial processing. During this period, contributions from Faraday[35] and Lemoine[36] in addition to many more led to a substantial increase in the understanding of catalysis and how it affected chemical kinetics. Soon, catalysts were being utilized in numerous large-scale industrial processes such as the preparation of nitric acid[37], the contact process[30] and the synthesis of NH_3 from H_2 and N_2[30]. A growing global demand for petroleum in the early 20th century led to extensive research in oil refining and methods for the development of new raw materials. Perhaps the highlight of this era was the development of Fischer-Tropsch catalysis, which made it possible to obtain hydrocarbons from coal gasification with excellent efficiency[30, 38]. The technological advances accomplished during the remainder of the 20th century allowed for the development of new tools for the study of catalysts.

Today, catalysts are employed in over 90 % of industrial chemical processes and the diminishing stocks of fossil fuels has led to the investigation of alternative sources of fuels.

1.4. Reaction over Heterogeneous Gold Catalysts

Until fairly recently, gold was considered to be catalytically inert[39]. It wasn't until 1973 that Bond[40] demonstrated that the impregnation of aurochloric acid onto metal oxides served as an active catalyst for the hydrogenation of alkenes. Well over a decade later, Haruta[41] and Hutchings[42] observed that gold supported catalysts were extremely active for the oxidation of CO and the hydrochlorination of ethyne to vinyl chloride. Subsequent work by Haruta and co-workers revealed that Au supported on TiO_2 was highly effective for the selective epoxidation of propene[43]. Later, work by Prati and Rossi revealed the potential of Au catalysts for the selective oxidation of alcohols and carbohydrates[44]. These works provided a foundation for the study of heterogeneous gold catalysis in which scientific interest has continued to grow. As such, there have been numerous reviews published documenting development in this field[39, 45-49].

The reasoning behind why gold nanoparticles are so active for certain catalytic transformations is still not fully understood. The activity of supported Au nanoparticles has been linked with a number of different phenomena[50], including, quantum size effects[51-53], the Au oxidation state[54-56], the low co-ordination of Au atoms in nanoparticles[57, 58] in addition to various support effects such as charge transfer[59, 60] and oxygen spill-over[61, 62]. It is likely that the highly active nature of these nanoparticles is attributed to a collection of these features.

The activity of supported metal catalysts has long be associated with the size of supported nanoparticles[18]. The Au particle size in supported gold catalysts is undoubtedly critical to the overall performance of the catalyst[63-65]. The catalyst preparation method can significantly influence the size and distribution of these particles which can consequentially impact the catalytic performance. It is now commonly known that Au nanoparticles must exhibit a diameter less than 5 nm in order to display a significant degree of activity[64]. Perhaps the most commonly used preparation technique from an industrial perspective is the impregnation method. Interestingly, this was the first method used for the preparation of supported Au nanoparticles as shown by Bond *et al.*[40]. This method can produce

nanoparticles within the desired activity region but with little control over the size distribution. A recent modification of this method proposed by Meenakshisundaram *et al.*[66], allows for the preparation of sub 5nm Au particles with minimal deviations from the mean. The relationship between particle size and activity was subsequently demonstrated when the catalyst prepared by the modified impregnation method was used for the aerobic oxidation of alcohols[67].

Much of the work pioneered by Haruta involved the preparation of supported Au catalysts by the deposition precipitation method[68, 69]. This method has shown to consistently give supported Au catalysts with exceptional metal dispersion within the desired activity region. More recent work which involved the production of Au/Fe_2O_3 using the co-precipitation method was reported to produce a large population of exceptionally small nanoparticles[55]. Large quantities of the work investigating the performance of Au catalysts for the oxidation of alcohols employed the sol-immobilisation technique[70]. This technique involves the utilisation of a stabilising ligand to control particle size and impede agglomeration. Exceptionally small particles with well-defined distributions can be produced in this manner, the size and shape of which can be controlled through the choice and quantity of the stabilising ligand[71, 72].

The alloying of Au with Cu[73], Ag[74], Pd[75] and Pt[76] to form bimetallic nanoparticles can increase catalytic performance in a range of oxidation reactions. The synergistic interaction observed between the metals is believed to be a result of numerous possible effects. These effects include the additional metal being far more easily oxidised than Au resulting in a greater concentration of adsorbed oxygen in the vicinity of the active site[77], electronic effects – a change in the band structure of the Au through electronic promotion or demotion[76] and geometric effects - the formation of core shell or alloyed structures which may further enhance the electronic effects of the additional metal[78].

1.4.1. The Direct Synthesis of Hydrogen Peroxide

H_2O_2 is a high value commodity chemical which has applications in industry and in everyday household cleaning goods. The current industrial method for its production utilizes the anthraquinone process which was developed by BASF in 1939. Although

reasonably effective, there are concerns regarding the carbon efficiency of the process and environmental hazards associated with its implementation.

There has been significant scientific interest in the direct synthesis of H_2O_2 over the last decade which has been documented in a number of reviews[79, 80]. Direct synthesis from H_2 and O_2 would greatly enhance the efficiency of its production and significantly reduces the carbon footprint of its production and distribution. There are a number of limitations involved with the direct synthesis which are currently preventing its application on an industrial scale. Mixtures of H_2 and O_2 are explosive in certain concentrations and as a result, must be diluted in an inert carrier gas which can then impact potential productivity[79, 81, 82]. In addition, the activation of H_2 (considered to be the RDS[83]) is a difficult feat to achieve effectively. There are also sequential hydrogenation and decomposition pathways which can cause further issues and reduce the selectivity of the reaction. These unfavourable sequential transformations are displayed in scheme 1.2. In order for this process to be consider industrially viable, further development is required.

$$H_2 + O_2 \longrightarrow H_2O_2 \nearrow^{H_2} 2H_2O$$
$$\searrow H_2O + 1/2\ O_2$$
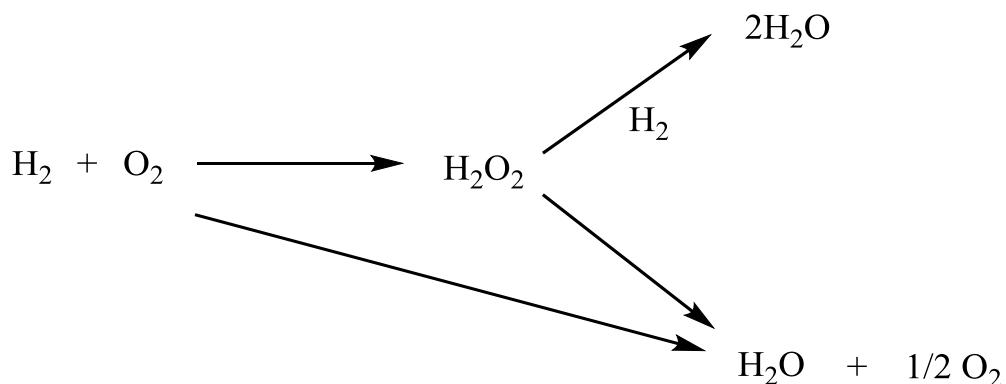
Scheme 1.2. Reaction profile for the direct synthesis of H_2O_2 from O_2 and H_2. The unfavourable sequential hydrogenation and decomposition of H_2O_2 are displayed.

Hutchings and co-workers[84] were the first to show that supported Au nanoparticles on Al_2O_3 were active for the direct synthesis of H_2O_2. In the same publication, it was determined that alloying Pd with Au could enhance the activity of the catalyst further. Subsequent work conducted by this group revealed that these alloys were also active on additional metal oxide supports with a noticeable increase in activity reported when

supported on sulphated carbon supports[85]. Ishihara *et al.*[86] developed the idea that greater catalytic productivity could be achieved using acidic supports (silica and zeolites). Further work by Hutchings an co-work involved the testing of AuPd supported on Al_2O_3[87], Fe_2O_3[88] and TiO_2[89] for the direct synthesis of H_2O_2. Through application of extensive microscopy, it was determined that these systems all exhibited Au[CORE]Pd[SHELL] structures. The productivity of these catalysts was comparable, with TiO_2 appearing to exhibit the highest performance.

The effect of the reaction medium can also affect the productivity of supported AuPd catalysts. Choudhary and co-workers have published numerous papers investigating the nature of the reaction medium[90-93]. Acidification of the reaction medium and incorporation of halides into the system can significantly enhance the productivity of hydrogen peroxide through the suppression of the unfavourable sequential hydrogenation and decomposition pathways. The efficiency of the halide in suppressing these unfavourable reactions is believed to be dependent on the oxidation of the active metal[94].

A significant leap forward in this field was achieved when active carbon was used as a support for the AuPd nanoparticles[95]. It was determined that the acid pre-treatment of the support prior to metal immobilisation significantly reduced the unfavourable sequential reactions. It was postulated that this increase in performance was a result of the formation of a higher population of small nanoparticles which were Pd rich alloys. It was also determined that these species induced a higher proportion of Pd metal which exhibited a 2+ oxidation state. This was suggested to be crucial to the catalysts performance. This influenced subsequent work in this field which focussed on the application of exceptionally acidic supports such as HPA's[96, 97] and zeolites[98]. It is clear that increasing the isoelectric point of the support has a huge influence on the productivity of the AuPd catalysts. It is clear that the direct synthesis of H_2O_2 requires further development before the process can be applied in industry.

1.4.2. The Selective Epoxidation of Olefins

Epoxides have long been desirable chemicals from an industrial perspective, with their application in the manufacture of a range of important commercial products[99]. The current industrial method for the production of small chain epoxides involves selective oxidation

from the corresponding olefin over a supported Ag catalyst[100]. This method can deliver an exceptional selectivity to the epoxide.
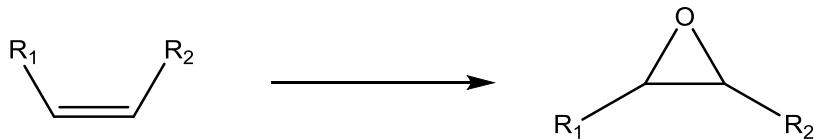
Scheme 1.3. The selective oxidation of olefins to produce epoxides.

Haruta and co-workers were the first to recognise that supported Au nanoparticles were viable for this selective oxidation[43]. Subsequent work by this group demonstrated that an Au/TiO$_2$ catalyst could selectively oxidise propene to propene oxide in the presence of O$_2$ and sacrificial H$_2$. It was determined that the H$_2$ allows for the activation of O$_2$ at low temperatures[68]. Subsequent publications revealed that the selectivity could be further promoted through optimisations of the TiO$_2$ suport[101, 102].

Mechanistic studies determined that the propene adsorbs to the TiO$_2$ to form a bidentate propoxy species[103]. The simultaneous production of a peroxy species on the Au nanoparticle interacts with this species allowing for the reactive desorption of the epoxide. Additional work by this group revealed that the Au nanoparticles merely facilitate the production of these peroxy species and that the epoxidation of the substrate takes place only in active sites located on the Ti[104]. The catalyst preparation conditions are considered to be crucial in controlling the reaction selectivity, as the active Au particle size is considered to be < 2 nm in diameter[68].

More recent work conducted by Hughes *et al.*[105] revealed that the sacrificial H$_2$ is not crucial. Instead, catalytic quantities of peroxides were used and high epoxide selectivity was achieved for the epoxidaton of a series of unsaturated cyclic substrates. This is perhaps further evidence in support of the role of the surface bound peroxy species mentioned previously[103].

From an industrial perspective, the hydrogen selectivity is far too low in order to make the process cost effective. For this reason, the use of water as a possible hydrogen source for the epoxidation of propene over Au/TiO$_2$ was investigated by Ojeda *et al.*[106]. As anticipated, a significant reduction in the conversion and epoxide selectivity was observed.

11

This work was subsequently followed with contributions from Haruta and co-workers, who determined that the inclusion of alkali ions in the system could promote both epoxide selectivity and activity when using an Au-TS1 catalyst[107, 108]. It was determined that the cationic halides stabilise the O_2^- species over the Au clusters facilitating the production of Au bound peroxy species.

1.4.3. The Selective Oxidation of Alcohols and Aldehydes

The selective oxidation of alcohols and aldehydes is of significant interest from both industrial and research perspectives. With the growing importance of utilization of green routes for chemical synthesis, new methods for the synthesis of high value chemicals from by-products and platform chemicals are being investigated. Current industrial applications rely on the use of stoichiometric equivalents of various reagents. The reagents are often considered to be hazardous, hereby allowing for an alternative method of oxidation using heterogeneous catalysts and molecular O_2. Prati and Rossi were the first to discover that supported gold nanoparticles were highly active for the oxidation of alcohols[109], which subsequently has led to increased interest in the field. Many different substrates have been investigated in the literature[110-113]. For the purpose of the work in this thesis, only a few of these reactions will be discussed.

1.4.3.1. Benzyl Alcohol Oxidation
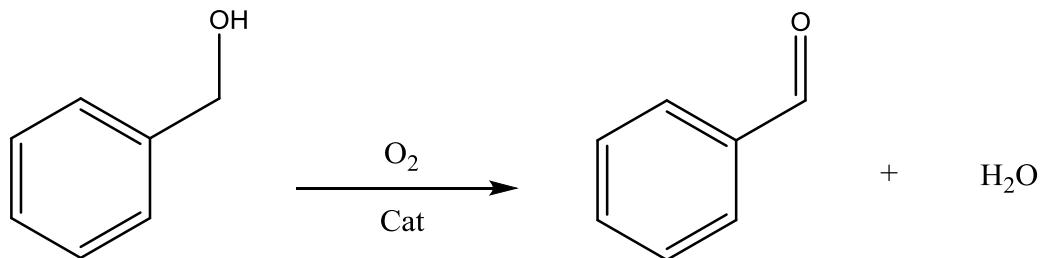
Scheme 1.4. The oxidative dehydrogenation of benzyl alcohol to benzaldehyde

The desired product from the selective oxidation of benzyl alcohol is benzaldehyde which has applications in both the cosmetic and pharmaceutical industries. Hutchings and co-workers were the first to demonstrate that supported gold nanoparticles were active for the solvent free liquid phase oxidation of benzyl alcohol[114]. It was determined that the support and preparation method could significantly affect the performance of the catalyst. Choudhary and co-workers[115] subsequently investigated the effect of the Au nanoparticle support. It was observed that U_3O_8, MgO, Al_2O_3 and ZrO_2 were the most effective supports for this reaction. It was later determined that supported Au catalysts prepared by the sol-immobilisation method were highly active for this reaction.[116]

Once again, synergistic effects created from the incorporation of Pd into Au nanoparticles were found to improve catalytic performance[117]. Hou *et al.*[75] subsequently conducted an in-depth study investigating the effect of the metal ratio on the performance of AuPd containing sols. A ratio of 1:3 AuPd was observed to give the highest activity and selectivity to benzaldehyde. The preparation method of supported AuPd catalysts was found to significantly impact catalytic performance. Supported AuPd alloys prepared by sol-immobilisation, impregnation and deposition precipitation were compared and it was determined that the sol-immobilisation method gave the best overall catalytic performance[118]. Additional work by Hutchings and co-workers[119] revealed that AuPd/C catalysts prepared by this method were also suitable for this reaction. Interestingly, the catalysts used in this study were also highly active for the direct synthesis of H_2O_2, leading to the postulation that both reactions are catalysed by the same metal active sites.

The complex mechanistic profile of this reaction makes it an interesting model for the study of catalytic alcohol oxidation. Benzyl alcohol can be oxidised directly to benzaldehyde and undergo sequential oxidations to the corresponding acid and ester. Another reaction route involves disproportionation of the surface bound intermediate to form toluene[120]. Nowicka *et al.*[121] determined that it is the Pd in the AuPd alloys which facilitates the unfavourable disproportionation. However, it is the incorporation of Pd which also promotes the catalytic activity of the AuPd alloys. It was later determined that this unfavourable pathway could be suppressed through utilization of basic supports such MgO or reaction spiking with small quantities of base[121]. This work suggests that the application of more acidic supports such as TiO_2 and carbon may promote the unfavourable disproportionation. Further work conducted by Hutchings and co-workers investigated the effect of AuPd/TiO_2 catalysts under anaerobic conditions. Stoichiometric quantities of benzaldehyde and Toluene were

observed which implied that both products may arise from a single transition state through interaction of the catalyst surface with two additional molecules of subsrate[120, 122]. Subsequent publications revealed that doping the AuPd alloys with Bi[123] and Pt[124] could reduce the disproportionation through the blocking of specific active sites and changing the co-ordination of the substrate to the catalyst.

An additional complexity of this system is the absence of benzoic acid when reactions are conducted under aerobic conditions. This is unusual, as benzaldehyde readily undergoes auto oxidation to benzoic acid in air at room temperature. This paradox was revealed to be a result of benzyl alcohol suppressing the auto oxidation reaction through the interception of benzoyl peroxy radicals[125]. Other publications have postulated that benzoic acid[126] and benzoate[127] can reduce the performance of AuPd alloys in this reaction through product inhibition. The addition of basic potassium salts was also observed to reduce this inhibition[126]. It was also suggested that the Au facilitates the desorption of these species.

There are a number of other examples of AuPd alloys supported on interesting materials such as biomass[128] , porous steel fibre[129], nanopaper[130] and even encapsulated in metal organic frameworks[131]. In addition, there are also numerous examples of AuPd alloys catalysing this reaction in flow [132, 133].

1.4.3.2. The Selective Oxidation of 1,2-Propane Diol

Diols and triols are produced in large quantities as by-products from the industrial production of bio-diesel. Although they are considered to be waste chemicals in this process, they have been identified as key platform chemicals for further synthesis[134]. If efficient catalytic routes can be derived for the further synthesis of these compounds, it would ultimately make the synthesis of bio-diesel more economically viable from an industrial perspective.

Lactic acid (LA) is considered to be the desired product from the selective oxidation of 1,2-propanediol due to its application as an intermediate in the industrial production of biodegradable polymers[135]. The observation that supported Au nanoparticles were suitable for this selective oxidation was first observed by Prati and Rossi[44]. This extensive and informative article revealed that the support, preparation technique and experimental conditions could have a profound impact on the activity and selectivity of the Au

nanoparticles. It was observed that stoichiometric quantities of base were required in order to yield a suitable catalytic performance. The authors determined that there were two possible pathways for the synthesis of LA; (i) oxidation of the primary alcohol species *via* lactaldehyde, or (ii) through the simultaneous oxidation of both alcohol species followed by an intermolecular Cannizzaro reaction of the pyruvaldehyde. It was suggested that the latter of these reactions was highly dependent on the presence of the sacrificial base. This reaction profile is displayed in Scheme 1.5.
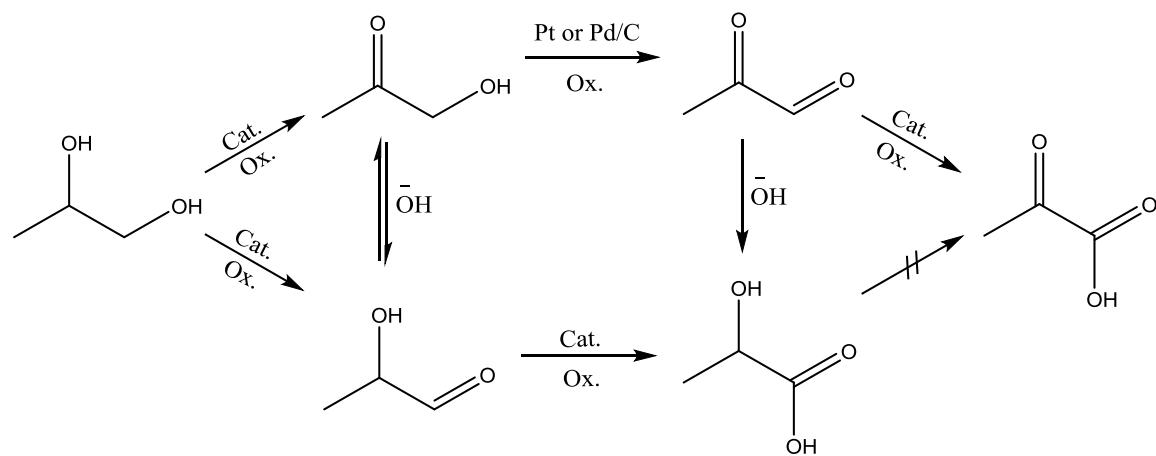
Scheme 1.5. The two proposed pathways for the synthesis of LA from 1,2-propanediol.

Hutchings and co-workers investigated the effect of incorporating Pd into the supported Au catalysts[134]. A synergistic effect on catalyst activity was observed. This study also compared the preparation technique and determined that catalysts prepared by sol-immobilisation were more active than catalyst prepared by impregnation. It was postulated that the enhanced performance was attributed to the higher population of small nanoparticles in the sol-immobilised catalyst. This observation was confirmed by Ma *et al.*[136] who noted that the particle size of AuPd alloys supported on Mg(OH)$_2$ effected catalytic performance. A DFT study revealed that the rate enhancement observed with AuPd alloys compared with monometallic Pd catalysts was a result of the Au facilitating the desorption of strongly bound surface species[137].

AuPt/C was also found to be effective for this oxidation under ambient conditions (40 °C, air) in the presence of a sacrificial base[135]. Supported AuPd and AuPt have also been investigated for the oxidation of 1,2-propanediol under base free conditions. Ryabenkova *et al.*[111] noted that base free oxidation over AuPd sol-immobilised catalysts was possible

but substantial losses in activity and selectivity were observed. This observation was consistent regardless of the catalyst support. Tongsakul *et al.*[138] prepared 'green' AuPt/HT catalysts by sol-immobilisation where starch was used as both the stabiliser and reducing agent. The catalysts displayed excellent activity for oxidation under ambient and base free conditions. It was postulated that this increase in performance was a result of electronic donation from the Au and starch to the active Pt surface sites.

1.4.3.3. The Selective Oxidation of 5-Hydroxymethyl-2-Furfural (HMF)
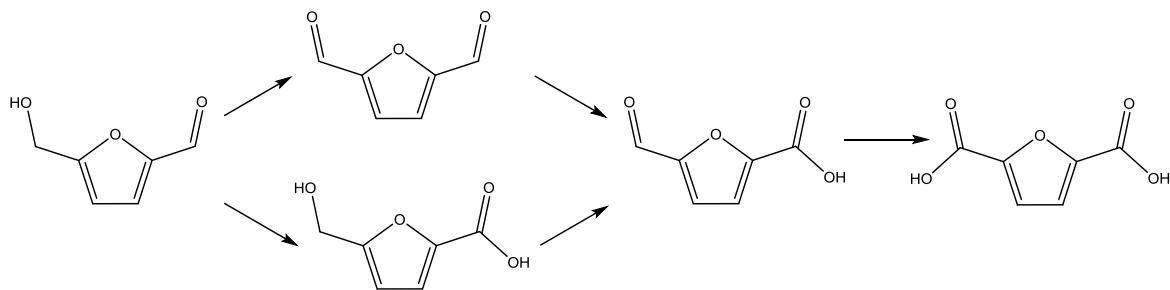
Scheme 1.6. Reaction profile for the oxidation of HMF to FDCA.

HMF is produced on a large scale industrially through the hydrolysis of lignocellulose. It is considered a key platform chemical for the development of derivatives with multiple applications, such as the preparation of pharmaceuticals and as polymer precursors[112, 139]. The desired reaction product from the oxidation of HMF is 2,5-furandicarboxyllic acid (FDCA) as it has been identified as possible replacement for terephthalic acid (TPA), the industrial precursor commonly used in the manufacture of polyethylene terephthalate (PET). An efficient method for the synthesis of FDCA from a bio-renewable route would be advantageous from an industrial perspective.

Davis and co-workers[140] have compared the activity of Au, Pd and Pt nanoparticles supported on carbon in a basic reaction medium for the oxidation of HMF. The Au monometallic catalyst was found to be the most active in terms of HMF conversion but was unable to activate the alcohol. By comparison, the Pd and Pt catalyst were able to activate the hydroxyl group which ultimately led to a greater desirable reaction selectivity. A subsequent publication by the same group provided a possible mechanism for the

reaction which was determined using O^{18} isotopic labelling experiments[141]. It was determined that the oxygen in the acid products was sourced only from the water in the aqueous phase. It was suggested that the gaseous O_2 had an indirect yet crucial role in the reaction mechanism. The authors postulated that the role of the O_2 is to scavenge electrons from surface of the active metals, ultimately liberating the active sites for catalysis.

Bimetallic Au containing catalysts were found to increase catalytic performance through activation of the hydroxyl species. It is well known that the activation of hydroxyl species is often the RDS whenever successive aldehyde oxidation is desired[56, 112, 142]. The incorporation of Cu^{143} and Pd^{144} separately into supported Au nanoparticles was found to increase the reaction selectivity to FDCA by facilitating the activation of the hydroxyl group. The Pd and Cu were also found to increase the stability of the Au nanoparticles as they maintained a higher degree of activity upon subsequent uses.

The support can clearly influence the performance of the Au nanoparticles. Cai *et al.*[145] supported Au in HY zeolitic supercage structures. This support significantly outperformed the other supports tested and gave close to a 100 % yield of the desired FCDA. This exceptional reaction activity and selectivity was postulated to be a result of the small mean Au particles size (1 nm) and the high population of acidic hydroxyl groups found in close proximity to the Au nanoparticles. Similar trends have been observed from the optimisation of carbon supports. Davis *et al.*[146] revealed that increasing the population of OH species on carbon nanofiber supports increased the performance of the Au nanoparticles when compared with conventional carbon supports. Subsequently, Wan *et al.* revealed that the surface of carbon nanotubes could be refined in order to promote the performance of the AuPd nanoparticles in the base free selective oxidation of HMF[147]. It was observed that increasing the population of surface bound hydroxyl species increased catalytic performance by promoting the adsorption of HMF and other reaction intermediates to the catalysts surface. The presence of carboxyl species was reported to facilitate the opposite.

Wilson and co-workers later published an in-depth discussion on the use of alkali free Mg-Al hydrotalcites to support Au nanoparticles for this reaction[148]. It was reported that in the absence of base, HMF and the other reaction intermediates bind strongly to the catalyst, ultimately reducing its activity. It was suggested that the addition of base increased the rate of the reaction by promoting the desorption of these species, thus liberating the Au active sites. It was also proposed that the aqueous base is involved in the activation of the O-H

species, although Cavani and co-workers have also suggested that it promotes the production of FDCA by initiating intramolecular Cannizzaro reactions[149].

1.5. The Selective Oxidation of Bio-derived Feedstocks

1.5.1. The Energy Crisis

The consumerist outlook adopted by much of the western world has led to a significant increase in global energy dependence. This has indirectly resulted in the energy industry playing a crucial role in controlling economic growth. Over the past century, significant emphasis was placed on the use of fossil fuel feedstocks such as natural gas, coal and oil to quench the increasing global energy demand. The development of infrastructure for the refining of these feedstocks has enabled the preparation of many different products from these materials[150, 151]. Despite the attributes associated with these feedstocks, numerous concerns regarding the sustainability and environmental impact of this industry have been raised[151].

The natural stores of these materials are diminishing at a rapid rate. In addition, CO_2 emitted from the combustion of these fuels is considered to be a primary contributor to global warming which has been observed in recent decades[151]. This increase in the global temperature is understood to be linked with the recent observations of climate change and dramatic ecological damage. In addition, the catastrophic industrial disasters in this industry can have a devastating impact on the localised environment and habitats. The unfavourable attributes of this industry has led to the search for sustainable and environmentally benign alternatives for the production of energy.

Numerous alternative technologies have been developed[152]. Of these, a substantial quadrant utilize natural energy sources found on earth such as wind, solar and tidal phenomena. Although these technologies have shown promise in small scale processing, significantly increased development is required for them to be a feasible replacement to fossil fuels. Nuclear fission is another alternative for energy production with the potential to fill the void which will be created by diminishing fossil fuel stocks. Furthermore, a substantial amount of research is currently being undertaken in the development of infrastructure which can allow for the utilization of energy from nuclear fusion[153-155]. If the attempts to

harness this energy source are successful it could almost certainly be a viable replacement to fossil fuels. The utilization of nuclear energy comes at a cost with radioactive waste produced and the prospect of catastrophic industrial disasters as seen in Chernobyl in 1986 and Fukushima in 2011 limit its widespread application.

Biofuels produced from bio-renewable feedstocks are another alternative for energy production. The viability of these materials to replace conventional fossil fuels has potential which has resulted in significant scientific interest in recent years[156-158].

1.5.2. Bio-renewables for the Production of Fuels and Fine Chemicals

The production of bio-fuels from bio-renewable feedstocks is considered to be a promising alternative to conventional energy processes. Fuels produced in this way offer a method of harnessing energy with reduced emissions of greenhouse gases and noxious chemicals. The diversity of available feedstocks allows for new processes to be developed for the synthesis of fine chemicals.

First generation biofuels are isolated from crops and such as soybean, sugar cane and corn. These substances can be used as feedstocks for the production of bio-diesel, bio gas and ethanol. Although these processes are considered fairly efficient and offer an annually renewable fuel, sourcing these fuels from feedstocks which are fit for human consumption has led to an ethical dilemma[159]. The universal development of infrastructure for the production of biodiesel would lead to severe poverty in some areas of the world as well as an inevitable rise in the staple food prices. This limits 1st generation bio-fuels as a global replacement for fossil fuels but is certainly suitable for small scale regional development.

Bio-diesel is predominantly composed of fatty acid methyl esters[151]. It is produced from the transesterification of vegetable oils with alcohols in the presence of a homo- or heterogeneous catalyst[6]. Bio-diesel has very similar properties to conventional diesel which is what makes it such a desirable replacement for petroleum derived diesel. Glycerol is produced as a co-product from this reaction[160] which has subsequently sparked extensive research into its application as a platform chemical.
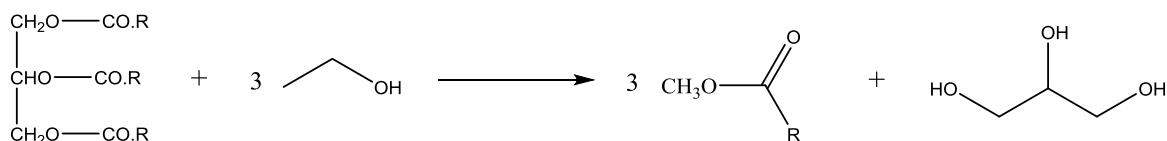
Scheme 1.7. Triglycerides found in 1st generation feedstocks undergo esterification in the presence of a primary alcohol to produce fatty acid-esters (biodiesel) and glycerol.

Second generation biofuels are predominantly produced from lignocellulosic materials[161, 162]. For this reason, it is considered more viable from an ethical and renewable perspective, as the feedstocks are generally not competitive with food stocks. Fuels produced in this manner are also considered to exert less of a carbon footprint than first generation biofuels. The lignocellulosic feedstock consists predominantly of plant cell walls of which, approximately 75 % is composed of polysaccharides[151, 163]. The hydrolysis of these materials can allow for the extraction of numerous sugars from the feedstock which can be used for the further development of fuels and fine chemicals.
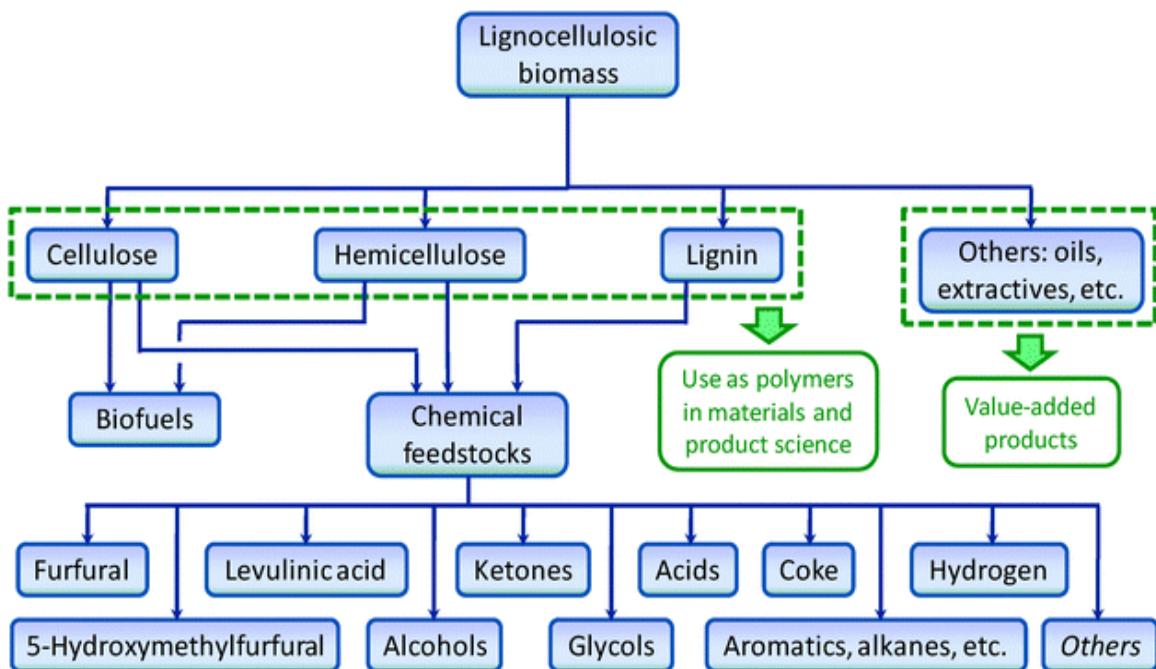
Scheme 1.8. The large distribution of products which can be produced from treatment of lignocellulose. Figure has been republished[164] with permission from the RSC.

20

Despite the many merits associated with second generation fuels, the extensive treatment steps and current inefficiency of these processes mean that fuels produced in this way are not yet cost effective. Further development is required in order to make these processes more viable industrially.

1.5.3.   The Selective Oxidation of Glycerol

The development and utilisation of bio-diesel as an alternative fuel resource appears a promising alternative to conventional fossil fuels; with many nations opting to invest heavily in infrastructures to facilitate the development and exploitation of bio-fuels. Currently, bio fuels are not considered a viable alternative to fossil fuels. A primary limitation associated with bio fuels is a lack of atom efficiency manifested through the production of waste chemicals. It is imperative that methods are developed so that these waste chemicals are recycled for further applications.
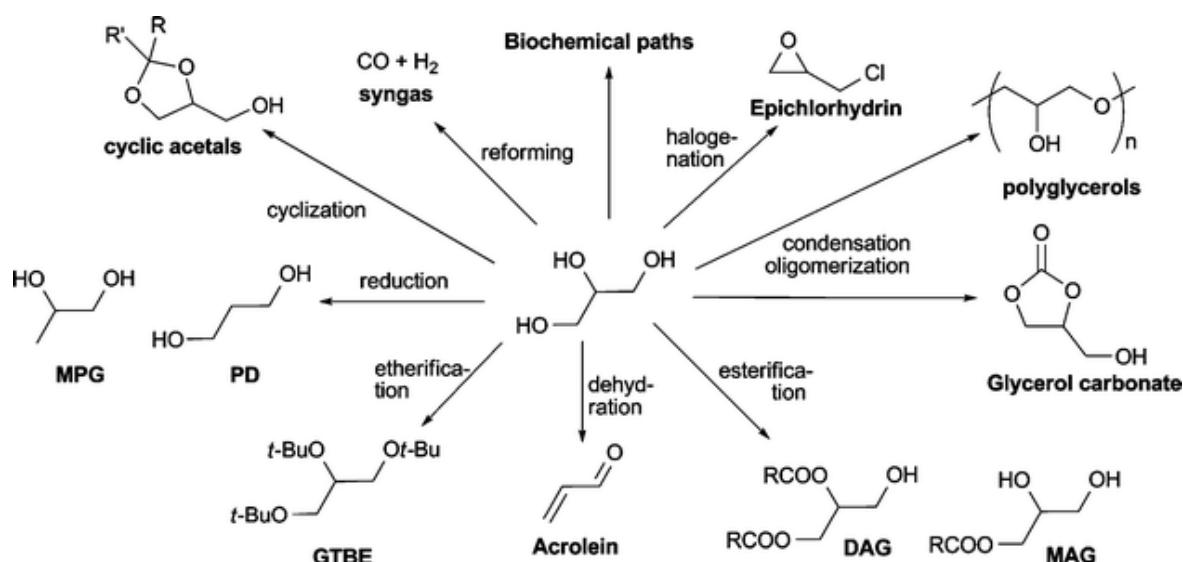
Scheme 1.9. Glycerol is considered to be a key platform chemical and can be used for the synthesis of many other compounds. Scheme republished with permission from the RSC[165].

Glycerol is a C_3 tri-ol containing three hydroxyl groups. Its primary industrial production comes as a bi-product of biodiesel production *via* the transesterification of triglycerides

sourced predominantly from soybean or palm oils. Its three hydroxyl groups mean that it possess excellent potential for development into other fine chemicals. The EU directive (2009/28/EC) features renewable energy targets for the countries in the EU and as a result, the industrial production of glycerol is projected to increase in the coming years. This projection has left a huge area of research for the exploitation of glycerol as a platform chemical. Glyceric acid (GA), tartronic acid (TA), LA, dihydroxyacetone (DHA), mesoxalic acid (MA) and glycolic acid (GLA) are all fine chemicals which can be synthesised from glycerol. The selective oxidation using heterogeneous catalysts has proven to be an exceptional method in attaining these fine chemicals from glycerol[165, 166].

The first pioneering research on the catalytic oxidation of glycerol involved the use of Bi doped Pt catalysts for the production of DHA[167]. The authors showed that the addition of Bi to a supported Pt catalyst increased the selectivity to DHA from 10% to 80%. A subsequent publication explained that the role of the Bi was to prevent over oxidation of the products. Additionally, it was proposed that the Bi ad-atoms selectively oriented the substrate on the surface to promote the oxidation of the additional hydroxyl group[168]. Garcia *et al.*[169] confirmed this work but also revealed that high yields of GA could be achieved for the oxidation of glycerol over a 5% Pd/C catalyst. It was also determined that the experimental conditions can significantly alter the selectivity of the catalyst. Rossi and Prati and co-workers were the first to determine that supported Au catalysts in the presence of O_2 could selectively oxidise glycerol[109]. In the same publication they showed how the choice of support and the preparation method can profoundly affect the performance of the catalyst. Following on from this, Hutchings and co-workers[170] showed that Au/Graphite was an excellent catalyst for the selective oxidation of glycerol to GA. These works triggered a cascade of additional publications from both the Prati and Hutchings groups whose contributions to the use of Au in this field of research was summarised in a recent review[166].

The preparation of bimetallic catalysts containing Au can affect both catalyst activity and selectivity. It has been reported that AuPd bimetallic catalysts can significantly enhance activity and C_3 selectivity when compared to their monometallic counterparts[75, 171-174]. Work by Davis and co-workers[175] showed that the incorporation of Pd into Au has shown to increase the C_3 selectivity with GA being the predominant product. It is suggested that the role of Pd is to catalyse the decomposition of H_2O_2 bi-product which is believed to be responsible for C-C cleavage and leads to the production of unfavourable C_1 and C_2

products. Furthermore, metal particle size can also have a huge impact on the performance of a catalyst for this reaction[176] which highlights the importance of the preparation method. Catalyst preparation and particle size effects have shown to be a crucial feature associated with catalytic performance in a range of other oxidation reactions; benzyl alcohol oxidation[177], CO oxidation[69] and the epoxidation of olefins[68].

The reaction conditions can also play a significant role in the selectivity of the catalyst. Gil *et al.*[178] reported in detail, the significant effect operation conditions can have on the selective oxidation of glycerol using Au nanoparticles supported on a range of different carbonaceous materials. It was observed that an increase in oxygen pressure slightly increased the rate of glycerol consumption but significantly enhanced the selectivity to GA for all catalysts tested. It was suggested that the increase in GA came predominantly at the expense of the sequential oxidation to TA. It was postulated that this increase in C_3 selectivity was a result of a decrease in the in-situ production of H_2O_2 which has been suggested to be responsible for some of the C-C cleavage observed in the oxidation of glycerol[65, 171, 179, 180]. H_2O_2 is believed to be produced as a consequence of O_2 reduction prior to its dissociation[179, 181, 182], with the water acting as a sacrificial oxidant toward the diatomic oxygen. It is not clear in the current literature how the H_2O_2 interacts with the substrate/products to instigate the C-C cleavage.

$$O_2* + H_2O* \rightarrow OOH* + HO*$$

$$OOH* + H_2O* \rightarrow H_2O_2* + HO*$$

$$HO* + e^- \leftrightarrow HO^- + *$$
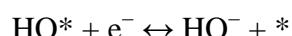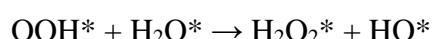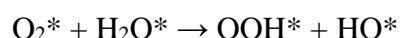
Scheme 1.10. The equations highlights the role of H_2O in the activation of oxygen, with H_2O_2 being produced as a by-product. * depicts a site on the surface of the metal. Image courtesy of Davis and co-workers

The temperature in which the reaction is conducted can also have a significant effect on the selectivity of the reaction. As with most catalytic processes increasing reaction temperature increases the rate of glycerol consumption which links back to the role of temperature in basic collision theory. A publication by Valverde and co-workers[178] reported that increasing temperature not only increased the rate of glycerol consumption,

but also affected the selectivity of the reaction. With an increasing temperature, a higher selectivity of GA and oxalic acid (OA) was observed. Another study by Prati and co-workers [183] also showed that reactions occurring at 50 ℃ showed greater selectivity toward GA than at 30 ℃ using bimetallic Au, Pd and Pt catalysts. Valverde and co-workers[178] postulated that the reason for this was that glycolic GLA production is directly related to the presence of H_2O_2 and pointed out that previous studies investigating the production of H_2O_2 have shown that less H_2O_2 is made with increasing temperature[85]. This is not the case as the reason the observed concentration H_2O_2 at high temperatures decreases is because it decomposes rapidly at elevated temperatures. This opinion is consistent throughout the literature as the direct synthesis of H_2O_2 from H_2 and O_2 has to be carried out at temperatures close to 0 ℃ to inhibit the subsequent decomposition[84, 85, 89, 95]. Other publications suggest that the formation of GLA is attributed to the oxidation of intermediate species such as DHA and glyceraldehyde (GLAD) proceeding *via* different mechanistic pathways[170, 184, 185].

It has been well documented that the pH of the aqueous solution drastically affects the rate of glycerol oxidation and the selectivity of the products[168, 179, 181, 186]. Prati and Rossi were the first to postulate the role of NaOH in the oxidation of alcohols when Au supported catalysts were used for the oxidation of C_3 diols[44]. They suggested that the external hydroxyl group plays an integral role in the initial dehydrogenation of the alcohol group to form the carbonyl. In the absence of a sacrificial base, the cleavage of the C-H bond and subsequent H-abstraction of the hydrogen atom adjacent to the target alcohol group is incredibly difficult. This theory was later supported by the Hutchings group[187]. Furthermore, increasing concentrations of base have shown to enhance C3 selectivity through the base promoted decomposition of H_2O_2[171] which as discussed previously, is widely believed to be responsible for the C-C cleavage in the catalytic oxidation of glycerol. Since this work, significant contributions from Davis and co-workers[179, 181, 186] give a more defined and detailed description of the role of external hydroxyl groups in the oxidation of alcohols. Using density functional theory, Davis and co-workers[181] explained that surface-bound hydroxide intermediates significantly lower the energy barrier for C-H and O-H bond activation with Au nanoparticles. The formation of the initial alkoxy intermediate is also possible in solution alone, but the energy barrier for the subsequent C-H activation is significantly reduced when adsorbed hydroxyl intermediates are involved.

Thus, both the OH ion and the heterogeneous catalyst have pivotal roles in the dehydrogenation of the alcohol species to form the aldehyde.

A significant amount of recent work has focussed on the oxidation of glycerol in a base free / neutral aqueous medium. For the industrialisation of such a process, the sacrificial consumption of NaOH is not favourable. Early work suggested that supported platinum catalysts displayed great promise with particle size proving an essential attribute for activity[188]. Further work and by Brett *et al.*[189] involved the preparation of supported AuPt alloys. These alloys were found to display high activities in a base free environment. In addition, this publication highlighted the importance of support selection, which appears to have a significant impact on a given catalysts activity under base-free conditions. An additional contribution from Tongsakul *et al.*[190] suggested that the incorporation of Au into Pt changes the electronic and geometric nature of the Pt, hereby promoting its catalytic activity. Further work from Villa *et al.*[191] suggested that under base free conditions basic supports promote activity but also enhance C-C cleavage with acidity promoting the selectivity to C3 products. It was stated that the performance of these acidic supported catalyst was not dependent on the type of acidic site, but the quantity.

1.5.4. The Selective Oxidation of Furfural

A fundamental disadvantage for the universal exploitation of biodiesel as an alternative to fossil fuels is the considerable waste of carbon which is produced as unfavourable bi-products. One possible method of resolving this problem would be to utilize these waste materials as platform chemicals. Furfural (FF) is a heterocyclic C_5 aldehyde formed from the acid hydrolysis of lignocellulosic agricultural residues. FF has limited applications but has significant potential as a platform chemical[192-194]. To date, the majority of work in this area has focussed on the hydrogenation of FF to furfuryl alcohol (FOH) and subsequently tetrahydrofurfuryl alcohol, tetrahydrofuran and 2-methyltetrahydrofuran, which are considered promising 2nd generation fuels[195-200]. In addition, FF has also been used to produce furan by using a supported palladium catalyst through vapour phase decarbonylation[201]. Due to the vast amount of research focussing on these transformations, the potential for the selective oxidation of FF to value added products appears to have been somewhat overlooked.

Maleic acid (MEA) is one of many products which can be produced from the selective oxidation of FF. Commercially, MEA is produced from maleic anhydride through vapour phase oxidation of petroleum derivatives over vanadium phosphate catalysts at temperatures exceeding 250 ºC[202]. MEA is a crucial starting material for the formation of unsaturated polyester resins[203]. In light of the concerns regarding the depletion of fossil fuel stocks, it is important to replace the conventional petroleum based starting materials for MEA formation with something that is renewable. Yin and co-workers[204] were the first to identify that FF could be used as a starting material for the formation of MEA. In their first publication, they showed that using phosphomolybdic heteropolyacids (HPA) in the presence of $Cu(NO_3)_2$ could give yields of up to 35.3 % with a selectivity of 39.3 %. Although this was the first publication in this area, significant amounts of carbon are believed to be lost as a result of resin formation which the $Cu(NO_3)_2$ was stated to reduce. A subsequent publication by the same group showed that similar yields of MEA could be obtained but with a greater selectivity of 50.3 % using a biphasic system[205]. It was stated that the biphasic system allowed for the substrate to be released gradually from the organic layer. From this it was postulated that the reduction in substrate concentration in the aqueous layer minimised the formation of resins through intramolecular substrate interactions. The most recent publication from Yin and co-worker revealed that a further increase of MEA yield was obtainable through use of phosphomolybdic HPAs in the presence of copper(II)triflate[206]. MEA yields of up to 54 % were reported. The triflate complex was suggested to increase selectivity by both trapping the carbon radicals which facilitate resin formation and re-oxidising the reduced catalyst in-situ. An alternative approach was proposed by Granados and co-workers[207] who showed that using a titanosilicate zeolite (TS-1) in the presence of H_2O_2 could give MEA yields of up to 78 % after 24 h.

The formation of succinic acid (SA) from bio-renewable FF also appears to be an attractive target. SA has a range of different applications on a commercial scale including use as an acidity regulator in the food industry, a foaming agent in surfactants, and as an additive in the pharmaceutical industry for the production of antibiotics and vitamins[208]. There are a number of recent reviews highlighting the potential of SA as a platform chemical for the synthesis of high value compounds[139, 194, 209] which include the formation of specialised polyesters[210]. As with MEA, SA is conventionally sourced from maleic anhydride which is synthesised from petroleum based compounds[202]. As discussed previously, this is no

26

longer favourable and an alternative approach from bio-renewable materials would be much more viable. There is a significant amount of literature showing that SA can be made directly from lignocellulosic materials[211, 212] with reasonable yields, but literature reporting the direct synthesis of SA from FF is limited. A two-step process was proposed by Kunioka and co-workers[213]. The first step involves the liquid phase oxidation of FF in the presence of sodium chlorate and vanadium pentoxide to form fumaric acid. This was subsequently hydrogenated using a 5 wt.% Pd/C catalyst to give SA with almost 100 % atom efficiency. Choudhary and co-workers were the first to propose a method for the one pot synthesis of SA from FF in the liquid phase [214]. A SA yield of 74.2 % was reported after 24 h when catalysed by amberlyst-15 under relatively mild reaction conditions using H_2O_2 as the oxidant. The remaining 25.8 % of carbon was unaccounted for, and it was proposed that this loss may be attributed to resin formation. A subsequent, paper by the same group showed that SA could be produced from HMF under the same conditions but with significantly lower yields[215]. This paper also showed that the SA selectivity was considerably higher when lower temperatures were used in the presence of high H_2O_2 concentrations.

The oxidative esterification of FF to form alkoxy furoates is also a possible option. These compounds are in high demand for their application as flavour and fragrance components in the fine chemical industry[216]. Taarning *et al.*[217] were the first to show that the oxidative esterification of FF to methyl furoate was possible through the application of specific reaction conditions and in the presence of a Au supported heterogeneous catalyst. A subsequent publication by Corma and co-worker showed that higher yields of the product could be achieved through use of an Au/nano-CeO$_2$ catalyst. High yields of desired product were obtained when pressurising the reaction vessel with 10 bar of bubbled O$_2$ at 130 ºC. These reaction conditions were considerably more intensive than those used by Taarning *et al.*[217]. A more recent paper revealed that a Au/ZrO$_2$ could successfully catalyse this transformation in the absence of a base[216]. A selectivity in excess of 90 % was achieved using 6 bar O$_2$ at 120 ºC. Catalysts with varying Au particle sizes were assessed and increasing Au particle sizes was shown to severely reduce catalytic performance. An additional publication from Boccuzzi et al.[69] followed on from this, showing that the application of Au/TiO$_2$ in the absence of base was also capable of catalysing the oxidative esterification of FF with methanol. The important link between Au nanoparticle size and catalytic performance was reiterated in this work. A subsequent publication by the same

group[218] used the same reaction conditions in order to conduct a support study for this reaction. Au nanoparticles were supported on CeO_2, TiO_2 and ZrO_2 and it was reported that Au/ZrO_2 performed the best. It was postulated that ZrO_2 was the superior support as it was the least likely metal oxide to be poisoned by organic bi-products. Very recent work by Tong *et al.[219]* reveals that FF can undergo oxidative esterification with propanol in the presence of Au nanoparticles. It was also determined that a subsequent condensation of the coupled product could be achieved through the addition of K_2CO_3.

Furoic acid (FA) is another compound which can be produced directly from FF. FA is predominantly used as a precursor to form furoyl chloride, which is a key compound in the pharmaceutical industry for the production of drugs and insecticides[220]. It is currently produced on an industrial scale *via* the Cannizzaro reaction with NaOH. This process requires the subsequent separation of the corresponding alcohol and acid which may be considered costly due to the additional time and financial constraints associated with this process. The direct catalytic oxidation of FF to FA has previously been considered unfeasible on an industrial scale as the substrate can also take part in a competitive oxidation process resulting in the formation of other unfavourable bi-products due to ring cleavage[220]. Despite this, there have been some promising publications. Parpot *et al.* undertook an electrochemical investigation of the oxidation and reduction of FF in an aqueous medium[221]. Yields of up to 80 % of FA were obtained using Nickel anodes in a highly basic aqueous medium. This selectivity was noticeably higher when compared with the use of Pt and Au anodes. An additional study by Sha and co-workers[222] showed that yields of up to 92 % can be achieved in the presence of an Ag_2O/CuO heterogeneous catalyst under optimised reaction conditions. A temperature of 70 °C and 30 wt.% of Ag_2O was required in order to obtain these excellent yields. Deviation from these optimised conditions resulted in significant decreases in FA yield. Furthermore, re-usability tests showed that catalyst deactivation due to erosion by the FA produced in-situ was a problem which limits the possible industrialisation of this process.

FF is an extremely reactive compound and can participate in a range of unfavourable reactions which may impact its use as a platform chemical. These unfavourable transformations include: self-polymerisation[223], oxidative ring opening[220] and degradation[224].

28
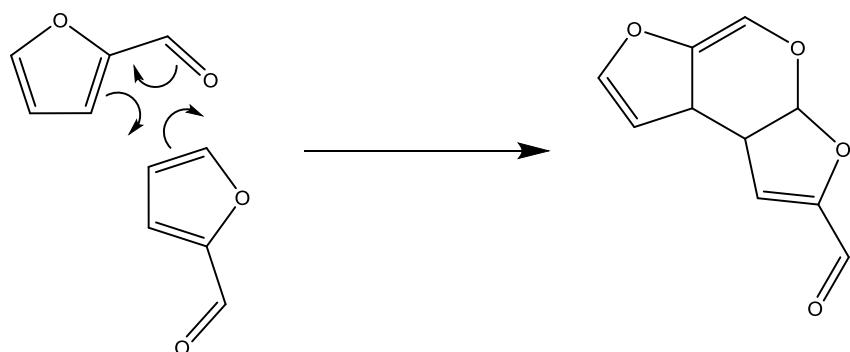
Scheme 1.11. Example of acid promoted Diels-Alder reaction between two FF compounds as proposed by Tanskanan and co-workers[225].

The unfavourable polymerisation of FF has been noted in publications attempting to yield succinic acid and MEA from FF using heterogeneous catalysts. A study by Yin and co-workers[206] proposed a mechanism for this unfavourable polymerisation. It was suggested that this process is initiated through the abstraction of a hydrogen atom from the furan ring to leave a radically charged furan species. Additional work by Tanskanen and co-workers[225, 226] involved the derivation of a kinetic model to fit the polymerisation of FF. Here, FF was exposed to formic acid in an aqueous medium. It was suggested that the acidity of the aqueous medium promoted the polymerisation pathway and that it occurred through a Diels-Alder interaction between two of the FF compounds.
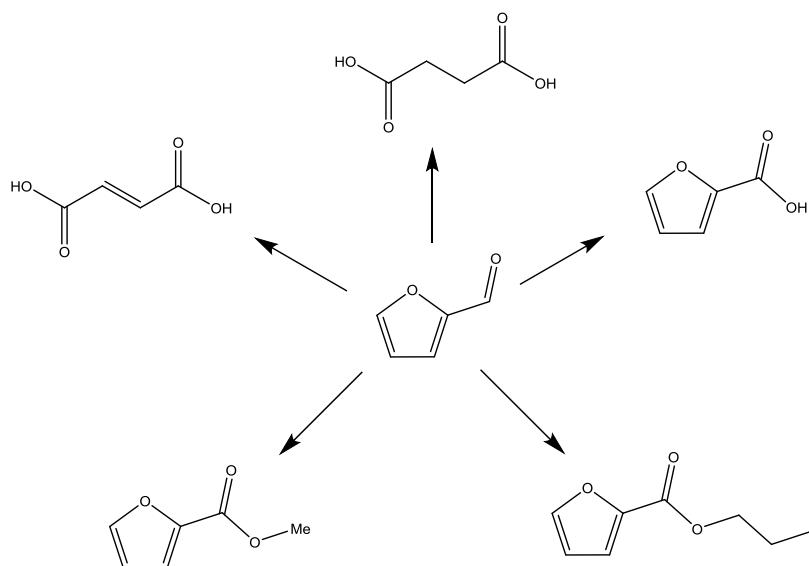
Scheme 1.12. The literature suggests that FF can be selectively oxidised to a range of different products in the presence of heterogeneous catalysts.

29

It is clear that FF is an exceptionally difficult compound to work with. Almost all of the publications associated with its selective oxidation have reported the formation of resins or a significant loss in mass balance.

1.6. Organic Mechanisms

There are a number of organic transformations which will be mentioned during this work. These are given below.

1.6.1. Dakin Oxidation Reaction
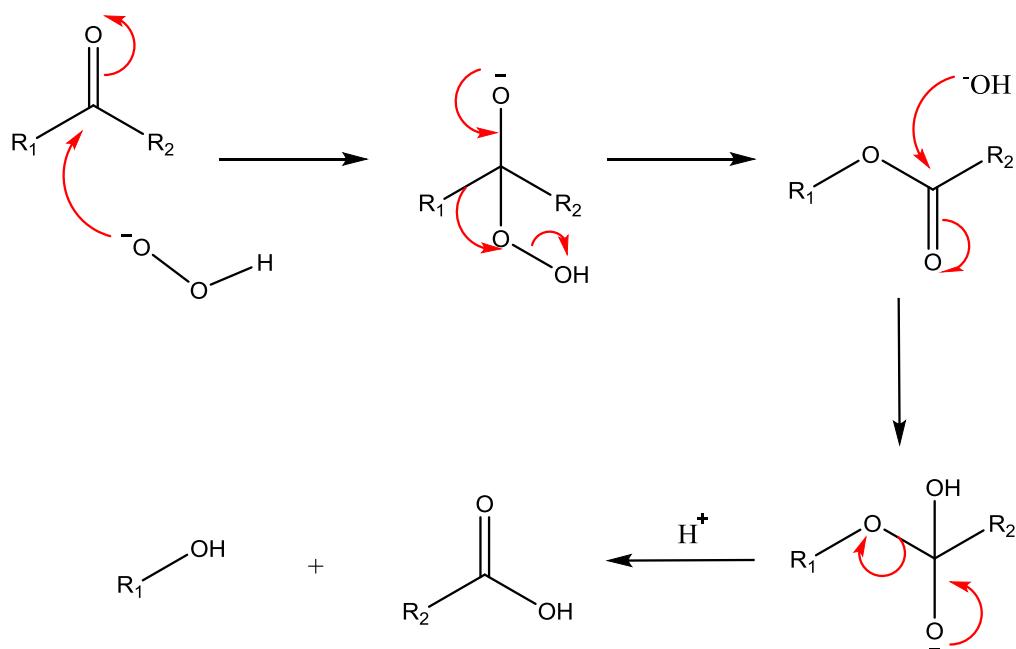
Scheme 1.13. Mechanism for the Dakin Oxidation redox reaction. Typically occurs when a hydroxylated phenyl aldehyde or ketone reacts with H_2O_2 in the presence of base to form a benzenediol and a carboxylate.

1.6.2. Diels-Alder Reaction
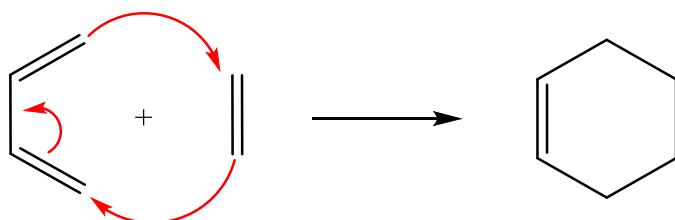
Scheme 1.14. Mechanism for the Diels-Alder reaction between a conjugated diene and a dienophile.

1.6.3. The Cannizzaro Reaction
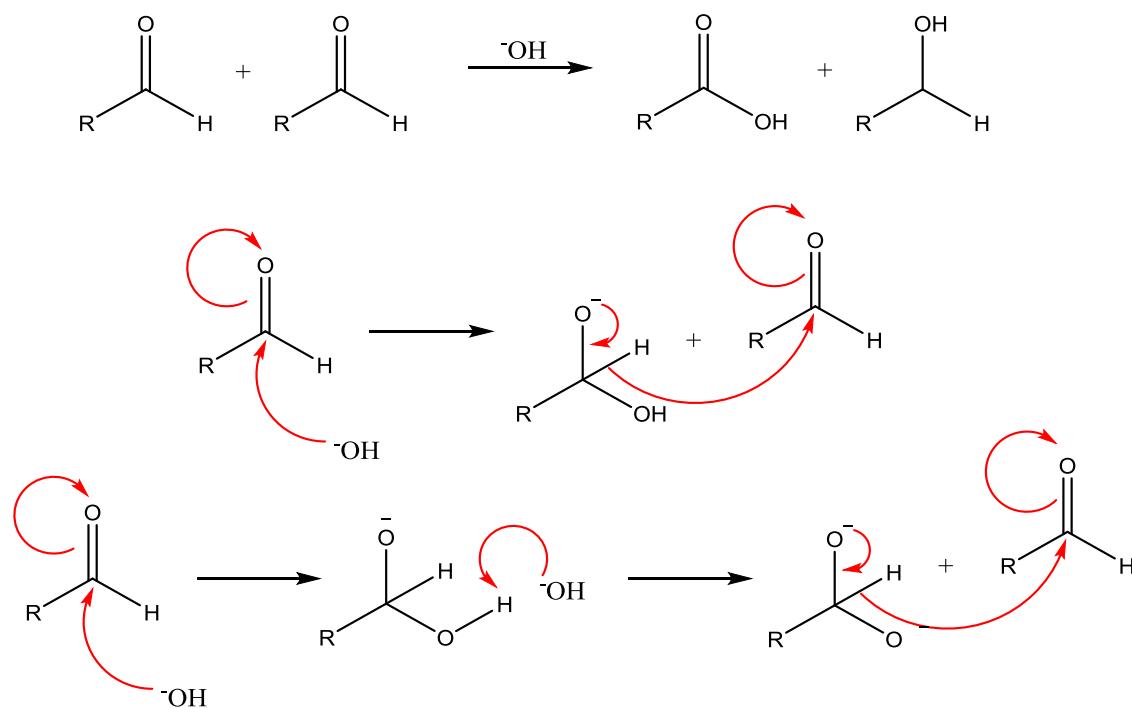
Scheme 1.15. Mechanism for the Cannizzaro reaction which involves the base induced disproportionation of two carbonyl species. The disproportionation leads to the formation of stoichiometric equivalents of the corresponding alcohol and aldehyde. The concentration of the base determines how the reaction proceeds.

1.7. References

1. M. Bowker, *The basis and applications of heterogeneous catalysis*, Oxford University Press, 1998.

2. P. Anastas and N. Eghbali, *Chemical Society Reviews*, 2010, **39**, 301.

3. P. T. Anastas, L. B. Bartlett, M. M. Kirchhoff and T. C. Williamson, *Catalysis Today*, 2000, **55**, 11.

4. C. A. Busacca, D. R. Fandrick, J. J. Song and C. H. Senanayake, *Advanced Synthesis & Catalysis*, 2011, **353**, 1825.

5. R. A. Sheldon, *Journal of Chemical Technology and Biotechnology*, 1997, **68**, 381.

6. F. R. Ma and M. A. Hanna, *Bioresource Technology*, 1999, **70**, 1.

7. P. T. Anastas and M. M. Kirchhoff, *Accounts of Chemical Research*, 2002, **35**, 686.

8. A. Kudo and Y. Miseki, *Chemical Society Reviews*, 2009, **38**, 253.

9. E. Pelizzetti and C. Minero, *Electrochimica Acta*, 1993, **38**, 47.

10. H. E. Schoemaker, D. Mink and M. G. Wubbolts, *Science*, 2003, **299**, 1694.

11. M. Beller, B. Cornils, C. D. Frohning and C. W. Kohlpaintner, *Journal of Molecular Catalysis A-Chemical*, 1995, **104**, 17.

12. R. Noyori and T. Ohkuma, *Angewandte Chemie-International Edition*, 2001, **40**, 40.

13. S. N. Riduan, Y. G. Zhang and J. Y. Ying, *Angewandte Chemie-International Edition*, 2009, **48**, 3322.

14. T. J. Colacot, *Platinum Metals Review*, 2011, **55**, 84.

15. D. J. Cole-Hamilton, *Science*, 2003, **299**, 1702.

16. I. E. Wachs, *Catalysis Today*, 1996, **27**, 437.

17. I. E. Wachs, *Catalysis Today*, 2005, **100**, 79.

18. A. T. Bell, *Science*, 2003, **299**, 1688.

19. K. Karaskova, L. Obalova, K. Jiratova and F. Kovanda, *Chemical Engineering Journal*, 2010, **160**, 480.

20. A. C. Gluhoi and B. E. Nieuwenhuys, *Catalysis Today*, 2007, **119**, 305.

21. R. Schlogl, *Angewandte Chemie-International Edition*, 2003, **42**, 2004.

22. G. K. Boreskov, *Heterogeneous Catalysis*, Nova Science Publishers, New York, 2003.

23. F. Banisharifdehkordi and M. Baghalha, *Fuel Processing Technology*, 2014, **120**, 96.

24.   G. Olah, A. Molnar, *Hydrocarbon Chemistry*, New Jersey, 2003

25.   A. Knell, P. Barnickel, A. Baiker and A. Wokaun, *Journal of Catalysis*, 1992, **137**, 306.

26.   J. Saavedra, H. A. Doan, C. J. Pursell, L. C. Grabow and B. D. Chandler, *Science*, 2014, **345**, 1599.

27.   G. C. Bond and D. T. Thompson, *Gold Bulletin*, 2000, **33**, 41.

28.   J. W. Mellor, *Journal of Physical Chemistry*, 1903, **7**, 557.

29.   S. Green, *Industiral Catalysis*, Macmillan Company, New York, 1928.

30.   B. Lindstrom and L. J. Pettersson, *Cattech*, 2003, **7**, 130.

31.   J. Döbereiner, *Schweigger's Journal*, 1822, 91.

32.   E. Davy, *Philosophical Transactions*, 1820, **108**.

33.   W. Henry, *Philosophical Magazine*, 1825, 269.

34.   R. L. Burwell, *Heterogeneous Catalysis - Selected American Histories*, American Chemical Society, Washington D.C., 1983.

35.   M. Faraday, *Philosophical Transactions, 124 (1834) 55*, 1834.

36.   G. Lemoine, *Chemical Physics*, 1877, **12**, 145.

37.   S. A. Topham, *Catalysis: Science and Technology*, Springer, New York, 1981.

38.   1925.

39.   A. S. K. Hashmi and G. J. Hutchings, *Angewandte Chemie-International Edition*, 2006, **45**, 7896.

40.   G. C. Bond, P. A. Sermon, G. Webb, D. A. Buchanan and P. B. Wells, *Journal of the Chemical Society-Chemical Communications*, 1973, 444.

41.   M. Haruta, T. Kobayashi, H. Sano and N. Yamada, *Chemistry Letters*, 1987, 405.

42.   G. J. Hutchings, *Journal of Catalysis*, 1985, **96**, 292.

43.   T. Hayasi, L. B. Han, S. Tsubota and M. Haruta, *Industrial & Engineering Chemistry Research*, 1995, **34**, 2298.

44.   L. Prati and M. Rossi, *Journal of Catalysis*, 1998, **176**, 552.

45.   M. Haruta and M. Date, *Applied Catalysis A-General*, 2001, **222**, 427.

46.   A. Corma and H. Garcia, *Chemical Society Reviews*, 2008, **37**, 2096.

47.   R. Sardar, A. M. Funston, P. Mulvaney and R. W. Murray, *Langmuir*, 2009, **25**, 13840.

48.   C. Della Pina, E. Falletta and M. Rossi, *Chemical Society Reviews*, 2012, **41**, 350.

49.   G. C. Bond and D. T. Thompson, *Catalysis Reviews-Science and Engineering*, 1999, **41**, 319.

50. B. Hvolbaek, T. V. W. Janssens, B. S. Clausen, H. Falsig, C. H. Christensen and J. K. Norskov, *Nano Today*, 2007, **2**, 14.

51. M. Valden, X. Lai and D. W. Goodman, *Science*, 1998, **281**, 1647.

52. M. Chen, Y. Cai, Z. Yan and D. W. Goodman, *Journal of the American Chemical Society*, 2006, **128**, 6341.

53. Z. X. Yang, R. Q. Wu and D. W. Goodman, *Physical Review B*, 2000, **61**, 14066.

54. J. Guzman and B. C. Gates, *Journal of the American Chemical Society*, 2004, **126**, 2672.

55. G. J. Hutchings, M. S. Hall, A. F. Carley, P. Landon, B. E. Solsona, C. J. Kiely, A. Herzing, M. Makkee, J. A. Moulijn, A. Overweg, J. C. Fierro-Gonzalez, J. Guzman and B. C. Gates, *Journal of Catalysis*, 2006, **242**, 71.

56. P. Haider, J. D. Grunwaldt, R. Seidel and A. Baiker, *Journal of Catalysis*, 2007, **250**, 313.

57. N. Lopez, T. V. W. Janssens, B. S. Clausen, Y. Xu, M. Mavrikakis, T. Bligaard and J. K. Norskov, *Journal of Catalysis*, 2004, **223**, 232.

58. S. Carrettin, P. Concepcion, A. Corma, J. M. L. Nieto and V. F. Puntes, *Angewandte Chemie-International Edition*, 2004, **43**, 2538.

59. J. A. van Bokhoven, C. Louis, J. T Miller, M. Tromp, O. V. Safonova and P. Glatzel, *Angewandte Chemie-International Edition*, 2006, **45**, 4651.

60. A. Sanchez, S. Abbet, U. Heiz, W. D. Schneider, H. Hakkinen, R. N. Barnett and U. Landman, *Journal of Physical Chemistry A*, 1999, **103**, 9573.

61. M. F. Camellone and S. Fabris, *Journal of the American Chemical Society*, 2009, **131**, 10473.

62. X. Tang, J. Schneider, A. Dollinger, Y. Luo, A. S. Worz, K. Judai, S. Abbet, Y. D. Kim, G. F. Gantefor, D. H. Fairbrother, U. Heiz, K. H. Bowen and S. Proch, *Physical Chemistry Chemical Physics*, 2014, **16**, 6735.

63. J. T. Miller, A. J. Kropf, Y. Zha, J. R. Regalbuto, L. Delannoy, C. Louis, E. Bus and J. A. van Bokhoven, *Journal of Catalysis*, 2006, **240**, 222.

64. M. Haruta, *Catalysis Today*, 1997, **36**, 153.

65. W. C. Ketchie, Y. L. Fang, M. S. Wong, M. Murayama and R. J. Davis, *Journal of Catalysis*, 2007, **250**, 94.

66. M. Sankar, Q. He, M. Morad, J. Pritchard, S. J. Freakley, J. K. Edwards, S. H. Taylor, D. J. Morgan, A. F. Carley, D. W. Knight, C. J. Kiely and G. J. Hutchings, *ACS Nano*, 2012, **6**, 6600.

67. M. Morad, M. Sankar, E. H. Cao, E. Nowicka, T. E. Davies, P. J. Miedziak, D. J. Morgan, D. W. Knight, D. Bethell, A. Gavriilidis and G. J. Hutchings, *Catalysis Science & Technology*, 2014, **4**, 3120.

68. T. Hayashi, K. Tanaka and M. Haruta, *Journal of Catalysis*, 1998, **178**, 566.

69. F. Boccuzzi, A. Chiorino, M. Manzoli, P. Lu, T. Akita, S. Ichikawa and M. Haruta, *Journal of Catalysis*, 2001, **202**, 256.

70. F. Porta, L. Prati, M. Rossi, S. Coluccia and G. Martra, *Catalysis Today*, 2000, **61**, 165.

71. I. Gandarias, P. J. Miedziak, E. Nowicka, M. Douthwaite, D. J. Morgan, G. J. Hutchings and S. H. Taylor, *Chemsuschem*, 2015, **8**, 473.

72. R. Y. Zhong, X. H. Yan, Z. K. Gao, R. J. Zhang and B. Q. Xu, *Catalysis Science & Technology*, 2013, **3**, 3013.

73. C. L. Bracey, P. R. Ellis and G. J. Hutchings, *Chemical Society Reviews*, 2009, **38**, 2231.

74. A. Wittstock, V. Zielasek, J. Biener, C. M. Friend and M. Baumer, *Science*, 2010, **327**, 319.

75. W. B. Hou, N. A. Dehm and R. W. J. Scott, *Journal of Catalysis*, 2008, **253**, 22.

76. D. Mott, J. Luo, P. N. Njoki, Y. Lin, L. Y. Wang and C. J. Zhong, *Catalysis Today*, 2007, **122**, 378.

77. A. Wang, X. Y. Liu, C. Y. Mou and T. Zhang, *Journal of Catalysis*, 2013, **308**, 258.

78. H. C. Ham, G. S. Hwang, J. Han, S. W. Nam and T. H. Lim, *Journal of Physical Chemistry C*, 2010, **114**, 14922.

79. J. K. Edwards, S. J. Freakley, R. J. Lewis, J. C. Pritchard and G. J. Hutchings, *Catalysis Today*, 2015, **248**, 3.

80. C. Samanta, *Applied Catalysis A-General*, 2008, **350**, 133.

81. J. K. Edwards, A. F. Carley, A. A. Herzing, C. J. Kiely and G. J. Hutchings, *Faraday Discussions*, 2008, **138**, 225.

82. J. K. Edwards and G. J. Hutchings, *Angewandte Chemie-International Edition*, 2008, **47**, 9192.

83. S. Chinta and J. H. Lunsford, *Journal of Catalysis*, 2004, **225**, 249.

84. P. Landon, P. J. Collier, A. J. Papworth, C. J. Kiely and G. J. Hutchings, *Chemical Communications*, 2002, 2058.

85. P. Landon, P. J. Collier, A. F. Carley, D. Chadwick, A. J. Papworth, A. Burrows, C. J. Kiely and G. J. Hutchings, *Physical Chemistry Chemical Physics*, 2003, **5**, 1917.

86. T. Ishihara, Y. Ohura, S. Yoshida, Y. Hata, H. Nishiguchi and Y. Takita, *Applied Catalysis A-General*, 2005, **291**, 215.

87. B. E. Solsona, J. K. Edwards, P. Landon, A. F. Carley, A. Herzing, C. J. Kiely and G. J. Hutchings, *Chemistry of Materials*, 2006, **18**, 2689.

88. J. K. Edwards, B. Solsona, P. Landon, A. F. Carley, A. Herzing, M. Watanabe, C. J. Kiely and G. J. Hutchings, *Journal of Materials Chemistry*, 2005, **15**, 4595.

89. J. K. Edwards, B. E. Solsona, P. Landon, A. F. Carley, A. Herzing, C. J. Kiely and G. J. Hutchings, *Journal of Catalysis*, 2005, **236**, 69.

90. V. R. Choudhary, C. Samanta, T. V. Choudhary, *Journal of Molecular Catalysis A-Chemical*, 2006, **260**, 115.

91. V. R. Choudhary, C. Samanta and T. V. Choudhary, *Applied Catalysis A-General*, 2006, **308**, 128.

92. C. Samanta,V. R. Choudhary, *Catalysis Communications*, 2007, **8**, 2222.

93. C. Samanta, V. R. Choudhary, *Catalysis Communications*, 2007, **8**, 73.

94. V. R. Choudhary and P. Jana, *Catalysis Communications*, 2008, **9**, 2371.

95. J. K. Edwards, B. Solsona, A. F. Carley, A. A. Herzing, C. J. Kiely and G. J. Hutchings, *Science*, 2009, **323**, 1037.

96. S. Park, D. R. Park, J. H. Choi, T. J. Kim, Y. M. Chung, S.H. Oh and I. K. Song, *Journal of Molecular Catalysis A-Chemical*, 2010, **332**, 76.

97. E. N. Ntainjua, M. Piccinini, S. J. Freakley, J. C. Pritchard, J. K. Edwards, A. F. Carley and G. J. Hutchings, *Green Chemistry*, 2012, **14**, 170.

98. N. Gemo, P. Biasi, P. Canu, F. Menegazzo, F. Pinna, A. Samikannu, K. Kordas, T. O. Salmi and J. P. Mikkola, *Topics in Catalysis*, 2013, **56**, 540.

99. G. Grigoropoulou, J. H. Clark and J. A. Elings, *Green Chemistry*, 2003, **5**, 1.

100. J. R. Monnier, P. J. Muehlbauer, *U.S. Patent*, 292 589, 1990.

101. A. K. Sinha, S. Seelan, T. Akita, S. Tsubota and M. Haruta, *Applied Catalysis A-General*, 2003, **240**, 243.

102. A. K. Sinha, S. Seelan, T. Akita, S. Tsubota and M. Haruta, *Catalysis Letters*, 2003, **85**, 223.

103. T. A. Nijhuis, T. Visser and B. M. Weckhuysen, *Journal of Physical Chemistry B*, 2005, **109**, 19309.

104. T. A. R. Nijhuis, T. Visser and B. M. Weckhuysen, *Angewandte Chemie-International Edition*, 2005, **44**, 1115.

105. M. D. Hughes, Y. J. Xu, P. Jenkins, P. McMorn, P. Landon, D. I. Enache, A. F. Carley, G. A. Attard, G. J. Hutchings, F. King, E. H. Stitt, P. Johnston, K. Griffin and C. J. Kiely, *Nature*, 2005, **437**, 1132.

106. M. Ojeda and E. Iglesia, *Chemical Communications*, 2009, 352.

107. J. Huang, T. Takei, T. Akita, H. Ohashi and M. Haruta, *Applied Catalysis B-Environmental*, 2010, **95**, 430.

108. J. Huang, T. Takei, H. Ohashi and M. Haruta, *Applied Catalysis A-General*, 2012, **435**, 115.

109. L. Prati and M. Rossi, *3rd World Congress on Oxidation Catalysis*, 1997, **110**, 509.

110. N. Dimitratos, J. A. Lopez-Sanchez, D. Morgan, A. F. Carley, R. Tiruvalam, C. J. Kiely, D. Bethell and G. J. Hutchings, *Physical Chemistry Chemical Physics*, 2009, **11**, 5142.

111. Y. Ryabenkova, P. J. Miedziak, N. F. Dummer, S. H. Taylor, N. Dimitratos, D. J. Willock, D. Bethell, D. W. Knight and G. J. Hutchings, *Topics in Catalysis*, 2012, **55**, 1283.

112. O. Casanova, S. Iborra and A. Corma, *Journal of Catalysis*, 2009, **265**, 109.

113. M. H. Ab Rahim, Q. He, J. A. Lopez-Sanchez, C. Hammond, N. Dimitratos, M. Sankar, A. F. Carley, C. J. Kiely, D. W. Knight and G. J. Hutchings, *Catalysis Science & Technology*, 2012, **2**, 1914.

114. D. I. Enache, D. W. Knight and G. J. Hutchings, *Catalysis Letters*, 2005, **103**, 43.

115. V. R. Choudhary, A. Dhar, P. Jana, R. Jha and B. S. Uphade, *Green Chemistry*, 2005, **7**, 768.

116. N. Dimitratos, J. A. Lopez-Sanchez, D. Morgan, A. Carley, L. Prati and G. J. Hutchings, *Catalysis Today*, 2007, **122**, 317.

117. G. Li, D. I. Enache, J. Edwards, A. F. Carley, D. W. Knight and G. J. Hutchings, *Catalysis Letters*, 2006, **110**, 7.

118. P. Miedziak, M. Sankar, N. Dimitratos, J. A. Lopez-Sanchez, A. F. Carley, D. W. Knight, S. H. Taylor, C. J. Kiely and G. J. Hutchings, *Catalysis Today*, 2011, **164**, 315.

119. J. Pritchard, L. Kesavan, M. Piccinini, Q. He, R. Tiruvalam, N. Dimitratos, J. A. Lopez-Sanchez, A. F. Carley, J. K. Edwards, C. J. Kiely and G. J. Hutchings, *Langmuir*, 2010, **26**, 16568.

120. S. Meenakshisundaram, E. Nowicka, P. J. Miedziak, G. L. Brett, R. L. Jenkins, N. Dimitratos, S. H. Taylor, D. W. Knight, D. Bethell and G. J. Hutchings, *Faraday Discussions*, 2010, **145**, 341.

121. M. Sankar, E. Nowicka, R. Tiruvalam, Q. He, S. H. Taylor, C. J. Kiely, D. Bethell, D. W. Knight and G. J. Hutchings, *Chemistry-A European Journal*, 2011, **17**, 6524.

122. G. Kovtun, T. Kameneva, S. Hladyi, M. Starchevsky, Y. Pazdersky, I. Stolarov, M. Vargaftik and I. Moiseev, *Advanced Synthesis & Catalysis*, 2002, **344**, 957.

123. A. Villa, D. Wang, G. M. Veith and L. Prati, *Journal of Catalysis*, 2012, **292**, 73.

124. Q. He, P. J. Miedziak, L. Kesavan, N. Dimitratos, M. Sankar, J. A. Lopez-Sanchez, M. M. Forde, J. K. Edwards, D. W. Knight, S. H. Taylor, C. J. Kiely and G. J. Hutchings, *Faraday Discussions*, 2013, **162**, 365.

125. M. Sankar, E. Nowicka, E. Carter, D. M. Murphy, D. W. Knight, D. Bethell and G. J. Hutchings, *Nature Communications*, 2014, **5**, 6.

126. E. Skupien, R. J. Berger, V. P. Santos, J. Gascon, M. Makkee, M. T. Kreutzer, P. J. Kooyman, J. A. Moulijn and F. Kapteijn, *Catalysts*, 2014, **4**, 89.

127. A. Villa, D. Ferri, S. Campisi, C. E. Chan-Thaw, Y. Lu, O. Krocher and L. Prati, *Chemcatchem*, 2015, **7**, 2534.

128. K. Deplanche, I. P. Mikheenko, J. A. Bennett, M. Merroun, H. Mounzer, J. Wood and L. E. Macaskie, *Topics in Catalysis*, 2011, **54**, 1110.

129. H. Guo, M. Kemell, A. Al-Hunaiti, S. Rautiainen, M. Leskela and T. Repo, *Catalysis Communications*, 2011, **12**, 1260.

130. Y. Guan, N. Zhao, B. Tang, Q. Q. Jia, X. H. Xu, H. Liu and R. I. Boughton, *Chemical Communications*, 2013, **49**, 11524.

131. J. Zhu, P. C. Wang and M. Lu, *Applied Catalysis A-General*, 2014, **477**, 125.

132. E. Cao, M. Sankar, E. Nowicka, Q. He, M. Morad, P. J. Miedziak, S. H. Taylor, D. W. Knight, D. Bethell, C. J. Kiely, A. Gavriilidis and G. J. Hutchings, *Catalysis Today*, 2013, **203**, 146.

133. H. Alex, N. Steinfeldt, K. Jaehnisch, M. Bauer and S. Huebner, *Nanotechnology Reviews*, 2014, **3**, 99.

134. N. Dimitratos, J. A. Lopez-Sanchez, S. Meenakshisundaram, J. M. Anthonykutty, G. Brett, A. F. Carley, S. H. Taylor, D. W. Knight and G. J. Hutchings, *Green Chemistry*, 2009, **11**, 1209.

135. Y. Ryabenkova, Q. He, P. J. Miedziak, N. F. Dummer, S. H. Taylor, A. F. Carley, D. J. Morgan, N. Dimitratos, D. J. Willock, D. Bethell, D. W. Knight, D. Chadwick, C. J. Kiely and G. J. Hutchings, *Catalysis Today*, 2013, **203**, 139.

136. H. Ma, X. Nie, J. Y. Cai, C. Chen, J. Gao, H. Miao and J. Xu, *Science China-Chemistry*, 2010, **53**, 1497.

137. M. B. Griffin, A. A. Rodriguez, M. M. Montemore, J. R. Monnier, C. T. Williams and J. W. Medlin, *Journal of Catalysis*, 2013, **307**, 111.

138. D. Tongsakul, S. Nishimura, C. Thammacharoen, S. Ekgasit and K. Ebitani, *Industrial & Engineering Chemistry Research*, 2012, **51**, 16182.

139. A. Corma, S. Iborra and A. Velty, *Chemical Reviews*, 2007, **107**, 2411.

140. S. E. Davis, L. R. Houk, E. C. Tamargo, A. K. Datye and R. J. Davis, *Catalysis Today*, 2011, **160**, 55.

141. S. E. Davis, B. N. Zope and R. J. Davis, *Green Chemistry*, 2012, **14**, 143.

142. T. Mallat and A. Baiker, *Chemical Reviews*, 2004, **104**, 3037.

143. S. Albonetti, T. Pasini, A. Lolli, M. Blosi, M. Piccinini, N. Dimitratos, J. A. Lopez-Sanchez, D. J. Morgan, A. F. Carley, G. J. Hutchings and F. Cavani, *Catalysis Today*, 2012, **195**, 120.

144. A. Villa, M. Schiavoni, S. Campisi, G. M. Veith and L. Prati, *Chemsuschem*, 2013, **6**, 609.

145. J. Cai, H. Ma, J. Zhang, Q. Song, Z. Du, Y. Huang and J. Xu, *Chemistry-A European Journal*, 2013, **19**, 14215.

146. S. E. Davis, A. D. Benavidez, R. W. Gosselink, J. H. Bitter, K. P. de Jong, A. K. Datye and R. J. Davis, *Journal of Molecular Catalysis A-Chemical*, 2014, **388**, 123.

147. X. Y. Wan, C. M. Zhou, J. S. Chen, W. P. Deng, Q. H. Zhang, Y. H. Yang and Y. Wang, *ACS Catalysis*, 2014, **4**, 2175.

148. L. Ardemani, G. Cibin, A. J. Dent, M. A. Isaacs, G. Kyriakou, A. F. Lee, C. M. A. Parlett, S. A. Parry and K. Wilson, *Chemical Science*, 2015, **6**, 4940.

149. A. Lolli, S. Albonetti, L. Utili, R. Amadori, F. Ospitali, C. Lucarelli and F. Cavani, *Applied Catalysis A-General*, 2015, **504**, 408.

150. A. Demirbas, *Energy Sources*, 2004, **26**, 715.

151. S. N. Naik, V. V. Goud, P. K. Rout and A. K. Dalai, *Renewable & Sustainable Energy Reviews*, 2010, **14**, 578.

152. M. Z. Jacobson, *Energy & Environmental Science*, 2009, **2**, 148.

153. M. Dittmar, *Energy*, 2012, **37**, 35.

154. K. Tokimatsu, J. Fujino, S. Konishi, Y. Ogawa and K. Yamaji, *Energy Policy*, 2003, **31**, 775.

155. S. Lee and S. H. Saw, *Journal of Fusion Energy*, 2011, **30**, 398.

156. P. Kumar, D. M. Barrett, M. J. Delwiche and P. Stroeve, *Industrial & Engineering Chemistry Research*, 2009, **48**, 3713.

157. D. M. Alonso, J. Q. Bond and J. A. Dumesic, *Green Chemistry*, 2010, **12**, 1493.

158. P. M. Mortensen, J. D. Grunwaldt, P. A. Jensen, K. G. Knudsen and A. D. Jensen, *Applied Catalysis A-General*, 2011, **407**, 1.

159. P. B. Thompson, *Journal of Agricultural & Environmental Ethics*, 2008, **21**, 183.

160. M. G. Kulkarni, R. Gopinath, L. C. Meher and A. K. Dalai, *Green Chemistry*, 2006, **8**, 1056.

161. L. D. Gomez, C. G. Steele-King and S. J. McQueen-Mason, *New Phytologist*, 2008, **178**, 473.

162. A. Zabaniotou, O. Ioannidou and V. Skoulou, *Fuel*, 2008, **87**, 1492.

163. M. Pauly and K. Keegstra, *Plant Journal*, 2008, **54**, 559.

164. N. Sun, H. Rodriguez, M. Rahman and R. D. Rogers, *Chemical Communications*, 2011, **47**, 1405.

165. B. Katryniok, H. Kimura, E. Skrzynska, J.-S. Girardon, P. Fongarland, M. Capron, R. Ducoulombier, N. Mimura, S. Paul and F. Dumeignil, *Green Chemistry*, 2011, **13**, 1960.

166. A. Villa, N. Dimitratos, C. E. Chan-Thaw, C. Hammond, L. Prati and G. J. Hutchings, *Accounts of Chemical Research*, 2015, **48**, 1403.

167. H. Kimura, K. Tsuto, T. Wakisaka, Y. Kazumi and Y. Inaya, *Applied Catalysis A-General*, 1993, **96**, 217.

168. P. Fordham, R. Garcia, M. Besson and P. Gallezot, *11th International Congress on Catalysis - 40th Anniversary, Pts A and B*, 1996, **101**, 161.

169. R. Garcia, M. Besson and P. Gallezot, *Applied Catalysis A-General*, 1995, **127**, 165.

170. S. Carrettin, P. McMorn, P. Johnston, K. Griffin and G. J. Hutchings, *Chemical Communications*, 2002, 696.

171. N. Dimitratos, A. Villa and L. Prati, *Catalysis Letters*, 2009, **133**, 334.

172. A. H. A. Nadzri, N. Hamzah, A. Alias, J. Salimon and M. A. Yarmo, *X-Ray and Related Techniques*, 2011, **173**, 155.

173. A. Villa, N. Janjic, P. Spontoni, D. Wang, D. S. Su and L. Prati, *Applied Catalysis A-General*, 2009, **364**, 221.

174. N. Dimitratos, J. A. Lopez-Sanchez, J. M. Anthonykutty, G. Brett, A. F. Carley, R. C. Tiruvalam, A. A. Herzing, C. J. Kiely, D. W. Knight and G. J. Hutchings, *Physical Chemistry Chemical Physics*, 2009, **11**, 4952.

175. W. C. Ketchie, M. Murayama and R. J. Davis, *Journal of Catalysis*, 2007, **250**, 264.

176. N. Dimitratos, J. A. Lopez-Sanchez, D. Lennon, F. Porta, L. Prati and A. Villa, *Catalysis Letters*, 2006, **108**, 147.

177. W. H. Fang, J. S. Chen, Q. H. Zhang, W. P. Deng and Y. Wang, *Chemistry-A European Journal*, 2011, **17**, 1247.

178. S. Gil, M. Marchena, L. Sanchez-Silva, A. Romero, P. Sanchez and J. L. Valverde, *Chemical Engineering Journal*, 2011, **178**, 423.

179. W. C. Ketchie, M. Murayama and R. J. Davis, *Topics in Catalysis*, 2007, **44**, 307.

180. A. Villa, G. M. Veith, D. Ferri, A. Weidenkaff, K. A. Perry, S. Campisi and L. Prati, *Catalysis Science & Technology*, 2013, **3**, 394.

181. B. N. Zope, D. D. Hibbitts, M. Neurock and R. J. Davis, *Science*, 2010, **330**, 74.

182. C. Shang and Z.-P. Liu, *Journal of the American Chemical Society*, 2011, **133**, 9938.

183. C. L. Bianchi, P. Canton, N. Dimitratos, F. Porta and L. Prati, *Catalysis Today*, 2005, **102**, 203.

184. S. Demirel-Gulen, M. Lucas and P. Claus, *Catalysis Today*, 2005, **102**, 166.

185. F. Porta and L. Prati, *Journal of Catalysis*, 2004, **224**, 397.

186. M. S. Ide and R. J. Davis, *Accounts of Chemical Research*, 2014, **47**, 825.

187. S. Carrettin, P. McMorn, P. Johnston, K. Griffin, C. J. Kiely and G. J. Hutchings, *Physical Chemistry Chemical Physics*, 2003, **5**, 1329.

188. D. Liang, J. Gao, J. H. Wang, P. Chen, Z. Y. Hou and X. M. Zheng, *Catalysis Communications*, 2009, **10**, 1586.

189. G. L. Brett, Q. He, C. Hammond, P. J. Miedziak, N. Dimitratos, M. Sankar, A. A. Herzing, M. Conte, J. A. Lopez-Sanchez, C. J. Kiely, D. W. Knight, S. H. Taylor and G. J. Hutchings, *Angewandte Chemie-International Edition*, 2011, **50**, 10136.

190. D. Tongsakul, S. Nishimura and K. Ebitani, *ACS Catalysis*, 2013, **3**, 2199.

191. A. Villa, S. Campisi, K. M. H. Mohammed, N. Dimitratos, F. Vindigni, M. Manzoli, W. Jones, M. Bowker, G. J. Hutchings and L. Prati, *Catalysis Science & Technology*, 2015, **5**, 1126.

192. C. M. Cai, T. Y. Zhang, R. Kumar and C. E. Wyman, *Journal of Chemical Technology and Biotechnology*, 2014, **89**, 2.

193. A. Bohre, S. Dutta, B. Saha and M. M. Abu-Omar, *ACS Sustainable Chemistry & Engineering*, 2015, **3**, 1263.

194. P. Gallezot, *Chemical Society Reviews*, 2012, **41**, 1538.

195. J.-P. Lange, E. van der Heide, J. van Buijtenen and R. Price, *Chemsuschem*, 2012, **5**, 150.

196. H. Y. Zheng, Y. L. Zhu, B. T. Teng, Z. Q. Bai, C. H. Zhang, H. W. Xiang and Y. W. Li, *Journal of Molecular Catalysis A-Chemical*, 2006, **246**, 18.

197. S. Sitthisa and D. E. Resasco, *Catalysis Letters*, 2011, **141**, 784.

198. L. R. Baker, G. Kennedy, M. Van Spronsen, A. Hervier, X. J. Cai, S. Y. Chen, L. W. Wang and G. A. Somorjai, *Journal of the American Chemical Society*, 2012, **134**, 14208.

199. S. G. Wang, V. Vorotnikov and D. G. Vlachos, *ACS Catalysis*, 2015, **5**, 104.

200. S. Iqbal, X. Liu, O. F. Aldosari, P. J. Miedziak, J. K. Edwards, G. L. Brett, A. Akram, G. M. King, T. E. Davies, D. J. Morgan, D. K. Knight and G. J. Hutchings, *Catalysis Science & Technology*, 2014, **4**, 2280.

201. W. Zhang, Y. Zhu, S. Niu and Y. Li, *Journal of Molecular Catalysis A-Chemical*, 2011, **335**, 71.

202. G. Centi, F. Trifiro, J. R. Ebner and V. M. Franchetti, *Chemical Reviews*, 1988, **88**, 55.

203. K. J. Zeitsch, in *The chemistry and technology of furfural and its many by-products*, Elsevier, 2000, vol. 13, pp. 225-228.

204. S. Shi, H. Guo and G. Yin, *Catalysis Communications*, 2011, **12**, 731.

205. H. Guo and G. Yin, *Journal of Physical Chemistry C*, 2011, **115**, 17516.

206. J. H. Lan, Z. Q. Chen, J. C. Lin and G. C. Yin, *Green Chemistry*, 2014, **16**, 4351.

207. N. Alonso-Fagundez, I. Agirrezabal-Telleria, P. L. Arias, J. L. G. Fierro, R. Mariscal and M. L. Granados, *RSC Advances*, 2014, **4**, 54960.

208. J. G. Zeikus, M. K. Jain and P. Elankovan, *Applied Microbiology and Biotechnology*, 1999, **51**, 545.

209. C. Delhomme, D. Weuster-Botz and F. E. Kuehn, *Green Chemistry*, 2009, **11**, 13.

210. C.-J. Tsai, W.-C. Chang, C.-H. Chen, H.-Y. Lu and M. Chen, *European Polymer Journal*, 2008, **44**, 2339.

211. K. Chen, M. Jiang, P. Wei, J. Yao and H. Wu, *Applied Biochemistry and Biotechnology*, 2010, **160**, 477.

212. J. M. Yao, M. Jiang, H. Wu and K. Q. Chen, *Shengwu Jiagong Guocheng*, 2010, **8**, 66.

213. Y. Tachibana, T. Masuda, M. Funabashi and M. Kunioka, *Biomacromolecules*, 2010, **11**, 2760.

214. H. Choudhary, S. Nishimura and K. Ebitani, *Chemistry Letters*, 2012, **41**, 409.

215. H. Choudhary, S. Nishimura and K. Ebitani, *Applied Catalysis A-General*, 2013, **458**, 55.

216. M. Signoretto, F. Menegazzo, L. Contessotto, F. Pinna, M. Manzoli and F. Boccuzzi, *Applied Catalysis B-Environmental*, 2013, **129**, 287.

217. E. Taarning, I. S. Nielsen, K. Egeblad, R. Madsen and C. H. Christensen, *Chemsuschem*, 2008, **1**, 75.

218. F. Menegazzo, M. Signoretto, F. Pinna, M. Manzoli, V. Aina, G. Cerrato and F. Boccuzzi, *Journal of Catalysis*, 2014, **309**, 241.

219. X. L. Tong, Z. H. Liu, L. H. Yu and Y. D. Li, *Chemical Communications*, 2015, **51**, 3674.

220. K. J. Zeitsch, in *The chemistry and technology of furfural and its many by-products* Elsevier, 2000, vol. 13, pp. 159-163.

221. P. Parpot, A. P. Bettencourt, G. Chamoulaud, K. B. Kokoh and E. M. Beigsir, *Electrochimica Acta*, 2004, **49**, 397.

222. Q. Y. Tian, D. X. Shi and Y. W. Sha, *Molecules*, 2008, **13**, 948.

223. A. Gandini and M. N. Belgacem, *Actualite Chimique*, 2002, 56.

224. D. L. Williams and A. P. Dunlop, *Industrial and Engineering Chemistry*, 1948, **40**, 239.

225. K. Lamminpaa, J. Ahola and J. Tanskanen, *RSC Advances*, 2014, **4**, 60243.

226. K. Lamminpaa, J. Ahola and J. Tanskanen, *Industrial & Engineering Chemistry Research*, 2012, **51**, 6297.

Chapter 2

Experimental

2.1. <u>Chemicals – Source and Purity</u>

All chemicals used in my research are given below, along with their corresponding source and approximate purity.

Water, HPLC grade, **Fisher Scientific**

Phosphoric Acid (85 wt.% in H_2O), $\geq$ 99.99%, **Sigma Aldrich**

Palladium Chloride, **Johnson Matthey**

Chloroauric acid, **Johnson Matthey**

Chloroplatinic acid, **Johnson Matthey**

Polyvinylalcohol (M_w 9000-10000), 80% hydrolysed, **Sigma Aldrich**

Tetrakis(hydroxymethyl)phosphonium chloride (THPC), 80% in water, **Sigma Aldrich**

Sodium borohydride, $\geq$ 98 %, **Sigma Aldrich**

Sulphuric Acid, $\geq$ 95 (w/w) %, **Fisher Scientific**

Titainia P.25, $\geq$ 99.5%, **Degussa**

Magnesium Oxide, **BDH**

Graphite, Powder (< 20 micron) synthetic, **Aldrich**

XC-72R, vulcan - powder, **CABOT**

Glycerol, $\geq$ 99 %, **SigmaUltra**

DL-Glyceraldehyde dimer, $\geq$ 97 %, **Sigma-Aldrich**

DL-Glyceric acid hemicalcium salt hydrate, $\geq$ 98 %, **Sigma-Aldrich**

Glycolic acid, $\geq$ 97 %, **Sigma-Aldrich**

1,3-Dihydroxyacetone acetone dimer, $\geq$ 97 %, **Sigma-Aldrich**

DL-Lactic acid, 85 (w/w) %, **Sigma**

Tartonic acid, $\geq$ 97 %, **Sigma-Aldrich**

β-Hydroxypyruvic acid, $\geq$ 95 %, **Sigma-Aldrich**

Oxalic acid, $\geq$ 98 %, **Sigma-Aldrich**

Formic acid, $\geq$ 96 %, **Sigma-Aldrich**

Furfural, $\geq$ 99 %, **Sigma-Aldrich**

Furfuryl Alcohol, $\geq$ 98 %, **Aldrich**

Furoic Acid, $\geq$ 98 %, **Aldrich**

Hydrogen Peroxide, 60 (w/w) % Aqueous

Sodium Hydroxide, $\geq$ 97% Powder, **Sigma-Aldrich**

Na_2SO_3, $\geq$ 98 %, **Sigma-Aldrich**

$NaNO_3$, $\geq$ 99 %, **Sigma**

2.2. Definitions

$$Conversion\ (\%) = \left(\frac{Moles\ of\ Substrate\ Converted}{Moles\ of\ Substrate}\right)\ x\ 100$$

$$Selectivity\ (\%) = \left(\frac{Moles\ of\ Product}{Moles\ of\ Substrate\ Converted}\right)\ x\ 100$$

$Carbon\ Balance\ (\%)$
$$= \left(\frac{Moles\ of\ Carbon\ Detected}{Moles\ of\ Carbon\ at\ the\ Beginning\ of\ the\ Reaction}\right)\ x\ 100$$

$$Turn\ Over\ Frequency\ (TOF) = \left(\frac{\left(\frac{Moles\ of\ Substrate\ Consumed}{Moles\ of\ Active\ Metal}\right)}{Time}\right)\ x\ 100$$

$$Reduction\ in\ Oxidation\ Activity\ (\%) = \left(\frac{TOF_{STANDARD} - TOF_{NEW}}{TOF_{STANDARD}}\right)\ x\ 100$$

$$Rate\ (K) = k \cdot cat \cdot [A]^a [B]^b [C]^c$$

$$Rate\ Constant\ (k) = Ae^{\frac{-Ea}{RT}}$$

2.3. Catalyst Preparation

The way in which a catalyst is prepared can greatly affect its performance. Typically, supported Au catalysts exhibit higher activities as particle size decreases[1, 2]. In addition, the Au particle size can also affect selectivity of the reaction as different size particles can promote different reaction pathways[3]. As a consequence, metal particle size is a key parameter which, if controlled correctly, has the potential to significantly enhance catalytic performance. Particle size is greatly affected by the catalyst preparation technique and thus it is crucial that the appropriate preparation technique is selected in order to obtain optimum catalyst performance

2.3.1. The Sol –Immobilisation Technique

The sol-immobilisation technique is a modern method for the preparation of highly dispersed supported metal nanoparticles. It involves the application of a stabilising agent to control and stabilise particle size. Typically, metal(s) are encapsulated with the stabilising agents and are subsequently reduced using a powerful reducing agent. In most cases, acidification of the solution is required in order to reduce the pH to a lower value than the isoelectric point of the support to ensure full metal immobilisation. This is generally not required with basic supports such as $Mg(OH)_2$ and ZrO_2. This preparation technique delivers supported metal nanoparticles which are finely dispersed and have exceptionally small size distributions[4-7]. A limitation of this technique is that the stabilising agent is often difficult to remove and can hinder the movement of a substrate in and out of the active site[8].

2.3.2. Conventional Sol-immobilisation

The following details the preparation of 1g of a 1 wt.% Au/TiO_2 catalyst by the conventional sol-immobilisation technique.

$HAuCl_4.3H_2O$ (0.8 mL, 12.5 g / L) was added to H_2O (400 mL) and stirred. To this solution, polyvinyl alcohol (1 wt.% solution, Aldrich, weight average molecular weight Mw ¼ 9000–10 000 g mol^{-1}, 80% hydrolysed) was added. Subsequently, $NaBH_4$ (0.1 M, $NaBH_4$/Au (mol/mol) = 5) was then introduced. After 30 minutes of sol generation, the colloid was immobilised by adding TiO_2 (0.99 g) and the solution was acidified to pH 1 (0.1 M, H_2SO_4) under vigorous stirring. After 1 h the slurry was filtered, the catalyst washed thoroughly with distilled water, and dried at 110 ºC for 16 h.

2.3.3. Modified Sol-Immobilisation

The immobilisation of Au can be problematic with some supports using the conventional sol-immobilisation technique; namely CeO_2 and graphite. For this reason, an alternative method of immobilising metal sols was created where Tetrakis(hydroxymethyl) phosphonium chloride (THPC) acts as both the stabilising agent and reducing agent. This method has also been shown to produce small nanoparticles with narrow particle size distributions[7]. The procedure for producing 1 g of a 1 wt.% Au/Graphite catalysts in this manor is displayed below.

Sodium hydroxide (2.4 mL, 0.2 M) and Tetrakis(hydroxymethyl)phosphonium chloride (1.427 mL of 10 % vol aqueous solution) were added to H_2O (47 mL) and stirred for 3 minutes. $HAuCl_4.3H_2O$ (0.8 mL, 12.5 g/L) was subsequently added and the solution was left to equilibrate for 0.5 h. Graphite (0.99 g) was added to the mixture and the solution was acidified to pH 1 (0.1 M, H_2SO_4) and left to stir for an additional 1 h. The catalyst was filtered, washed thoroughly and dried at 110 ºC for 16 h.

The sol-immobilisation technique can also be used to produce bi- and tri-metallic catalysts. Additional metals are added at the same stage as the Au. Bimetallic and trimetallic catalysts containing combinations of Au, Pd and Pt prepared this way are reported in the literature[4, 6, 9, 10].

2.3.4. Impregnation (IMP)

The impregnation technique is a quick and simple method for supporting metal nanoparticles. This method gives a reasonably broad particle size distribution. Impregnated catalysts typically provide their projected metal loadings but often require a post preparation treatment step in order to increase the support metal interaction. This additional heat treatment can cause particle agglomeration in some cases. Furthermore, due to the lack of particle size control, impregnated catalysts can often be difficult to reproduce. The procedure for producing a 0.5 g of a 1 wt.% Au/TiO_2 catalyst is given below.

TiO_2 (0.495 g) was inserted into a beaker (10 mL) attached with a magnetic stir bar. $HAuCl_4.3H_2O$ (0.4 mL, 12.5 g / L) and H_2O (1.6 mL) was subsequently added to the beaker and the solution was stirred slowly at 80 ℃. The consistency of the mixture is monitored and the beaker removed when a thick paste is formed. The paste was dried at 110 ℃ for 16 h and the subsequent material was finely ground and calcined at 400 ℃ under static air for 3 h with a ramp rate of 20 ℃ / min.

2.3.5. Modified Impregnation (Mod-IMP)

This technique for preparing AuPd nanoparticles was only recently discovered[11]. It offers the ability to prepare small nanoparticles containing Au and Pd, with no stabilising agent. The impregnation method is modified by using excess chloride during the preparation to provide more particle size control. This method for the preparation of 1 g of a 1 wt.% AuPd (molar) /TiO_2 is provided below.

To a 50 mL round bottom flask attached with a magnetic stir bar, $HAuCl_4.3H_2O$ (0.519 mL, 12.5 g / L) and $PdCl_2$ (0.585 mL, 6 g / L) was added. H_2O (14.896 mL) was subsequently added in order to bring the total volume of the flask up to 16 mL. The flask was immersed in an oil bath at room temperature and stirred vigorously. Over a period of 10 minutes, the temperature of the oil bath was raised to 60 ℃. Once the temperature had stabilised, TiO_2 (0.99 g) was added slowly to the mixture over an additional 10 minutes with constant stirring. Once this was complete, the slurry was stirred for a further 15 minutes. The temperature was raised to 95 ℃ and stirred for an additional 16 h. The solid powder was subsequently retrieved and ground to a fine powder. Following this, the catalyst was reduced at 400 ℃ for 3 h under a steady flow of 5% H_2 in air. The sample was heated at a ramp rate of 10 ℃ / min.

2.4.   Catalyst Evaluation

All catalyst testing was conducted for the development in understanding of two reactions:

(i)   The oxidation of glycerol

(ii)   The oxidation of furfural

Both chemicals are formed as products from the production of biofuels[12, 13]. Many modifications of the standard testing was conducted in order to gain further understanding of catalysts stabilities and the mechanistic features of each reaction. The standard reaction conditions are detailed below, along with the testing modifications of each reaction.

2.4.1.   Selective Oxidation of Glycerol

Reactions were carried out using a 50 mL Colover glass reactor. To this, glycerol (5 mL, 0.6 M in H_2O) and NaOH (5 mL, 1.2 M in H_2O) was added to the reactor vessel, sealed and the resulting solution was left for 5 minutes in order to reach the desired temperature (60 °C unless stated otherwise). The desired amount of catalyst (stated in the corresponding caption) was subsequently added to the solution. The reactor was purged three times and pressurised with O_2 (3 bar). The reaction mixture was stirred at 1200 rpm for a stated time. In some cases, reaction samples were taken from the reactor, after which the reactor was re-purged three times and pressurised with O_2 (3 bar). After the reaction was complete, the reactor vessel was cooled to room temperature and the final reaction sample was taken. All reaction samples were diluted 10 fold in H_2O, filtered and subsequently analysed by high performance liquid chromatography (HPLC).

The substrate was often exchanged for reaction products in order to assess how the catalysts affect them under these reaction conditions. For these tests, the exact same testing procedure was used with the 0.3 M solution of glycerol being substituted with a 0.3 M of a different compound.

2.4.2.   Glycerol Product Inhibition Studies

Reactions were carried out using a 50 mL Colover glass reactor. To this, 5 mL of a solution comprising of glycerol (0.6 M in H_2O) and the product (0.1 M in H_2O) under investigation was added. NaOH (5 mL, 1.2 M in H_2O) was subsequently added and the vessel was sealed and the resulting solution was left for 5 minutes under vigorous stirring (1200 rpm) in order

to reach the desired temperature (60 ℃ unless stated otherwise). The desired amount of catalyst (stated in the corresponding caption) was subsequently added to the solution. The reactor was purged three times and finally pressurised with O_2 (3 bar pressure). The reaction mixture was stirred at 1200 rpm for a stated time. In some cases, reaction samples were taken from the reactor after which, the reactor was re-purged three times and pressurised with O_2 (3 bar). After the reaction was complete, the reactor vessel was cooled to room temperature and the final reaction sample was taken. All reaction samples were diluted 10 fold in H_2O, filtered and subsequently analysed by HPLC.

2.4.3. Radical Testing in the Oxidation of Glycerol

Reactions were carried out using a 50 mL Colover glass reactor. The glycerol solution (0.3 M in H_2O and NaOH–glycerol ratio = 2, mol/mol) was added to the reactor. An additional, Na_2SO_3 (10 mg) or $NaNO_3$ (10 mg) was added and the resulting solution was left for 5 minutes in order to reach the desired temperature (60 ℃ unless stated otherwise). The desired amount of catalyst (stated in the corresponding caption) was subsequently added to the solution. The reactor was purged three times with O_2 and finally pressurised to 3 bar. The reaction mixture was stirred at 1200 rpm for a stated time. In some cases, reaction samples were taken from the reactor, after which the reactor was re-purged three times and pressurised with O_2 (3 bar). After the reaction was complete, the reactor vessel was cooled to room temperature and the final reaction sample was taken. All reaction samples were diluted 10 fold in H_2O, filtered and subsequently analysed by HPLC.

2.4.4. The Selective Oxidation of Furfural

Reactions were carried out using a 50 mL Colover glass reactor. An oil bath was heated to the desired temperature (30 ℃ unless stated otherwise) and left to stabilize for 30 minutes. The desired amount of catalyst (stated in the corresponding caption) was added to the reactor with NaOH (5 mL, 0.3 M in H_2O) and H_2O (4.752 mL). The resulting solution was stirred at 1000 rpm for 5 minutes. Furfural (0.248 mL) was added under continuous stirring so that the total concentration of furfural in solution equated to approximately 0.3 M. Subsequently, the reactor was purged three times and pressurized with O_2 (3 bar pressure). In some cases, reaction samples were taken from the reactor, after which the reactor was

re-purged three times and pressurised with O_2 (3 bar). All reaction samples were diluted 10 fold in H_2O, filtered and subsequently analysed by HPLC.

2.4.5. The Selective Oxidation of Furfural Alcohol

Reactions were carried out using a 50 mL Colover glass reactor. An oil bath was heated to the desired temperature (30 ℃ unless stated otherwise) and left to stabilize for 30 minutes. The desired amount of catalyst (stated in the corresponding caption) was added to the reactor with NaOH (5 mL, 0.3 M in H_2O) and H_2O (4.74 mL). The resulting solution was stirred at 1000 rpm for 5 minutes. Furfural (0.260 mL) was added under continuous stirring so that the total concentration of furfural in solution equated to approximately 0.3 M. Subsequently, the reactor was purged three times and pressurized with O_2 (3 bar pressure). In some cases, reaction samples were taken from the reactor, after which the reactor was re-purged three times and pressurised with O_2 (3 bar). All reaction samples were diluted 10 fold in H_2O, filtered and subsequently analysed by HPLC.

2.4.6. Short Term Sampling Experiments

In order to determine the reaction orders, rate constants and activation energies for the catalytic oxidations of furfural and furfuryl alcohol, short term reaction sampling was conducted in order to monitor the reactions progress at low substrate conversions. The same experimental procedures were used (detailed above), however, samples were taken every 5 minutes. The reactor was subsequently purged three times and charged with O_2 (3 bar) after each sample was taken.

2.5. Catalyst Stability

The stability of a catalyst is a crucial factor to consider when assessing its industrial viability. Some supported metal nanoparticles are susceptible to leaching, particularly in the liquid phase[14]. The preparation technique and post preparation heat treatment of the catalyst can increase the metal-support interaction and consequently reduce or even prevent metal leaching.

2.5.1. Microwave Plasma Atomic Emission Spectroscopy (MP-AES)

Atomic Emission Spectroscopy (AES) has been widely used for obtaining quantitative elemental analysis of liquid phase samples for a number of years. The principle is simple; as a given element is exposed to an influx of energy, its valence electrons undergo transitions to higher energy levels. When these excited electrons relax, they emit light and the spectral lines observed are indicative of the unique electronic transitions of a given element.
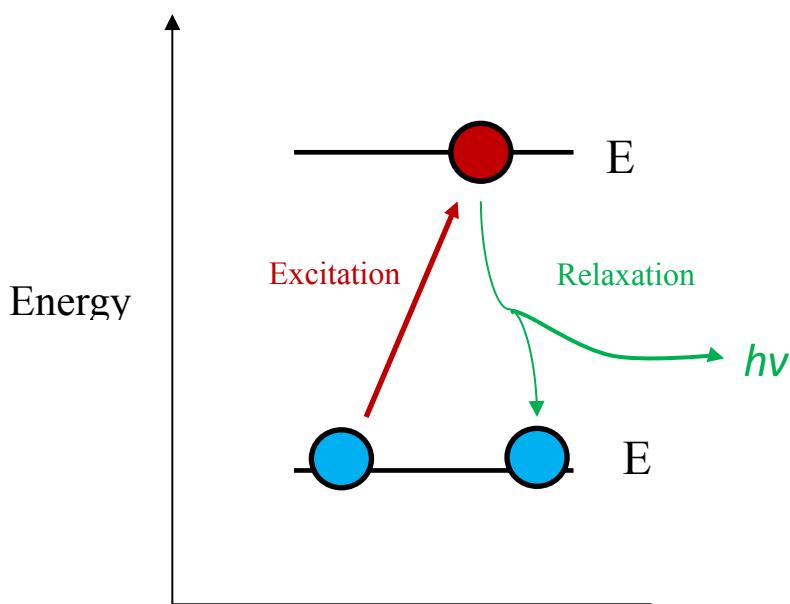
Figure 2.1. Diagram representing the process responsible for photon emission.

MP-AES utilizes this theory as a method of obtaining quantitative elemental analysis of liquid phase samples to an exceptional degree of accuracy. Nitrogen is fed through a water trap and gas filter to the torch, where microwave radiation heats the gas to approximately 5000 °C. Under these conditions, the nitrogen is broken down and ionised forming a stream of nitrogen plasma. Upon exposure to this plasma, elements are atomised and their electrons are excited and subsequently relax emitting photons with defined energies and wavelengths which are characteristic of each element. Mirrors surrounding the torch chamber collect and focus the emitted light onto a monochromatic detector.

MP-AES is an exceptionally useful tool for the study of heterogeneous catalyst. Information regarding metal loadings, elemental ratios, metal leaching and even catalytic poisons can be determined using this technique.

Experimental

Procedure for the elemental analysis of an Au/TiO$_2$ catalyst is displayed below.

The analysis was conducted using an Agilent 4100 MP-AES. Au content was analysed using two emission lines. A known mass of Au/TiO$_2$ was added to aqua regia solution (2 % in H$_2$O, 50 mL) and left to digest overnight. The samples were filtered using PTFE filters (Acrodisc PVDF 0.45 μl). Samples were introduced into a stream of nitrogen plasma *via* a single pass spray chamber at a pressure of 120 kPa in the absence of any air injection. The instrument was calibrated with 2.5 ppm, 5 ppm and 10 ppm of Au standards. Samples were tested three times and an average of the three results was taken.

2.5.2. Catalyst Re-usability Tests

Reusability experiments were conducted as a method of investigating whether the catalyst performance changed in subsequent tests. Multiple tests were conducted under standard reaction conditions and the catalyst was recovered from each reactor. The catalysts were dried in at 110 ℃ for 16 h and subsequently combined and retested under the standard reaction conditions.

2.6. Product Analysis

There are multiple methods which can be used to analyse the contents of aqueous solutions. HPLC was the primary method used for analysis of reaction samples in this work.

2.6.1. High Performance Liquid Chromatography (HPLC)

HPLC allows for the separation of poorly volatile samples. The technique is based on the fundamental principles associated with product separation in organic synthesis; using silica

columns. The technique allows for accurate quantitative analysis of a liquid phase solution and is made up of two fundamental constituents; the mobile phase and stationary phase. A schematic diagram shown in Figure 2.2 is a diagrammatic representation of a HPLC detailing its key components.
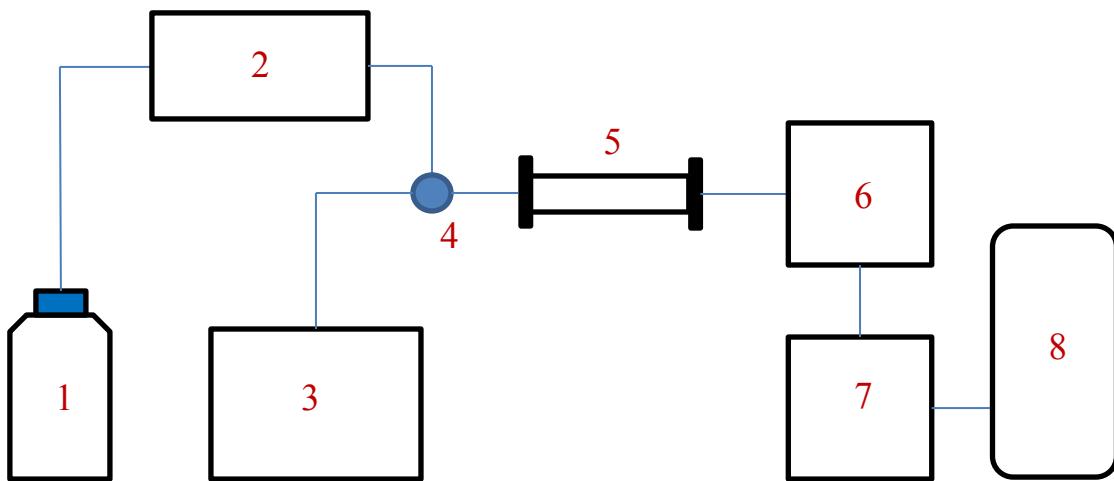
Figure 2.2. Schematic diagram for the HPLC used to analyse the reaction effluents of the catalytic reactions. 1. Solvent reservoir, 2. HPLC Pump, 3. Autosampler, 4. Rheodyne valve, 5. Column, 6. Refractive Index detector, 7. Diode array detector, 8. Data acquisition.

The solvent reservoir is where the mobile phase is stored. Multiple solvents may be applied as the mobile phase and the selection is crucial to obtaining accurate quantitative data. When multiple solvents are used, the mobile phase can be either gradient (composition of solvents changes with time) or isocratic (composition of solvents is kept constant) in nature. The HPLC pump is required to withstand very high pressures and controls the flow of the mobile phase throughout the system. It is important that the flow rate is controlled to a high level of accuracy in order to maintain consistent retention factors. The auto-sampler is responsible for introducing the sample into the mobile phase. The volume injected must be consistent as it could severely influence the accuracy of results in the absence of an internal or external standard.

Once the sample is introduced into the mobile phase, it is pumped into the column. There are many different types of HPLC columns and the selection can be dependent on the given reaction. The columns consist of the stationary phase which is generally made of silica based microporous materials, polymers or gels. Interactions between the mobile phase and the stationary phase play a role in attaining consistent and accurate results. As the mobile phase is passed into the column, compounds from the sample interact and equilibrate with the stationary phase, leading to differing retention times. Once, they pass out the column they are carried in the mobile phase to the detectors.

There are many different detectors used in HPLC. The choice of which, is dependent on the nature of the samples and mobile phase. The two detectors which were used in this were work were a refractive index detector (RID) and a diode array detector (DAD). The column eluent is first fed through to the RID into a sample cell, where it is passed over a beam of light. The refractive index of the mobile phase is subsequently measured. The greater the difference in the RI of the sample and mobile phase, the higher the observed sensitivity.
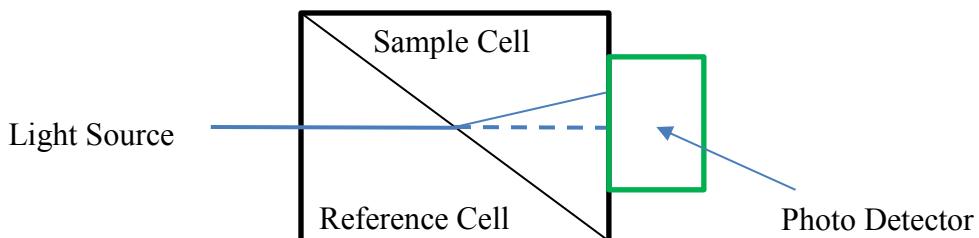
Figure 2.3. Schematic representation of a refractive index detector.

The primary advantage of using an RID is that it has a universal response. Every liquid phase species will refract light to some extent. Unfortunately, sensitivity can be an issue, which can limit its accuracy when compared against other detectors. For this reason, it is better to use RID's in combination with an additional source of detection.

DAD detectors can detect ultra-violet and visible light at the same time. The detector allows for the 3-dimensional projection of products. A beam of light from the deuterium and quartz halogen lamps is passed over a sample in the reference cell. Here, the absorbance of light is monitored and the greater the absorbance, the higher the sensitivity. DAD detectors give significantly higher sensitivities than RID's. However, the samples must consist of molecular components, which absorb light. For this reason, detection is limited to compounds containing unsaturated, aromatic or carbonyl compounds.

To monitor the oxidation of glycerol and furfural a HPLC fixed with RID and DAD detectors was used. The experimental details are displayed below;

Experimental

The analysis was carried out using HPLC with ultraviolet and refractive index detectors. Reactants and products were separated using a Metacarb 67 H column. The eluent was an aqueous solution of H_3PO_4 (0.01 M) and the flow was 0.25 ml min^{-1}. Samples of the reaction mixture (0.5 ml) were diluted (to 5 ml) using the eluent. Products were identified by comparison with authentic samples. For the quantification of the amounts of reactants consumed and products generated, an external calibration method was used.

2.7.   Catalyst Characterisation

There are numerous different analytical and spectroscopic techniques which can provide qualitative data of a given material. For the study of heterogeneous catalysts, these tools are crucial in correlating physical properties with activity.

2.7.1.   X-ray photoelectron Microscopy (XPS)

The fundamental principles of XPS are based on the photoelectric effect, where photons are absorbed by atoms resulting in the subsequent ejection if a photoelectron. The kinetic energy (KE) of the ejected photoelectron can be expressed as a function of the binding energy of ejected atom (E_b) and the energy of the photon (hv).

$$KE = hv - E_b$$

XPS can provide the user with information regarding the oxidation states of a given materials elemental components. It can also provide quantitative data associated with the elemental makeup of the materials surface.
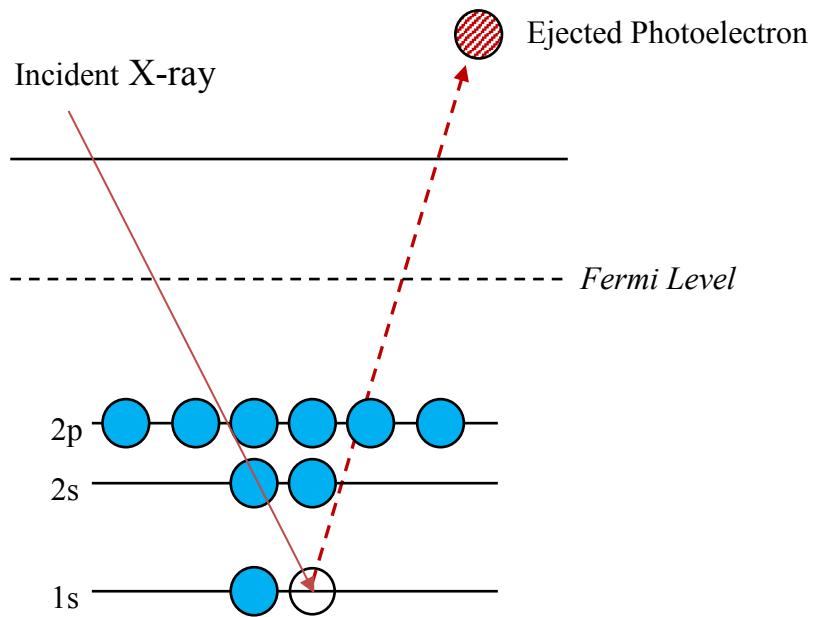
Figure 2.4. Depicts the ejection of a photoelectron by X-ray radiation

Following this process, the atom relaxes and one of two things occurs: (i) The vacancy is filled as a result of fluorescence or (ii) the emission of auger electrons occurs. Auger electrons are emitted as a result of an electron from a higher energy level filling the lower energy vacancy. Auger effects are observed less commonly with heavy elements as a result of larger discrepancies in energy between the core electron vacancy and the outer shell electrons.

For this work, Al Kα X-rays are fired at the surface of a catalyst in order to obtain information regarding its elemental constituents and their respective oxidation states. The ejected electrons are subsequently collected and their respective KE's are measured. By using a modified version of the given equation which includes the work function of the XPS, it is possible to accurately determine the E_b of each electron emitted and thus receive quantitative data of the nature of the catalysts surface. By looking closely at the binding energies of the elements, it is possible to derive the relative oxidation states of the samples elemental components. The energy states of a given atom change depending on its oxidation state. This is a result of the altered attractive force exerted by the nucleus with differing quantities of orbiting electrons. Fewer electrons results in a higher attractive force

experienced by the other electrons which ultimately, leads to a shift in the atomic binding energies.

Experimental

All the catalysts assessed using XPS in this thesis were characterised at the Cardiff University XPS centre by Dr David Morgan. A VG EscaLab 220i spectrometer equipped with an AlKα X-ray 300 W source was used for this work. The relative binding energies were standardised against a C 1 s reference (284.7 Ev).

2.7.2. Powder X-ray Diffraction (XRD)

XRD is a powerful analytical technique, which is primarily used for the identification of crystalline materials. This technique is typically used as a method of obtaining information regarding the bulk structure of materials such as phase identification, determination of unit cell dimensions and crystallite size and quality[16].
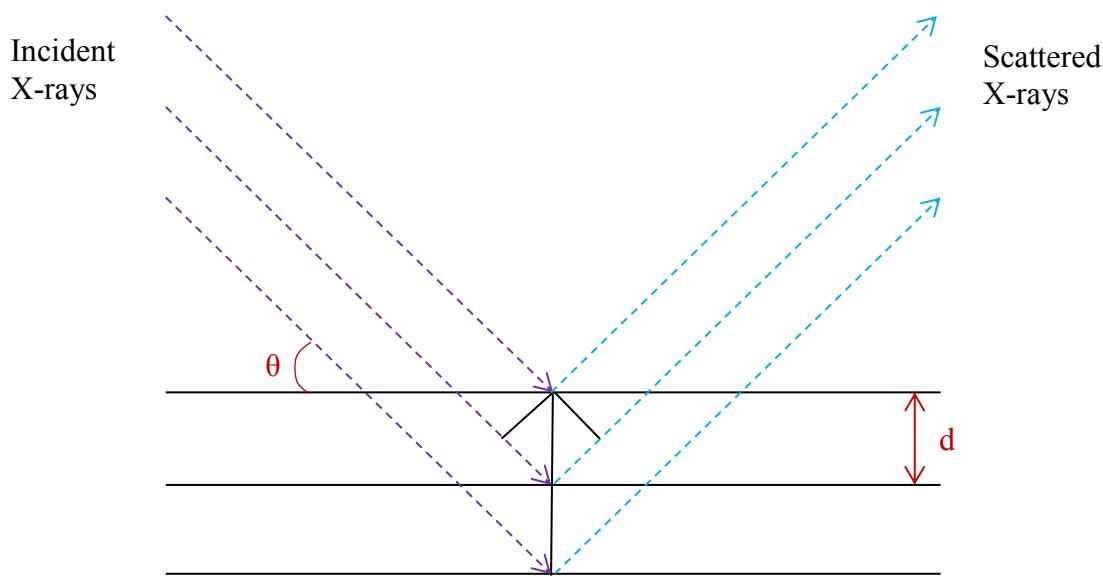
Figure 2.5. As incident X-rays contact a surface they are elastically scattered. The Bragg law can be used to identify the lattice spacing (d) using the angle (θ) and wavelength (λ) of the incident radiation.

X-rays are produced through the bombardment of a copper target with high energy electrons. Electrons within the copper are excited to high energy levels. As they relax, energy is emitted as Kα and Kβ X-rays. Kβ electrons are omitted using a filter leaving only the Kα radiation. These X-rays are focussed onto the sample and elastically scattered by the respective atoms. The scattered radiation can undergo either constructive or destructive interference. The angle of the X-ray source changes from 10 ° to 80 ° during the run. Constructive interference gives high intensity reflections which gives information regarding the long term order of the crystalline structure. Poorly crystalline samples give significantly more destructive interference. All the scattered radiation is collected using a moving detector.

Bragg's law is used to calculate the lattice spacing (d) within a sample by unifying the wavelength of X-rays (λ), the order of the reflection (n) and the angle between the incident x-rays and the normal plane in one equation.

$$n\lambda = 2d \sin \theta$$

Bragg Law: Method for obtaining lattice parameters of a given powder XRD.

The crystallinity of the sample can be assessed by looking at the full width half max (FWHM) of the most intense peaks. Highly crystalline solids with good long-term order will exhibit sharp narrow diffraction peaks whereas solids consisting of poor morphologies will give less intense, broader peaks. The Scherrer equation is a further tool which can be used for assessing the morphologies of crystalline solids using XRD. This equation allows for the accurate determination of the crystallite size (τ)

$$\tau = \frac{K\lambda}{\beta \, COS \, \theta}$$

Scherrer Equation: Method for the derivation of crystallite sizes in conjunction with powder XRD.

Experimental

Powder X-ray diffraction (XRD) was conducted using a PANalytical X'Pert Pro system fitted with a CuKα X-ray source run at 40 kV and 40 mA. An X'Celerator detector was used in order to assess the scattered media. Each sample was scanned from $2\theta = 10$ º to 80 º for 30 minutes. Catalysts were ground into a fine powder and loaded onto a silicon wafer. The corresponding results were compared directly with the data held in the ICDD library.

2.7.3. Transmission Electron Microscopy (TEM)

Electron microscopes are powerful tools which use accelerated electrons to construct 2D images of small areas with exceptional resolution. Such properties are of great use for investigating the surface of catalytic materials and can give a significant amount of information regarding particles size, metal distribution and dispersion. A schematic diagram of a typical transmission microscope is displayed in Figure 2.6. A schematic diagram of a conventional electron microscope.

Conventional TEMs provide exceptional magnification and resolution. An extremely high voltage of electricity is required in order to adequately activate the cathode in the electron gun. The heated filament generates a high energy beam of electrons which are passed through electromagnetic coils on their way to the sample. The first electromagnetic coil is responsible for focussing the electron beam into a thin direct stream of electrons and the second focussed the beam onto a small selected area of the sample. The sample sits on a thin copper holder and the electron beam passes straight through both. The electrons subsequently pass through a projector lens and onto a fluorescent screen which projects the image of the surface.

There are numerous modifications of conventional TEM's which are now operational such as HAADF and TEM-EDX. These modifications have allowed for even greater qualitative analysis of heterogeneous catalysts.

Experimental

Transmission electron microscopy (TEM) was conducted using an Ieol 2100 fixed with a LaB$_6$ filament operating at 200 KV. Powdered catalyst samples were dispersed in ethanol and dropped onto lacey carbon films over a 300 mesh copped grid.
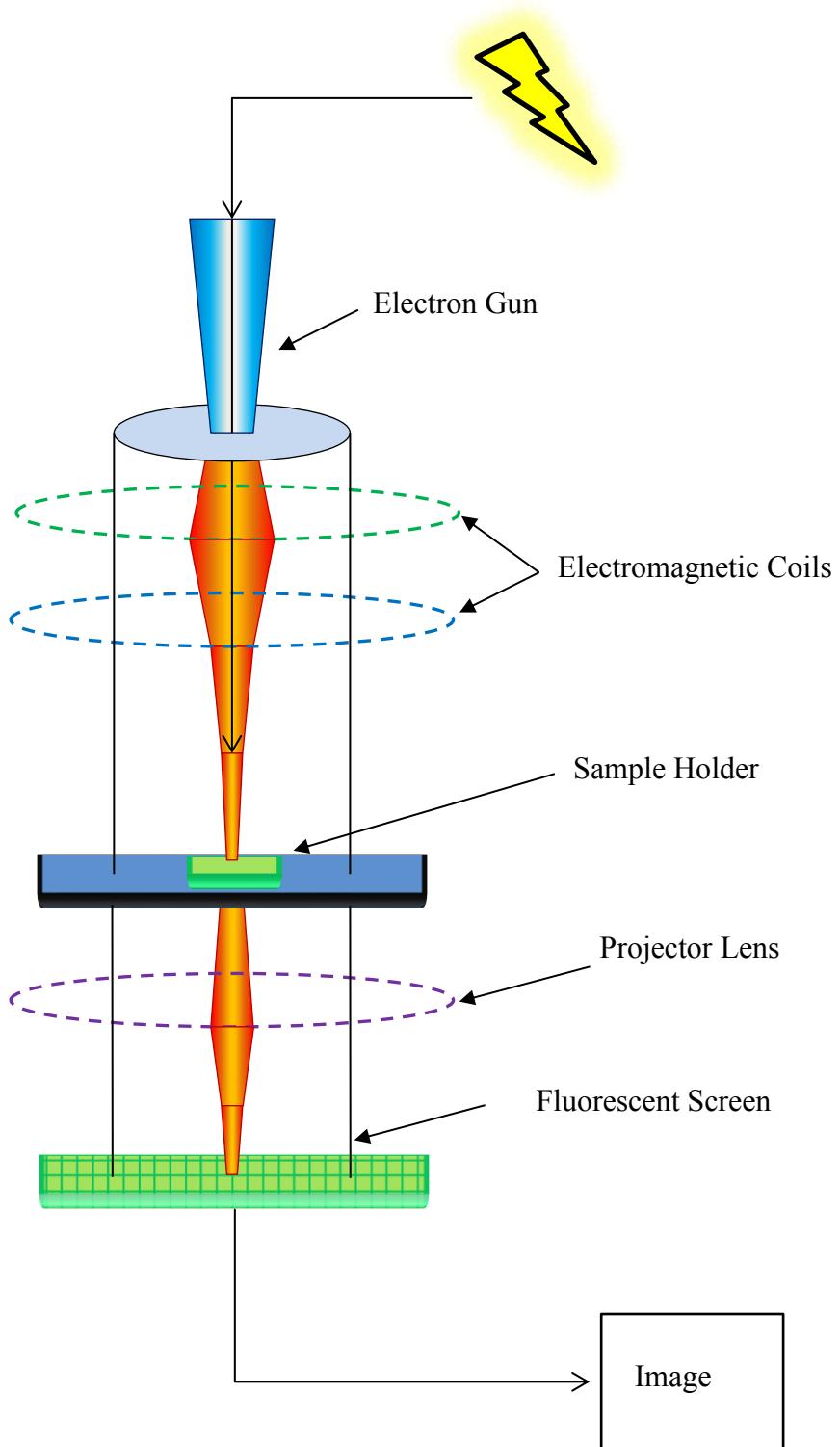
Figure 2.6. A schematic diagram of a conventional electron microscope.

2.7.4. Thermogravimetric Analysis (TGA)

TGA is a useful technique, which monitors the weight of a given sample as a function of temperature and/or time under controlled atmospheric conditions. It can provide a range of information regarding phase transitions such as adsorption, desorption, vaporisation and sublimation. In addition, it can allow for the determination of chemical phenomena such as oxidations/reductions, chemisorptions, decompositions and dehydrations. TGA can be an exceptionally useful tool for the characterisation of catalytic materials. A schematic diagram of a typical TGA is displayed below.

Various modifications of TGA are available with additional equipment attached to enhance its applications. TGA are often fitted with mass spectrometers which aid the determination of the gasses lost.
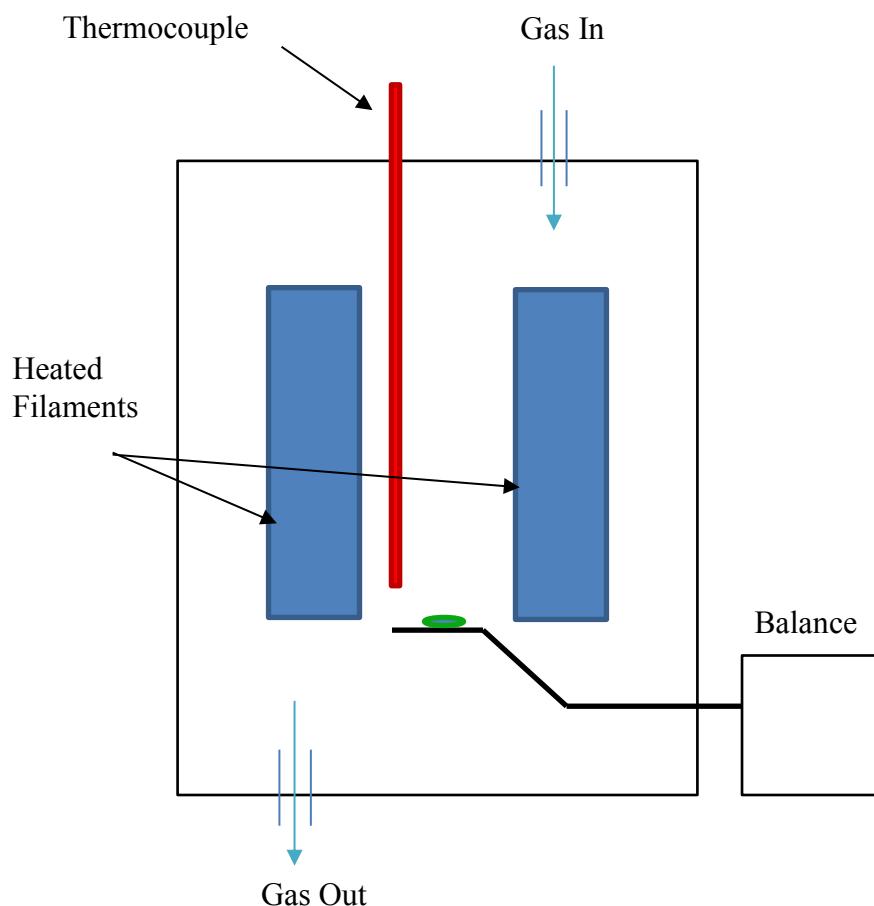
Figure 2.7. A schematic diagram of a conventional TGA set-up

Experimental

TGA was conducted using a Setram Labsys TGA/DTA instrument. Catalyst samples were heated from 30 to 800 ℃ under flowing air (15 mL min^{-1}) at a heating rate of 10 ℃ per minute. The change in the mass of the catalyst was monitored with increasing temperature.

2.8.   <u>References</u>

1.   M. Haruta and M. Date, *Applied Catalysis A-General*, 2001, **222**, 427.

2.   A. Wolf and F. Schuth, *Applied Catalysis A-General*, 2002, **226**, 1.

3.   S. L. Chen, L. F. Luo, Z. Q. Jiang and W. X. Huang, *ACS Catalysis*, 2015, **5**, 1653.

4.   S. A. Kondrat, P. J. Miedziak, M. Douthwaite, G. L. Brett, T. E. Davies, D. J. Morgan, J. K. Edwards, D. W. Knight, C. J. Kiely, S. H. Taylor and G. J. Hutchings, *Chemsuschem*, 2014, **7**, 1326.

5.   J. A. Lopez-Sanchez, N. Dimitratos, P. Miedziak, E. Ntainjua, J. K. Edwards, D. Morgan, A. F. Carley, R. Tiruvalam, C. J. Kiely and G. J. Hutchings, *Physical Chemistry Chemical Physics*, 2008, **10**, 1921.

6.   N. Dimitratos, J. A. Lopez-Sanchez, D. Morgan, A. F. Carley, R. Tiruvalam, C. J. Kiely, D. Bethell and G. J. Hutchings, *Physical Chemistry Chemical Physics*, 2009, **11**, 5142.

7.   F. Porta, L. Prati, M. Rossi, S. Coluccia and G. Martra, *Catalysis Today*, 2000, **61**, 165.

8.   I. Gandarias, P. J. Miedziak, E. Nowicka, M. Douthwaite, D. J. Morgan, G. J. Hutchings and S. H. Taylor, *Chemsuschem*, 2015, **8**, 473.

9.   Q. He, P. J. Miedziak, L. Kesavan, N. Dimitratos, M. Sankar, J. A. Lopez-Sanchez, M. M. Forde, J. K. Edwards, D. W. Knight, S. H. Taylor, C. J. Kiely and G. J. Hutchings, *Faraday Discussions*, 2013, **162**, 365.

10.   G. L. Brett, Q. He, C. Hammond, P. J. Miedziak, N. Dimitratos, M. Sankar, A. A. Herzing, M. Conte, J. A. Lopez-Sanchez, C. J. Kiely, D. W. Knight, S. H. Taylor and G. J. Hutchings, *Angewandte Chemie-International Edition*, 2011, **50**, 10136.

11.   M. Sankar, Q. He, M. Morad, J. Pritchard, S. J. Freakley, J. K. Edwards, S. H. Taylor, D. J. Morgan, A. F. Carley, D. W. Knight, C. J. Kiely and G. J. Hutchings, *ACS Nano*, 2012, **6**, 6600.

12.   F. R. Ma and M. A. Hanna, *Bioresource Technology*, 1999, **70**, 1.

13.   A. Bohre, S. Dutta, B. Saha and M. M. Abu-Omar, *ACS Sustainable Chemistry & Engineering*, 2015, **3**, 1263.

14.   R. Redon, N. G. G. Pena and F. R. Crescencio, *Recent Patents on Nanotechnology*, 2014, **8**, 31.

15.   P. Atkins, W. and J. Paula, D., Oxford University Press, 6 edn., 2012.

16.   W. Niemantsverdriet J, John Wiley & Sons, 3 edn., 2008.

Chapter 3

The Selective Catalytic Oxidation of Glycerol

3.1. Introduction

Glycerol is a C_3 polyol produced as major co-product from the transesterification of 1st generation bio-fuel feedstocks[1]. Each carbon atom is bound to a hydroxyl group which gives it great potential for exploitation as a platform chemical. For this reason, the selective oxidation of glycerol over heterogeneous catalysts has long been a subject of scientific interest[2, 3]. It has been determined that the choice of catalyst[4], the size of the metal nanoparticles[5] and the reaction conditions[6, 7] can all significantly influence the selectivity and the rate of the reaction.
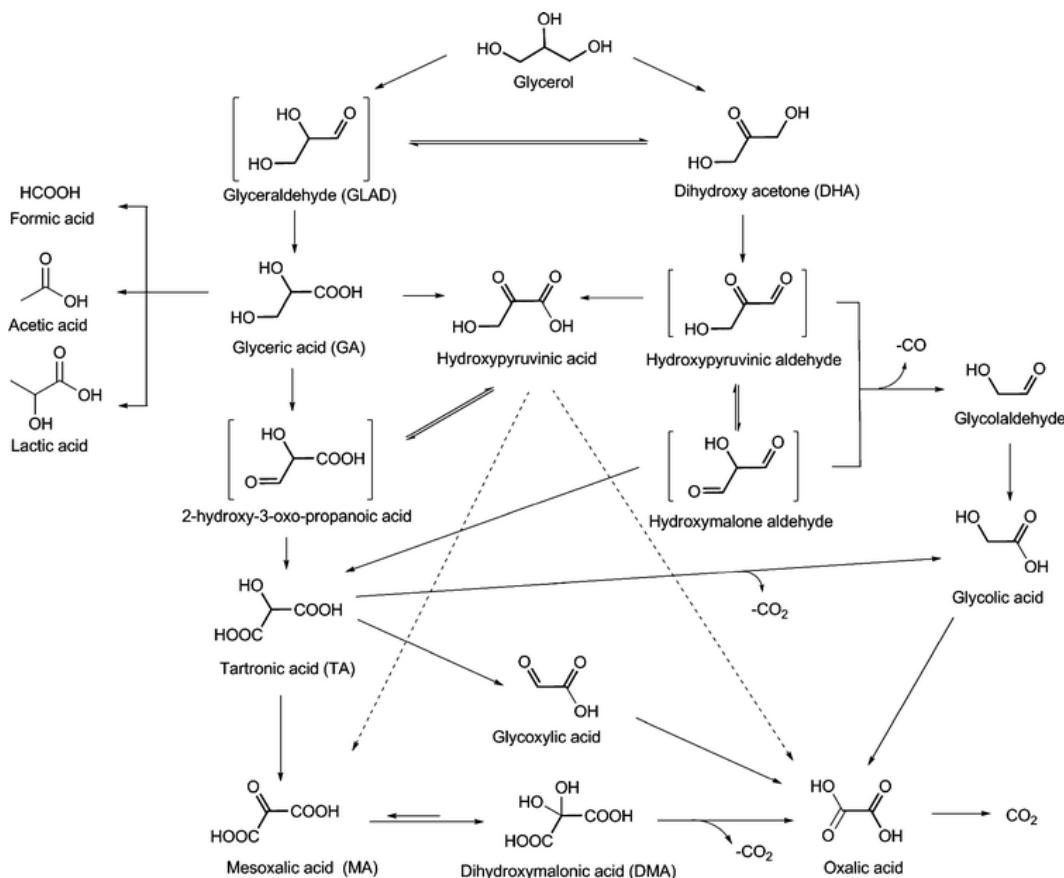

Figure 3.1. A scheme detailing the products which can be formed from the oxidation of glycerol. This scheme has been republished[8] with permission from the RSC.

Figure 3.1 shows the large distribution of products which can be formed from the oxidation of glycerol. The application of heterogeneous catalysts for this process allows for an additional avenue to control reaction selectivity. Prati and co-workers were the first to demonstrate that supported Au catalysts were active for the selective oxidation of glycerol[9]. Since then, it has been discovered that alloying Pd[6, 10, 11] and Pt[12, 13] into the supported Au nanoparticles can significantly enhance catalytic performance. A number of different products can be formed from the catalytic oxidation of glycerol. C_3 products such as lactic acid (LA), glyceric acid (GA) and tartronic acid (TA) are considered to be the most desirable oxidation products, and as a consequence, avoiding C-C cleavage is crucial. It is believed that this unfavourable cleavage is a result of the in-situ production of H_2O_2 from the reduction of O_2 by H_2O on the catalysts surface[14-16]. The application of hydrophobic materials as supports for the metal nanoparticles has been shown to reduce this unfavourable cleavage[4, 17].

It has been determined that the reaction conditions can significantly influence the product selectivity and rate of the reaction. Increasing the reaction temperature has been found to increase the C_3 selectivity[7, 18, 19]. It was suggested that this was a result of the decreased stability of H_2O_2 at elevated temperatures. Increasing the pH of the aqueous reaction medium was also found to increase the C_3 selectivity[19]. It was postulated that the observed reduction in C-C cleavage was a result of the base facilitating the decomposition of H_2O_2. In addition, the presence of a sacrificial base has also been found to increase the rate of the reaction. It was proposed that the presence of base significantly increases the initial deprotonation reaction to produce the corresponding alkoxide[14]. From an industrial perspective, base free oxidation is more desirable as it reduces reagent costs and would not require any additional purification steps. There have been a number of publications investigating the oxidation of glycerol under base free conditions[13, 20-22]. It has not yet however, been possible to replicate the high rates observed under basic reaction conditions[4]. O_2 is considered to play a pivotal role in the activation of the catalyst[23] however it is also believed to be involved in the production of H_2O_2. Therefore as a result, varying the O_2 concentration could generate a trade-off between reaction rate and C_3 product selectivity.

It is clear that there are two fundamental areas in the literature that require attention:

(i)   Oxidation of glycerol under base free conditions

(ii)   Determination of the route(s) to the unfavourable C-C cleavage

The research in this chapter is focussed towards resolving these current issues.

3.2. Aims and Objectives of the Project

3.2.1. Objective

Investigate the role of Au supported heterogeneous catalysts for the selective oxidation of glycerol. Emphasis is placed on the oxidation of the substrate under base free conditions and for its selective oxidation to produce C_3 products.

3.2.2. Aims

- Assess how the experimental conditions affect the performance of a 1 wt.% $AuPt/TiO_2$ catalyst for the selective oxidation of glycerol.

- Develop a greater understanding of the reaction profile in the presence of a 1 wt.% $AuPt/TiO_2$ catalyst.

- Investigate the oxidation of glycerol under base free conditions using mono-, bi- and trimetallic heterogeneous catalysts containing Au, Pd and Pt.

- Attempt to determine the factor(s) which lead to the unfavourable C-C cleavage. Investigate whether modification of the catalyst can reduce this unfavourable transformation.

3.3. A Benchmark Catalyst for the Selective Oxidation of Glycerol

AuPt alloys have been found to be highly active for the oxidation of glycerol on a range of different supports[18, 24, 25]. For this reason, a 1wt.% AuPt/TiO$_2$ catalyst was prepared by the conventional sol-immobilisation method[26] using PVA as the stabiliser. The catalyst was tested under standard reaction conditions and the corresponding reaction profile is displayed in Figure 3.2.
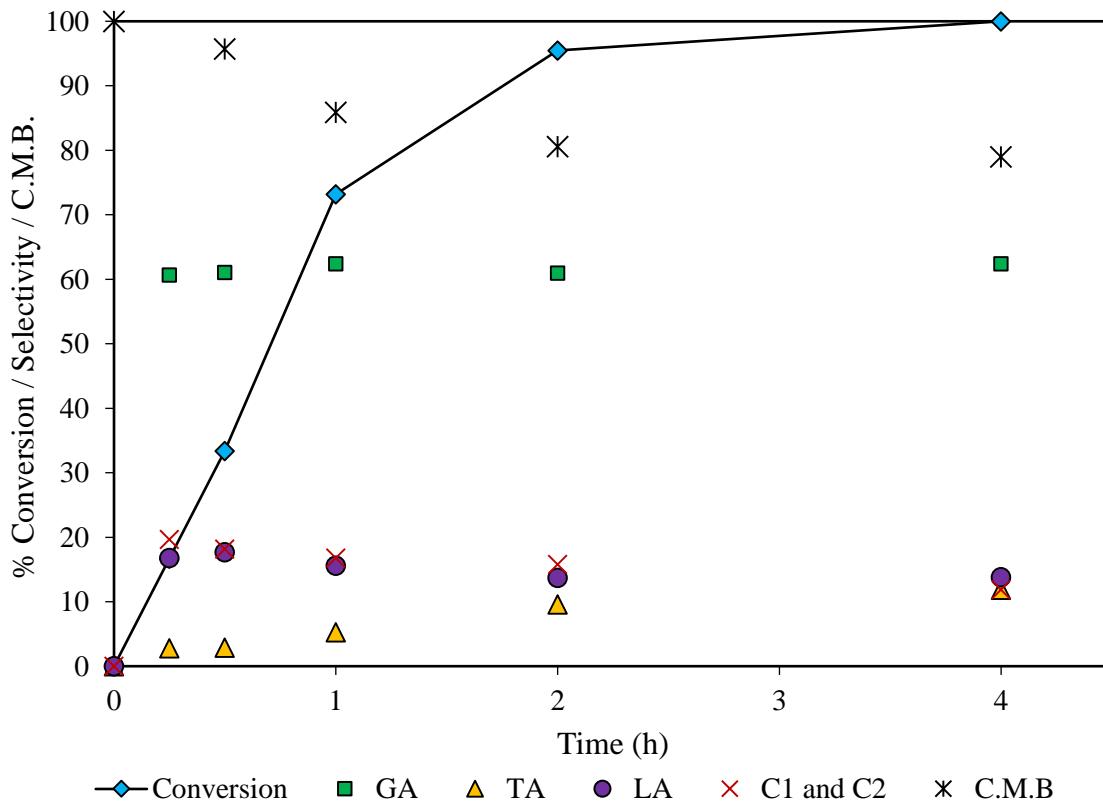
Figure 3.2. Time online profile for the oxidation of glycerol over the 1 wt.% AuPt/TiO$_2$ catalyst. **Reaction conditions:** 10 mL, glycerol (0.3 M), NaOH (0.6 M), substrate:metal ratio = 2000, 60 °C, 4 h.

The consumption of glycerol appears to be fairly controlled, the rate of which appears to slow with its diminishing concentration. GA appears to be the favoured product across the reaction. The selectivity towards TA gradually increases as the reaction proceeds with time which is likely a result of the sequential oxidation of GA. It is thought that the formations of all the above products proceed through either dihydroxy acetone (DHA) or

68

glyceraldehyde (GLAD), but these two products have never been observed when reactions have been carried out in a basic reaction medium. The selectivity to LA and C-C cleavage products appears to be at a peak at 0.25 h. This may suggest that the formation of these products comes predominantly from the rapid base catalysed consumption of DHA and GLAD. It is possible that the C-C cleavage is a result of GLAD undergoing Dakin Oxidation. These reactions typically involve the elimination of a terminal carbonyl group with an electron rich migrating group in the presence of H_2O_2 and base. It is possible that the catalyst is acting as an electron rich sink, hereby allowing the Dakin Oxidation to proceed. To my knowledge, the link between C-C cleavage and Dakin Oxidation has never been made in the catalytic liquid phase oxidation of alcohols.

The 1 wt.% AuPt/TiO$_2$ catalyst was subsequently characterised by XPS and the resulting spectrum is displayed in Figure 3.3.
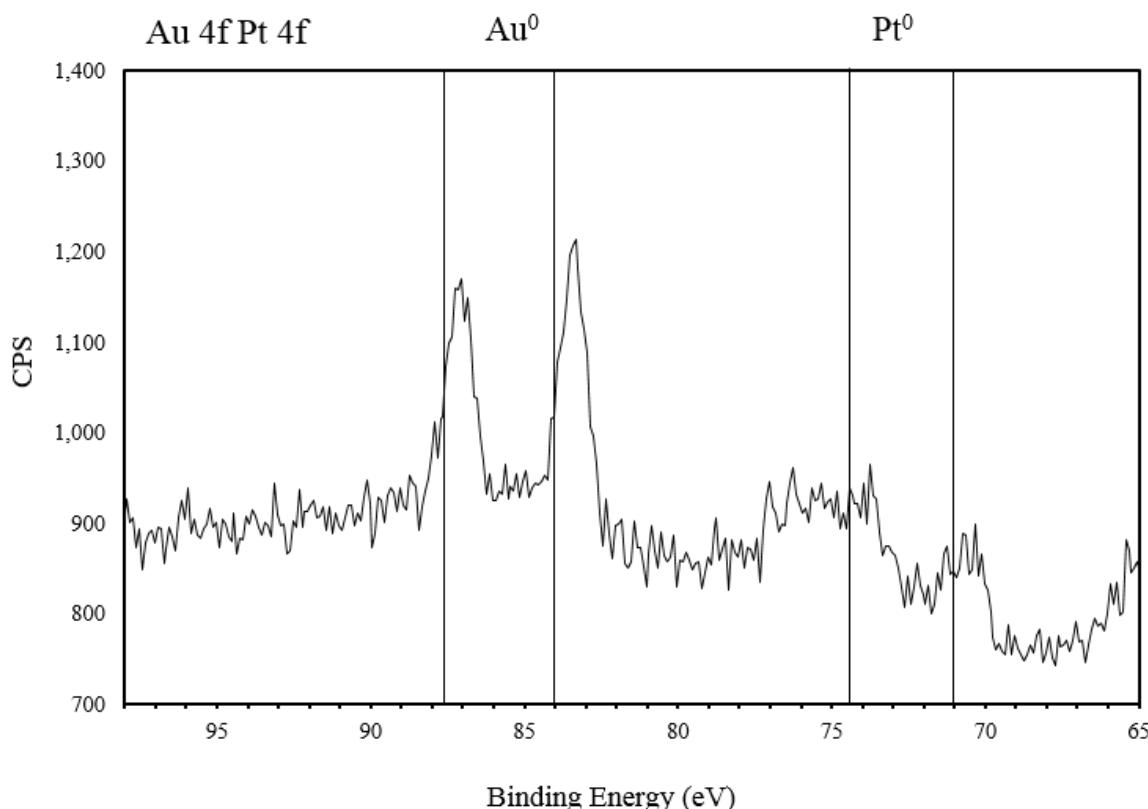
Figure 3.3. XPS spectrum of Au 4f and Pt 4f regions for the 1 wt.% AuPt/TiO$_2$ catalyst.

The XPS spectra shown in Figure 3.3 suggests that Au and Pt are present in their metallic states. This is typical of supported Au and Pt catalyst prepared by the sol-immobilisation

technique[13]. The peaks at 83.2 and 87.1 eV correspond to the $Au4f_{7/2}$ and $Au4f_{5/2}$ species associated with Au^0. This is unusual as the $Au4f_{7/2}$ peak associated with Au^0 is typically observed at a binding energy of 84.0 eV[27]. This downward shift in binding energy has previously been observed with Au/TiO_2[28] and was attributed to the interaction of metallic Au clusters with surface Ti^{3+} centres at defects in the TiO_2[28, 29]. Other studies have suggested that the downward shift in binding energy is evidence of AuPt alloy structures[30]. The evaluation of the Pt4f spectrum was difficult as the region was partially overlapped by the Ti3s satellite peak[31]. Nevertheless, careful extraction of this peak allowed for the determination of the peaks associated with the Pt^0 state. The peaks associated with $Pt4f_{7/2}$ and $Pt4f_{5/2}$ were observed at binding energies of 71.0 and 74.4 eV and are typical of the binding energies associated with Pt^0 [32, 33].

In order to investigate the metal loading of the catalyst, MP-AES analysis was conducted to determine the metal loading of Au and Pt.

Table 3.1. The total metal loading and ratio of Au and Pt determined using MP-AES.

	Total Metal Loading (%)	Au (molar %)	Pt (molar %)
$AuPt/TiO_2$	0.77	54.06	45.94

The AES data (Table 3.1) confirms that the Au and Pt content in the catalyst is close to the expected stoichiometry. The total metal loading is lower than the expected metal loading which may be attributed to inefficient immobilisation of the metals to the support during preparation. No TEM was conducted for this catalyst but this preparation method has previously shown to produce well dispersed nanoparticles with well-defined particle diameters between 2 and 5 nm[13, 26].

As discussed in the introduction, the pH of the aqueous reaction mixture can significantly influence the rate in which glycerol is consumed. It has been suggested that the presence of surface-bound hydroxyl groups reduces the energy barrier required for the initial C-H bond activation[14]. Table 3.2 shows how the incorporation of base into the system can affect the performance of the $AuPt/TiO_2$ catalyst in this reaction.

Table 3.2 Glycerol oxidation under basic and base free conditions over the AuPt/TiO$_2$ catalyst. **Reaction conditions:** 10 mL, glycerol (0.3 M), NaOH equivalents stated, O$_2$ (3 bar), substrate:metal ratio = 2000, 60 °C, 4 h.

NaOH Equivalents	Time (h)	Con (%)	Selectivity (%)								C.M.B. (%)
			GA	GLAD	TA	LA	DHA	GLA	OA	FOA	
2	0.25	17	61	0	3	17	0	10	1	9	100
	0.5	33	61	0	3	18	0	9	1	9	96
	1	73	62	0	5	16	0	8	1	8	86
	2	96	61	0	10	14	0	8	1	7	81
	4	100	62	0	12	14	0	8	1	2	79
0	0.25	1	10	4	1	0	79	2	5	0	100
	0.5	1	9	5	2	0	73	3	9	0	99
	1	1	11	7	3	0	67	5	6	0	102
	2	2	17	11	5	0	45	15	8	0	99
	4	3	13	11	3	0	35	11	5	23	99

As anticipated, the catalytic activity decreases significantly under base free conditions. Furthermore, the selectivity profile is changed. This is a good example of how the reaction is sensitive to environmental conditions in which it occurs. In order to develop a greater understanding on how the experimental conditions effect the performance of the AuPt/TiO$_2$ catalyst, parameter mapping experiments need to be conducted.

In order to gain a greater insight into the role of base in this reaction, further tests were conducted using 0.5, 1, 2 and 4 equivalents of NaOH. The results are shown in Table 3.3.

Interestingly, the NaOH concentration appears to have a non-linear relationship with substrate conversion. An increase in the catalytic turnover is observed as the NaOH concentration increases up to two molar equivalents. A decrease in conversion is subsequently observed at four molar equivalents. This relationship between conversion and NaOH can be explained by the product distribution.

An increase in LA selectivity and a decrease in selectivity to C$_1$ and C$_2$ products is observed as the concentration of NaOH is increased. Increasing the hydroxyl concentration appears to inhibit either the formation of H$_2$O$_2$, or its interaction with the substrate species. It has

been suggested previously that C-C cleavage occurs as a result of the in-situ formation of H_2O_2[16]. It has also been reported that increasing the pH of the aqueous phase promotes the decomposition of H_2O_2[19]. It is therefore feasible to suggest that the decrease in C-C cleavage is a result of the base promoted decomposition of H_2O_2. The reduction in the levels of H_2O_2 in the aqueous phase may be the reason why the substrate conversion decreases at higher concentrations of NaOH. If this is true, it can be postulated that a proportional relationship exists between H_2O_2 concentration and catalytic activity.

Table 3.3. Glycerol oxidation over the AuPt/TiO$_2$ catalyst. The effect of NaOH concentration on catalyst performance is assessed. **Reaction conditions:** 10 mL, glycerol (0.3 M), NaOH equivalents stated, O$_2$ (3 bar), substrate:metal ratio = 2000, 60 ℃, 4 h.

NaOH Equivalents	Time (h)	Con (%)	Selectivity (%)						C.M.B. (%)
			GA	TA	LA	GLA	OA	FOA	
0.5	0.25	16	51	5	9	21	1	12	96
	0.5	23	53	5	9	19	2	12	94
	1	26	69	7	3	14	2	5	91
	2	32	72	6	2	14	2	4	88
	4	42	63	6	4	14	2	12	94
1	0.25	12	59	3	10	15	1	12	95
	0.5	23	60	4	9	14	1	13	96
	1	29	69	6	2	14	2	8	83
	2	50	70	6	5	14	2	3	81
	4	58	71	6	5	15	2	1	82
2	0.25	17	61	3	17	10	1	9	100
	0.5	33	61	3	18	9	1	9	96
	1	73	62	5	16	8	1	8	86
	2	96	61	10	14	8	1	7	81
	4	100	62	12	14	8	1	2	79
4	0.25	7	55	4	41	0	0	0	94
	0.5	16	49	4	43	0	4	0	93
	1	40	45	4	45	2	1	3	93
	2	87	42	9	45	2	1	3	82
	4	100	14	37	45	2	2	2	81

The mechanistic route to form LA from glycerol is somewhat unclear. It has long been known that base can promote the dehydration-rearrangement-rehydration of polyols to produce LA[34]. A likely route involves the initial oxidative dehydrogenation of a terminal alcohol group to form GLAD. This would then be followed by a dehydration step and

possibly a rearrangement to form LA. It is known that under reaction conditions GLAD and DHA are equilibrium[35, 36]. For this reason, it is difficult to assess which of these intermediates undergoes the dehydration. A recent article by Crabtree and co-workers propose a different mechanistic route[37]. They suggest that a terminal alcohol group of GLAD is dehydrated to form 2-hydroxyacrylaldehyde. This compound subsequently undergoes oxidation to produce methylglyoxal which can then be consumed *via* a base promoted intermolecular Cannizzaro reaction to produce LA. It is clear that increasing the NaOH concentration increases the production of LA and it could therefore be postulated that external hydroxyl groups play a pivotal role in the dehydration of either DHA or GLAD. This would explain the poor LA selectivity observed for the oxidation of glycerol under base free conditions[38, 39].
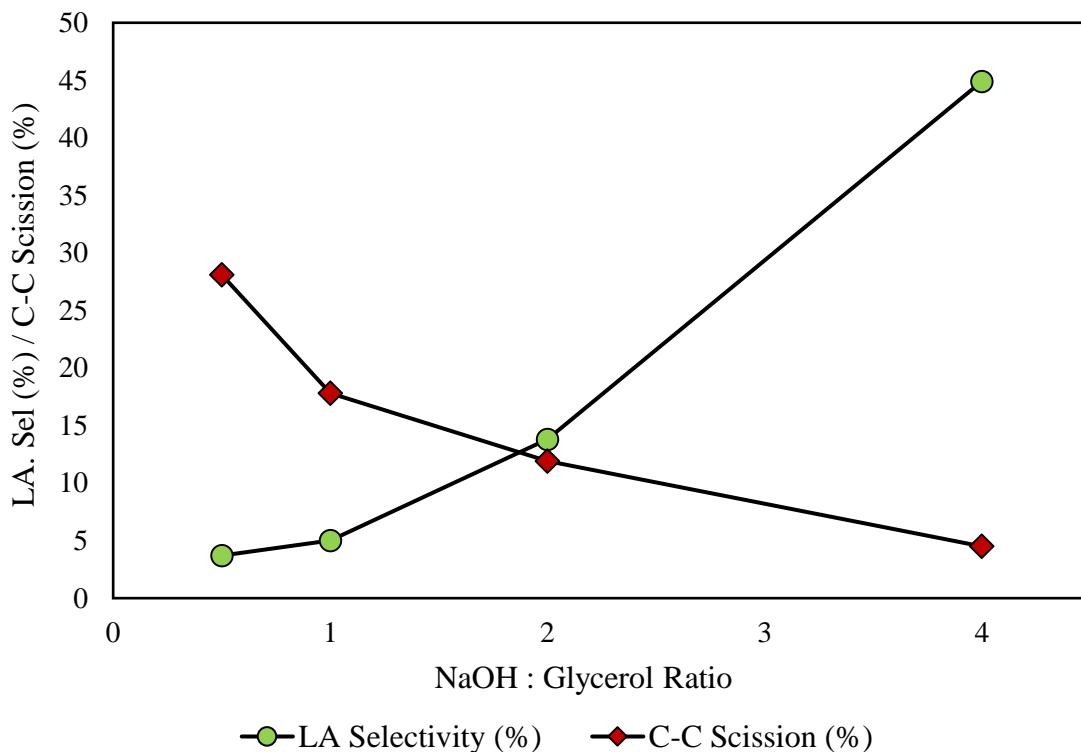
Figure 3.4. LA selectivity appears to have an inversely proportional relationship with C-C scission. Both are clearly influenced by the NaOH : glycerol ratio.

LA selectivity appears to have a proportional relationship with C_3 selectivity. This suggests that LA is stable under reaction conditions and that the parallel oxidation reaction which leads to the formation of GA and TA must therefore facilitate the unfavourable C-C

cleavages. The relationship between C-C scission and LA selectivity is demonstrated in Figure 3.4.

The role of oxygen in the catalytic oxidation of glycerol has also been discussed in detail in the literature[19, 23]. In order to investigate the effect of O_2 pressure on the AuPt/TiO$_2$ catalyst, a series of tests were conducted where the pressure of O_2 was varied in the reactor.

Table 3.4. The effect of the O_2 pressure on the oxidation of glycerol over the AuPt/TiO$_2$ catalyst under standard reaction conditions is assessed. **Reaction conditions:** 10 mL, glycerol (0.3 M), NaOH:substrate = 2, O_2 (pressure stated), substrate:metal ratio = 2000, 60 ℃, 4 h. He corresponds to reaction conducted under 3 bar He).

O_2 Pressure (bar)	Time (h)	Con (%)	Selectivity (%)						C.M.B. (%)
			GA	TA	LA	GLA	OA	FOA	
He	0.25	1	46	0	54	0	0	0	100
	0.5	1	40	0	60	0	0	0	100
	1	2	12	1	27	8	7	46	102
	2	2	11	1	40	10	6	32	102
	4	2	9	1	47	11	5	26	99
1	0.25	9	46	2	50	0	1	4	98
	0.5	17	47	3	46	0	1	4	97
	1	34	43	3	49	2	1	4	96
	2	70	48	4	43	2	0	2	93
	4	100	48	11	36	2	1	3	92
2	0.25	10	53	1	26	10	1	10	99
	0.5	16	56	2	24	8	1	9	100
	1	43	54	3	30	6	1	7	98
	2	90	59	5	26	5	1	5	101
	4	98	57	9	24	5	1	5	105
3	0.25	17	61	3	17	10	1	9	100
	0.5	33	61	3	18	9	1	9	96
	1	73	62	5	16	8	1	8	86
	2	96	61	10	14	8	1	7	81
	4	100	62	12	14	8	1	2	79

It is evident from Table 3.4 that oxygen has a substantial impact on the performance of the catalyst in this reaction. As oxygen pressure is increased, the conversion significantly

increases. This proportional relationship between catalyst turnover and O_2 pressure is typical of oxidation reactions catalysed by heterogeneous catalysts[23].

The O_2 pressure also appears to have a significant impact on the selectivity profile of the reaction. There is a noticeable increase in C_2 and C_1 products with increasing O_2 pressure, particularly in the final stages of the reaction. As discussed previously, H_2O_2 is a product of the reduction of O_2 by H_2O[15]. It is therefore likely that increasing the oxygen pressure may be promoting the production of H_2O_2 in the reaction. Additionally, the selectivity to GA and LA increase and decrease respectively as the pressure is increased. This suggests that oxygen may be inhibiting the LA pathway through the promotion of the competitive direct oxidation pathway.
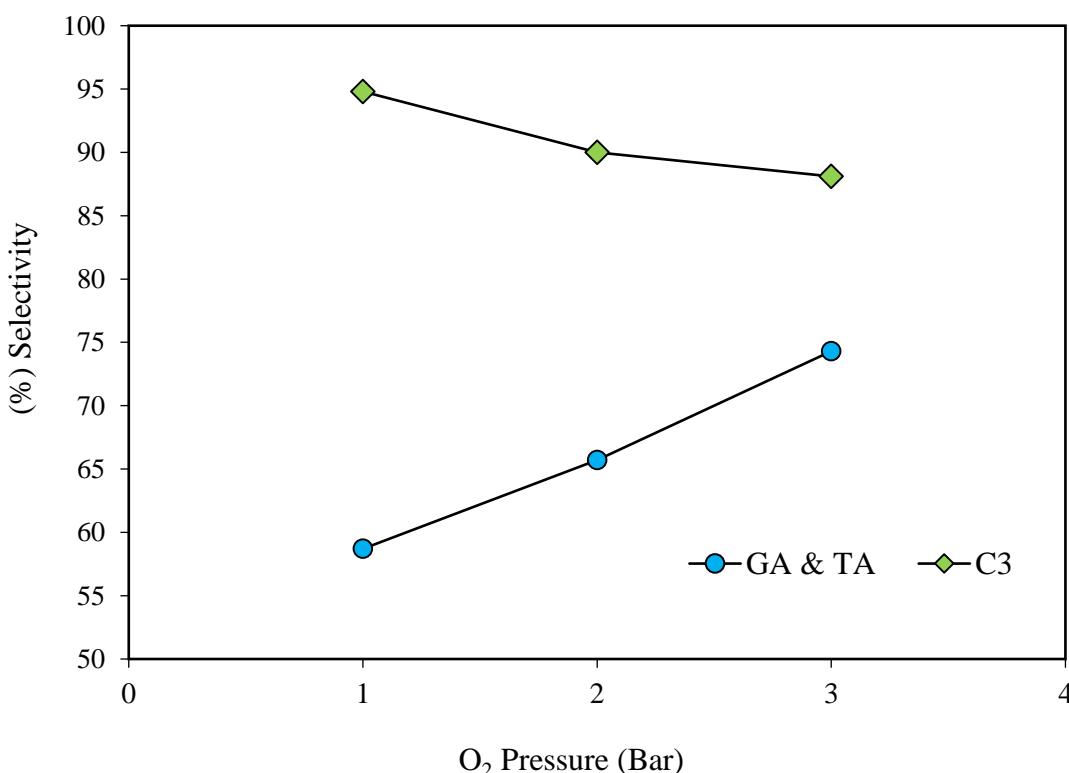
Figure 3.5. The selectivity to GA and TA increases with increasing O_2 pressure. In addition, the unfavourable C-C scission appears to have a proportional relationship with O_2 pressure. Data points reflect samples taken after 4 h of reaction.

Under anaerobic conditions, the catalyst still appears to be active. This could suggest that oxygen from the support or oxygen from the base can also take part in reaction.

Interestingly, products formed from C-C cleavages are still observed under anaerobic conditions. This could imply that H_2O_2 is not only produced from the reduction of O_2 by H_2O or that there is an additional mechanistic route which can result in C-C scission. It is very possible that the C_3 acid species may undergo decarboxylation leading to the formation of a C_2 species and CO_2.

Increasing the reaction temperature for the oxidation of glycerol has previously shown to not only promote catalytic activity, but also increase the selectivity to GA in the presence of supported Au containing catalysts[7, 18, 19]. For this reason, it was necessary to assess the effect temperature had on the performance of the 1% $AuPt/TiO_2$ catalyst for this reaction. The results of these tests are displayed in Table 3.5.

Table 3.4. The effect of reaction temperature on the oxidation of glycerol over the $AuPt/TiO_2$. **Reaction conditions:** 10 mL, glycerol (0.3 M), NaOH:substrate = 2, O_2 (3 bar), substrate:metal ratio = 2000, temperature stated, 4 h.

Temperature (ºC)	Time (h)	Con (%)	Selectivity (%)						C.M.B. (%)
			GA	TA	LA	GLA	OA	FOA	
40	0.25	12	60	3	9	16	1	12	102
	0.5	26	60	3	8	16	1	12	99
	1	53	62	4	8	14	1	10	97
	2	96	63	9	6	12	2	8	87
	4	99	64	11	6	12	2	5	85
60	0.25	17	61	3	17	10	1	9	100
	0.5	33	61	3	18	9	1	9	96
	1	73	62	5	16	8	1	8	86
	2	96	61	10	14	8	1	7	81
	4	100	62	12	14	8	1	2	79
80	0.25	14	52	2	36	4	1	5	95
	0.5	27	49	2	40	4	0	6	90
	1	59	49	3	38	4	0	6	91
	2	96	49	11	33	4	1	3	77
	4	100	46	14	34	4	1	1	76
100	0.25	29	29	1	67	2	0	1	97
	0.5	55	28	2	64	2	1	3	93
	1	100	29	7	57	2	1	5	81
	2	100	21	14	57	2	2	4	84
	4	100	16	18	57	2	3	4	91

As expected, there is a proportional relationship between glycerol conversion and reaction temperature. This trend can be explained by fundamental collision theory. Interestingly, substantial changes in the product selectivity is observed as the reaction temperature is increased. A proportional relationship between the temperature and C_3 selectivity is observed despite the selectivity to GA and TA decreasing. The increase in C_3 selectivity can be explained by the instability of H_2O_2 at elevated temperatures. There is also a substantial increase in selectivity to LA observed. Increasing the reaction temperature may promote the dehydration of a terminal alcohol group; believed to be key step in the formation of LA from glycerol. This is also further evidence to suggest that LA is reasonably stable in the reaction medium and that LA is less prone to decarboxylation than the other C_3 organic acids.
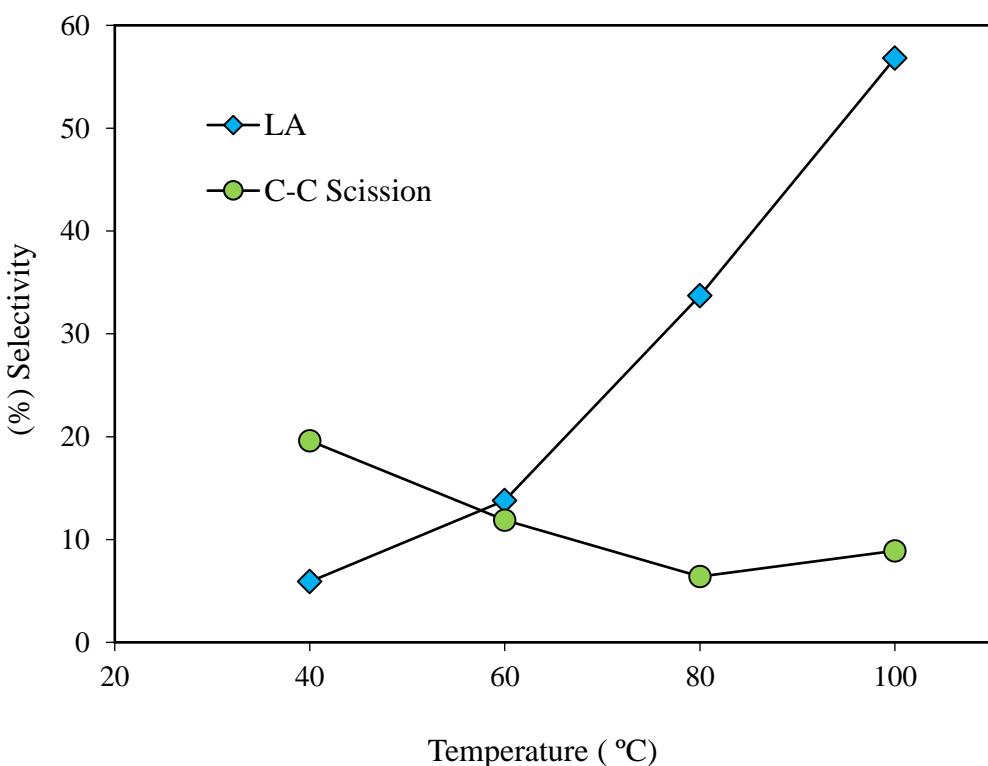
Figure 3.6. C-C scission decreases as LA selectivity increases as the reaction temperature is increased. High temperatures may facilitate the dehydration of terminal alcohols and promote H_2O_2 decomposition. Data points reflect samples taken after 4 h.

From the parameter mapping experiments it is clear that the reaction conditions can have a substantial impact on the performance of the AuPt/TiO$_2$ for the oxidation of glycerol. A greater understanding of the promotional effects affecting the different reaction pathways has been established. The knowledge acquired from this investigation will act as a foundation moving forward.

3.4.   A Mechanistic Overview of the Reaction Profile

In order promote desirable reaction selectivity, it is important to consider how the reaction products are effected by the catalyst and the reaction conditions. For this reason, a series of tests were constructed where the major products from the oxidation of glycerol were used as the reaction substrates. These tests were conducted in order to assess how they were affected by the catalyst under reaction conditions in a basic and base free reaction medium. Once again, a 1 wt.% AuPt/TiO$_2$ catalyst prepared by conventional sol-immobilisation was used as the standard catalyst. XPS and MP-AES was conducted on the catalyst to ensure its reproducibility.
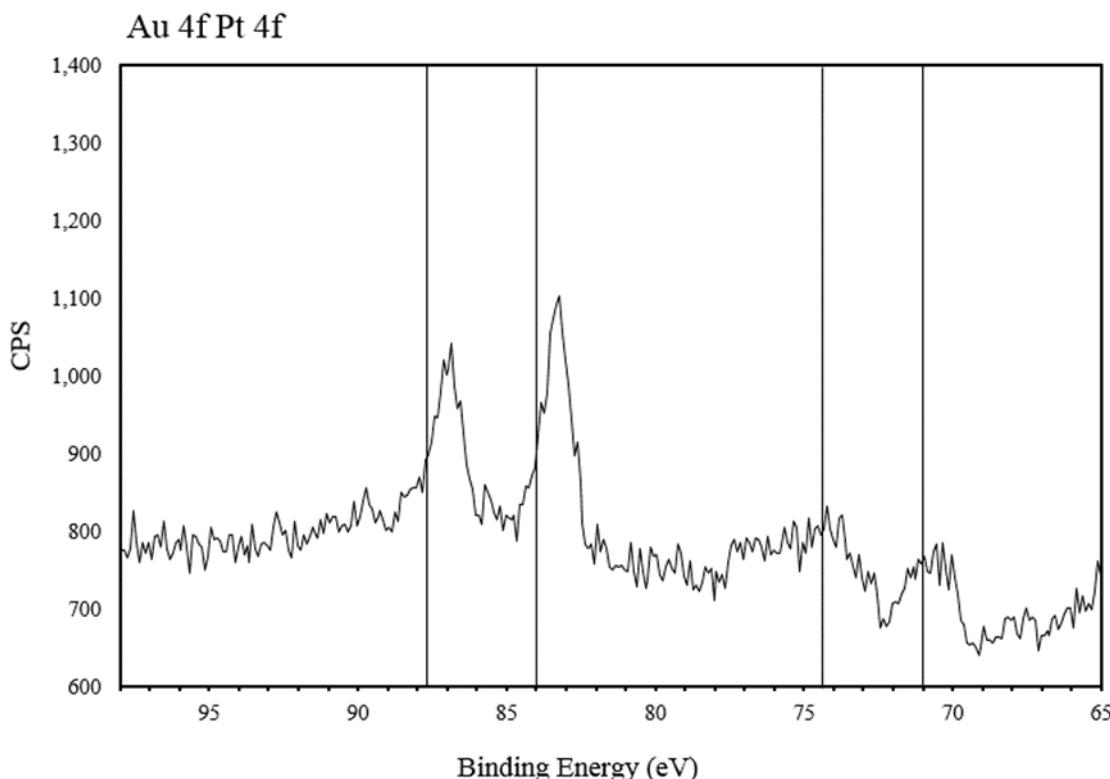
Figure 3.7. XPS spectrum of Au 4f and Pt 4f regions for the 1 wt.% AuPt/TiO$_2$ catalyst.

The XPS spectra in Figure 3.7 shows that both the Au and Pt is present in their metallic state. The Au $4f_{7/2}$ and $4f_{5/2}$ peaks are observed at binding energies of 83.25 and 87.0 eV. Once again the Au peaks appear at a slightly lower binding energy than expected[27]. This could be a result of the Au nanoparticles interacting with defect sites in the Ti[28] or indicate that AuPt alloy structures are present[30]. The Pt $4f_{7/2}$ and $4f_{5/2}$ peaks observed at binding energies of 71.1 and 74.2 eV respectively are characteristic of Pt^0 states[32, 33]. The catalyst was subsequently assessed for its metal loading by MP-AES and the results are displayed in Table 3.6.

Table 3.6. The total metal loading and ratio of Au and Pt is determined using MP-AES

	Total Metal Loading (%)	Au (molar %)	Pt (molar %)
1% AuPt/TiO$_2$	0.81	52.36	47.64

Once again, the total metal loading was lower than expected but was consistent with the catalyst prepared in Section 3.3. The first group of experiments were designed to assess the reactivity of each product under basic reaction conditions and in the presence of the 1 wt%. AuPt/TiO$_2$ catalyst. The results from these tests are displayed in Table 3.7.

Under the standard reaction conditions, DHA and GLAD appear to be consumed immediately, with no traces of the two compounds observed after 0.5 h of reaction. To my knowledge, no previous studies which have investigated the oxidation of glycerol in a basic reaction medium have reported observing either of these compounds. Various publications reporting the oxidation of glycerol under base free conditions have observed both GLAD and DHA [4, 12, 39, 40]. This suggests that in the presence of base, these two products immediately react in a base catalysed transformation. It is known that the two compounds are in equilibrium, leaving either the primary or secondary alcohol prone to nucleophilic attack. Their selectivity profiles after reaction completion are similar, with the DHA favouring the formation of LA as opposed to the direct oxidation pathway.

There is also significantly less C$_3$ products formed from the oxidation of these two products when compared with the oxidation of glycerol. It is possible that the sudden transformation

of these species in solution may make them susceptible to homogeneous intermolecular interactions, resulting in C-C cleavage. The low C.M.B.'s observed from the oxidation of these species suggest that there may be additional unidentified products formed. The fact that similar reaction profiles aren't observed for the oxidation of glycerol could suggest that LA and GA are primary oxidation products. Aldol type reactions between GLAD or DHA and an additional unsaturated product could be occurring which would lead to the formation of C_5 and even C_6 compounds. For this reason, even if small quantities of the substrate and/or product(s) took part in these reaction it may account for a substantial quantity of the missing carbon.

Table 3.7. Products formed from oxidation of glycerol were used as substrates and their reactivity was assessed under standard reaction conditions in the presence of a AuPt/TiO$_2$ catalyst. TOF's are calculated at 0.5 h and conversion, selectivity and mass balance data reflects samples after 4 h of reaction. **Reaction conditions:** 10 mL, substrate (0.3 M), NaOH:substrate = 2, O$_2$ (3 bar), substrate:metal ratio = 2000, 60 °C 4 h.

	TOF (h^{-1})	Con (%)	Selectivity (%)									C.M.B. (%)
			GLY	DHA	GLAD	LA	GA	TA	GLA	OA	FOA	
GLY	1649	100	X	0	0	14	62	12	8	1	2	79
DHA	4938	100	0	X	0	37	33	4	7	1	17	47
GLAD	4938	100	0	0	X	29	31	11	13	3	13	57
LA	0	0	0	0	0	X	0	0	0	0	0	100
GA	89	8	0	0	0	0	X	9	24	21	46	93
TA	0	0	0	0	0	0	0	X	0	0	0	100
GLA	79	9	0	0	0	0	0	0	X	100	0	101
OA	0	0	0	0	0	0	0	0	0	X	0	100
FOA	138	17	0	0	0	0	0	0	0	0	X	84

When GA is used as the substrate, an unexpected result is observed. Significant quantities of TA were observed when glycerol was used as the substrate. On the contrary, an exceptionally small TOF and overall conversion is observed, with selectivity favouring the production of C_2 and C_1 compounds. The GA precursor used for these tests was a hemi calcium salt; perhaps the presence of Ca in the reaction medium had a negative impact on the performance of the catalyst. Davis and co-workers have reported a similar observation when they looked into the oxidation of 0.05 M solution of GA over Au/TiO$_2$[16]. Davis postulated that in order to continue with the subsequent oxidation to TA, the primary alcohol group needs to be activated by an external hydroxyl group. However, as the

carboxylic acid group is far more acidic than the terminal alcohol, it inhibits the deprotonation of the alcohol. Another possible explanation for the poor activity observed is that TA may be a primary oxidation product.

The GO appeared to oxidise to OA in a fairly controlled fashion but at a low rate which can also be explained by Davis' theory. FOA is also consumed under these reaction conditions. Previous electrochemical studies have suggested that the oxidation of glycerol can lead to the formation of CO_2[41, 42]. No conversion was observed when OA, TA and LA were used as the substrates.

The next group of experiments assessed the reactivity of each product under base free conditions and in the presence of the $AuPt/TiO_2$ catalyst. The results from these tests are displayed in Table 3.8.

Table 3.8. Products formed from the oxidation of glycerol were used as substrates and their reactivity was assessed under base free conditions in the presence of the $AuPt/TiO_2$ catalyst. TOF's are calculated at 0.5 h and conversion, selectivity and mass balance data reflects samples after 4 h of reaction. **Reaction conditions:** 10 mL, substrate (0.3 M), O_2 (3 bar), substrate:metal ratio = 2000, 60 ºC 4 h.

	TOF (h^{-1})	Con (%)	Selectivity (%)									C.M.B. (%)
			GLY	DHA	GLAD	LA	GA	TA	GLA	OA	FOA	
GLY	35	3	X	35	11	0	13	3	11	5	23	99
DHA	128	9	0	X	0	0	0	12	70	18	0	92
GLAD	316	34	0	0	X	0	99	0	0	0	0	100
LA	0	0	0	0	0	X	0	0	0	0	0	100
GA	84	4	0	0	0	0	X	70	20	5	5	96
TA	0	0	0	0	0	0	0	X	0	0	0	100
GLA	0	0	0	0	0	0	0	0	X	0	0	100
OA	509	72	0	0	0	0	0	0	0	X	0	28
FOA	0	0	0	0	0	0	0	0	0	0	X	100

From the TOF's displayed in Table 3.8, it appears GLAD is more easily consumed than DHA under base free conditions. The oxidation of GLAD to GA appears to proceed in an exceptionally controlled fashion as a selectivity close to 100 % is observed. On the contrary, the oxidation of DHA appears to proceed *via* a different mechanistic pathway.

TA and other sequential oxidation products are observed, but no GA is present. Katryniok *et al.*[8] proposed that TA can be formed from DHA *via* hydroxypyruvaldehyde and hydroxymalone intermediate species. This would explain the absence of GA in the reaction solution. The large quantities of GO and OA observed also support this theory, as it was suggested that glycolaldehyde can be formed from these two intermediates. Furthermore, it is postulated that OA can be formed from the oxidative decarbonylation of 2-hydroxy-3-oxo-propanoic acid [8]. The presence of these additional products and intermediates would account for the poor carbon mass balance observed for the oxidation of DHA. A lack of external hydroxyl groups appears to shut off the pathway to LA, providing further evidence that homogeneous hydroxyl groups are essential for the dehydration of primary alcohols in this reaction.

Once again, extremely poor GA consumption is observed. As mentioned previously, the terminal alcohol of the GA requires activation from an external hydroxyl group[16]. It is likely that the absence of NaOH in the reaction would make this even more unfavourable. However, the TOF for GA in the presence and absence of NaOH is comparable, which underlines the negative impact the acidity of the carboxylic acid is having on the activation of the remaining primary alcohol group. TA appears to be stable under these conditions which indicates that C-C cleavage must occur prior to TA formation. LA, GO, and FOA also appear to be stable under these reaction conditions. OA is consumed at a fairly high rate which could be attributed to the sequential oxidation to other C_1 derivatives.

The last set of experiments were constructed to assess the reactivity of each product in a basic environment and in the absence of a catalyst. The results from these experiments are displayed in Table 3.9.

In the absence of a catalyst; glycerol, LA, TA, GO, OA and FOA all appear to be stable under the standard reaction conditions. This underlines the important role of the catalyst in the oxidation of these compounds. It also suggests that the catalyst is responsible for the over oxidation of products, and that these unfavourable reactions can be inhibited through the development of catalyst design. Once again, small quantities of GA are consumed, predominantly undergoing C-C cleavage to produce C_1 and C_2 products. This could suggest that the catalyst is not essential for the production of H_2O_2 or that there are additional homogeneous pathways which can lead to the unfavourable C-C scission such as the possibility of decarboxylation reactions, as discussed previously.

Table 3.9. Products formed from the oxidation of glycerol were used as substrates and their reactivity was assessed under basic condition and in the absence of a catalyst. TOF's are calculated at 0.5 h and conversion, selectivity and mass balance data reflects samples after 4 h of reaction. **Reaction conditions:** 10 mL, substrate (0.3 M), O_2 (3 bar), NaOH:substrate = 2, 60 °C, 4 h.

	TOF (h^{-1})	Con (%)	Selectivity (%)									C.M.B. (%)
			GLY	DHA	GLAD	LA	GA	TA	GLA	OA	FOA	
GLY	0	0	X	0	0	0	0	0	0	0	0	100
DHA	4938	100	0	X	0	38.7	26.6	2.7	9.7	1.8	20.4	51.1
GLAD	4938	100	0	0	X	17.6	34.7	2	19.8	0.8	25.1	52.3
LA	0	0	0	0	0	X	0	0	0	0	0	100
GA	54.3	6.4	0	0	0	0	X	5.5	22.6	16.7	55.1	100.5
TA	0	0	0	0	0	0	0	X	0	0	0	100
GLA	14.8	1	0	0	0	0	0	0	X	0	0	99.7
OA	0	0	0	0	0	0	0	0	0	X	0	100
FOA	0	0	0	0	0	0	0	0	0	0	X	100

The TOFs of GLAD and DHA are identical to those observed under standard conditions. It appears as though the catalyst has very little impact on the reaction selectivity associated with the oxidation of both DHA and GLAD. Slightly more C-C cleavage is observed in the absence of catalyst suggesting that the catalyst provides an element of control to the system. Furthermore, both DHA and GLAD have very similar selectivity profiles, suggesting that the two molecules can readily interconvert under these reaction conditions. DHA slightly favours the production of LA where oxidation to TA appears to be more favourable from GLAD.

These tests have revealed how complex this reaction is. The catalyst and environmental conditions can affect the reaction intermediates in different ways, adding further complexities when trying to control the product selectivity. The substantial losses in carbon from some species suggest that there may be additional products being produced which are not accounted for. The tests also indicate that there could be multiple catalytic pathways for the production of the same products. Nevertheless, the oxidation of glycerol under base free conditions does appear to be possible with a high selectivity to C_3 products. As a result, this research appears to be promising moving forward.
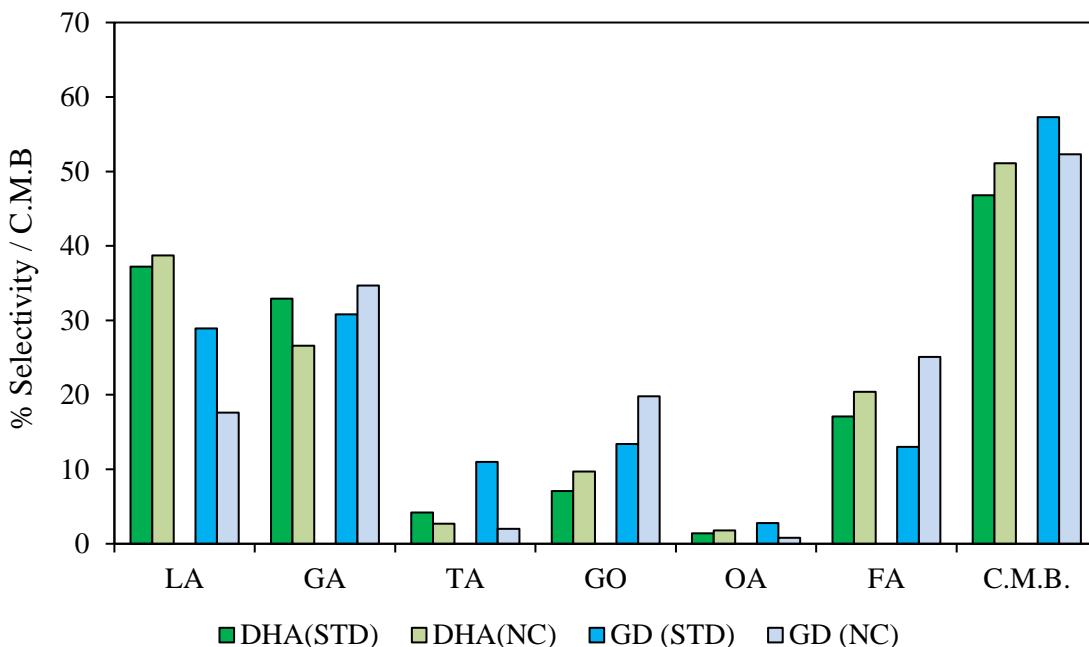
Figure 3.8. The reaction selectivity and carbon mass balances are compared for the oxidation of GLAD and DHA under standard conditions (STD) and in the absence of any catalyst (NC). These figures correspond to the reaction after 4 h. GD corresponds to glyceraldehyde. **Reaction conditions:** 10 mL, substrate (0.3 M), O_2 (3 bar), NaOH:substrate = 2, 60 ℃, 4 h.

3.5. Base Free Oxidation of Glycerol

The ability to selectively oxidise glycerol under base free conditions enhances the potential for the industrialisation of this reaction. For this reason, there has been a lot of development in this area of research in recent times[13, 22, 38, 40]. Supported platinum catalysts have shown to be fairly active under base free conditions but are also believed to promote the unfavourable C-C scission[39]. Prati and co-workers demonstrated that gold containing catalysts were inactive for this process in the absence of sacrificial base[43]. On the contrary, AuPt catalysts supported on $Mg(OH)_2$ have proven to be active, highlighting the importance in the selection of the support and metal nanoparticles[13]. Irrespective of this, it was stated that small amounts of Mg^{2+} leached from the support forming homogeneous $Mg(OH)_2$, which could account for the high activity observed.

Table 3.10. The activity of Au, Pd and Pt containing bimetallic catalysts are assessed for their ability to oxidise glycerol under standard reaction conditions in the absence of base. **Reaction conditions:** 10 mL, substrate (0.3 M), O_2 (3 bar), substrate:metal ratio = 2728, 60 ºC, 24 h.

Catalyst	Time (h)	Con (%)	Selectivity (%)								C.M.B.
			GA	TA	DHA	LA	GLA	OA	βHA	FOA	
AuPdPt	0.5	4	54	0	42	0	0	1	0	3	97
	1	6	58	0	39	0	2	1	1	0	96
	2	8	60	1	37	0	2	1	1	0	96
	4	10	64	1	32	0	2	1	1	0	95
	24	18	65	1	30	0	3	0	1	0	95
AuPd	0.5	1	74	16	0	0	0	10	0	0	97
	1	2	77	16	0	0	0	7	0	0	98
	2	2	76	18	0	0	0	6	0	0	98
	4	3	41	8	48	0	0	3	0	0	98
	24	8	40	7	48	0	0	5	0	0	93
AuPt[*]	0.5	0	0	0	0	0	0	0	0	0	100
	1	0	0	0	0	0	0	0	0	0	100
	2	0	0	0	0	0	0	0	0	0	100
	4	0	0	0	0	0	0	0	0	0	100
	24	0	0	0	0	0	0	0	0	0	100
PdPt	0.5	3	54	2	41	0	0	3	0	0	98
	1	3	62	3	33	0	0	1	0	0	98
	2	4	60	2	36	0	0	1	1	0	98
	4	6	66	1	0	0	1	31	1	0	97
	24	14	70	1	2	0	0	26	1	0	94

It has already been determined in this chapter that AuPt nanoparticles supported on TiO_2 are active for the oxidation of glycerol under base free conditions. For this reason, a series of Au, Pd and Pt containing catalysts supported on TiO_2 were prepared by the conventional sol-immobilisation technique. The catalysts were subsequently assessed for the oxidation of glycerol under base free conditions. The results of these tests are displayed in Table 3.10.

The bimetallic catalysts exhibited poor activities after 24 h of reaction. Previous studies have reported that supported AuPt nanoparticles were highly active for the oxidation of glycerol under these conditions[12, 13]. The results in Table 3.10 contradict this, as no reaction was observed with the AuPt/TiO_2 catalyst after the 24 h reaction. The PdPt/TiO_2 catalyst

appeared to be the most active, with 13.8 % of the substrate being consumed after 24 h. It's possible that Au may be inhibiting the performance of the catalysts in some way.

Table 3.11. The activity of Au, Pd and Pt containing bimetallic catalysts are assessed for their ability to oxidise glycerol at 100 ºC and in the absence of base. **Reaction conditions:** 10 mL, substrate (0.3 M), O_2 (3 bar), substrate:metal ratio = 2728, 100 ºC, 4 h.

Catalyst	Time (h)	Con (%)	Selectivity (%)								C.M.B (%)
			GA	TA	GLA	LA	OA	DHA	βHA	FOA	
AuPdPt	0.5	9	55	1	3	0	0	39	1	1	97
	1	18	56	1	3	0	0	38	2	0	93
	2	22	56	1	5	0	0	36	2	0	95
	4	37	55	2	7	0	0	35	1	1	87
AuPd	0.5	0	50	0	0	0	3	47	0	0	100
	1	1	42	0	0	0	0	58	0	0	100
	2	4	34	1	8	0	0	56	1	0	99
	4	8	30	1	10	0	0	58	1	0	97
AuPt*	0.5	0	0	0	0	0	0	0	0	0	100
	1	0	0	0	0	0	0	0	0	0	100
	2	0	0	0	0	0	0	0	0	0	100
	4	0	0	0	0	0	0	0	0	0	100
PdPt	0.5	4	61	1	0	0	0	37	1	0	100
	1	12	63	1	0	0	0	34	2	0	96
	2	29	63	1	4	0	0	31	2	0	87
	4	39	64	1	6	0	0	28	1	0	83

The AuPd/TiO$_2$ catalyst was found to give the highest C$_3$ selectivity. Supported Pt monometallic catalysts have previously been found to facilitate C-C cleavage. The higher C$_1$ and C$_2$ selectivity of the PdPt/TiO$_2$ could indicate that monometallic Pt islands are present on the surface of the catalyst. Interestingly, a recent study found that the addition of small amounts of Pt to supported clusters of AuPd supressed the hydrogenation and decomposition of H_2O_2[44]. H_2O_2 is believed to be directly responsible for C-C cleavage in the selective oxidation of glycerol[15]. It is possible that the Pt is stabilising the H_2O_2 formed in the reaction, and as a result, is indirectly responsible for the increased C-C scission observed with the PdPt/TiO$_2$ catalyst. The trimetallic AuPdPt/TiO$_2$ catalyst displayed the highest overall activity and maintained a good degree of C$_3$ selectivity; 96 % selectivity at

18 % conversion. The Au may facilitate the alloying of the three metals, which would reduce the quantity of monodispersed Pt on the surface of the catalyst.

In order to gain a greater understanding of how these catalysts function, further tests were conducted under base free conditions at 100 ℃. The results from these tests are displayed in Table 3.11. Even at elevated temperatures, poor activities were observed for the AuPt/TiO$_2$ and AuPd/TiO$_2$ catalysts. On the contrary, a significant increase in activity was observed for the PdPt/TiO$_2$ and tri-metallic AuPdPt/TiO$_2$ catalysts, which displayed conversions of 39.3 and 36.9 % respectively. Interestingly, a significant reduction in C-C scission was observed with the PdPt/TiO$_2$ catalyst and a C$_3$ selectivity comparable with the AuPd/TiO$_2$ catalyst was detected. It has been previously determined that increasing the reaction temperature can enhance the C$_3$ selectivity of a catalyst[19]. It was postulated that this was a result of decreasing H$_2$O$_2$ stability as temperature is increased. This may be the reason why a higher C$_3$ selectivity is observed at 100 ℃ than 60 ℃. A higher C$_3$ selectivity was also observed with the AuPdPt/TiO$_2$ catalyst at an increased reaction

Once again, no conversion was observed with the AuPt/TiO$_2$ catalyst. In order to gain a greater understanding as to why this catalyst is not active, MP-AES was used to determine the specific weight loadings of each catalyst. These results are displayed in Table 3.12.

Table 3.12. The metal weight loadings of each catalyst were determined by MP-AES.

Catalyst	Total metal loading (%)	Metal loading (molar %)			Adjusted Metal ratios*
		Au	Pd	Pt	
AuPd/TiO$_2$	0.31	29.3	70.7	-	1:2 (Au:Pd)
PdPt/TiO$_2$	0.96	-	45.4	54.6	1:1 (PdPt)
AuPt/TiO$_2$	0.17	31.0	-	69.0	1:2 (AuPt)
AuPdPt/TiO$_2$	0.92	23.4	29.4	47.2	1:1:2 (Au:Pd:Pt)

It is clear that the metal weight loadings are not consistent across the series of catalysts. The PdPt/TiO$_2$ and AuPdPt/TiO$_2$ catalysts appear to be close to the target metal loading of 1 wt.%, whereas the AuPd and AuPt/TiO$_2$ catalysts appear to have significantly lower metal loadings than anticipated. This data immediately explains why there is such a considerable different in activity exhibited by the two sets of catalysts. Furthermore, there appears to be discrepancies in the molar ratios between the metals. All the catalysts were prepared with

an intended total weight loading of 1 % with equimolar ratios between the metals. Nevertheless, the catalysts can still provide an insight into the activity and selectivity requirements for the base free oxidation of glycerol. Due to the significant differences in metal loadings between the catalysts, it is difficult to compare their performance directly from the reaction results. It seems more appropriate to assess them in term of their TOF as this accounts for the moles of metal involved.

Table 3.13. The Turnover frequencies for the bi- and trimetallic catalysts were determined at 60 ℃ and 100 ℃. The initial rate measurement was conducted after 0.5 h.

Catalyst	TOF (h^{-1}) at 0.5 h reaction time	
	60 °C reaction temperature	100 °C reaction temperature
AuPd/TiO$_2$	86	38
PdPt/TiO$_2$	152	210
AuPt/TiO$_2$	-	-
AuPdPt/TiO$_2$	174	378

The turnover frequencies for each of the corresponding catalysts revealed that the trimetallic AuPdPt/TiO$_2$ catalyst is the most active. This increase in activity is could indicate that a synergistic interaction between the three metals is observed. Interestingly, there was a decrease in the TOF for the AuPd/TiO$_2$ catalyst when the temperature was increased from 60 ℃ to 100 ℃. This could be a result of an increase in sintering of the AuPd nanoparticles at higher reaction temperatures.

The fresh catalysts were subsequently characterised by TEM. The images received and the corresponding particle size distributions (PSDs) are displayed in figure 3.9. The AuPd/TiO$_2$, PdPt/TiO$_2$ and AuPdPt/TiO$_2$ catalysts all consisted of small nanoparticles with mean particle sizes ranging from 2.0 to 2.3 nm. The AuPt/TiO$_2$ catalyst however, consisted of unusually small nanoparticles with an exceptionally narrow PSD; 1.19 nm average particle size with a standard deviation from the mean particle size of 0.37 nm. It is likely that the small well defined PSD observed for this catalyst is a result of its low metal loading.

The TEM images are in agreement with literature which reports that the conventional sol-immobilisation technique generates small nanoparticles with well-defined PSDs[26]. In addition, it is evident that the particles sizes of these catalysts fall within the required region in order to be active for alcohol oxidation.
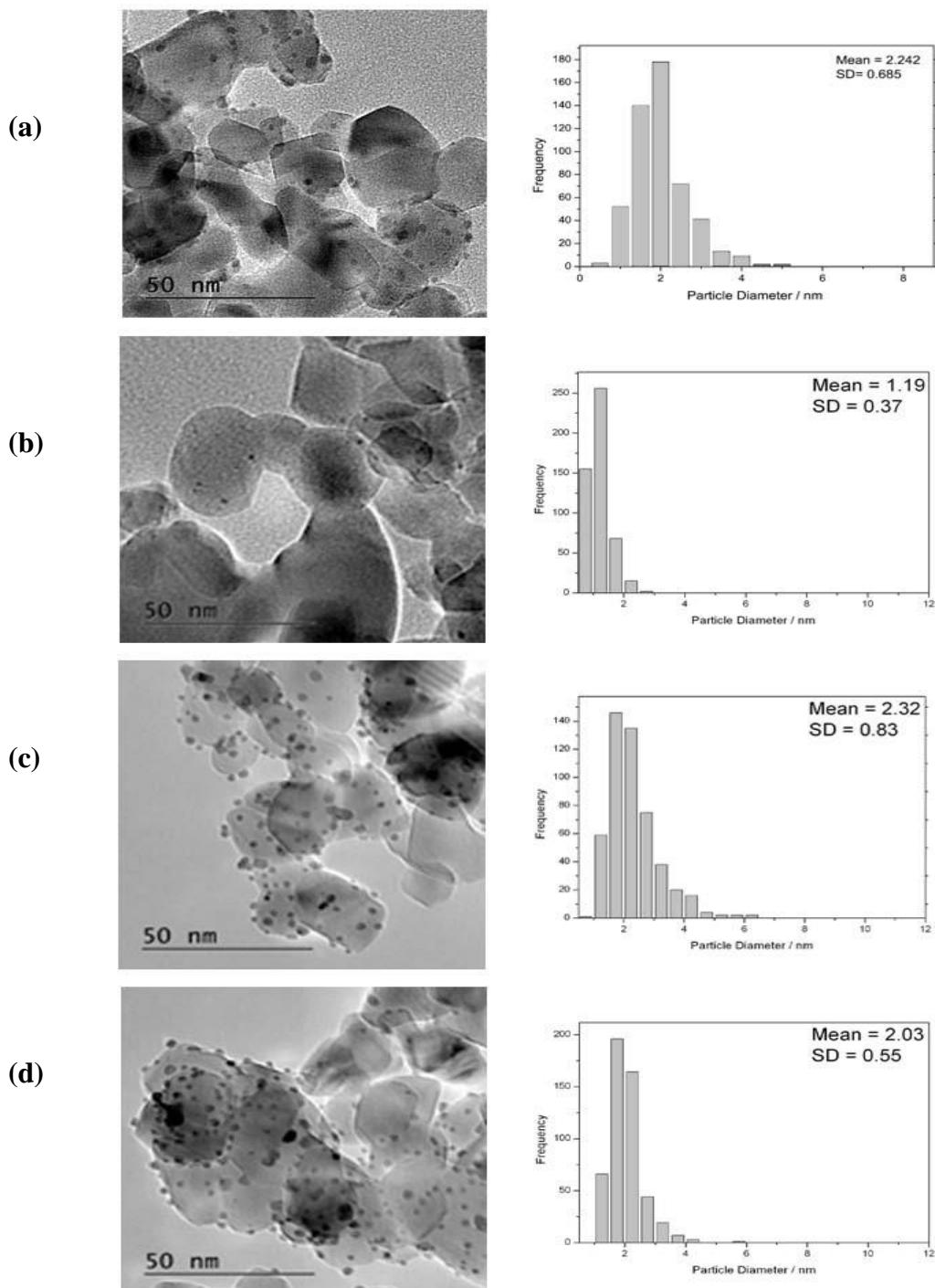

Figure 3.9. Images and PSD's retrieved for the catalysts by TEM:
(a) AuPd/TiO$_2$, (b) AuPt/TiO$_2$, (c) PdPt/TiO$_2$ and (d) AuPdPt/TiO$_2$

XPS was conducted on each of the catalysts in order to determine the oxidation state of the metallic species and their distribution on the surface of the TiO_2. The XPS spectra of the catalysts are displayed in Figures 3.10 and 3.11.
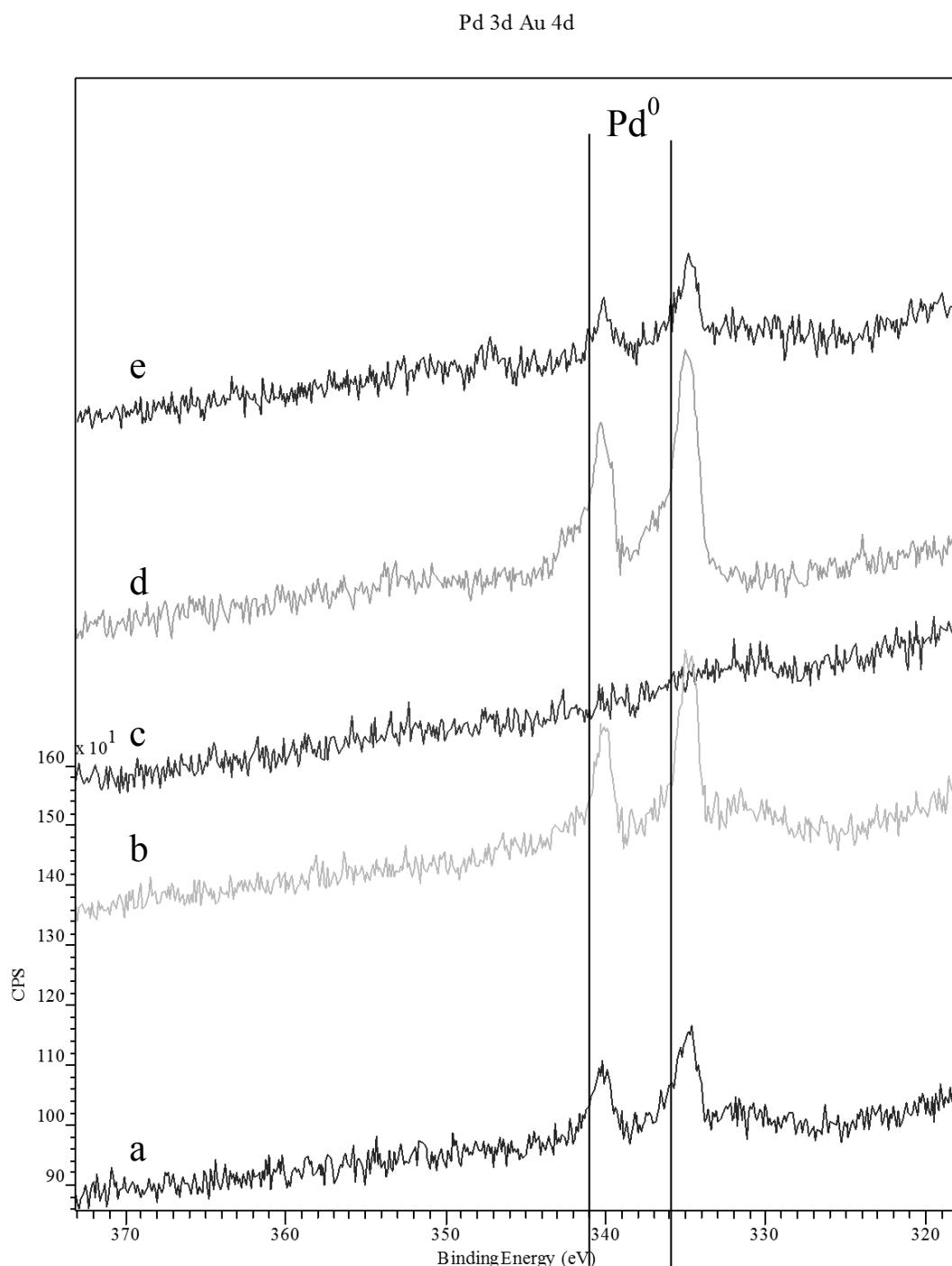

Figure 3.10. XPS spectra showing the Pd 3d region for each of the catalysts. The spectra reveal that Pd is only ever present in its metallic state. (a) AuPdPt/TiO$_2$, (b) PdPt/TiO$_2$, (c) AuPt/TiO$_2$, (d) AuPd/TiO$_2$ and (e) AuPdPt/TiO$_2$ used.
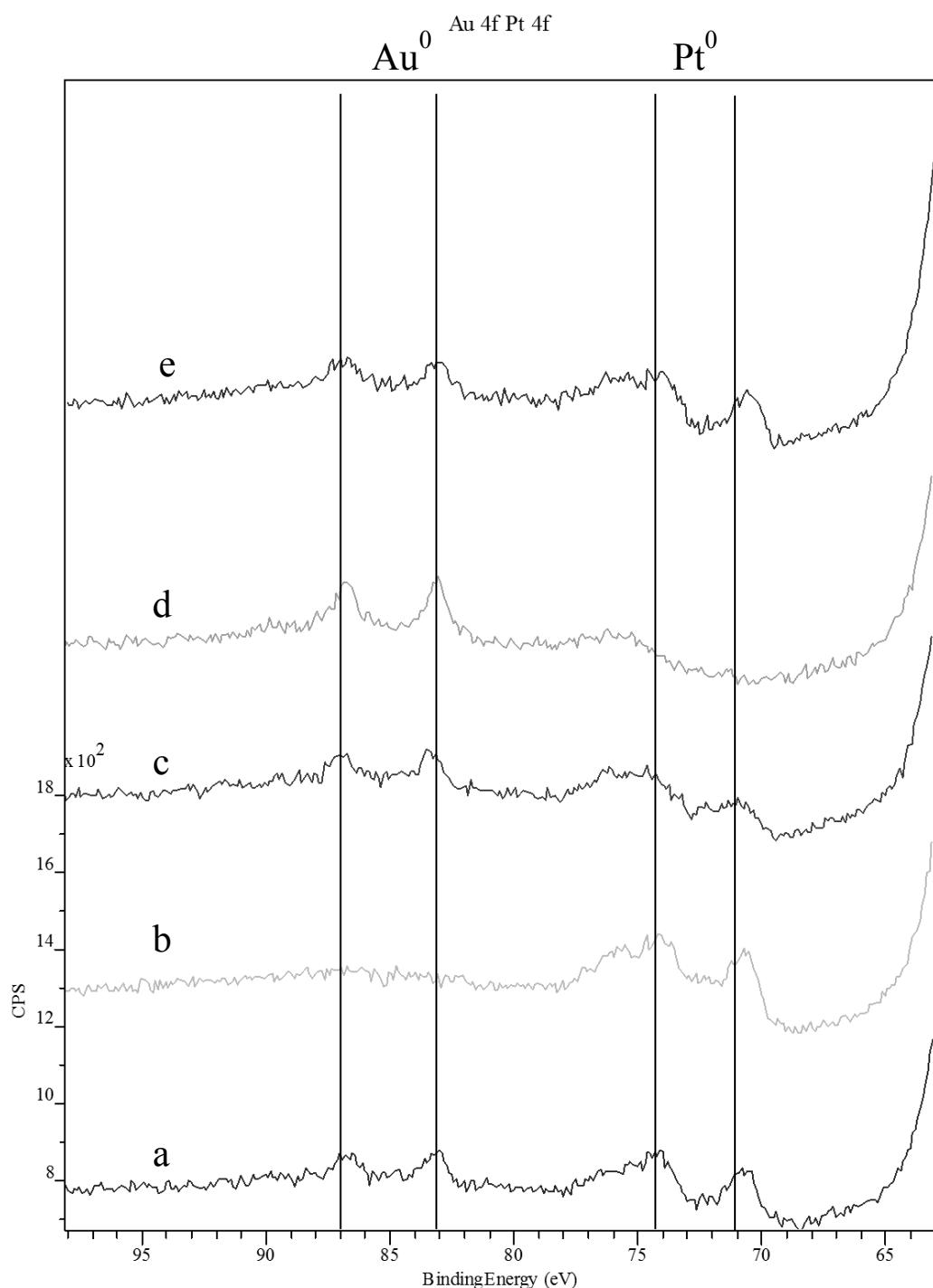
Figure 3.11. XPS spectra showing the Au 4f and Pt 4f regions for each of the catalysts. The spectra reveal that both the Pt and Au are only ever present in their metallic state. (a) AuPdPt/TiO$_2$, (b) PdPt/TiO$_2$, (c) AuPt/TiO$_2$, (d) AuPd/TiO$_2$ and (e) AuPdPt/TiO$_2$ used.

The acquired data suggested that all the metals are present in their metallic states. The observed binding energies for Au, Pd and Pt were 83.2, 335.0 and 70.7 eV respectively. The binding energies associated with the Pd $3d_{5/2}$ and the Pt $4f_{7/2}$ peaks are characteristic of metallic Pd and Pt species[32, 45]. Au $4f_{7/2}$ peaks are typically observed at 84.0 eV [27]. This downward shift in binding energy is likely a result of the Au particles interacting with Ti^{3+} centres at defect sites[28]. The quantity of Au on the surface of the trimetallic catalyst appears to be lower than the amount determined by MP-AES when compared against Pd and Pt. This may be a due to the formation of core-shell like structures which have an Au rich core. Looking at the nanoparticles in closer detail using TEM-EDX could provide further evidence for this theory.

Table 3.14. The atomic ratios of the elemental constituents associated of each catalyst was determined using XPS.

Catalyst	Atomic weight (%)						Atomic ratios		
	Pd	Au	Pt	O	Ti	O/Ti	Pd/Au	Pd/Pt	Pt/Au
1% AuPdPt/TiO$_2$	0.27	0.07	0.18	68.84	30.63	2.25	3.19	1.51	2.44
1% PdPt/TiO$_2$	0.41	0.00	0.28	68.35	30.96	2.21	-	1.49	-
1% AuPt/TiO$_2$	0.00	0.08	0.10	68.76	31.05	2.21	-	-	1.29
1% AuPd/TiO$_2$	0.42	0.12	0.00	68.38	31.08	2.20	3.00	-	-
1% AuPdPt/TiO$_2$ used	0.10	0.05	0.10	69.04	30.71	2.25	1.55	1.03	1.99

From an industrial perspective, the stability of a catalyst is crucially important. For this reason, re-suability studies were conducted to assess the stability of the trimetallic AuPdPt/TiO$_2$ catalyst over subsequent uses.

There is evidence to suggest that the catalyst may be undergoing a change upon subsequent uses. There is very little change in the performance of the catalyst in the 1st re-use test. A small increase in activity is observed which could indicate that some residual PVA was washed off during the first test. A previous study has showed that refluxing the catalyst at 90 ºC in H$_2$O can remove large quantities of PVA from the surface of the catalyst[46],

conditions which are not too dissimilar from the reaction conditions used for these tests. It has previously be shown that stabilisers can cause reductions in catalytic activity due to the blocking of active sites.[47]. This could explain the increase in activity of the AuPdPt/TiO$_2$ in the first re-use test. Nevertheless, the slight increase in conversion almost certainly falls within experimental error and so this theory cannot be supported with such limited evidence.

Table 3.15. The re-usability of the AuPdPt/TiO$_2$ catalysts for the oxidation of glycerol under base free conditions is assessed over subsequent runs. **Reaction conditions:** 10 mL, substrate (0.3 M), O$_2$ (3 bar), substrate:metal ratio = 2728, 60 ℃, 24 h.

Run	Con at 24 h (%)	Selectivity (%)							C.M.B. (%)
		GA	TA	GLA	OA	DHA	βHA	FOA	
Initial	18	65	1	3	0	30	1	0	95
Re-use 1	18	60	1	2	0	35	1	1	88
Re-use 2	8	50	3	2	1	43	1	1	95

Interestingly, a substantial loss in activity and change in selectivity is observed in the 2nd reuse test. PSD were determined for the catalysts (Figure 3.12) which were obtained at each stage of testing shows a dramatic increase in the mean particle size between the 1st and second reuse tests; from 2.64 to 4.34 nm respectively. This increase in particle size supports the activity data in Table 3.15, as it is known that smaller nanoparticles are more active for alcohol oxidation[48]. There appears to be considerable change in C$_3$ selectivity which indicates that the formation of H$_2$O$_2$ is not dependent on the particle size. However, the selectivity to DHA appears to increase at the expense of GLAD which may suggest that the size of the metal particles could affect the position of the equilibrium between DHA and GLAD.

Previous studies have shown that the support can significantly affect the performance of Au nanoparticles for the selective oxidation of glycerol[4]. For this reason, the trimetallic AuPdPt complex was supported on a range of different supports and the resulting catalysts were assessed for their ability to oxidise glycerol under base free conditions. The corresponding results are displayed in Table 3.16.
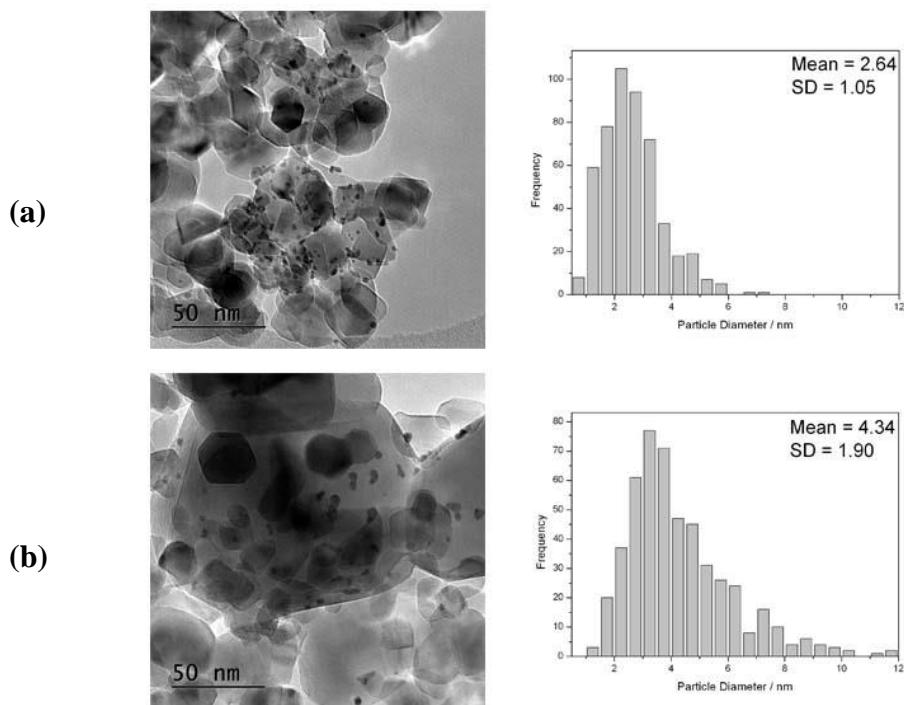
Figure 3.12. Images and PSD's retrieved for the re-use catalysts by TEM: (a) AuPdPt/TiO$_2$ after first re-use and (b) AuPdPt/TiO$_2$ after the second re-use

The variation in the observed conversions highlights the importance of the support selection for the base free oxidation of glycerol. Mg(OH)$_2$ appears to be the most active support for the trimetallic system, displaying conversions of 20.3 and 68.3 at 0.5 h and 24 h respectively. Mg(OH)$_2$ has previously been discarded as a viable support for base free oxidation as it has been shown that Mg^{2+} ions can leach from the support, inducing a homogeneous base catalysed system[13]. As discussed previously, no DHA or GLAD are observed when this reaction is conducted in the presence of NaOH. Interestingly, high quantities of DHA were observed with the Mg(OH)$_2$ after 0.5 h, which could indicate that the leaching of Mg from the support is minimal. If this is the case, it is likely that the high activity is attributed to the highly basic nature of the Mg(OH)$_2$. This would also explain the observed deactivation of the catalyst with time. If OH$^-$ species from the support are playing an active role in the catalysis, it may be difficult to replenish these sites given the base free reaction medium. A similar deactivation is observed with all the other supports.

Table 3.16. AuPdPt nanoparticles were immobilised on a range of catalytic supports and assessed for their performance to oxidise glycerol under base free conditions. ([a] corresponds to catalysts prepared by the conventional sol-immobilisation technique and [b]corresponds to catalysts prepared by the modified sol-immobilisation technique). **Reaction conditions:** 10 mL, substrate (0.3 M), O_2 (3 bar), substrate:metal ratio = 2728, 60 ºC, 24 h.

Support	Time (h)	Con (%)	Selectivity (%)								C.M.B. (%)
			GA	TA	GLA	LA	OA	DHA	βHA	FOA	
TiO$_2$[a]	0.5	4	54	0	0	0	1	42	0	3	97
	1	6	58	0	2	0	1	39	1	0	96
	2	8	60	1	2	0	1	37	1	0	96
	4	10	64	1	2	0	1	32	1	0	95
	24	18	65	1	3	0	0	30	1	0	95
Mg(OH)$_2$[a]	0.5	20	46	0	0	0	3	50	0	1	97
	1	39	54	8	8	0	2	27	0	1	86
	2	46	59	10	10	0	4	13	0	1	83
	4	55	63	10	12	0	6	7	0	2	75
	24	68	52	17	15	0	14	2	0	1	68
Graphite[a]	0.5	4	47	1	0	0	0	50	1	1	98
	1	8	51	0	1	0	1	45	1	0	96
	2	16	53	1	1	0	0	43	2	0	91
	4	21	55	1	1	0	0	41	3	0	89
	24	43	56	1	3	0	0	37	4	0	84
CeO$_2$[b]	0.5	2	36	0	0	0	3	56	0	6	98
	1	3	50	0	0	0	2	46	0	3	98
	2	4	48	0	0	0	0	50	0	2	97
	4	5	50	0	0	0	1	47	1	2	97
	24	16	58	0	3	0	0	38	2	1	90
ZrO$_2$[a]	0.5	2	34	0	0	0	2	59	59	5	98
	1	3	33	0	0	0	2	62	62	3	97
	2	5	34	0	10	0	2	53	53	2	97
	4	6	33	0	7	0	1	57	57	2	96
	24	22	48	0	6	0	0	45	45	1	84
CeZrO$_4$[b]	0.5	3	24	0	31	0	0	45	0	0	98
	1	5	37	0	0	0	2	56	2	4	97
	2	6	45	1	0	0	2	47	2	3	96
	4	7	47	1	4	0	1	43	2	2	96
	24	20	51	0	5	0	1	41	1	1	84

The C_3 selectivity appears to be relatively consistent across all the supports except for the $Mg(OH)_2$ and ZrO_2. There is significantly more glycolic acid (GLA) observed with these supports which could indicate that these materials are promoting the production of H_2O_2. The H_2O_2 is believed to be formed from the reduction of O_2 by H_2O, however if this was the case, the C_3 selectivity of all the catalysts would be comparable. This indicates that there may be additional pathways responsible for the C-C cleavage which are promoted by surface bound hydroxyl species.

The choice of support also appears to affect the substrates ability to undergo sequential oxidations reactions. The AuPdPt/graphite catalysts gives a high selectivity to GA and DHA, even at relatively high conversions; a combined GA and DHA selectivity of 92.9 % is observed at a conversion of 42.7 %. On the contrary, a combined selectivity of 72.1 % for GA and DHA is observed at a conversion of 54.6 % with the AuPdPt/$Mg(OH)_2$ system. The carbon mass balances associated with all the catalysts are relatively low considering the small quantities of glycerol converted. It has been shown that CO_2 can be formed as a results of sequential oxidations in this reaction[41] but considering the fairly low selectivity to C_1 and C_2 products, it is likely that products are being produced which are not being accounted for in the analysis.

To summarise, a trimetallic AuPdPt/TiO_2 was found to be more active than corresponding bimetallic catalysts containing Au, Pd and Pt for the base free oxidation of glycerol. It was not possible to replicate the high activity observed in the presence of a sacrificial base. Nevertheless, it was determined that the choice of the support can clearly have a significant impact on activity which certainly leaves room for further development moving forward.

3.6. The Selective Oxidation of Glycerol to Tartronic Acid

Tartronic acid (TA) can be produced from the oxidation of glycerol in the presence of a heterogeneous catalyst. It has previously be shown that TA can be used as a precursor for the formation of mesoxalic acid using bismuth promoted Pt catalysts[49]. In addition, the use of TA as a target compound for the selective oxidation of glycerol could act as a model for the formation of other high value products through the selective catalytic oxidation of alcohols.

To my knowledge, there are no current publications whose objective is solely based on the production of TA from glycerol using a heterogeneous catalyst. The limiting obstacle to overcome is the C-C cleavage which readily occurs as a result of in-situ H_2O_2 production under reaction conditions[15, 16]. Very recent studies have suggested that hydrophobic supports can reduce the production of H_2O_2 during the reaction[4]. Prati and co-workers[50] recently showed that controlling the hydrophobicity of carbon supports can reduce the unfavourable C-C cleavage. It was revealed that increasing the hydrophobic nature of the supports led to the formation of less C_1 and C_2 products.

To determine the influence of the catalyst support on H_2O_2 production, a series of 1% Au catalysts were prepared on a range of supports and tested for the oxidation of glycerol under standard reactions conditions. The corresponding results are displayed in Table 3.17. It is clear from these tests that the support can significantly influence both the activity and selectivity of the catalyst. Of the supports tested, TiO_2 was found to be the least active for this reaction with only 48.7 % of the substrate converted after an 8 h reaction. On the contrary, all the other catalysts gave 100 % conversions, with graphite appearing to be the most active in the early stages of the reaction. The Au/Graphite gave a conversion 56.2% after just 0.5 h of reaction.

SnO_2 and $CeZrO_4$ were found to favour the production of LA more than the other catalyst supports. The high LA selectivity of these supports was predominantly observed at the beginning of the reactions with selectivity appearing to decrease as the reaction proceeds. It is unlikely that this decrease is a result of LA consumption as it was shown previously that LA is fairly stable under standard reaction conditions in the presence of a 1% $AuPt/TiO_2$ catalyst.

Table 3.17. Au nanoparticles were immobilised on a range of supports and tested for the oxidation of glycerol under standard conditions. Catalyst were prepared by the sol-immobilisation technique, (catalysts with * prepared by modified sol technique). **Reaction conditions:** 10 mL, substrate (0.3 M), O_2 (3 bar), substrate:metal ratio = 500:1, NaOH:substrate = 2, 60 ℃, 4 h.

Catalyst	Time (h)	Con (%)	Selectivity (%)						TA Yield (%)	C.M.B. (%)
			GA	TA	LA	GLA	OA	FOA		
Au/TiO₂	0.5	15	68	3	7	9	3	11	3	93
	1	21	66	3	6	8	2	15	6	99
	2	36	68	4	7	10	1	11	12	100
	4	39	68	4	7	11	1	9	15	103
	8	49	69	3	6	10	1	10	16	100
Au/Graphite*	0.5	56	57	17	9	8	4	5	8	93
	1	71	57	19	8	8	5	5	12	93
	2	88	58	20	7	7	5	4	16	92
	4	98	50	27	6	7	5	5	24	92
	8	100	36	40	6	7	7	5	37	92
Au/Mg(OH)₂	0.5	19	56	26	5	4	3	2	6	102
	1	44	58	27	5	5	3	3	11	98
	2	82	54	31	3	6	3	3	22	91
	4	98	47	37	3	6	4	3	30	84
	8	100	38	45	3	6	4	3	26	58
Au/XC72R*	0.5	46	53	13	7	15	4	7	7	103
	1	79	52	16	5	14	5	7	12	92
	2	93	50	20	5	14	5	7	17	92
	4	99	47	24	4	13	5	7	21	91
	8	100	44	27	4	13	5	7	25	93
Au/CeZrO₄*	0.5	21	61	9	22	4	3	3	2	102
	1	70	63	12	15	4	3	3	7	91
	2	90	65	12	13	4	3	3	11	98
	4	100	62	14	12	4	5	3	14	96
	8	100	58	16	12	4	7	4	15	94
Au/BN*	0.5	42	56	21	9	7	4	4	7	90
	1	84	52	27	6	7	5	4	20	89
	2	99	46	33	5	6	6	4	29	89
	4	100	37	41	4	7	7	4	36	90
	8	100	32	46	4	7	8	4	42	91
Au/CB₄*	0.5	34	56	19	10	7	4	5	5	92
	1	57	54	19	9	8	7	6	10	92
	2	93	49	25	7	9	5	7	21	93
	4	100	42	32	6	8	6	7	27	86
	8	100	36	37	6	8	6	7	38	88
Au/SnO₂*	0.5	20	57	14	22	3	2	2	2	96
	1	41	59	15	21	3	2	2	5	92
	2	77	61	16	16	4	2	3	11	92
	4	99	59	20	13	4	2	3	18	88
	8	100	50	27	13	5	3	3	24	90

MP-AES was conducted in order to assess the Au loadings associated with each of the supports. The derived metal loadings corresponding to each catalyst are displayed in Table 3.18.

Table 3.18. MP-AES was used to determine the Au loadings of each of the catalysts.

Catalyst	Au Loading (wt.%)	TOF (h^{-1})
Au/BN	0.69	603
Au/Graphite	0.83	668
Au/TiO$_2$	0.94	163
Au/SnO$_2$	0.73	271
Au/Mg(OH)$_2$	0.93	205
Au/C$_4$B	0.58	576
Au/CeZrO$_4$	0.68	310

In order to determine the supports ability to facilitate C-C cleavage, it is important to consider the selectivity towards the C$_1$ and C$_2$ products. For this reason, the yields of GA and TA produced, were used as a means of assessing the selectivity of each catalyst. Furthermore, as it was difficult to compare the activities of each catalyst after the full reaction, each catalyst's activity was assessed in terms of the TOF it exhibited at 0.5 h.

The dashed box in Figure 3.13 shows the highest performing catalysts from both the perspectives of activity and selectivity. These catalysts were Au/BN, Au/C$_4$B and Au/Graphite. Interestingly, all these supports are considered to be hydrophobic, which provides further evidence to support Prati and co-workers, who postulated that hydrophobic supports reduce C-C cleavage[50]. As a result, these catalysts were selected for further assessment moving forward

As TA is a product of the sequential oxidation of GA, it was necessary to conduct some extended runs in order to determine whether higher yields of TA can be achieved after a longer reaction time. The extended reaction profiles for the oxidation of glycerol over Au/BN, Au/C$_4$B and Au/Graphite are displayed in Figures 3.14, 3.15 and 3.16.
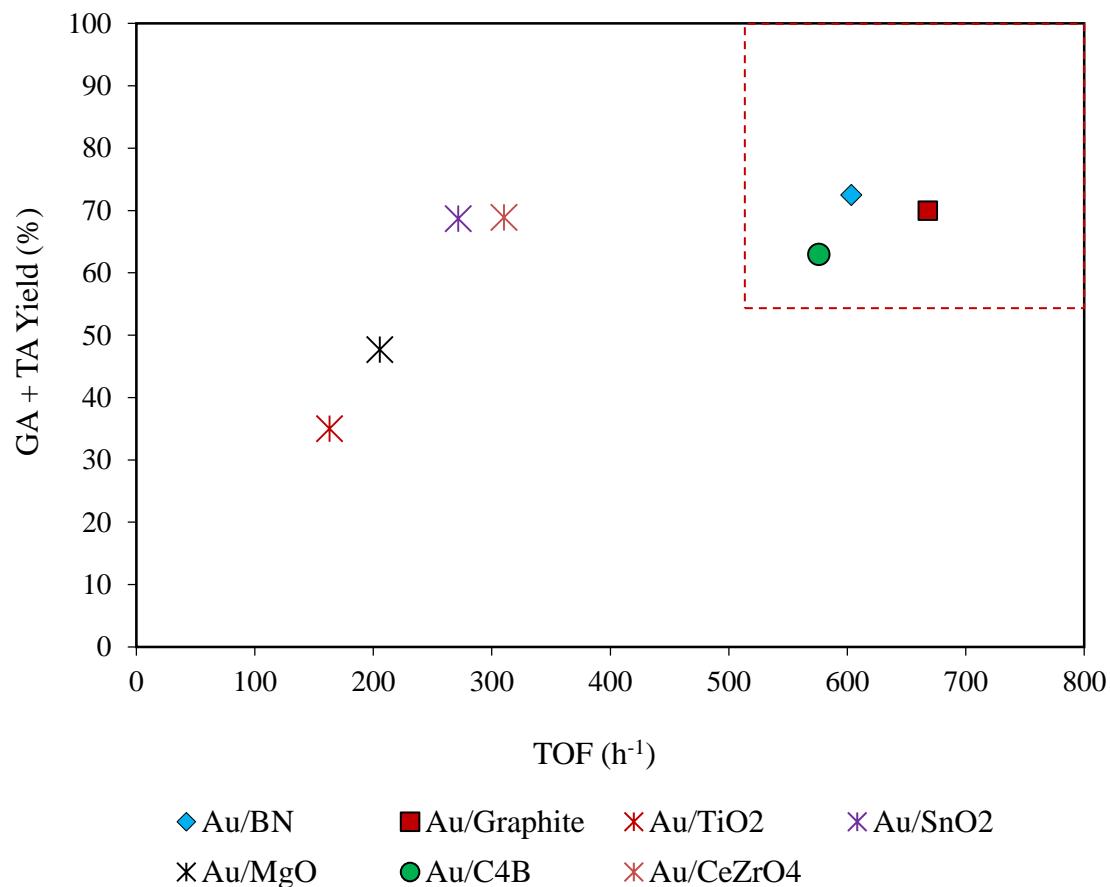
Figure 3.13. The combined yields of GA and TA are assessed as a function of TOF for the Au supported catalysts.

All three of the catalysts have similar reactions profiles over 24 h. Each catalyst gives a similar selectivity to LA, which is predominantly produced within the early stages of the reaction. The majority of the C_3 cleavage appears to take place within the first 8 h, as there appears to be no further increase in selectivity to C_1 and C_2 products after that time. At this point, all the glycerol, DHA and GLAD has been consumed, which could suggest that the cleavage predominantly occurs from these products. This supports the work by Davis and co-workers, who suggested that GLAD and DHA form a hydroperoxy adduct in the presence of supported Au nanoparticles, which in turn, leads to the formation of glycolic acid *via* a glycolaldehyde intermediate[16].
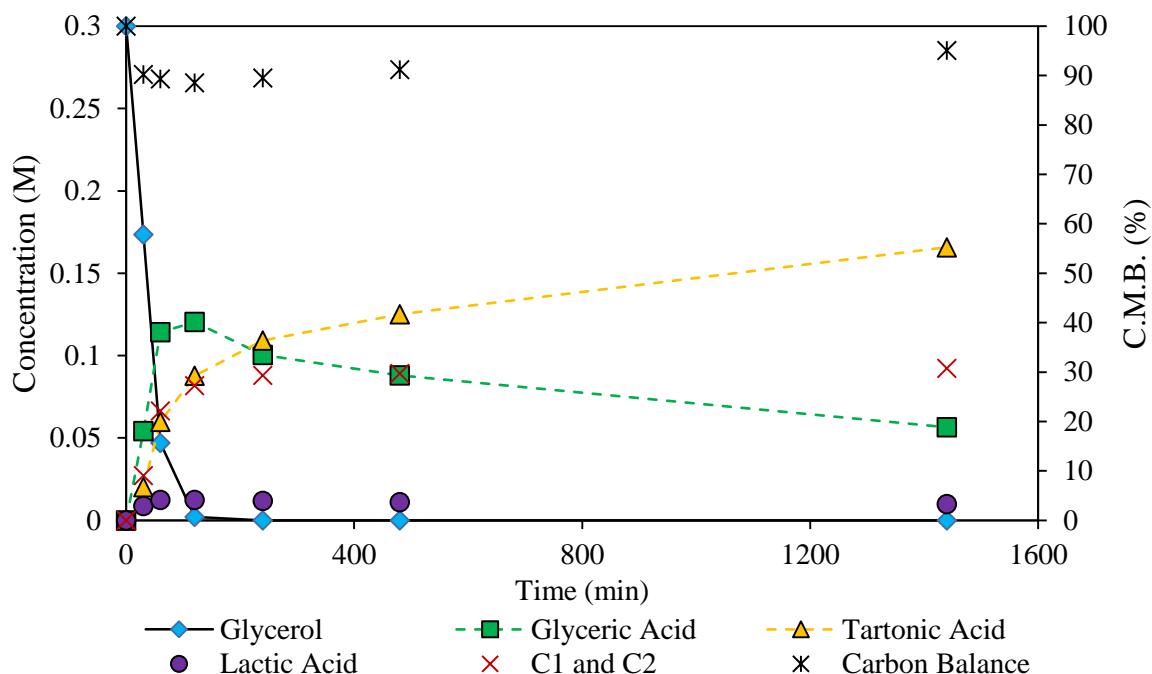
Figure 3.14. Plot displaying the performance of the Au/BN catalyst over 24 h. **Reaction conditions:** 10 mL, substrate (0.3 M), O_2 (3 bar), NaOH:substrate = 2, substrate:metal ratio = 500:1, 60 °C, 24 h.
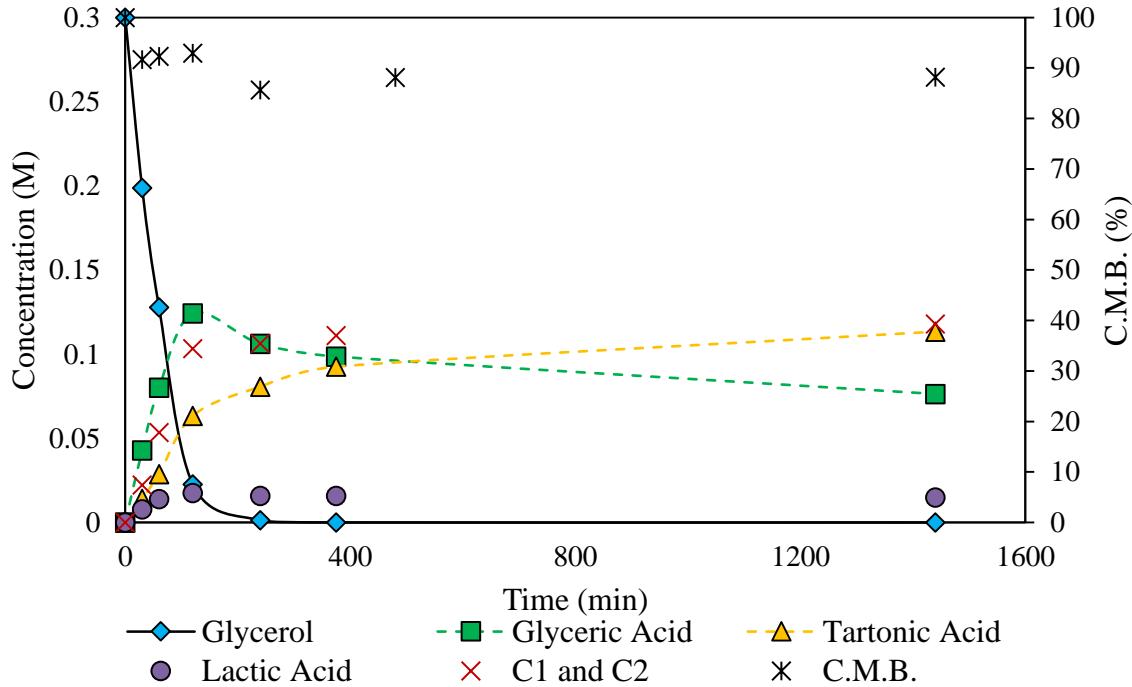
Figure 3.15. Plot displaying the performance of the Au/C$_4$B catalyst over 24 h. **Reaction conditions:** 10 mL, substrate (0.3 M), O_2 (3 bar), NaOH:substrate = 2, substrate:metal ratio = 500:1, 60 °C, 24 h.
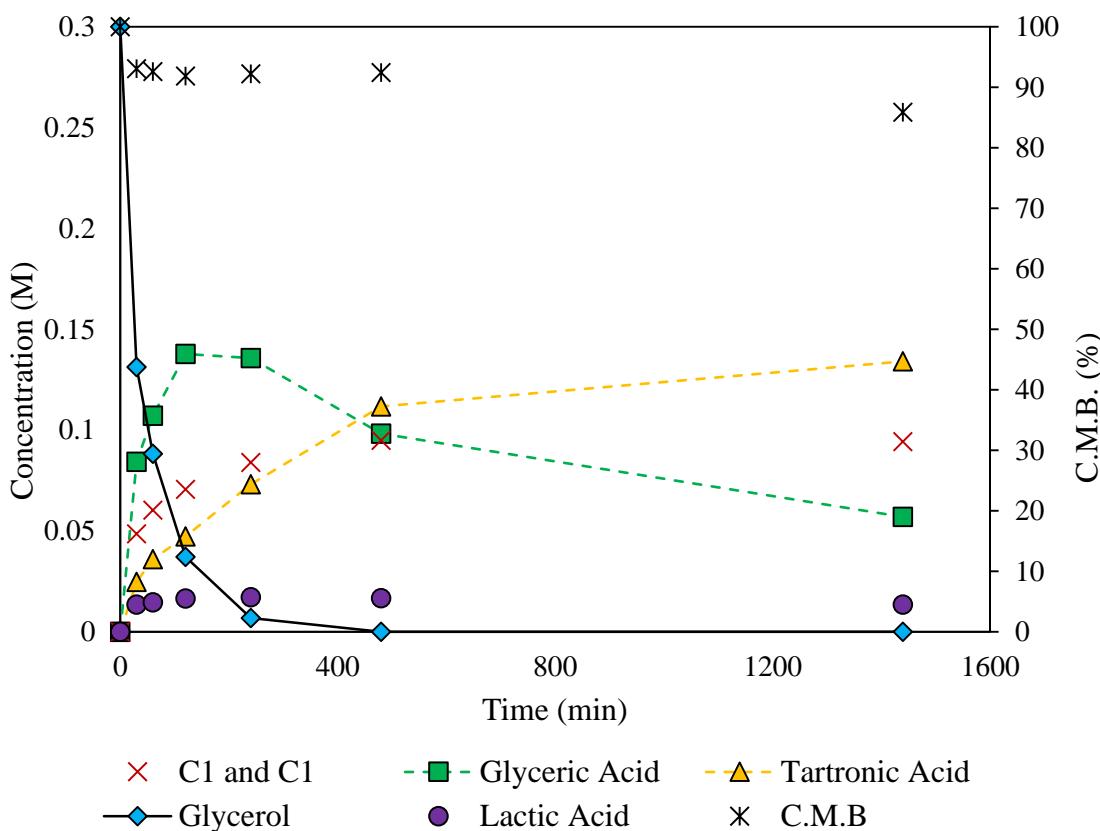
Figure 3.16. Plot displaying the performance of the Au/Graphite catalyst over 24 h. **Reaction conditions:** 10 mL, substrate (0.3 M), O_2 (3 bar), NaOH:substrate = 2, substrate:metal ratio = 500:1, 60 ℃, 24 h.

The purpose of increasing the reaction length was to determine whether greater yields of TA could be produced. The highest TA yield was observed with the Au/BN catalyst which gave a yield of 55.3 % after 24 h. This increase however, was fairly insignificant, as a yield of 41.5 % was originally observed after only 8 h. This trend was observed with all three of the catalysts, which could suggest that they are being deactivated during the reaction. In the initial stages of the reaction, GA appears to be converted to TA rapidly when compared to its conversion in the later stages. As the Au/BN catalyst gave the most favourable results, it was used for further experimentation and a new batch was produced. The Au weight loading of the new catalysts was confirmed as 0.893 wt. % by MP-AES. In order to assess why this deactivation was taking place, product inhibition studies were conducted, where 0.05 M of product was added to the standard reactants at the beginning of the reaction. The results of these tests are displayed in Table 3.19.

Table 3.19. The effect of reaction products on the activity of the Au/BN catalyst is assessed. * corresponds to the compound in which 0.05 M is added at the beginning on the reaction. The reduction in oxidation activity is determined by: $((TOF_{STANDARD}-TOF_{COMPOUND*}) / TOF_{STANDARD}) \times 100)$

Reaction	% Con at 0.5 h	% Con at 2 h	TOF (h^{-1})	Reduction in Oxidation Activity (%)
Standard	40	75	438	0
Oxalic Acid*	47	83	521	- 19.0
Glycolic Acid*	26	45	288	34.2
Formic Acid*	30	67	328	25.1
Na_2CO_3 *	50	82	555	- 26.8
Tartronic Acid*	40	82	441	- 0.8

It is evident that the incorporation of additional compounds at the beginning of the reaction can have an effect on the activity of the Au/BN catalyst. GLA and FOA appear to reduce the activity of the catalyst, as a reduction in oxidation activity of 34.2 and 25.1 % was observed respectively. This reduction in performance is also reflected in the corresponding glycerol conversions after two hours. Zope et al.[51] conducted a similar study and suggested that small organic compounds can affect the activity of Au supported catalysts. In their study, the addition of small amounts of TA was found to significantly deactivate a 1% Au/TiO$_2$. TA did not appear to have any effect on the activity of the Au/BN and so it can be speculated that the support may affect the deactivation of the catalysts. Interestingly, the presence of OA and Na_2CO_3 appears to promote the catalytic activity. Carbonates have previously been shown to poison Au catalysts in the oxidation of carbon monoxide[52]. Davis and co-workers have previously highlighted the important role of surface bound OH$^-$ species in the oxidation of glycerol[14]. It is possible that the Na_2CO_3 may be promoting activity of the catalyst through the donation of additional oxygen to the support. Once bound, it could easily pick up a hydrogen atom given the aqueous environment and subsequently provide an additional surface bound OH$^-$ species. In order to gain a further understanding into the effect of these species, the catalysts were retrieved after the reactions and characterised by TGA (Figure 3.17).
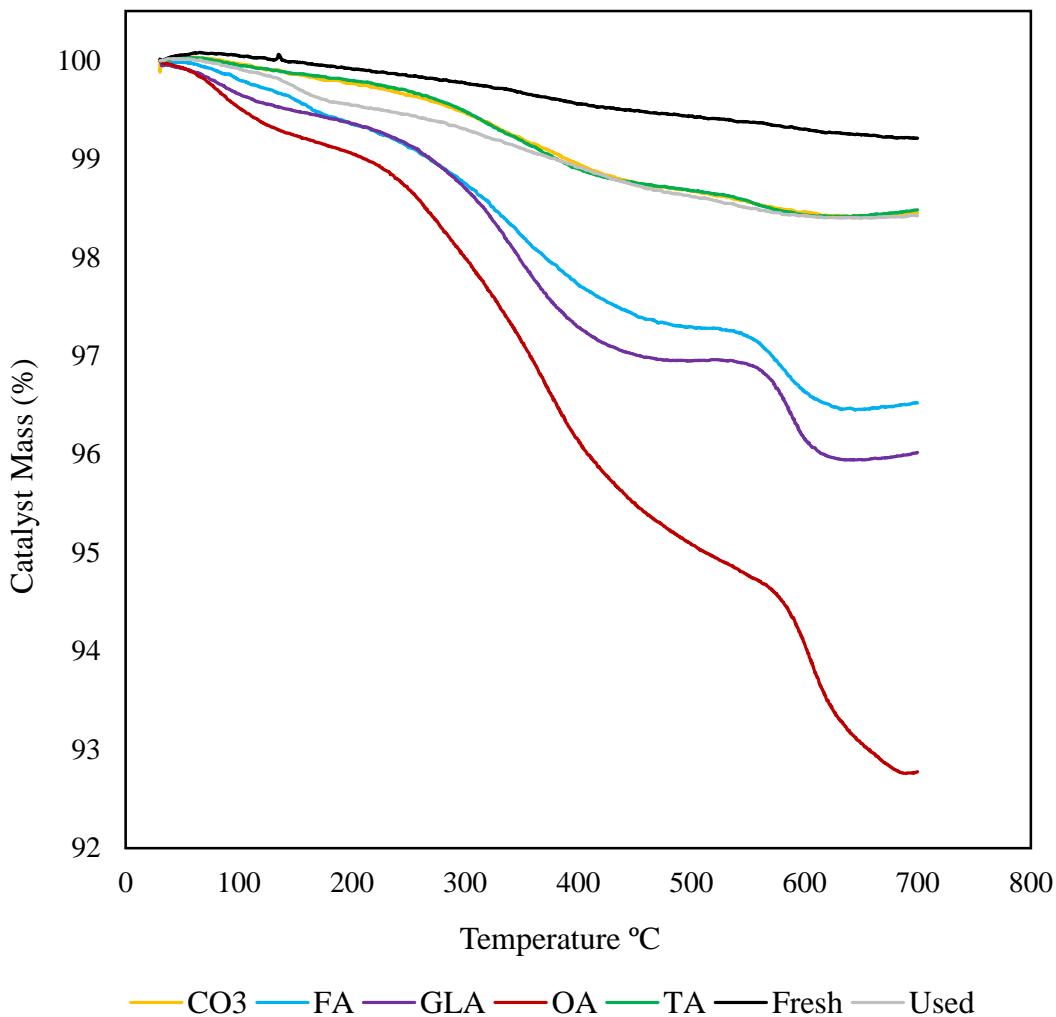
Figure 3.17. The TGA traces corresponding to Au/BN catalyst after exposure to an additional 0.05 M of a given compound at the beginning of the reaction. 'Used' corresponds to the Au/BN catalyst after a standard 4 h reaction. 'Fresh' corresponds to an unused sampled of the Au/BN catalyst.

There is a noticeable difference in mass lost as the catalysts are heated. The fresh catalyst had the smallest loss in mass; 0.8% after being heated to 700 ℃. Interestingly, higher losses in mass are observed for all the other catalysts, suggesting that the catalysts exposed to the reaction medium may be accommodating adsorbed organic species. Au/BN which was tested under standard conditions exhibited a loss in mass of 1.46 % at 700 ℃. This supports the theory that products produced in the reaction may be inhibiting the performance of the catalyst. The catalysts which were tested in the presence of additional quantities of CO_3 and TA showed almost identical TGA profiles as the used catalyst. This could indicate that

these compound neither promote catalyst deactivation themselves, nor lead to the formation of other catalytic inhibiting species. On the contrary, significant losses of mass were observed for OA, GLA and FOA of 7.23, 3.94 and 3.48 % respectively at 700 ºC.

The large losses of mass exhibited by the catalyst after exposure to additional quantities GLA and FOA support the experimental data in Table 3.19. It is evident that GLA and FOA bind strongly to the catalyst, which could be inhibiting the catalysts activity through the blocking of active sites. The highest mass loss observed was when Au/BN was exposed to additional quantities of OA at the beginning of the reaction. Interestingly, the experimental data in Table 3.19 shows a dramatic increase in catalyst oxidation activity was observed when additional OA was present in the reaction system. This may suggests that OA binds strongly to the catalyst, and has a promotional effect on its activity. It is possible that the OA predominantly adsorbs to the surface of the support, rather than the metal active sites.

It has been postulated for some time that H_2O_2 is responsible for the unfavourable C-C cleavage observed in the oxidation of glycerol. For this reason, a series of tests were conducted where varied quantities of H_2O_2 were added at the beginning of the reaction. The results for these tests are displayed in Table 3.20.

It is clear from the experimental data that H_2O_2 does have an effect on the C_3 selectivity of the reaction. Increasing the concentration of H_2O_2 at the beginning of the experiment appears to result in a decrease in C_3 selectivity, most noticeably at the beginning of the reaction. This relationship is displayed in Figure 3.18. Interestingly, there does not appear to be any significant decreases in C_3 selectivity after this time. This is likely a result of any excess of H_2O_2 rapidly breaking down in the reaction medium. H_2O_2 also appears to increase the rate of glycerol consumption. A proportional relationship between the quantity of H_2O_2 and initial substrate consumption is observed. This suggests that the H_2O_2 may play a role in the activation of glycerol.

The reactions run in the absence of catalyst reveal that both the catalyst and H_2O_2 are required for the C-C cleavage to occur. The H_2O_2 is unable to interact with the substrate independently of the catalyst, which further support the theory that C-C cleavage occurs through Dakin Oxidation. There does not appear to be any decrease in C_3 selectivity when H_2O_2 is added at different stages of the reaction which is unexpected. This may be due to

the majority of reactant having surpassed GLAD and DHA in the oxidation sequence when the additional H_2O_2 was added.

Table 3.5. Varying quantities of H_2O_2 were added to the Au/BN catalyst for the oxidation of glycerol under standard reaction conditions. *Ratio of H_2O_2 added at 0, 0.5, 1 and 2 h of the reaction. [b] reaction in absence of catalyst but presence of base, [bf] reaction in absence of both catalyst and base. **Reaction conditions:** 10 mL, substrate (0.3 M), O_2 (3 bar), NaOH:substrate = 2, substrate:metal ratio = 500:1, H_2O_2:metal stated, 60 °C, 4 h.

H_2O_2 : Metal	Time (h)	Con (%)	Selectivity (%)						C.M.B. (%)	C_3 Sel (%)
			GA	TA	LA	GLA	OA	FOA		
0	0.5	40	52	25	8	6	5	4	90	85
	1	75	50	28	5	7	5	4	89	83
	2	97	46	33	4	7	6	4	87	83
	4	100	43	36	4	7	6	4	87	83
106.3	0.5	47	50	26	5	8	6	5	92	81
	1	84	48	28	4	8	7	5	91	81
	2	98	45	32	4	8	7	5	89	81
	4	100	42	36	3	7	7	5	90	81
212.6	0.5	54	49	26	5	9	6	5	94	80
	1	85	48	29	4	9	6	5	90	80
	2	97	45	32	3	8	7	5	90	80
	4	99	42	35	3	8	7	5	91	80
318.9	0.5	60	48	27	4	9	7	5	93	79
	1	90	45	31	3	8	8	5	96	79
	2	99	41	36	3	8	9	5	105	79
	4	100	31	44	3	8	10	5	105	78
212.6 *	0.5	52	51	25	6	9	5	5	90	81
	1	81	50	27	5	9	5	5	90	81
	2	97	48	30	4	8	5	5	89	82
	4	99	46	32	4	8	6	5	88	82
212.6 [b]	0.5	0	0	0	0	0	0	0	100	-
	1	0	0	0	0	0	0	0	100	-
	2	0	0	0	0	0	0	0	100	-
	4	0	0	0	0	0	0	0	100	-
212.6 [bf]	0.5	0	0	0	0	0	0	0	100	-
	1	0	0	0	0	0	0	0	100	-
	2	0	0	0	0	0	0	0	100	-
	4	0	0	0	0	0	0	0	100	-
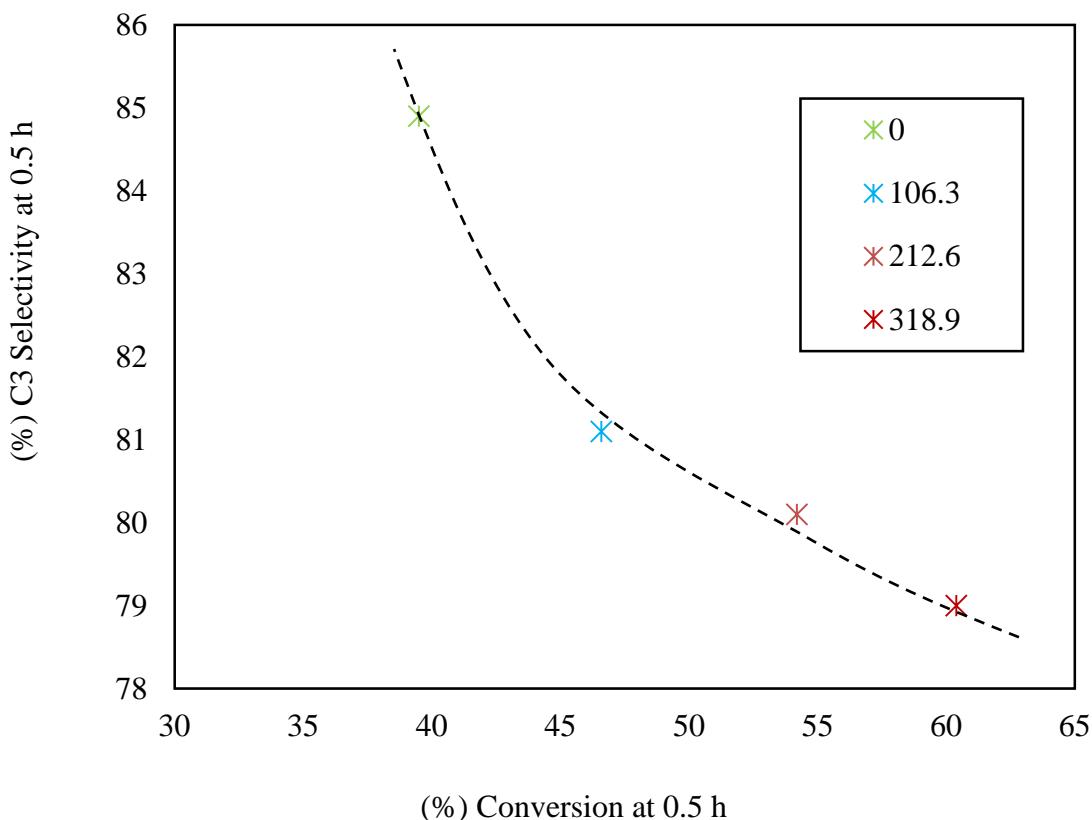
Figure 3.18. The C_3 selectivity appears to decrease as the quantity of H_2O_2 added at the beginning of the reaction is increased. The insert corresponds to the H_2O_2 : metal ratio. **Reaction conditions:** 10 mL, substrate (0.3 M), O_2 (3 bar), NaOH:substrate = 2, substrate:metal ratio = 500:1, 60 °C, 4 h.

Although the addition of external H_2O_2 does appear to result in additional C-C cleavage, it does not seem plausible that it could account for the entirety of the cleavage observed. If this were the case, excessively large quantities of H_2O_2 would need to be produced *in-situ*. It is more likely that peroxy intermediate species formed on the metal nanoparticle adjacent to adsorbed substrate is what leads to unfavourable cleavage. Peroxy radicals have shown to have played significant roles in the oxidation of CO to CO_2 [53, 54]. Davis and co-workers postulated that peroxy intermediate species are formed during the oxidation of glycerol by the reduction of O_2 with H_2O [15]. Na_2SO_3 and $NaNO_3$ can act as radical quenchers for *OH and *OOH respectively. Hutchings and co-workers have previously used these reagents in order to gain a further understanding of the mechanisms associated with methane activation [55]. As a result, a series of tests were constructed in order to determine the effect

*OH and *OOH radicals have on the oxidation of glycerol in the presence of Au/BN. The results of these tests are displayed in Table 3.21.

Table 3.21. All tests were conducted under standard reactions conditions. Re-use* corresponds to a reaction where Au/BN has been collected at the end of the Na_2SO_3 reaction, dried and re-tested. **Reaction conditions:** 10 mL, substrate (0.3 M), O_2 (3 bar), NaOH:substrate = 2, substrate:metal ratio = 500:1, radical scavenger (10 mg), 60 ℃, 4 h.

Reaction	Time (h)	Con (%)	Selectivity (%)						C.M.B. (%)
			GA	TA	LA	GLA	OA	FOA	
Standard	0.5	40	52	25	8	6	5	4	90
	1	75	50	28	5	7	5	4	89
	2	97	46	33	4	7	6	4	87
	4	100	43	36	4	7	6	4	87
NaNO₃	0.5	50	52	24	5	7	7	4	94
	1	86	49	28	4	7	8	4	90
	2	100	44	33	3	7	9	4	91
	4	100	38	38	3	7	10	4	90
Na₂SO₃	0.5	12	0	8	0	92	0	0	89
	1	15	44	1	0	32	0	22	92
	2	19	42	1	5	33	0	19	96
	4	30	45	1	4	30	0	20	97
Re-use *	0.5	44	63	16	7	8	2	5	102
	1	68	64	17	6	7	2	5	100
	2	82	64	18	5	6	1	5	103
	4	94	63	20	5	6	1	6	102
No Cat Na₂SO₃	0.5	0	0	0	0	0	0	0	100
	1	0	0	0	0	0	0	0	100
	2	0	0	0	0	0	0	0	100
	4	0	0	0	0	0	0	0	100

The *OOH radical scavenger did not appear to have a significant impact on the reaction profile when compared to the standard reaction. There is a slight increase in activity but the selectivity profile is almost identical. From this, it is clear that *OOH radicals do not play a major role in the C-C cleavage mechanism. On the contrary, the *OH radical quencher severely inhibited the activity of the catalyst. A drop in conversion from 39.5 % to 11.9 % is observed at 0.5 h when Na_2SO_3 was added at the beginning of the reaction.

The selectivity profile is also effected. A dramatic increase in selectivity to C_1 and C_2 products is observed. Interestingly, when this catalyst was re-used in the absence of the quencher, the catalysts activity and selectivity profile was comparable with the standard reaction. This shows that the quencher has no poisoning effect on the catalyst, suggesting that the change in performance can only be attributed to the absence of *OH radicals in the system

It is clear that the *OH radicals play an important role in the oxidation of glycerol to GA and TA as this pathway appears to be shut off in the presence of the quencher. A previous study used theoretical analysis to investigate the interaction of OH* radicals with Au surfaces[56]. It was shown that *OH radicals chemisorb onto Au forming a covalent bond. It has previously been suggested that the oxidation of glycerol to GA is reliant on the presence of surface bound OH⁻ species[16]. The decrease in selectivity to GA could be a result of a reduction of Au-OH species, produced from *OH radicals. Increasing the population of Au-OH species could therefore reduce the C-C cleavage by instead promoting the favoured oxidation pathway. On the contrary, the cause of the C-C cleavage still remains unclear as the relative concentrations of the C_1 and C_2 products do not appear to have changed significantly despite significant variations in catalytic activity. Thus, it can be concluded that *OH radicals do not directly contribute to C-C cleavage but appear to play a pivotal role in the oxidation of glycerol to GA and TA.

In an attempt to further increase the TA selectivity, small quantities of Pd and Pt were incorporated into the Au/BN catalyst. The catalysts were prepared by the modified sol-immobilisation technique and subsequently tested for the oxidation of glycerol. The results of these tests are displayed in Table 3.22. In order to accurately assess the differences in activity between the catalysts, the metal weight loadings were determined using MP-AES and the corresponding TOF's were calculated.

It was determined that the AuPd/BN catalyst was the most active. Previous studies have shown that the incorporation of Pd to Au can both promote[57] and reduce[10] catalytic activity. This suggests that the support-metal interaction has a significant impact on the activity of AuPd nanoparticles in this reaction. The AuPt/BN catalyst was also found to be more active than the monometallic Au/BN catalyst. AuPt catalysts have previously been shown to be more active than monometallic Au catalysts for this reaction.[18, 25]. The data in Table 3.23 and table 24 reveals how the addition of small quantities of Pd or Pt can have a significant

impact on catalytic activity. Interestingly, a noticeable increase in C_3 selectivity is also observed with the AuPd/BN catalyst when compared with the other catalysts. A decrease in C-C scission has been reported previously when comparing the selectivity of supported AuPd clusters with monometallic Au catalysts[58]. It is possible that the decrease in C-C scission is a result of the Pd facilitating the decomposition of H_2O_2 formed in the reaction.

Table 3.22. The performance of AuPd/BN and AuPt/BN was assessed for the oxidation of glycerol under standard reaction conditions. The results are compared against the activity of the Au/BN catalyst. **Reaction conditions:** 10 mL, substrate (0.3 M), O_2 (3 bar), NaOH:substrate = 2, substrate:metal ratio = 500:1, 60 ºC, 4 h.

Catalyst	Time (h)	Con (%)	Selectivity (%)						C.M.B. (%)
			GA	TA	LA	GLA	OX	FOA	
Au/BN	0.5	40	52	25	8	6	5	4	90
	1	75	50	28	5	7	5	4	89
	2	97	46	33	4	7	6	4	87
	4	100	43	36	4	7	6	4	87
AuPd/BN	0.5	57	66	17	9	3	2	3	98
	1	86	65	20	7	3	2	3	96
	2	97	63	22	7	3	2	3	94
	4	99	62	24	7	3	2	3	94
AuPt/BN	0.5	65	57	10	20	7	1	6	98
	1	98	57	14	17	6	1	5	88
	2	100	54	17	16	6	2	5	88
	4	100	51	20	16	6	2	5	89

Table 3.23. The metal weight loadings of the Au, Pd and Pt containing catalysts were determined by MP-AES. TOF's were calculated using the corresponding metal weights.

Catalyst	Total Metal Loading (wt.%)	Metal Content (%)			(%) Con at 0.5 h	TOF (h^{-1})
		Au	Pd	Pt		
Au/BN	0.89	100.0	-	-	40	438
AuPt/BN	0.99	90.3	-	9.7	65	656
AuPd/BN	0.80	96.4	3.6	-	56	768

3.7. Conclusions

The selective oxidation of glycerol was investigated over supported Au containing heterogeneous catalysts. The work in this chapter was divided into four fundamental sections.

The first section focussed on the use of a 1 wt.% AuPt/TiO$_2$ catalyst for the oxidation of glycerol. The reaction parameters were varied in order to assess how they effected the product distribution and rate of reaction. It was determined that increasing the reaction temperature and the concentration of NaOH favoured the production of LA. It was suggested that an increasing reaction temperature promoted the dehydration of a terminal alcohol species, whereas increasing the NaOH concentration promoted the intermolecular Cannizzaro reaction of methylglyoxal to produce LA. Both of these steps were recently hypothesised by Crabtree and co-workers to be key in transformation of glycerol to LA[37]. It was also observed that increasing these parameters appeared to increase the overall C$_3$ selectivity. Although this is likely a result of these conditions promoting the LA pathway, it was also suggested that this may be due to the high temperatures and base promoting the decomposition of H$_2$O$_2$ formed in the reaction. Increasing the O$_2$ pressure in the reaction was found to favour the production of GA and TA at the expense of LA. As a conseqeunce it was suggested that O$_2$ plays a pivitol role in activation of this direct oxidation pathway. Increasing the O$_2$ pressure was also found to increase the unfavourable C-C scission which ultimately led to the increased formation of C$_1$ and C$_2$ products. It was postulated that this was a result of increased H$_2$O$_2$ production, as it is believed that H$_2$O$_2$ is produced through the reduction of O$_2$ by H$_2$O[15]. It is clear from this work that the reaction conditions can be used to tune the reaction selectivity.

The purpose of the work conducted in the second section was to gain a further understanding of how the reaction products were affected by a 1 wt.% AuPt/TiO$_2$ catalyst and the reaction conditions. For these tests, reactions were conducted under standard condtions with the substrate being replaced with different reaction products. It was found that DHA and GLAD were immediately consumed in base promoted reactions. Exteremely low activities were observed when reactions were conducted from GA. Interestingly, the C$_3$ selectivity of these reactions was significantly less when compared with reactions from glycerol, suggesting that GA and possibly even TA may be terminal reaction products (glycerol is converted to GA or TA in one asdorption cycle). LA, OA and TA were all

found to be stable under the reaction conditions and thus, the C-C cleavage can not occur from these compounds. The studies conducted under base free conditons suggest that the cleavage occurs predominantly from GLAD, DHA and possibly even GA. This work has contributed to a further understanding of the reaction profile. GLAD, DHA and GA have been identified as possible candidates from which the C-C cleavage occurs. Nevertheless, further work is required in order to confirm this theory.

The third section of this chapter focussed on the use of Au, Pd and Pt catalysts supported on TiO_2 for the oxidation of glycerol under base free conditions. The oxidation of glycerol under base free conditions would be far more suitable from an industrial perspective but previous publications determined that high reaction rates were far more difficult to achieve in the absence of sacrifical base. Of the bimetallic catalysts tested, $PdPt/TiO_2$ was found to be the most active which was unusual as supported AuPt nanoparticles had previously been shown to be highly active under base free conidions[13]. Discrepancies in the metal weight loadings of the catalysts made it difficult to compare the catalysts and as a result, it was determined that the best method of comparing catalyst activities was using TOF calculations. From these calculations, a trimetallic $AuPdPt/TiO_2$ catalyst was found to be the most active catalyst tested. Synergistic interactions between the three metals were proposed to be the reason behind the high activity observed for this catalyst. Re-use studies were conducted on this catalyst and it was determined that the catalyst was not very stable. A substantial loss in activity was observed when the catalyst was tested for the third time. TEM confirmed that this was a result of particle agglomeration. AuPdPt nanoparticles were subsequently immobilised on a range of different supports and tested for the oxidation of glycerol under base free conditions. It was determined that the support can significantly affect the activity and selectivity of the catalysts, offering a possible avenue for further work.

The aim of the final section of work was to gain a further understanding of the causes of C-C cleavage, and ultimately optimise a catalyst which could provide a good TA yield. To begin with, Au was immobilised on a range of different supports and the resulting catalysts were tested for the oxidation of glycerol under standard conditions. Of the supports tested, BN, graphite and C_4B were identified as the most promising as they combined good C_3 selectivity with a high catalytic activity. It was postulated that their favourable C_3 selectivity was a result of the hydrophobic nature of the supports. These catalysts however, were found to deactivate over time, limiting the TA yield to only 55.3 % after 24 h for the

Au/BN catalyst. In order to investigate this deactivation further, product inhibition studies were carried out using the Au/BN catalyst. It was determined that FOA and GLY inhibited the catalysts activity by binding irreversibly to the catalysts active sites. The in-situ formation of H_2O_2 has long been seen as the culprit responsible for activating the C-C cleavage. A series of tests were conducted in order to assess whether externally added H_2O_2 could imitate the peroxide formed inside the reaction. It was found that increasing the H_2O_2 added at the beginning of the reaction increased the C-C scission. A further study was designed investigate the role of *OH and *OOH radicals in the reaction. It was determined that *OH radicals are essential for the production of GA and TA and therefore play an important role in the mechanism. The incorporation of Pd and Pt into the Au/BN catalyst substantially increased the catalytic activity. The AuPd/BN catalyst also displayed enhanced selectivity to TA, which was attributed to the Pd promoting the decomposition of H_2O_2.

The conclusions from this chapter support the theory that H_2O_2 plays a pivotal role in C-C cleavage. Dakin Oxidation was suggested to be the mechanism by which this occurs, as this relies on the activation of the substrate by H_2O_2 in a basic reaction medium. GLAD, DHA and GA were identified as the compounds which may partake in Dakin Oxidation. Moving forward, isotopic labelling experiments would be an ideal method of confirming these postulations. It was also suggested that GA and TA are primary reaction products and that *OH radical species are crucial in the direct oxidation of glycerol to GA and TA. The base free oxidation of glycerol still remains to be a challenge. It was suggested that optimisation of the support could be one method of increasing the reaction rates.

3.8. References

1. M. G. Kulkarni, R. Gopinath, L. C. Meher and A. K. Dalai, *Green Chemistry*, 2006, **8**, 1056.

2. H. Kimura, K. Tsuto, T. Wakisaka, Y. Kazumi and Y. Inaya, *Applied Catalysis A-General*, 1993, **96**, 217.

3. R. Garcia, M. Besson and P. Gallezot, *Applied Catalysis A-General*, 1995, **127**, 165.

4. A. Villa, N. Dimitratos, C. E. Chan-Thaw, C. Hammond, L. Prati and G. J. Hutchings, *Accounts of Chemical Research*, 2015, **48**, 1403.

5. N. Dimitratos, J. A. Lopez-Sanchez, D. Lennon, F. Porta, L. Prati and A. Villa, *Catalysis Letters*, 2006, **108**, 147.

6. A. Villa, N. Janjic, P. Spontoni, D. Wang, D. S. Su and L. Prati, *Applied Catalysis A-General*, 2009, **364**, 221.

7. S. Gil, M. Marchena, L. Sanchez-Silva, A. Romero, P. Sanchez and J. L. Valverde, *Chemical Engineering Journal*, 2011, **178**, 423.

8. B. Katryniok, H. Kimura, E. Skrzynska, J.-S. Girardon, P. Fongarland, M. Capron, R. Ducoulombier, N. Mimura, S. Paul and F. Dumeignil, *Green Chemistry*, 2011, **13**, 1960.

9. L. Prati and M. Rossi, *3rd World Congress on Oxidation Catalysis*, 1997, **110**, 509.

10. W. C. Ketchie, M. Murayama and R. J. Davis, *Journal of Catalysis*, 2007, **250**, 264.

11. N. Dimitratos, J. A. Lopez-Sanchez, J. M. Anthonykutty, G. Brett, A. F. Carley, R. C. Tiruvalam, A. A. Herzing, C. J. Kiely, D. W. Knight and G. J. Hutchings, *Physical Chemistry Chemical Physics*, 2009, **11**, 4952.

12. A. Villa, S. Campisi, C. E. Chan-Thaw, D. Motta, D. Wang and L. Prati, *Catalysis Today*, 2015, **249**, 103.

13. G. L. Brett, Q. He, C. Hammond, P. J. Miedziak, N. Dimitratos, M. Sankar, A. A. Herzing, M. Conte, J. A. Lopez-Sanchez, C. J. Kiely, D. W. Knight, S. H. Taylor and G. J. Hutchings, *Angewandte Chemie-International Edition*, 2011, **50**, 10136.

14. M. S. Ide and R. J. Davis, *Accounts of Chemical Research*, 2014, **47**, 825.

15. B. N. Zope, D. D. Hibbitts, M. Neurock and R. J. Davis, *Science*, 2010, **330**, 74.

16. W. C. Ketchie, M. Murayama and R. J. Davis, *Topics in Catalysis*, 2007, **44**, 307.

17. L. Prati, A. Villa, C. E. Chan-Thaw, R. Arrigo, D. Wang and D. S. Su, *Faraday Discussions*, 2011, **152**, 353.

18. C. L. Bianchi, P. Canton, N. Dimitratos, F. Porta and L. Prati, *Catalysis Today*, 2005, **102**, 203.

19. N. Dimitratos, A. Villa and L. Prati, *Catalysis Letters*, 2009, **133**, 334.

20. A. Villa, S. Campisi, K. M. H. Mohammed, N. Dimitratos, F. Vindigni, M. Manzoli, W. Jones, M. Bowker, G. J. Hutchings and L. Prati, *Catalysis Science & Technology*, 2015, **5**, 1126.

21. D. Tongsakul, S. Nishimura and K. Ebitani, *ACS Catalysis*, 2013, **3**, 2199.

22. D. Liang, J. Gao, H. Sun, P. Chen, Z. Y. Hou and X. M. Zheng, *Applied Catalysis B-Environmental*, 2011, **106**, 423.

23. C. Della Pina, E. Falletta and M. Rossi, *Chemical Society Reviews*, 2012, **41**, 350.

24. Y. Shen, S. Zhang, H. Li, Y. Ren and H. Liu, *Chemistry-A European Journal*, 2010, **16**, 7368.

25. L. Prati, A. Villa, C. Campione and P. Spontoni, *Topics in Catalysis*, 2007, **44**, 319.

26. F. Porta, L. Prati, M. Rossi, S. Coluccia and G. Martra, *Catalysis Today*, 2000, **61**, 165.

27. M. T. Anthony and M. P. Seah, *Surface and Interface Analysis*, 1984, **6**, 95.

28. J. A. Moma, M. S. Scurrell and W. A. Jordaan, *Topics in Catalysis*, 2007, **44**, 167.

29. A. Golabiewska, W. Lisowski, M. Jarek, G. Nowaczyk, A. Zielinska-Jurek and A. Zaleska, *Applied Surface Science*, 2014, **317**, 1131.

30. Z. Bastl and S. Pick, *Surface Science*, 2004, **566**, 832.

31. R. Zimmermann, P. Steiner, R. Claessen, F. Reinert, S. Hufner, P. Blaha and P. Dufek, *Journal of Physics-Condensed Matter*, 1999, **11**, 1657.

32. J. Thiele, N. T. Barrett, R. Belkhou, C. Guillot and H. Koundi, *Journal of Physics-Condensed Matter*, 1994, **6**, 5025.

33. M. Romeo, J. Majerus, P. Legare, N. J. Castellani and D. B. Leroy, *Surface Science*, 1990, **238**, 163.

34. P. A. Shaffer and T. E. Friedemann, *Journal of Biological Chemistry*, 1930, **86**, 345.

35. R. W. Nagorski and J. P. Richard, *Journal of the American Chemical Society*, 2001, **123**, 794.

36.   R. K. P. Purushothaman, J. van Haveren, D. S. van Es, I. Melian-Cabrera, J. D. Meeldijk and H. J. Heeres, *Applied Catalysis B-Environmental*, 2014, **147**, 92.

37.   L. S. Sharninghausen, J. Campos, M. G. Manas and R. H. Crabtree, *Nature Communications*, 2014, **5**.

38.   J. Gao, D. Liang, P. Chen, Z. Hou and X. Zheng, *Catalysis Letters*, 2009, **130**, 185.

39.   D. Liang, J. Gao, J. H. Wang, P. Chen, Z. Y. Hou and X. M. Zheng, *Catalysis Communications*, 2009, **10**, 1586.

40.   R. Nie, D. Liang, L. Shen, J. Gao, P. Chen and Z. Hou, *Applied Catalysis B-Environmental*, 2012, **127**, 212.

41.   D. Z. Jeffery and G. A. Camara, *Electrochemistry Communications*, 2010, **12**, 1129.

42.   Y. Kwon, K. J. P. Schouten and M. T. M. Koper, *Chemcatchem*, 2011, **3**, 1176.

43.   A. Villa, G. M. Veith and L. Prati, *Angewandte Chemie-International Edition*, 2010, **49**, 4499.

44.   J. K. Edwards, J. Pritchard, L. Lu, M. Piccinini, G. Shaw, A. F. Carley, D. J. Morgan, C. J. Kiely and G. J. Hutchings, *Angewandte Chemie-International Edition*, 2014, **53**, 2381.

45.   K. S. Kim, A. F. Gossmann and N. Winograd, *Analytical Chemistry*, 1974, **46**, 197.

46.   J. A. Lopez-Sanchez, N. Dimitratos, C. Hammond, G. L. Brett, L. Kesavan, S. White, P. Miedziak, R. Tiruvalam, R. L. Jenkins, A. F. Carley, D. Knight, C. J. Kiely and G. J. Hutchings, *Nature Chemistry*, 2011, **3**, 551.

47.   I. Gandarias, P. J. Miedziak, E. Nowicka, M. Douthwaite, D. J. Morgan, G. J. Hutchings and S. H. Taylor, *Chemsuschem*, 2015, **8**, 473.

48.   P. Haider, B. Kimmerle, F. Krumeich, W. Kleist, J.-D. Grunwaldt and A. Baiker, *Catalysis Letters*, 2008, **125**, 169.

49.   P. Fordham, M. Besson and P. Gallezot, *Catalysis Letters*, 1997, **46**, 195.

50.   A. Villa, M. Plebani, M. Schiavoni, C. Milone, E. Piperopoulos, S. Galvagno and L. Prati, *Catalysis Today*, 2012, **186**, 76.

51.   B. N. Zope and R. J. Davis, *Green Chemistry*, 2011, **13**, 3484.

52.   J. Saavedra, C. Powell, B. Panthi, C. J. Pursell and B. D. Chandler, *Journal of Catalysis*, 2013, **307**, 37.

53.   D. A. H. Cunningham, W. Vogel and M. Haruta, *Catalysis Letters*, 1999, **63**, 43.

54. J. Saavedra, H. A. Doan, C. J. Pursell, L. C. Grabow and B. D. Chandler, *Science*, 2014, **345**, 1599.

55. C. Hammond, M. M. Forde, M. H. Ab Rahim, A. Thetford, Q. He, R. L. Jenkins, N. Dimitratos, J. A. Lopez-Sanchez, N. F. Dummer, D. M. Murphy, A. F. Carley, S. H. Taylor, D. J. Willock, E. E. Stangland, J. Kang, H. Hagen, C. J. Kiely and G. J. Hutchings, *Angewandte Chemie-International Edition*, 2012, **51**, 5129.

56. M. Suh, P. S. Bagus, S. Pak, M. P. Rosynek and J. H. Lunsford, *Journal of Physical Chemistry B*, 2000, **104**, 2736.

57. D. I. Enache, J. K. Edwards, P. Landon, B. Solsona-Espriu, A. F. Carley, A. A. Herzing, M. Watanabe, C. J. Kiely, D. W. Knight and G. J. Hutchings, *Science*, 2006, **311**, 362.

58. A. H. A. Nadzri, N. Hamzah, N. I. N. Yusoff and M. A. Yarmo, *Functional Materials Letters*, 2011, **4**, 309.

Chapter 4

The Selective Catalytic Oxidation of Furfural

4.1. <u>Introduction</u>

Furfural (FF) is a C_5 heterocyclic aldehyde, which can be isolated in large quantities through the treatment of lignocellulosic feedstocks. FF has potential as a platform chemical[1-3] which can undergo hydrogenation to produce valuable fuels such as tetrahydrofuran and 2-methyltetrahydrofuran[4-9]. In addition to the production of fuels, it is important that alternative methods are developed for the production of fine chemical from bio-renewable feedstocks. FF can be selectively oxidised into a range of different products which are either employed in industry[1, 10] or can undergo further transformations to form other high value products[3, 11, 12].

The selective oxidation of FF to maleic acid[13-16] (MEA) and succinic acid (SA)[17, 18] has generated a lot of scientific interest in recent times. MEA and SA can both be used as precursors to produce specialised polyester resins[19, 20]. SA also has a range of other uses including its use as an acidity regulator in the food industry and as an additive in the pharmaceutical industry to produce antibiotics and vitamins[10]. It has also been reported that FF can undergo oxidative esterification to produce alkyl furoates[21-24], which have various applications in the flavour and fragrance industries[25]. Au supported heterogeneous catalysts have been found to be highly active in these transformations. Furoic acid (FA) is an additional product which can be formed by the selective oxidation of FF. FA is predominantly used as a precursor to form furoyl chloride, which is widely used in the pharmaceutical industry to produce drugs and insecticides[26]. FA is currently produced industrially *via* the Cannizzaro reaction with NaOH. It was previously suggested that the application of a heterogeneous catalyst to improve the efficiency of this process was unfeasible, due to competitive pathways which lead to the formation of unfavourable by-products[26]. Nevertheless, there have been some attempts which have been largely unsuccessful[27, 28].

It is clear from the current literature that the polymerisation of FF in the solution is a problem, as numerous articles have reported substantial losses of carbon[13-16, 18, 29]. It is known that FF can undergo self-polymerisation[30] to produce resins. This polymerisation only appears to be a problem when reactions are conducted in H_2O, as losses in carbon did not appear to be a problem for the oxidative esterification of FF. It is believed that the self-polymerisation of FF is initiated through the abstraction of a hydrogen atom from the furan ring, leaving a radical furan species[15]. Further work conducted by Tanskanen and co-workers[31, 32] determined that the polymerisation is promoted by the acidity of the aqueous medium. Measures have been taken to reduce this polymerisation by using co-catalysts[15] and diluting the concentration of FF through the application of a biphasic system[33]. These reaction modifications did lead to some improvements but the extent of the polymerisation was still substantial.

4.2. Aims and Objectives

4.2.1. Objectives

Design and employ a reaction system whereby FF can be oxidised efficiently to FA using mild reaction conditions in the presence of a gold supported heterogeneous catalyst.

4.2.2. Aims

- Identify a Au supported heterogeneous catalyst which can selectively oxidise FF to FA
- Derive suitable reaction conditions and optimise the catalyst in order optimise catalytic performance
- Propose a suitable reaction profile for the system. Determine the affect each of the reaction conditions have on the performance of the catalyst in order to gain a further understanding of the reaction system.
- Vary the catalyst preparation method in order to gain an understanding of how the catalytic properties such as nanoparticle size effect catalytic performance.
- Assess the industrial viability of the catalyst. Assign kinetics to the system. Is the activation energy of the catalytic process competitive with the current industrial method for the production of FA.

4.3. Oxidation of Furfural over a 1 wt.% Au/TiO$_2$ Catalyst

It has been shown repeatedly in literature that Au nanoparticles supported on TiO$_2$ are highly effective catalysts for a range of oxidation reactions[34, 35]. For this reason, a 1 wt.% Au/TiO$_2$ catalyst was prepared by the conventional sol-immobilisation technique and subsequently tested for the oxidation of FF. The time online data for this reaction is displayed in Figure 4.1.
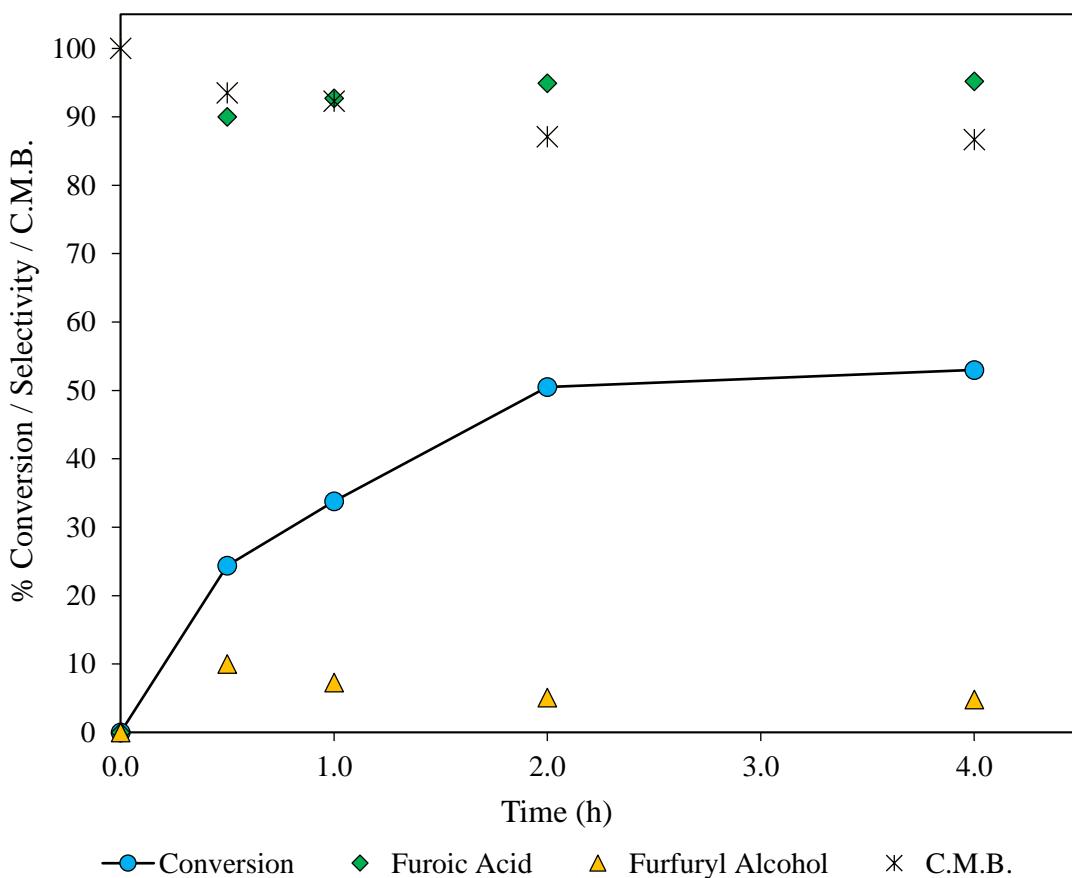
Figure 4.1. Time online reaction for the oxidation of FF over Au/TiO$_2$ under standard reaction conditions. **Reaction conditions:** 10 mL substrate (0.3 M), NaOH:substrate = 1, O$_2$ (3 bar), substrate:metal = 2000, 30 °C, 4 h.

The Au/TiO$_2$ catalyst gives a high selectivity to the desired FA product but a substantial decrease in the carbon mass balance is observed. A noticeable reduction in catalytic activity over time is also detected as the reaction proceed which could suggest that the catalyst is poisoned during the reaction. These observations could indicate that resins are formed in the reaction as reported in previous publications investigating the selective oxidation of

FF[13, 15]. If this is the case, it is clear that the formation of these species has a negative impact on the performance of the catalyst. It is believed that the formation of these species is caused by the interaction of two FF species[32]. For this reason, a possible method of reducing this may be to increase the quantity of catalyst in the reaction in order to reduce intermolecular interactions between the substrate species. Consequentially, further tests were conducted with higher quantities of catalyst in order to assess how this effected reaction profile. There results of these tests are displayed in Figure 4.3.
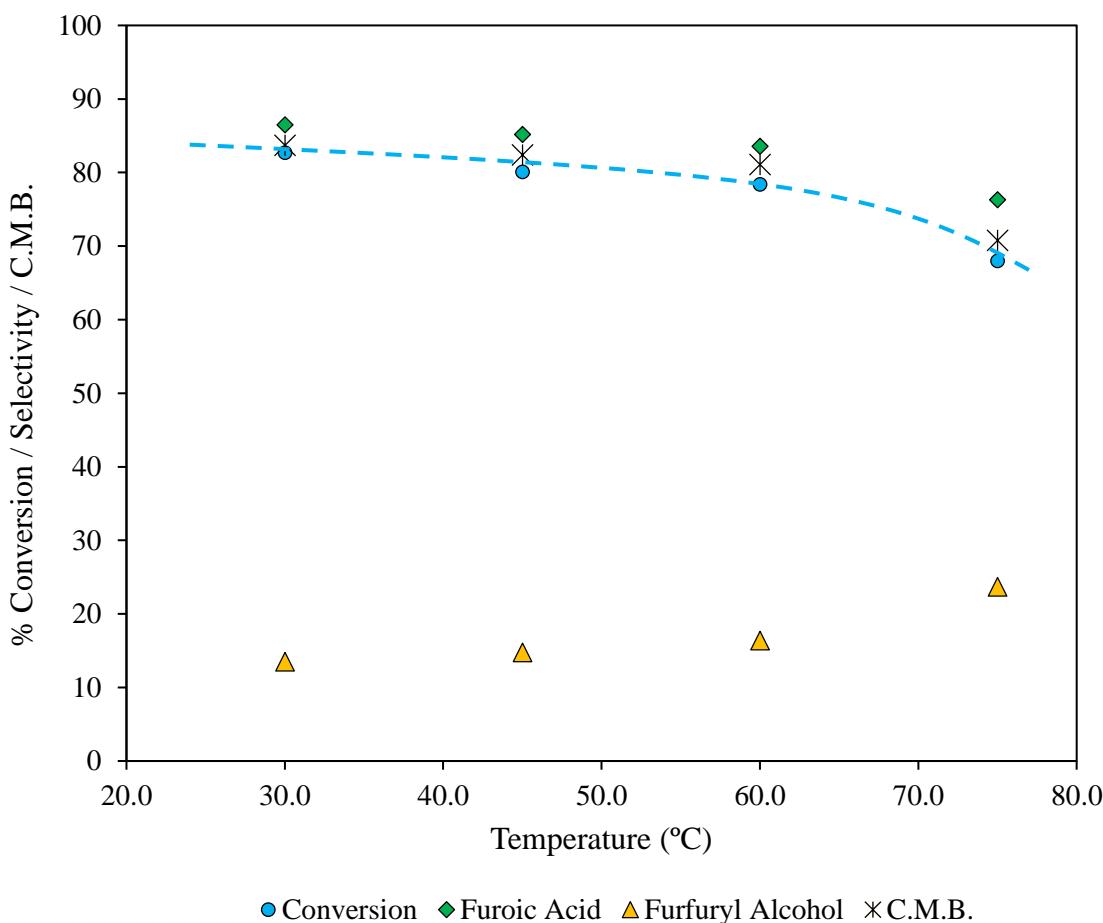
Figure 4.2. The effect of temperature on the performance of a 1% Au/TiO_2 catalyst for the oxidation of FF is displayed. Data reflects samples collected after 4 h of reaction. **Reaction conditions:** 10 mL substrate (0.3 M), NaOH:substrate = 1, O_2 (3 bar), substrate:metal = 2000, temperature stated, 4 h.

As expected, increasing the quantity of the catalyst had a positive effect on substrate conversion. Even at high quantities of catalyst, deactivation was still observed although the extent did appear to decrease. It is likely that the magnitude of resin formation is the same

with all the catalyst masses and the observed decrease in deactivation may just be attributed to the increase in active sites present.

In an attempt to gain a further understanding of the polymerisation pathway, further tests were conducted where the reaction temperature was increased. These tests are displayed in Figure 4.2.
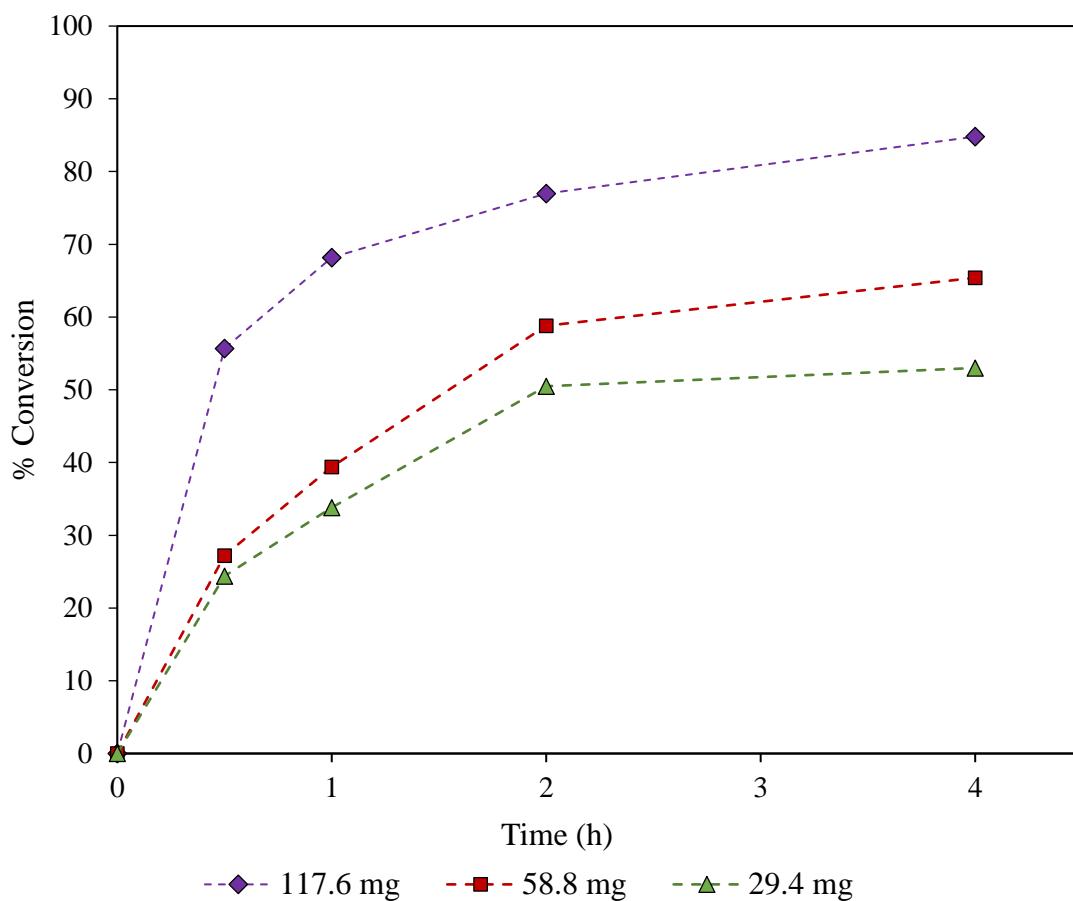
Figure 4.3. The effect of catalyst mass on the conversion of FF was assessed. A 1% Au/TiO$_2$ catalyst was used. **Reaction conditions:** 10 mL substrate (0.3 M), NaOH:substrate = 1, O$_2$ (3 bar), catalyst mass stated in legend, 30 °C, 4 h.

Interestingly, substrate conversion and CMB appears to have an inversely proportional relationship with reaction temperature. The selectivity to FA also appears to decrease at the expense of FOH. The previous postulation regarding catalyst poisoning appears to be relevant. Increasing the reaction temperature may have a promotional effect on the unfavourable polymerisation of FF. If this is the case, it is clear that the resins do poison the catalyst. In the article by Choudhary and co-workers[29] which was discussed previously,

higher yields of MEA were achieved when reaction temperature was reduced. Although it was not stated in the article, it likely that the decreased catalytic performance observed with higher reaction temperatures was a result of increased resin formation.

It is unlikely that the change in the selectivity profile is a result of increased resin formation. The increase in selectivity to FOH could indicate that an additional reaction pathway may be operational. The nature of substrate and the highly basic reaction medium make it a suitable environment for Cannizzaro reaction to occur between FF molecules. Given the highly oxidative conditions, it is unlikely that FOH is produced *via* a catalytic route. Increasing the reaction temperature would almost certainly promote this reaction pathway and is likely the reason why selectivity to FOH increases proportionally with temperature.

Another possible explanation for catalytic deactivation is product inhibition. The drop in catalytic activity can be correlated with increasing concentrations of FA present in the reaction. Previous articles have reported that the presence of carboxylic acid groups can inhibit the activation of alcohols in the presence of a base, as the external OH^- species favour the interaction with acidic COOH groups[36]. In order to assess whether this was the case in this reaction, a product inhibition study was conducted. For this, FA was added to the starting mixture which equated to 0.03 M. Substrate conversion was monitored with time and compared against the conversion observed under standard reaction conditions. The result of this test is displayed in Figure 4.4. The presence of additional FA at the beginning of the reaction does not appear to have any impact on the activity exhibited by the catalyst. This strengthens the theory that the deactivation observed is a result of resins poisoning the catalyst.

A 1% Au/TiO_2 catalyst can selectively oxidise FF to FA. FOH is produced as a by-product in the reaction which is likely a result of a base promoted Cannizzaro reaction. Increasing the temperature appears to promote this reaction as a greater FOH selectivity was observed as the reaction temperature was increased. The temperature also appears to have a negative impact on catalytic performance. It was postulated that increasing the temperature promotes the unfavourable formation of furan based resins which bind irreversibly to the catalysts active sites. A product inhibition test showed that FA has no detrimental effect on the activity of the catalyst, hereby strengthening the likelihood that catalyst deactivation is a result of resin formation.
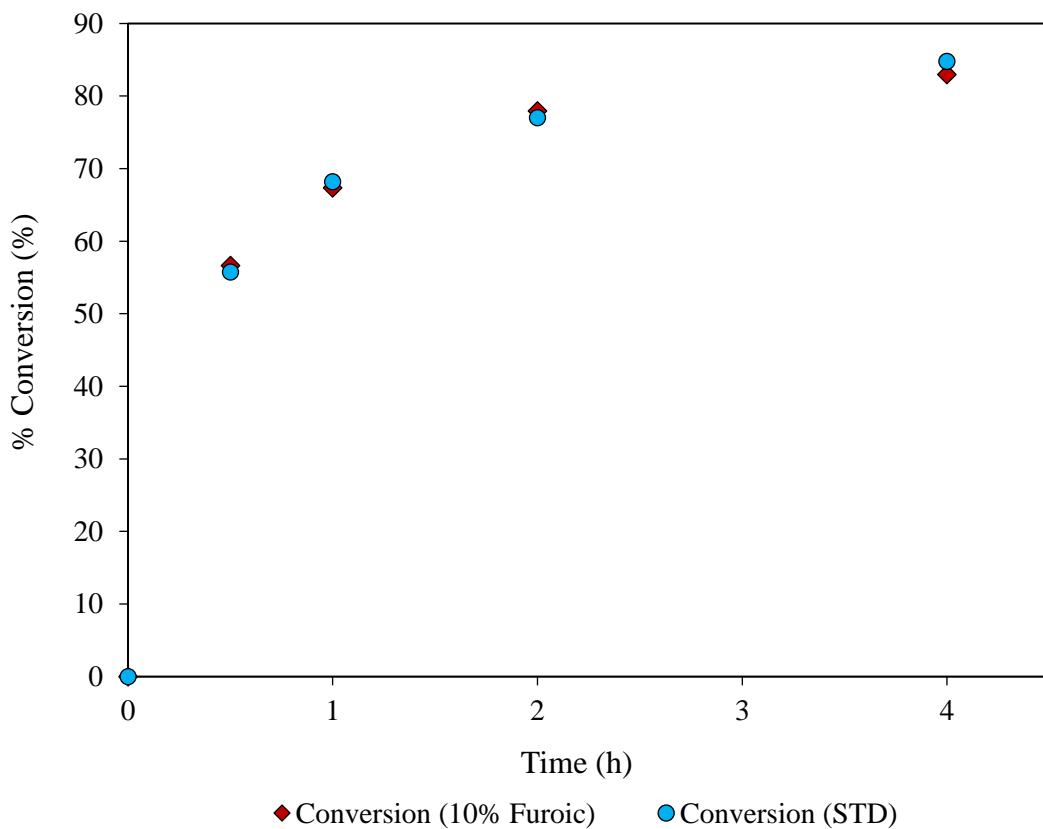
Figure 4.4. The effect of [FA] on catalytic activity is displayed. **Reaction conditions:** 10 mL substrate (0.3 M), NaOH:substrate = 1, O_2 (3 bar), substrate:metal = 500, 30 ℃, 4 h.

4.4. Optimisation of the Catalyst

The problems associated with the 1 wt.% Au/TiO_2 catalyst mean that it is not a suitable candidate for this process. Despite displaying promising reaction selectivity to FA, the losses in carbon to the formation of resins and the detrimental impact they appear to have on the catalyst is unfavourable. Modification of the catalyst is required in order to make the catalytic process more viable.

MgO has shown to be an exceptionally active support for Au nanoparticles for the oxidation of alcohols[37, 38]. For this reason, a 1% Au/MgO catalyst was prepared by the conventional sol-immobilisation technique and subsequently tested for the oxidation of FF. The results of this reaction are displayed in Figure 4.5
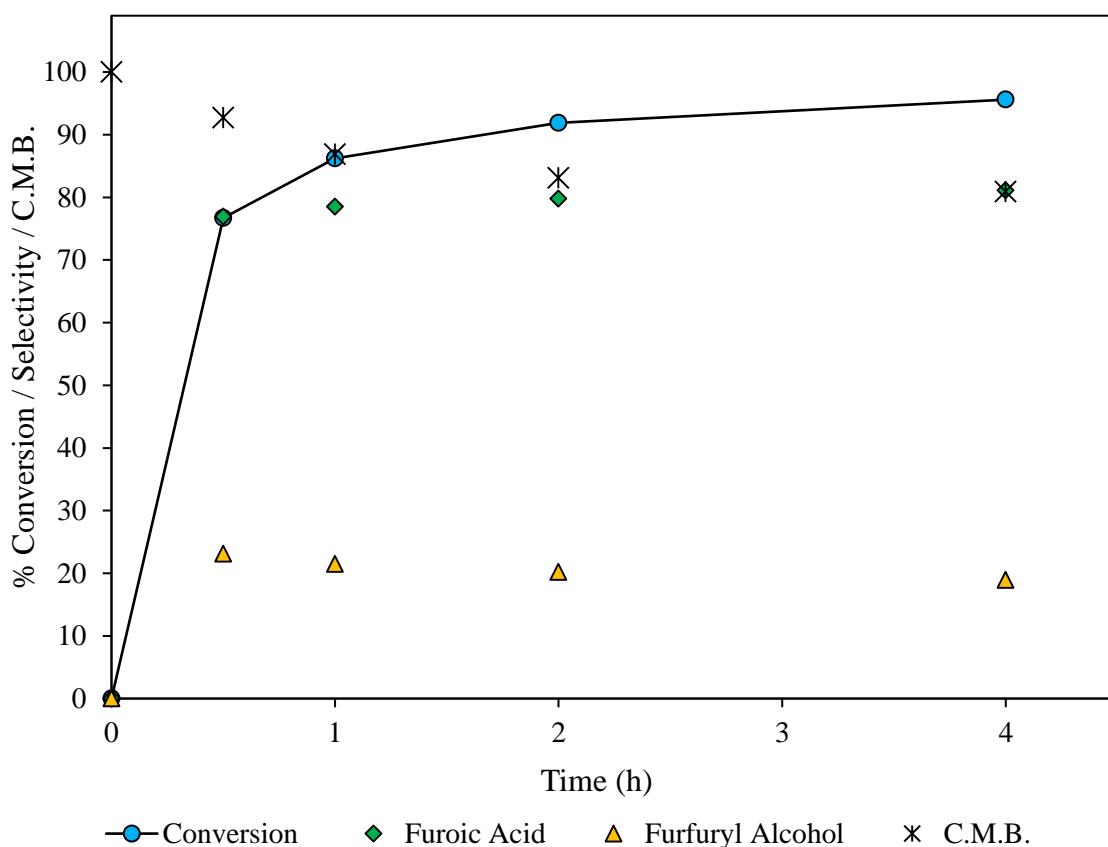
Figure 4.5. Time online reaction for the oxidation of FF over a 1% Au/MgO catalyst under standard reaction conditions. **Reaction conditions:** 10 mL substrate (0.3 M), NaOH:substrate = 1, O_2 (3 bar), substrate:metal = 500, 30 °C, 4 h.

It is evident that the support plays a significant role in the activity of the catalyst. An increase in conversion at 0.5 h from 24.4 % with the Au/TiO_2 catalyst to 34.9 % with the Au/MgO catalyst is observed. The selectivity to FOH is slightly higher suggesting that the MgO support may be promoting the Cannizzaro pathway. There still appears to be a significant loss of carbon which suggests that the MgO support does not inhibit the unfavourable polymerisation pathway; although the activity of the catalyst appears to be less affected.

The incorporation of Pd into Au supported catalysts has shown to significantly enhance catalytic activity in the oxidation of benzyl alcohol[39]. Rather than attempt to design a catalyst which switches off the polymerisation process it may be more viable to synthesise a catalyst which suppresses the unfavourable pathway through rapidly promoting the

desired pathway. If a catalyst is active enough for the transformation of FF to FA, it may indirectly suppress the polymerisation pathway. In order to assess this theory at 1 wt.% AuPd/MgO catalyst was prepared by the conventional sol-immobilisation pathway and subsequently tested for the selective oxidation of FF. The result of this test is displayed in Figure 4.6.
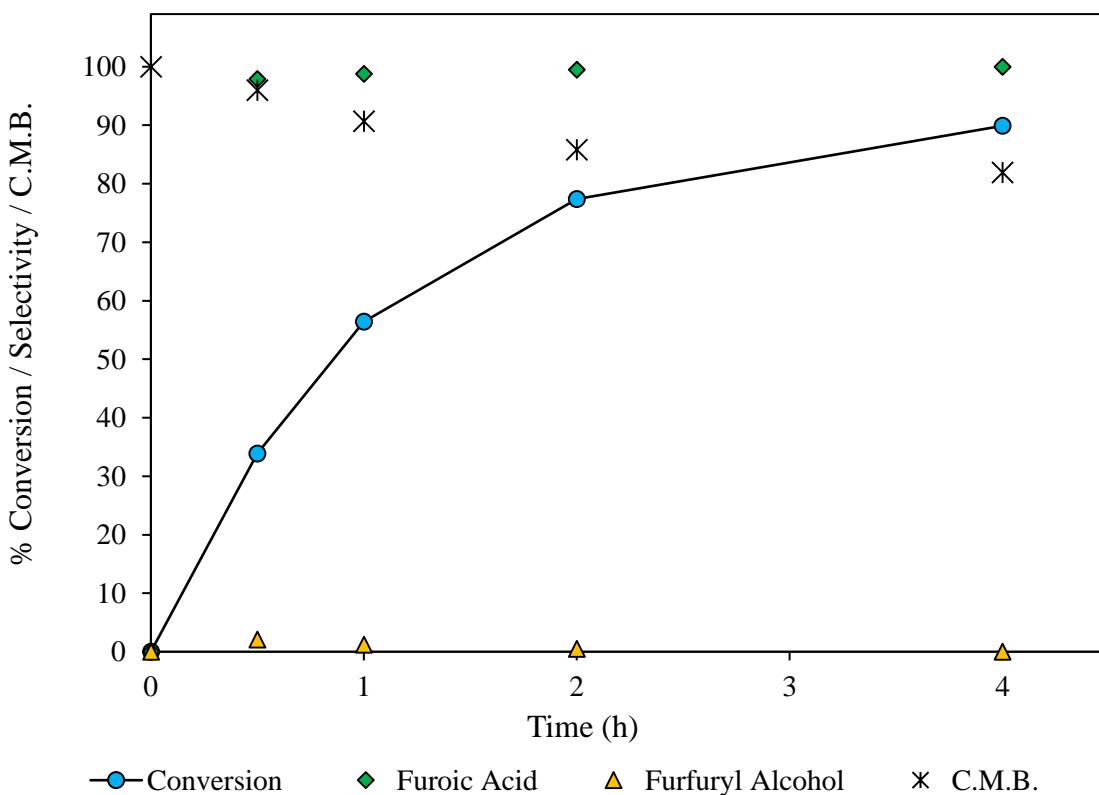
Figure 4.6. Time online reaction for the oxidation of FF over a 1% AuPd/MgO catalyst under standard reaction conditions. **Reaction conditions:** 10 mL substrate (0.3 M), NaOH:substrate = 1, O_2 (3 bar), substrate:metal = 500, 30 °C, 4 h.

The AuPd/MgO catalyst enhanced the selectivity to the desired compound at the expense of FOH. Only trace quantities of FOH were observed at the initial stages of the reaction, with none detected after reaction completion. One possible explanation for this is that the Pd is in some way inhibiting the Cannizzaro reaction. This is unlikely, as the Cannizzaro reaction is a homogeneous reaction promoted by the NaOH. A more feasible explanation is that the new AuPd clusters are facilitating a sequential oxidation step from FOH to FF. Synergistic interactions brought about from the alloying of Au and Pd have repeatedly proven to enhance catalytic performance in the oxidation of alcohols[39, 40]
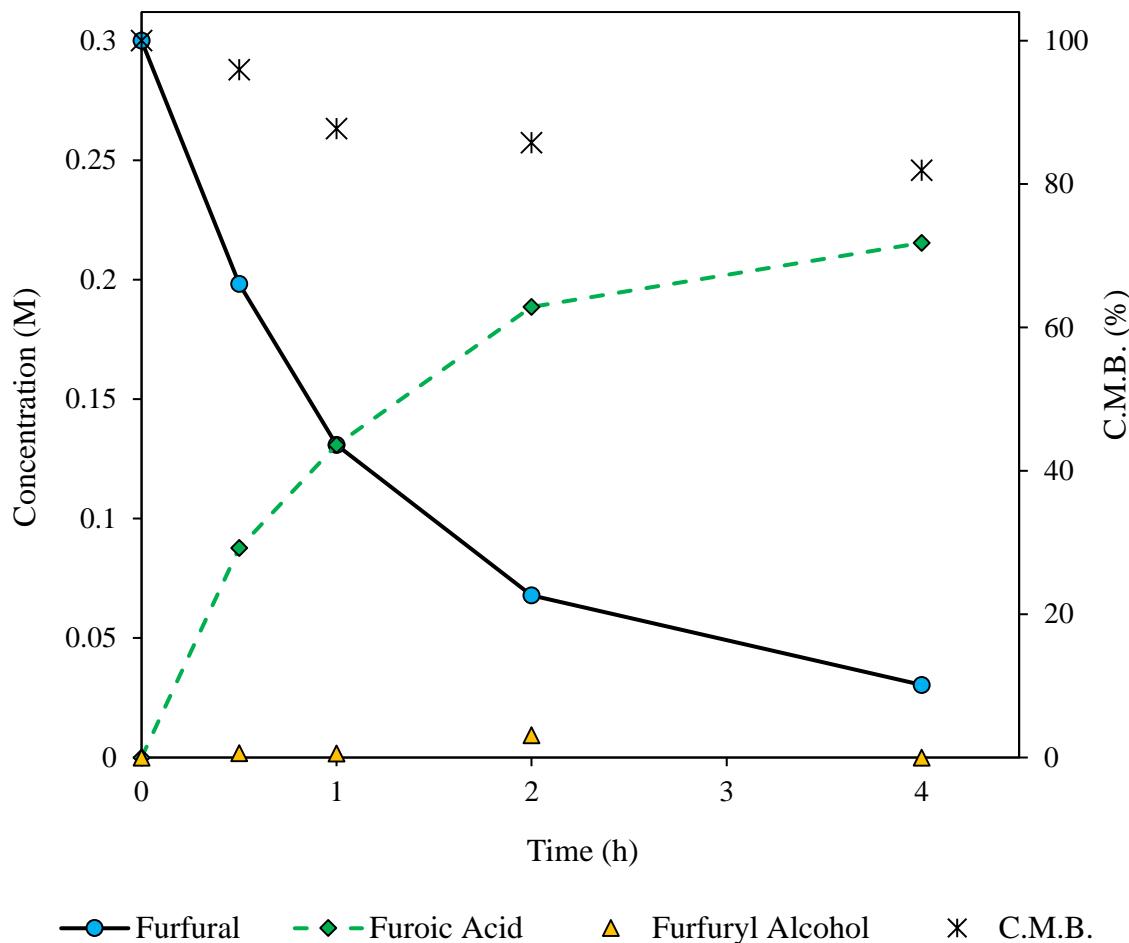
Figure 4.7. Time online plot highlighting the presence of substrate and products in terms of concentration (M). **Reaction conditions:** 10 mL substrate (0.3 M), NaOH:substrate = 1, O_2 (3 bar), substrate:metal = 500, 30 ℃, 4 h.

Despite the improved efficiency of the reaction with the modified catalyst, it is clear that substantial quantities of carbon are still missing. Approximately 20 % of the carbon is lost after 4 h which is comparable to the losses observed with the 1% Au/MgO and 1% Au/TiO$_2$ catalysts. For this reason, a more accurate method of presenting the reaction results is required. Figure 4.7 is an alternative method of presenting the reaction data which gives a more accurate method of following the reaction. Instead of conversions and selectivity, the quantity of the substrate and products are displayed in terms of their concentration in the aqueous reaction medium.

The plot in Figure 4.7 gives a clearer representation of how the reaction is proceeding with time. The concentration of FA appears to increase in an inversely proportional manner with respect to the concentration of FF. The presence of FOH appears to hit a maximum

concentration at 2 h which suggests that it is being produced and consumed in the reaction as none is observed after 4 h. This is further evidence to suggest that the AuPd nanoparticles are facilitating the sequential oxidation of FOH to FF. Although a 100 % FA selectivity was previously observed, Figure 4.7 shows that a FA yield of only 71.8 % is achieved after 4 h.

The 1 wt.% AuPd/MgO catalyst was subsequently characterised by XRD in an attempt to understand why this support is more active than the TiO$_2$. Although MgO is used for the catalyst preparation, previous studies have shown that MgO is converted to Mg(OH)$_2$ immediately when it comes into contact with water[38]. The X-ray diffraction patterns of the support prior to use and the catalyst are displayed in Figure 4.8.

Figure 4.8. X-ray diffraction patterns for (a) MgO support and (b) 1 % AuPd/Mg(OH)$_2$.
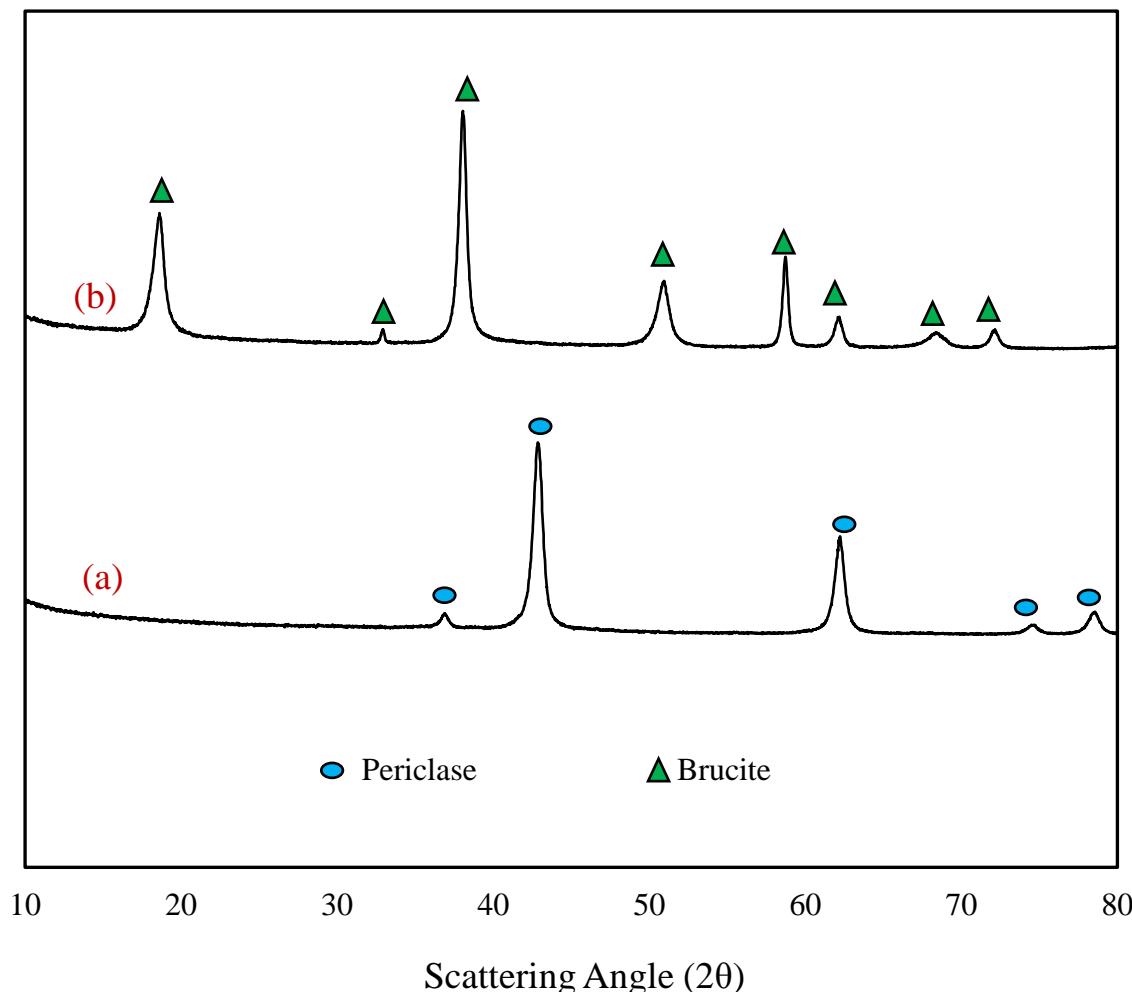
It is clear from the diffraction patterns that there is a phase change occurring during the preparation of the catalyst. Prior to preparation the support exhibits a periclase MgO crystal

structure. As postulated by Brett *et al.* H_2O appears to have facilitated a phase transition to brucite $Mg(OH)_2$. The detection of this phase change is important as it reveals that there is a greater population of hydroxide sites on the surface of the support than previously thought. Although there are a lot of other factors to consider when comparing catalytic supports, it is likely that the increase in catalytic performance is a result of the increased population of hydroxyl groups near the active site. Davis and co-workers have reported the importance of surface bound hydroxyl species have to the performance of Au supported heterogeneous catalysts for the oxidation of glycerol[36]. It was suggested that increasing the concentration of hydroxyl species on the surface increased the reaction rate as it enhanced the formation of surface bound peroxy species. It is possible that the formation of these species promote the catalytic oxidation of FF and FOH.

As discussed previously, there is evidence to suggest that a NaOH promoted Cannizzaro reaction is competing with the catalytic oxidation of FF to FA. In order to confirm whether this is the case, a series of tests were conducted and the corresponding results are displayed in Figure 4.9.
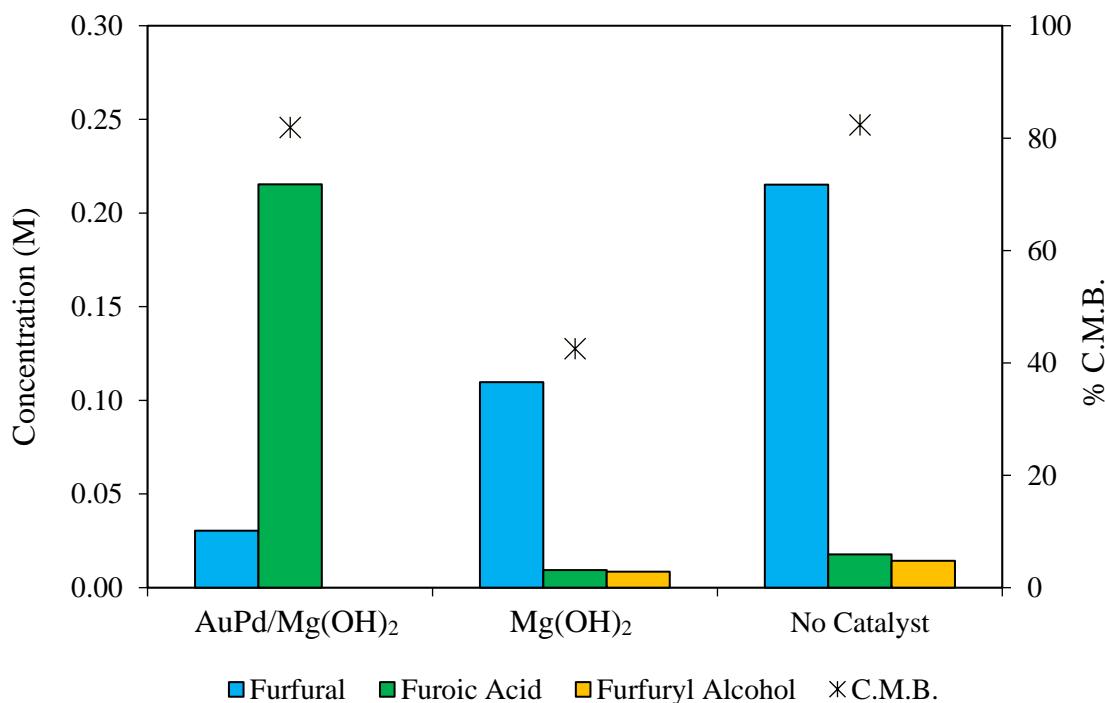
Figure 4.9. $AuPd/Mg(OH)_2$ and $Mg(OH)_2$ are assessed as catalysts for the oxidation of FF under standard conditions. An additional test in the absence of a catalyst is also displayed. Data is after a 4 h reaction. **Reaction conditions:** 10 mL substrate (0.3 M), NaOH:substrate = 1, O_2 (3 bar), substrate:metal = 500 where stated, 30 °C, 4 h.

The formation of FA and FOH in the absence of any catalyst confirms that a Cannizzaro reaction is taking place. It is also clear how important the presence of the AuPd nanoparticles are to the performance of the catalyst. Despite the highly basic surface of the Mg(OH)$_2$, it does not appear to have any promotional effect on the Cannizzaro reaction as the yields of FOH and FA observed in its presence are comparable with the blank reaction.

Interestingly, the CMB observed for the reaction with Mg(OH)$_2$ is noticeably lower than that observed in the blank reaction despite there being similar rates of disproportionation. This may suggest that the support is in fact promoting the polymerisation pathway. It was previously proposed that the polymerisation of FF is initiated by the abstraction of an H atom from the furan ring[15]. It is possible that the high population of hydroxyl groups on the surface of the support may be promoting this H$^+$ abstraction which would rationalize the low mass balance observed in the reaction with Mg(OH)$_2$. In the presence of the AuPd/Mg(OH)$_2$ catalyst, a comparable mass balance is observed to that in the absence of any catalyst. This could suggest that the AuPd nanoparticles may be inhibiting the polymerisation pathway through the promotion of the direct oxidation pathway.

Despite optimisation of the catalyst the formation of resins still appears to be a significant problem in the reaction system. It is clear that FF is incredibly susceptible to intermolecular interactions and so additional measures are required in order to minimise the extent of FF polymerisation. For this reason, a different experimental procedure was enforced in order to limit the contact time between FF compounds in the absence of any catalyst. The new experimental procedure involves the insertion of pure FF directly into the stirring aqueous reaction mixture containing the catalyst, NaOH and water. Once added, the reactor is immediately sealed and pressurised with O$_2$. In previous reactions, a bulk solution of FF (0.3 M) was made up prior to the reaction. A standard reaction was completed using the modified procedure and the comparison of the results with the previous method is displayed in Figure 4.10.

It is clear that the modified oxidation procedure is far more suitable for this process than the conventional method. Using the modified method an elevated conversion, FA yield and C.M.B. was achieved. It is likely that this desirable increase in performance is a result of less polymerisation taking place. Not only does this provide a more effective method of conducting the reactions but it also provides further evidence to the postulations provided previously regarding the formation of resins and their role in catalyst deactivation. Other

work has shown how limiting the contact time of FF compounds using a biphasic solvent system for the formation of MEA reduced resin formation. Despite the significant reduction in resin formation, a full conversion of the substrate was still not achieved using the modified experimental procedure.
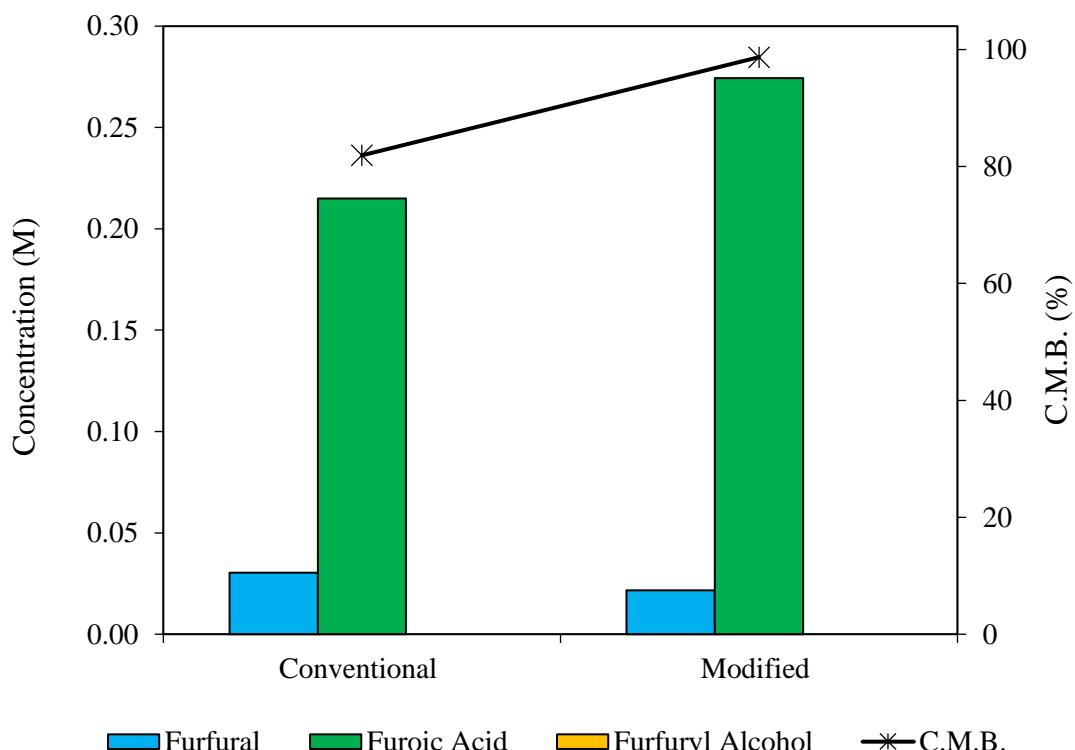
Figure 4.10. The oxidation of FF over a 1% AuPd/Mg(OH)$_2$ catalyst by conventional and modified experimental procedures. **Reaction conditions:** 10 mL substrate (0.3 M), NaOH:substrate = 1, O$_2$ (3 bar), substrate:metal = 500, 30 °C, 4 h.

Mg(OH)$_2$ appears to be a more suitable support for Au nanoparticles for this reaction than TiO$_2$. The nature of this phase was confirmed by XRD. The incorporation of Pd appears to promote the overall performance of the catalyst with a noticeable increase in the suppression of the unfavourable polymerisation pathway. A different method of analysis was determined which gives a more accurate representation of the reaction. The performance of blank reactions confirmed the occurrence of the Cannizzaro reaction. The Mg(OH)$_2$ support did not appear to have any promotional effect on this reaction although there is evidence to suggest that it promoted the polymerisation pathway. A new experimental method for running the reactions was determined which reduced the loss of carbon to resins. For this reason, all future testing in this chapter is conducted using this modified procedure.

4.5.   A Mechanistic Overview

In order to gain a greater understanding of the reaction system, it was necessary to conduct a full mechanistic study to gain an insight into how the reaction conditions and catalyst may be optimised to promote catalytic performance.

4.5.1.   The Oxidation of Furfural

A time online plot for the oxidation of FF over a 1% AuPd/Mg(OH)$_2$ catalyst is displayed in Figure 4.11. The catalyst was prepared twice and each batch was tested three times in order to gage the reproducibility and accuracy of the results. Error margins were applied in accordance with the standard deviation of the six tests.
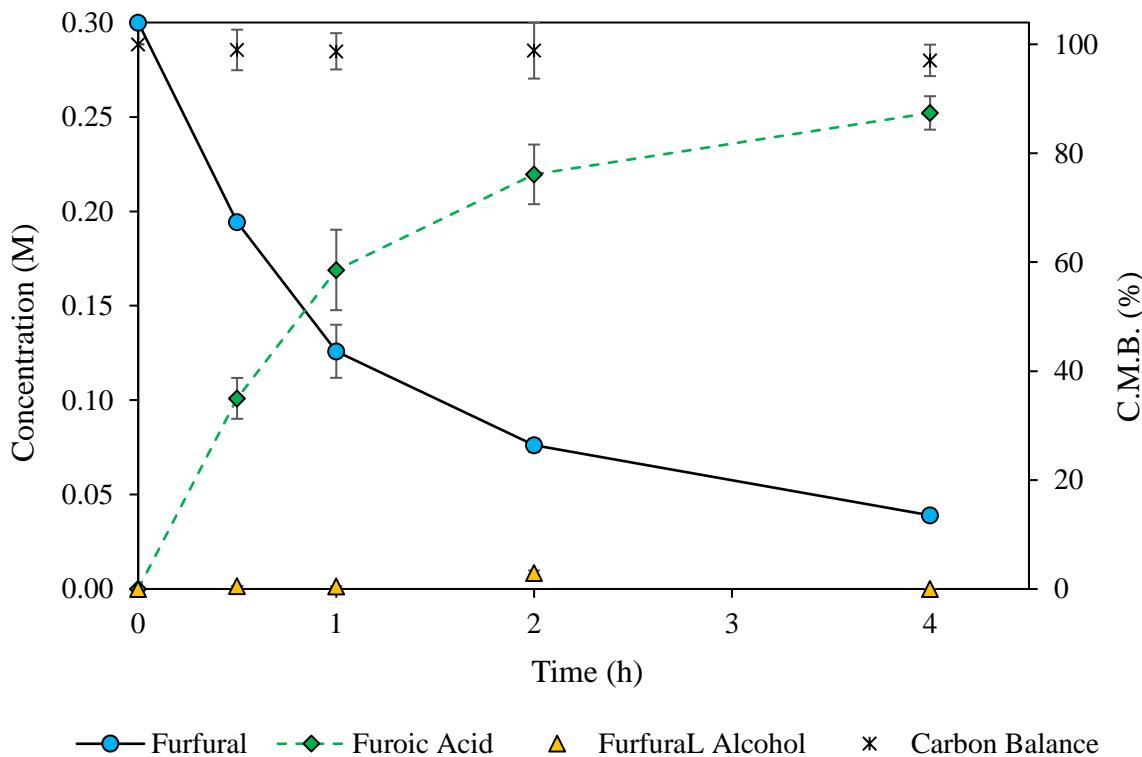
Figure 4.11. A time online plot for the oxidation of FF over a 1% AuPd/Mg(OH)$_2$ catalyst. Error margins were assigned in accordance with the standard deviation of 6 separate tests with 2 different catalyst batches. **Reaction conditions:** 10 mL substrate (0.3 M), NaOH:substrate = 1, O$_2$ (3 bar), substrate:metal = 500, 30 °C, 4 h.

The catalytic testing procedure is reproducible as the deviation away from the mean of the data points appears to be fairly low. This strengthens the industrial viability of this process as the susceptibility of the substrate to partake in competitive polymerisation reactions does not appear to be effect the reproducibility of the results.

The effect of base on the performance of the 1% AuPd/Mg(OH)$_2$ catalysts was assessed in an attempt to understand it's role on the oxidation of the aldehyde. For this, testing was conducted where the substrate to base ratio was varied and the catalytic performance monitored. The results of this set of experiments are displayed in Figure 4.12.
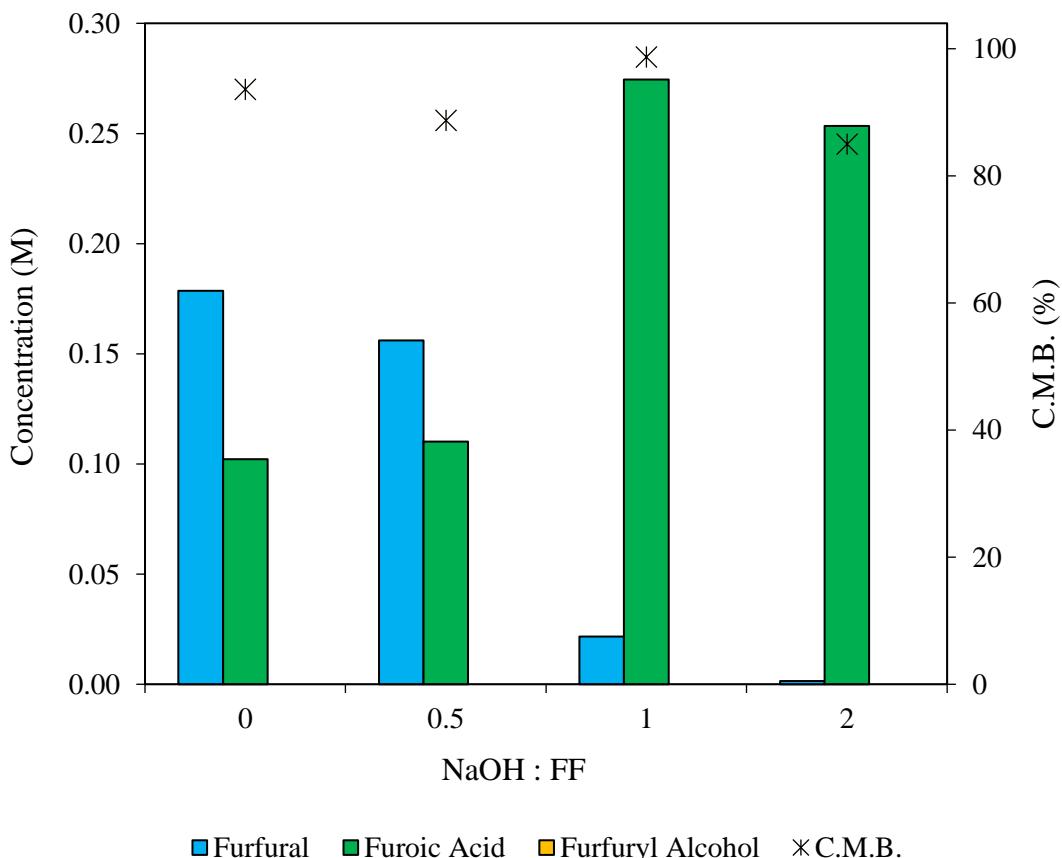
Figure 4.12. The base to substrate ratio is varied in order to assess the effect it has on the performance of the 1% AuPd/Mg(OH)$_2$ catalyst. Tests were conducted using the modified experimental procedure. Data reflects samples taken after of 4 h of reaction. **Reaction conditions:** 10 mL substrate (0.3 M), NaOH:substrate is stated, O$_2$ (3 bar), substrate:metal = 500, 30 °C, 4 h.

The activity of the catalyst clearly increases proportionally with the concentration of NaOH. This suggests that external hydroxide ions play a pivotal role in the catalyst reaction mechanism. It was previously displayed in Chapter 3 that some aldehydes and ketones are readily oxidised by NaOH in the absence of a catalyst. The results displayed in Figure 4.9 suggest that this is not the case with FF, as it appears that FA observed in the absence of the catalyst was produced from a Cannizzaro reaction between two FF compounds. It's possible that the adsorption of the substrate to the catalyst is required to weaken the C-H bond and allow for the subsequent oxidation to take place. The subsequent nucleophilic attack of the OH ion could occur through co-adsorption or directly from solution.

It was determined that the concentration of FA is at a maximum at a 1:1 base to substrate ratio. This could suggest that the NaOH may catalyse an additional pathway as well as the oxidation of the aldehyde to acid. It has already been postulated that base may promote the polymerisation pathway. The decrease in the C.M.B. observed at a NaOH ratio of 2 could be further evidence to suggest that the polymerisation of FF is promoted by OH ions. This is in agreement with work published by Lan *et al.*[15] who suggested that the polymerisation of FF is initiated through the abstraction of a hydrogen atom from the furan ring. In the absence of any base, the activity exhibited by the catalyst was comparable with that observed at a base to substrate ratio of 0.5. There are two possible explanations for this observation: (i) The surface of the $Mg(OH)_2$ support is highly populated with hydroxide groups which could be supplying the hydroxide ions required for the mechanism to proceed and (ii) Mg is leaching from the support, interacting with H_2O and to form a weak homogeneous base. The leaching of Mg from $Mg(OH)_2$ in water has been reported previously[38]. MP-AES was conducted on the post reaction effluent of the base free test and confirmed the presence of substantial quantities of Mg in the solution. This Mg leaching must be a consequence of the supports erosion by FA which is produced. No Mg was observed in the reaction effluent of the reactions conducted in the presence of base which is likely a result of the sodium interchanging with the proton of the acids and thus quenching their acidity. All these postulations suggest that the similar activity observed at base to substrate ratios of 0 and 0.5 are likely a result of contributions from both (i) and (ii).

The effect of oxygen pressure on the reaction system was also assessed. Oxygen has previously shown to have a significant effect on catalytic performance in oxidation

reactions[41, 42]. A series of experiments were conducted where the quantity of oxygen was varied. The results of these tests are displayed in Figure 4.13.
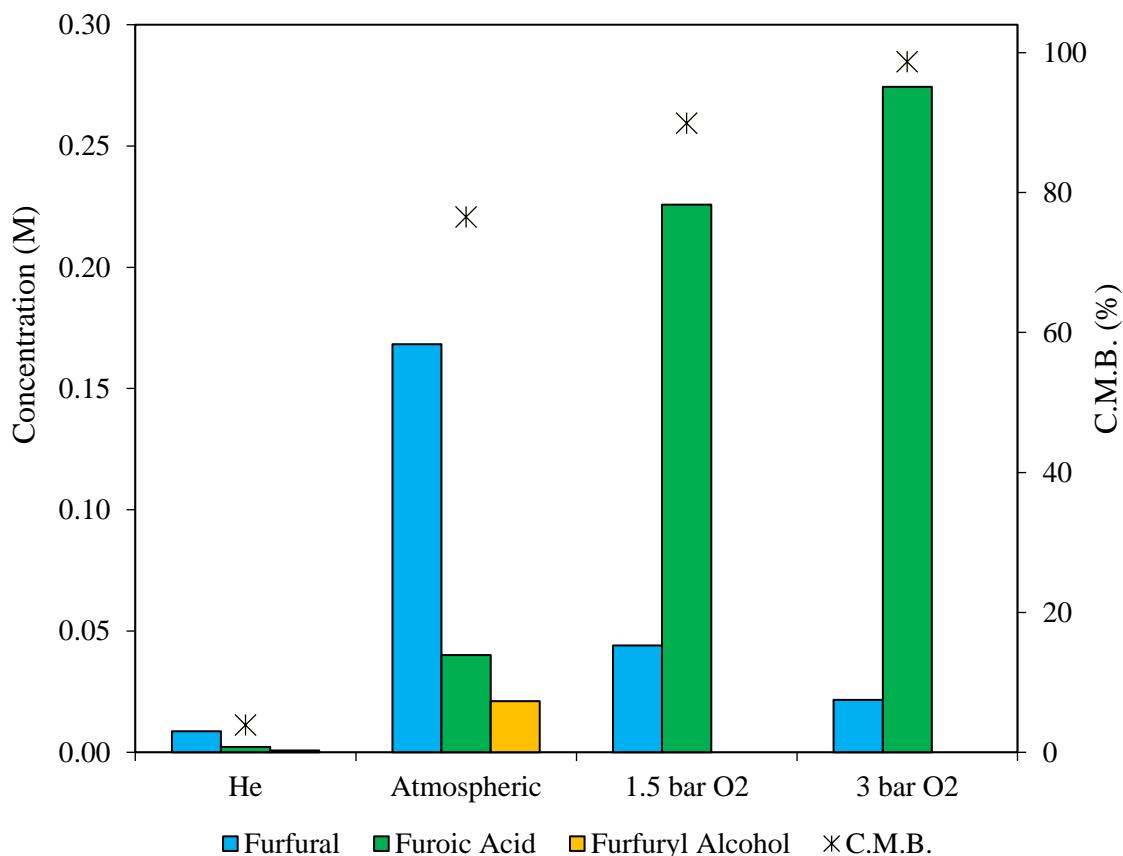

Figure 4.13. The quantity of oxygen is varied in order to assess the effect it has on the performance of the 1% AuPd/Mg(OH)$_2$ catalyst. Tests were conducted using the modified experimental procedure. He corresponds to the reactor purged 5 times and charged with 3 bar of Helium. Data reflects samples taken after of 4 h of reaction. **Reaction conditions:** 10 mL substrate (0.3 M), NaOH:substrate =1, O$_2$ pressure is stated, substrate:metal = 500, 30 °C, 4 h.

As with so many other oxidation reactions, it is clear that oxygen has a significant promotional effect on the reaction rate. Increasing the oxygen pressure increases the substrate consumption, FA yield and the CMB. It has been suggested previously that O$_2$ dissociates on the surface of Au through reduction with H$_2$O, yielding adsorbed OH species[43-45]. The importance of OH ions on catalytic performance for this reaction was previously highlighted in Figure 4.12. The significant promotional effect observed in O$_2$ rich environments further supports the postulation that O$_2$ dissociates to produce surface

bound hydroxyl species. Furthermore, this may suggest that surface bound hydroxide species are more likely to interact in the surface oxidation mechanism and that external hydroxide species must first adsorb to the catalyst prior to involvement in the mechanism. The proportional relationship between O_2 concentration and CMB could also indicate that O_2 inhibits the unfavourable polymerisation mechanism through the promotion of the catalytic aldehyde oxidation.

Under atmospheric conditions, there is noticeably more FA produced than FOH. This suggests that even under extremely low levels of O_2, the catalyst is still able to adsorb and dissociate O_2. The concentration of FOH observed is comparable with that observed in the absence of any catalyst which implies that the catalyst has no promotional effect on the production of FOH. In the absence of any atmospheric oxygen in the reactor, the polymerisation pathway appears to take complete control as exceptionally low CMBs are observed. Residual quantities of FA and FOH are also present which likely contributions from the Cannizzaro reaction. However, the quantities of FA and FOH are significantly lower than that observed in the absence of any catalyst. Furthermore, there appears to be no contribution from the catalytic aldehyde oxidation. This highlights the importance of O_2 in the catalytic oxidation of the aldehyde and also the importance of surface bound OH species. Furthermore, the rate of polymerisation appears to increase exponentially in the absence of O_2 which appears to have resulted in the suppression of the Cannizzaro reaction.

4.5.2.   The Cannizzaro Reaction

As it has been reported previously, two molecules of FF can interact in the presence of base to form a stoichiometric ratio of FOH and FA. Figure 4.14 shows how the Cannizzaro reaction proceeds with time under standard reaction conditions.

It is clear from the small quantities of FA and FOH observed throughout the reaction, that the rate of the Cannizzaro reaction is significantly slower than the catalytic aldehyde oxidation. The significant loss in carbon highlights the substantial polymerisation that takes place in the absence of the catalyst. This supports the statement made previously that the catalyst restricts the polymerisation through the promotion of the catalytic aldehyde oxidation. The rate of polymerisation appears to be faster than the rate of the Cannizzaro reaction. In order to assess how the Cannizzaro reaction and the polymerisation were

effected by base, a series of experiments were constructed where the NaOH to substrate ratio was varied. The results of these tests are displayed Figure 4.15.
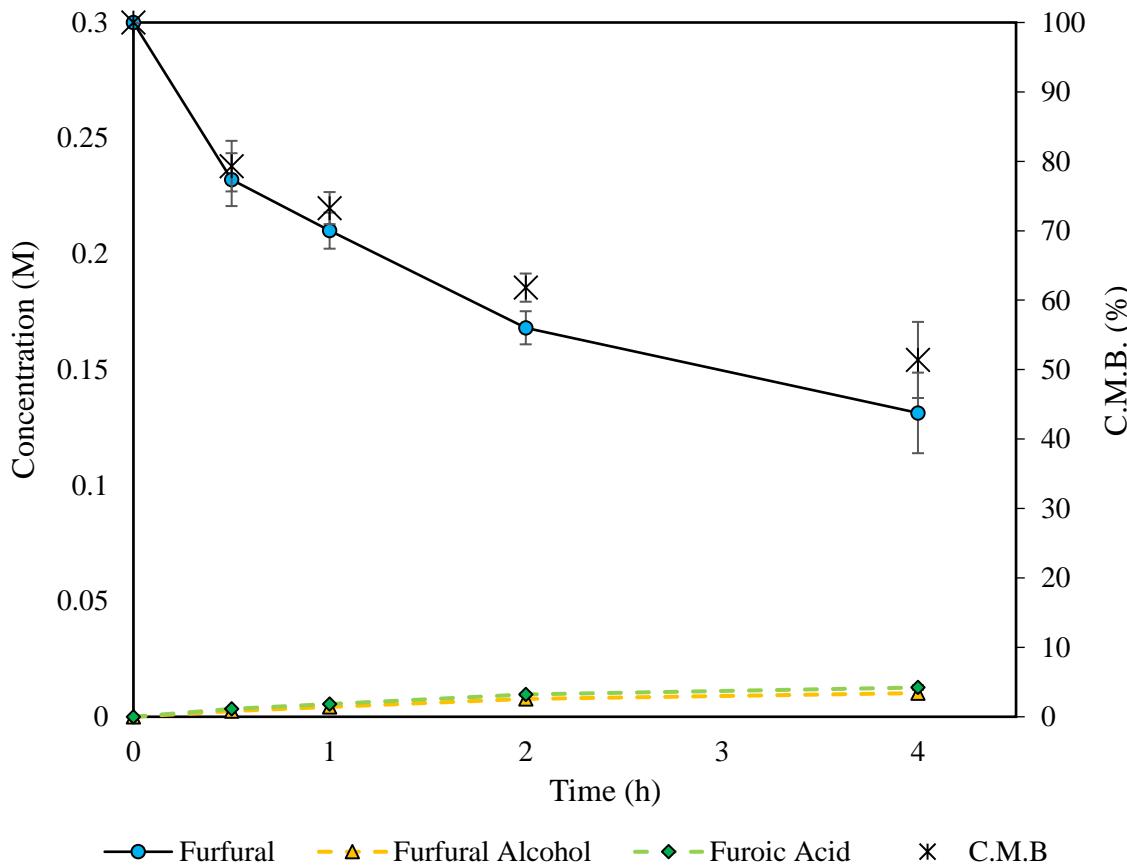
Figure 4.14. A time online plot for the Cannizzaro reaction in the absence of catalyst. Error margins were assigned in accordance with the standard deviation of 4 separate tests. Tests were conducted using the modified experimental procedure. **Reaction conditions:** 10 mL substrate (0.3 M), NaOH:substrate =1, O_2 (3 bar), substrate:metal = 500, 30 °C, 4 h.

It is clear that as the concentration of NaOH is increased the rate of the Cannizzaro reaction increases. This trend is expected as sacrificial hydroxyl groups are required for the initial activation of the substrate molecule. Interestingly, a higher concentration of FA than FOH is observed for each of the data points. The Cannizzaro reaction typically produces stoichiometric equivalents of each. This may suggest that FA is in fact more stable than FOH and that polymerisation can occur from FOH as well as from FF. The CMB appears

to decrease as the concentration of NaOH in the reaction increases. This is further evidence to suggest that polymerisation is instigated through interaction with base.
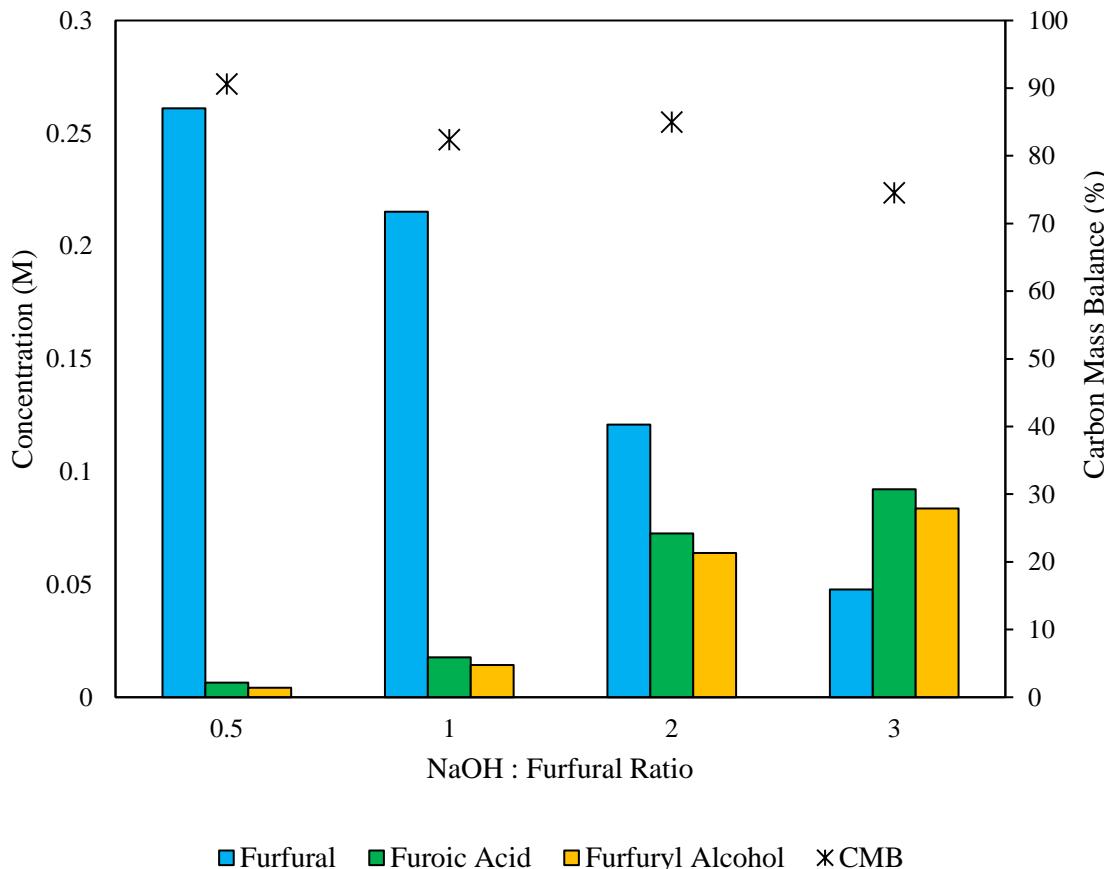
Figure 4.15. The base to substrate ratio is varied in order to assess the effect it has on the Cannizzaro reaction. Tests were conducted using the modified experimental procedure in the absence of any catalyst. Data reflects samples taken after of 4 h of reaction. **Reaction conditions:** 10 mL substrate (0.3 M), NaOH:substrate is stated, O_2 (3 bar), substrate:metal = 500, 30 °C, 4 h.

It is known that oxygen has no direct influence on the Cannizzaro reaction. The results displayed in Figure 4.16 support this, as the change in the concentrations of FA and FOH upon increasing the concentration of O_2 in the system is negligible. That said, the concentrations of these products do appear to decrease very slightly with increasing O_2 which may be a result of competition from the polymerisation route. The relative CMB of each data point appear to support this statement as they decrease with increasing O_2. This

can be correlated to the earlier postulation that O_2 can be reduced in the system to from *OH and OOH species (although this is generally only considered possible in the presence of a catalyst). If this reduction is occurring, the extra OH species could be contributing to the observed increase in polymerisation taking place with increasing O_2 concentrations.

Figure 4.16. The quantity of oxygen is varied in order to assess the effect on the Cannizzaro reaction. Tests were conducted using the modified experimental procedure. He corresponds to the reactor purged 5 times and charged with 3 bar of Helium. Data reflects samples taken after 4 h of reaction. **Reaction conditions:** 10 mL substrate (0.3 M), NaOH:substrate =1, O_2 pressure is stated, substrate:metal = 500, 30 ℃, 4 h.

It is known that oxygen has no direct influence on the Cannizzaro reaction. The results displayed in Figure 4.16 support this, as the change in the concentrations of FA and FOH upon increasing the concentration of O_2 in the system is negligible. That said, the concentrations of these products do appear to decrease very slightly with increasing O_2 which may be a result of competition from the polymerisation route. The relative CMB of

each data point appear to support this statement as they decrease with increasing O_2. This can be correlated to the earlier postulation that O_2 can be reduced in the system to from *OH and OOH species (although this is generally only considered possible in the presence of a catalyst). If this reduction is occurring, the extra OH species could be contributing to the observed increase in polymerisation taking place with increasing O_2 concentrations.

4.5.3.   The Oxidation of Furfuryl Alcohol

It has been discussed previously in this chapter that the oxidation of FOH may be possible in the presence of the 1% AuPd/Mg(OH)$_2$ catalyst and under the standard reaction conditions. For this reason, it was necessary to assess whether this was the case and a reaction consisting of interval sampling was constructed. As with the oxidation of FF, two batches of the 1 wt.% AuPd/Mg(OH)$_2$ were tested in order to derive error bars based on the standard deviation of each data point. The corresponding time online plot is displayed in Figure 4.17.

It is evident that the oxidation of the FOH does occur in the presence of the catalyst. The oxidation appears to proceed *via* FF to FA. The alcohol is initially oxidised to aldehyde before undergoing a sequential oxidation to the corresponding acid. A loss of carbon is also observed during this reaction but it is not yet clear whether this is occurring from the FOH or indirectly from FF. Interestingly, there is a noticeable increase in the loss of carbon when the concentration of FF in the system is at its maximum. This is evidence that polymerisation occurs predominantly from FF. FOH appears to be consumed at a slower rate than FF, which may suggest that oxidation of the alcohol is less thermodynamically favourable than the oxidation of the aldehyde. This supports work which shows that the oxidation of benzaldehyde proceeds spontaneously in the absence of any catalyst and under atmospheric conditions, while benzyl alcohol oxidation requires considerably harsher conditions and a catalyst[46]. In order to gain a greater insight into the promotional effect of NaOH on the alcohol oxidation, tests were conducted where the NaOH to substrate ratio was varied. The corresponding results are displayed in Figure 4.18
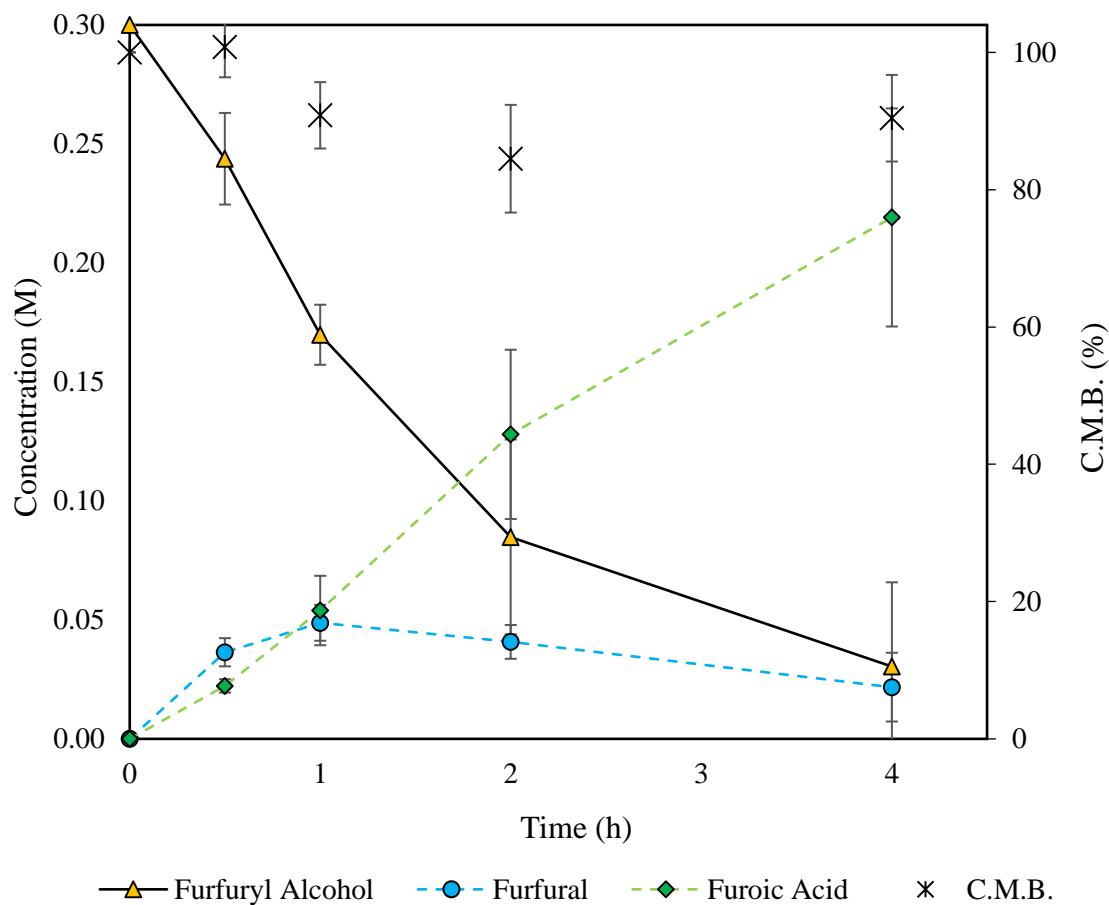
Figure 4.17. A time online plot for the oxidation of FOH over a 1% AuPd/Mg(OH)$_2$ catalyst. Error margins were assigned in accordance with the standard deviation of 4 separate tests with 2 different catalyst batches. Tests were conducted under standard reaction conditions using the modified experimental procedure. **Reaction conditions:** 10 mL substrate (0.3 M), NaOH:substrate =1, O$_2$ (3 bar), substrate:metal = 500, 30 ºC, 4 h.

As with the oxidation of FF, increasing the NaOH to substrate ratio clearly increases the performance of the catalyst for the oxidation of FOH in terms of both selectivity and activity. The presence of sacrificial hydroxide has been shown to significantly promote the activity of Au supported catalysts for alcohol oxidation reactions previously[41, 47]. The results displayed in Figur 4.18 are in agreement with this work as there is a clear increase in catalytic activity as the concentration of NaOH increases. Furthermore, an increased selectivity to the desired acid product with increasing NaOH concentration implies that the base not only facilitates the initial oxidative dehydrogenation but also the subsequent oxidation of the aldehyde. The increase in CMB observed with increasing base is further evidence to suggest that the alcohol can undergo polymerisation to form resins.
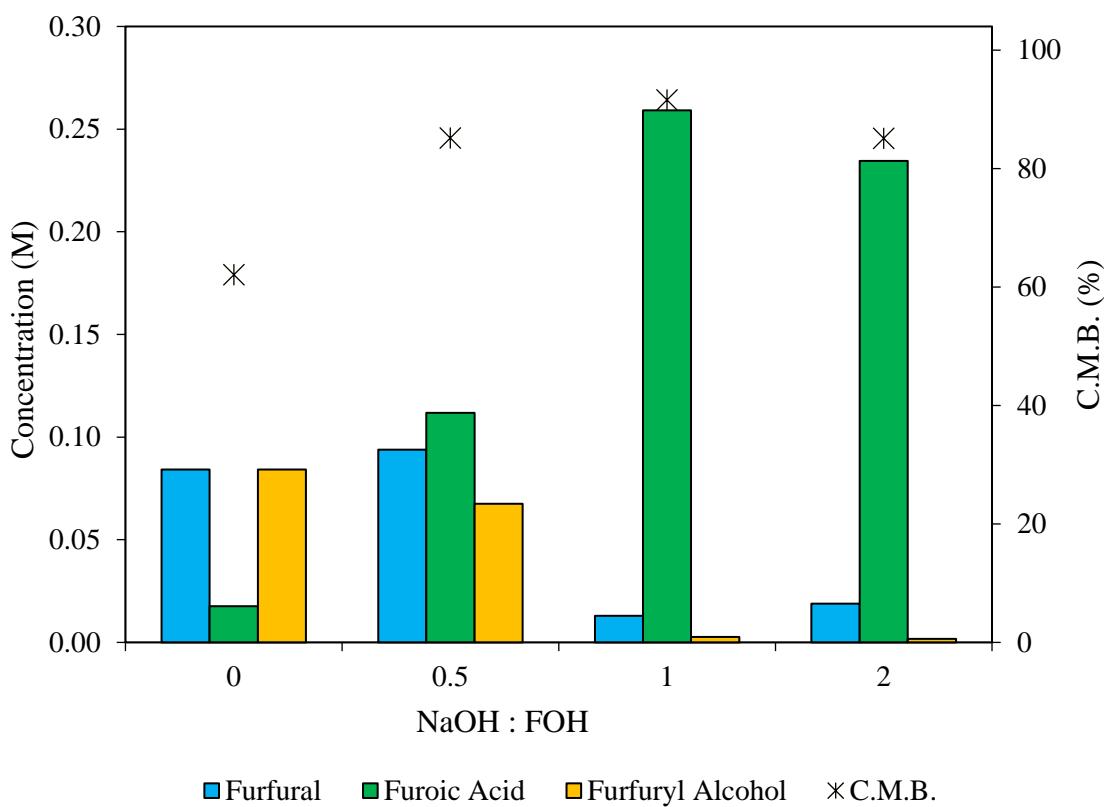
Figure 4.18. The base to substrate ratio is varied in order to assess the effect NaOH has on the performance of the 1% AuPd/Mg(OH)$_2$ catalyst. Tests were conducted using the modified experimental. Data reflects samples taken after of 4 h of reaction. **Reaction conditions:** 10 mL substrate (0.3 M), NaOH:substrate stated, O$_2$ (3 bar), substrate:metal = 500, 30 °C, 4 h.

The NaOH appears to be promoting the oxidative dehydrogenation pathway through the suppression of the polymerisation route. Interestingly, the CMB at low concentrations of base appears to be lower when compared with the mass losses observed for the reaction of FF. This may suggest that FOH may be more susceptible to undergo polymerisation than FF. It could also imply that the external hydroxyl groups play a more crucial role in the mechanism of the oxidative dehydrogenation. Oxygen pressure has also shown to have a significant impact on the catalytic performance of Au supported catalysts for the oxidation of alcohols[41, 48]. For this reason, a series of tests were conducted in order to assess the effect this variable had on the oxidation of FOH. The results of these tests are displayed in Figure 4.19.
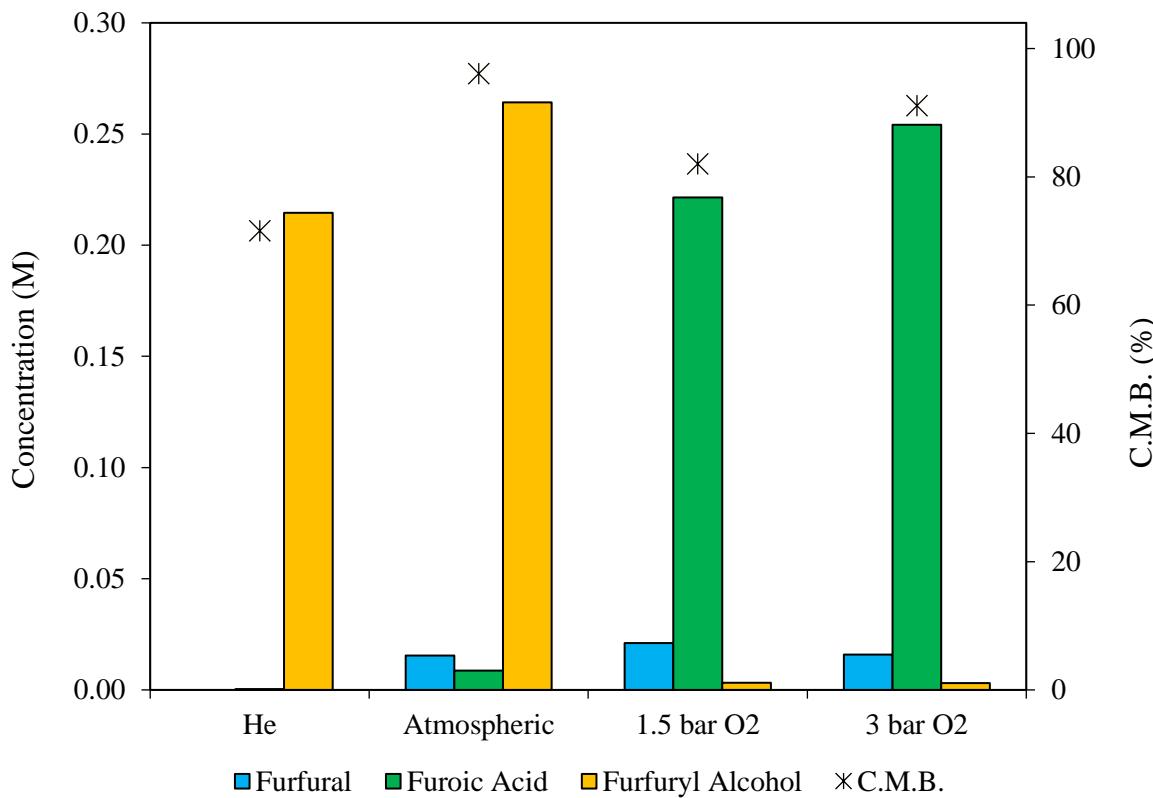
Figure 4.19. The quantity of oxygen is varied in order to assess the effect it has on the performance of the 1% AuPd/Mg(OH)$_2$ catalyst. Tests were conducted using the modified experimental procedure. He corresponds to the reactor purged 5 times and charged with 3 bar of Helium. Data reflects samples taken after 4 h of reaction. **Reaction conditions:** 10 mL substrate (0.3 M), NaOH:substrate = 1, O$_2$ pressure is stated, substrate:metal = 500, 30 ºC, 4 h.

As with the oxidation of FF, there is a clear increase in catalytic performance as the oxygen concentration is increased. Increasing the concentration of O$_2$ significantly increases the rate of FOH consumption at lower concentration. The effect on FOH consumption is less pronounced at high concentrations. This could suggest that the system is over saturated with O$_2$ at 1.5 bar, meaning that there is enough O$_2$ in the system at this pressure for the mechanistic process to be limited. If however we consider the CMB and the overall yield of FA of these two reactions, there is a notable increase in both data points at 3 bar of O$_2$ pressure. This could suggest that O$_2$ promotes the oxidation of the substrate through the competitive suppression of the polymerisation pathway. When tests were conducted under atmospheric conditions and in the presence of 3 bar of He, the activity and desired selectivity is significantly reduced. The presence of O$_2$ must also have a crucial role in the

143

reaction mechanism. The formation of resins appears to be less effected by oxygen concentration for the oxidation of FOH than FF. For this reason, it is possible that the route to the formation of resins is different for both FF and FOH.

4.5.4. Derivation of the Reaction Profile

The tests conducted in this section were designed to give an insight into the mechanistic profile for the catalytic oxidation of FF. The time online reaction of FF under standard reaction conditions revealed that trace amounts of FOH could be detected at the early stages of the reaction. The earlier studies conducted using Au/TiO_2 also revealed that the alcohol can be produced in fairly substantial quantities from FF. It was suggested that this was a results of a Cannizzaro reaction proceeding between the substrate and the aqueous NaOH. A time online plot of a reaction from FF in the absence of any catalyst confirmed that the Cannizzaro reaction is proceeding under the standard reaction conditions. This reaction does, however, appear to proceed significantly slower than the catalysed FF oxidation. Interestingly, a time online reaction from FOH under standard reaction conditions revealed that FA can be produced from the alcohol by a series of oxidations which appear to proceed *via* FF. For this reason it can be postulated that the absence of FOH at the end of the standard FF reaction is a result of the catalysts high affinity to catalyse the oxidation of any FOH which is produced *via* the Cannizzaro reaction. A proposed reaction profile is displayed in Figure 4.20.

A series of tests were also conducted where the concentrations of possible reactants were varied in order to gain a further understanding of the reaction mechanism. The selective catalytic oxidation of FF and FOH were clearly promoted by the presence of both NaOH and O_2. Increasing the quantities of both led to increased catalytic activity and favourable selectivity. Interestingly, both reactions require high levels of both O_2 and NaOH in order to achieve optimal results. Having the maximum quantity of one reactant and none of the other often led to poor activity and selectivity. This suggests that a synergistic interaction between the O_2 and NaOH could be responsible for achieving favourable results. Davis and co-workers[44, 49] have previously shown that both oxygen and an external hydroxide source

are required in order to yield the best activity for the oxidation of glycerol over Au supported catalysts.
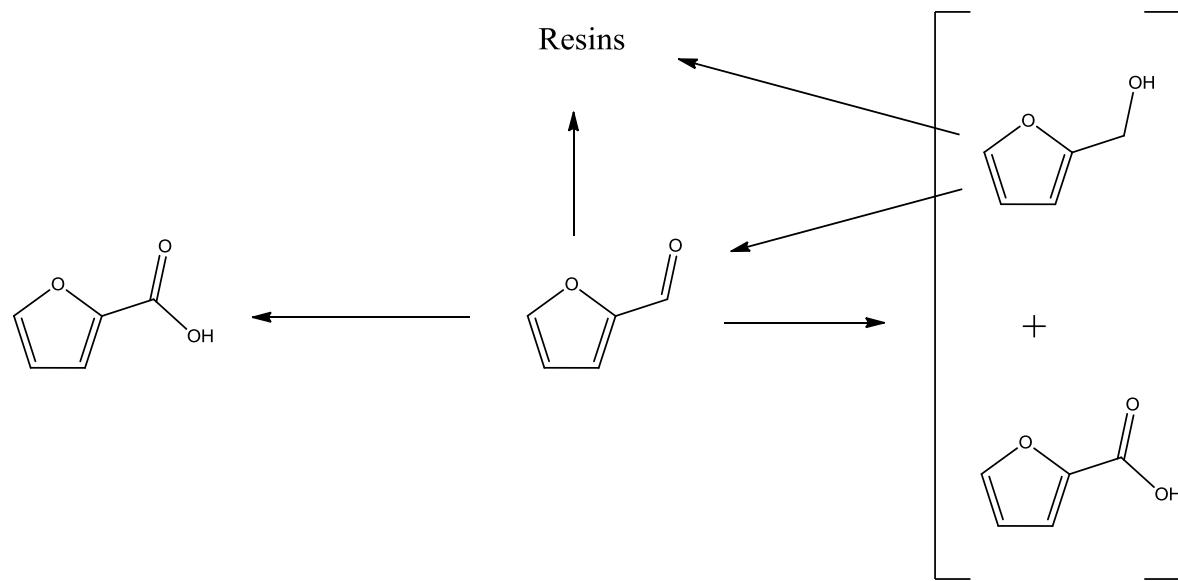

Figure 4.20. A proposed reaction profile for the oxidation of FF under standard reaction conditions.

The Cannizzaro reaction appears to proceed significantly slower than the two catalysed reactions. As expected the NaOH concentration has a substantial effect on the rate of this reaction. Oxygen pressure appeared to have a negligible impact on the rate of this reaction. In addition, substantial losses in carbon were observed as a result of the competing polymerisation pathway.

4.6. Investigation into the Reusability of the AuPd/Mg(OH)₂ Catalyst

When conducting academic research it is important to consider the industrial viability of a given process. A fundamental issue which is often encountered when facilitating the transfer of lab scale process to an industrial scale is catalyst reusability. For this reason, a series of experiments were conducted in order to assess the reusability of the 1 wt.% AuPd/Mg(OH)₂ catalyst for this reaction. The catalyst was removed from the reactor post reaction and subsequently washed, dried and retested under standard reaction conditions. In some cases, multiple reactions were required to ensure that enough catalyst tested was available for the subsequent tests. Three re-use tests were conducted and the corresponding results are displayed in Figure 4.21.
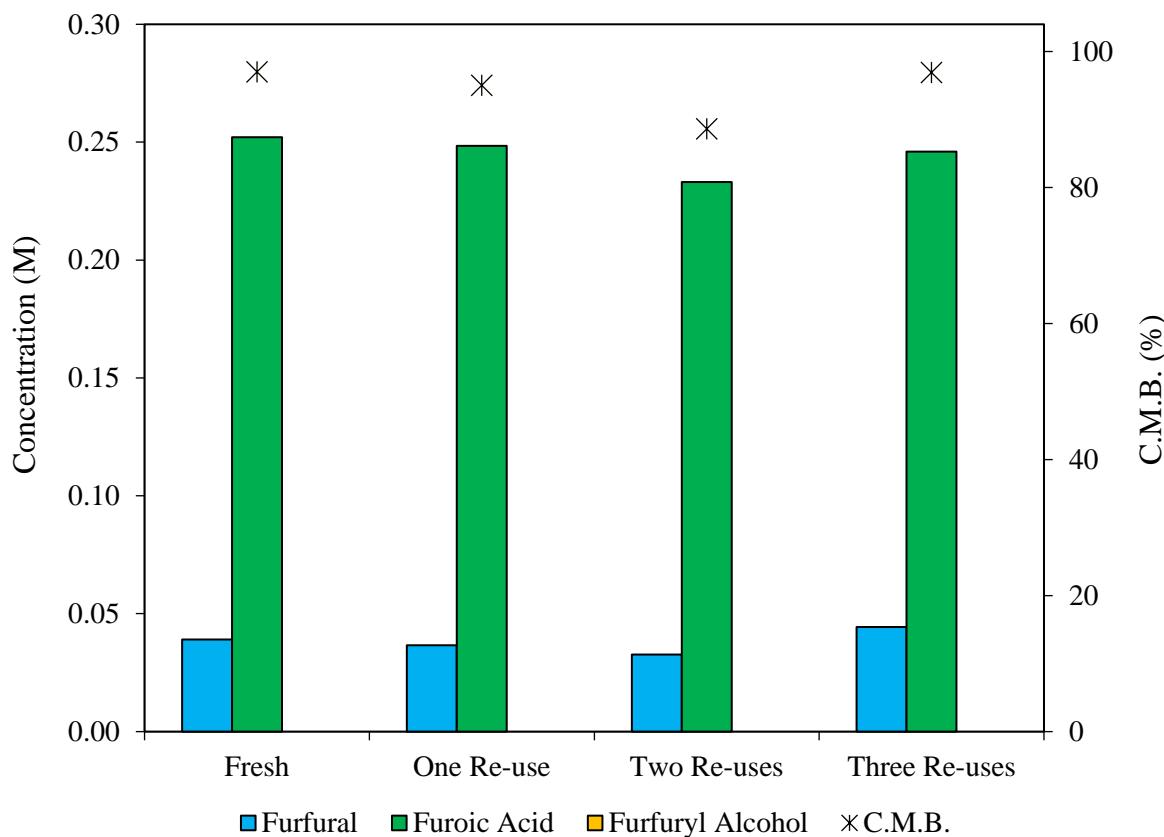
Figure 4.21. A re-use study for the oxidation of FF over fresh and used samples of the 1 wt.% AuPd/Mg(OH)₂ catalyst. Tests were conducted using the modified experimental procedure. Data reflects samples taken after of 4 h of reaction. **Reaction conditions:** 10 mL substrate (0.3 M), NaOH:substrate = 1, O₂ (3 bar), substrate:metal = 500, 30 ℃, 4 h.
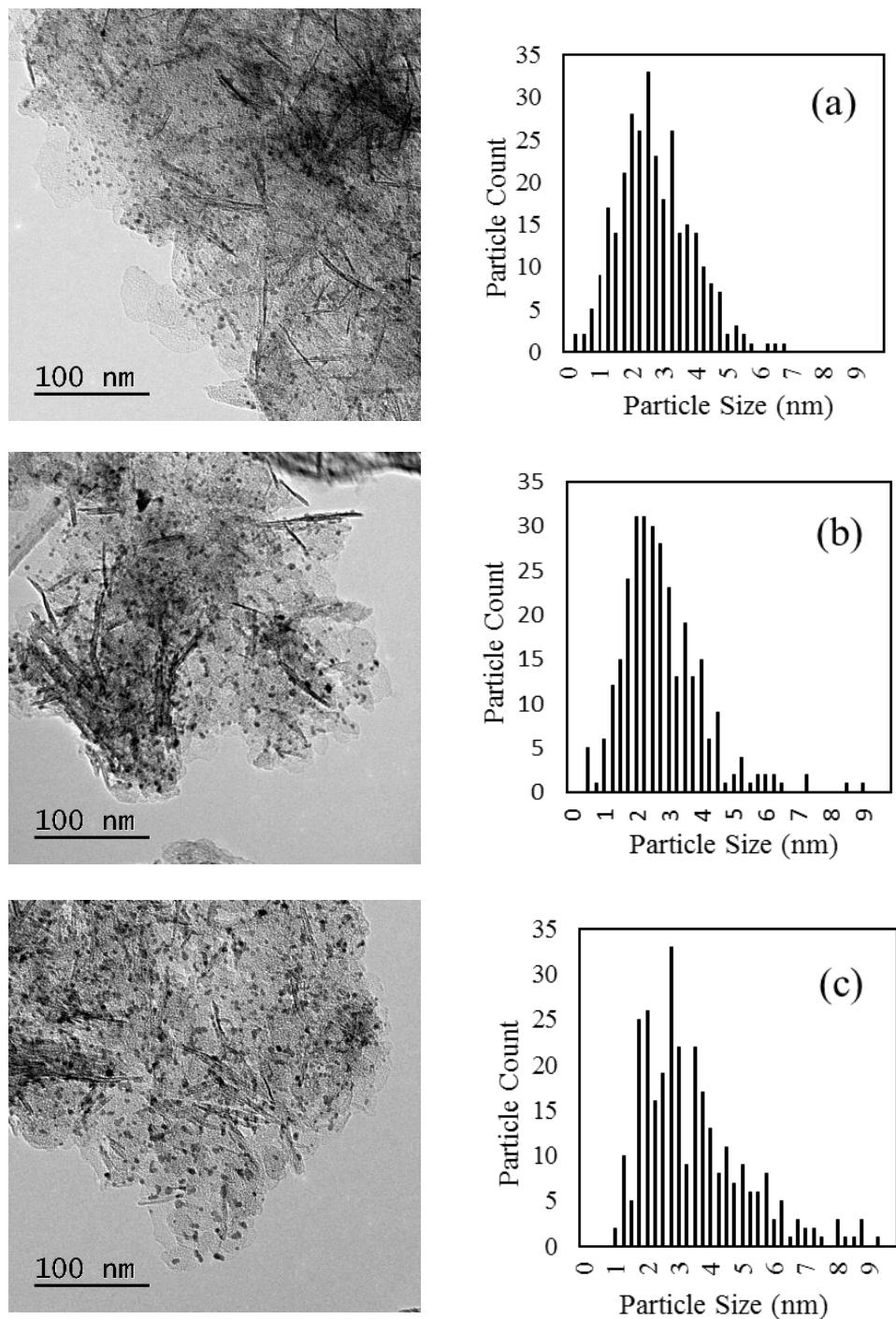
Figure 4.22. Images and PSD's corresponding to some of the catalysts. (a) Fresh catalyst, (b) used once and (c) used twice.

From the reaction data, there is no evidence to suggest that any catalyst deactivation is occurring

upon its re-use. The FA yield, FF conversion and CMB remain fairly constant across the four tests. Particle agglomeration is often associated with catalyst deactivation during extensive testing protocols. For this reason, TEM was conducted on the samples of the fresh catalyst and the catalyst tested once and twice. Images of these catalysts along with their corresponding particle size distributions (PSD's) are displayed in Figure 4.22.

From the PSD's it is clear that there is some evidence of particle agglomeration taking place between each use. Interestingly, this does not appear to have any impact on the performance of the catalysts which could suggest that particle size may not be crucial to catalytic performance. It is known that nanoparticles below 5 nm in diameter are active for alcohol oxidation[50, 51]. There is no substantial increase in the number of particles above 5 nm which may be why the activity of the catalyst remains constant across the reuse tests. It is difficult to assess at this point whether the agglomeration is a result of exposure to the experimental conditions or a result of extended exposure to high temperatures during the subsequent drying steps. Further work would be required in order to confirm this.

4.7. The Effect of Preparation Technique

In order to assess further the effect of particle size, a series of tests were conducted using 1 wt.% AuPd/Mg(OH)$_2$ catalysts which were prepared using different preparation techniques. It has been shown previously that the way in which a catalyst is prepared can significantly influence the performance of Au supported catalysts, which is often a result of a change in the mean particle size[52, 53]. AuPd/Mg(OH)$_2$ catalysts prepared by modified-impregnation and conventional impregnation were prepared and tested for the oxidation of FF under standard reaction conditions. The results of these tests are displayed in Figure 4.23, along with the results of the standard sol-immobilised AuPd/Mg(OH)$_2$ catalyst.

The catalysts prepared by sol-immobilisation and modified impregnation appear to have very similar reaction data with both catalysts displaying exceptional activity and selectivity to FA. Both of these preparation methods are believed to give highly dispersed metal nanoparticles with a well-defined PSD. These two preparation methods significantly outperformed the catalyst prepared by the conventional impregnation method. The conventional impregnation method is known to give a larger, less defined variation in particle size[52]. These results suggest that AuPd particle size is a crucial parameter to

consider. In order to verify this postulation, the three catalysts were examined using TEM. The images and PSD's of the corresponding catalysts are displayed in Figure 4.24.
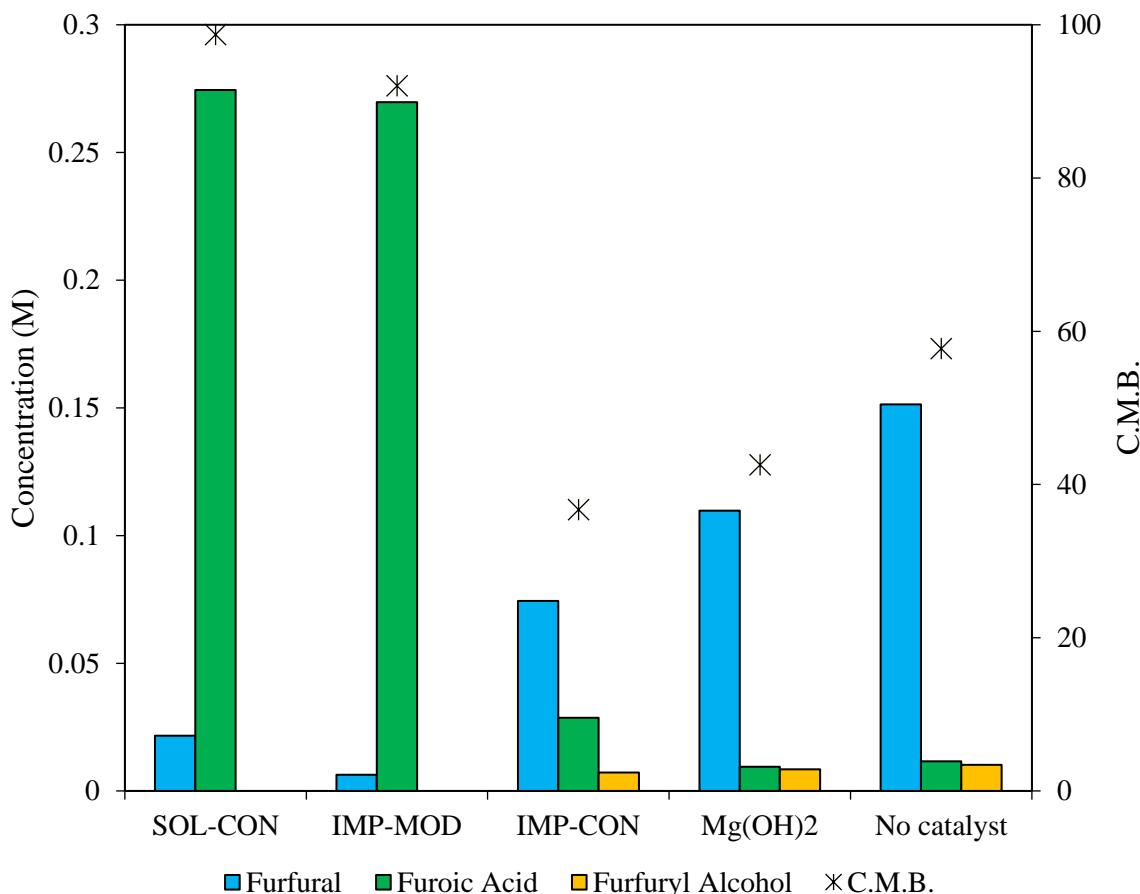

Figure 4.23. The oxidation of FF under standard reaction conditions over 1 wt.% AuPd/Mg(OH)₂ catalysts prepared by conventional sol-immobilisation (SOL-CON), modified impregnation (IMP-MOD) and conventional impregnation (IMP-CON). Additional tests were conducted using the blank support (Mg(OH)₂) and in the absence of any catalyst. All tests were conducted using the modified experimental procedure. Data reflects samples taken after of 4 h of reaction. **Reaction conditions:** 10 mL substrate (0.3 M), NaOH:substrate = 1, O₂ (3 bar), substrate:metal = 500, 30 ℃, 4 h.

The PSD's calculated from the TEM images of each catalyst it is evident that particle size of the active metal plays a pivotal role in the performance of the catalysts. The mean particle size determined for the catalysts prepared by the conventional sol immobilisation and modified impregnation techniques were 2.73 and 2.24 respectively. Due to the large
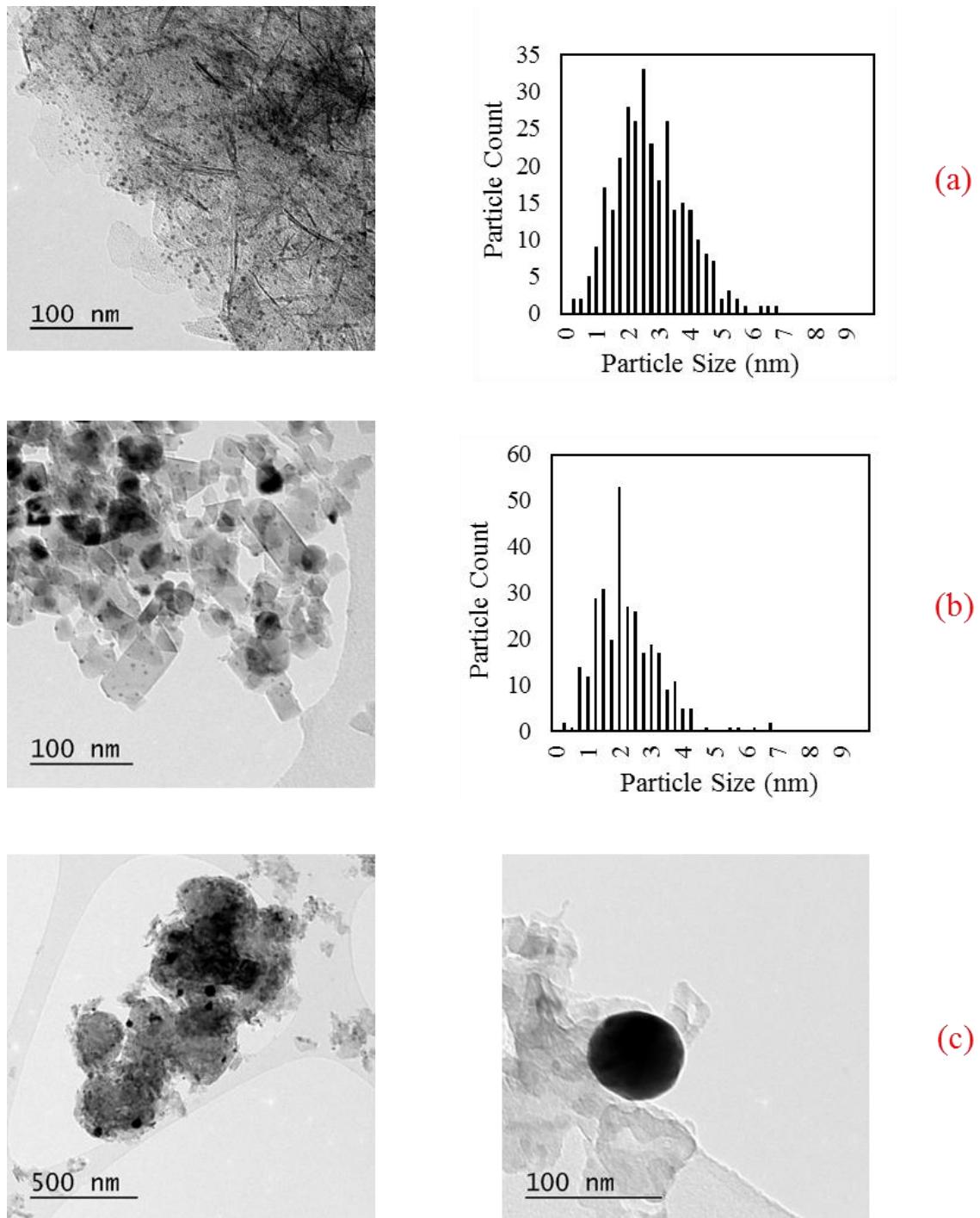
Figure 4.24. TEM images and PSD's corresponding to the catalysts prepared using different methods. (a) Conventional sol immobilisation, (b) modified impregnation and (c) conventional impregnation.

size of the particles in the conventional impregnation technique it was not possible to locate enough nanoparticles to satisfy the sampling criteria. It was however clear that the mean particle size of this catalyst was comparably higher than that of the other two catalysts with particles displaying diameters of up to 80 nm. The performance of this catalyst was poor when compared to the other two catalysts, and as a result it can be postulated that small nanoparticles are crucial in order to obtain high catalytic activity, desirable selectivity and reaction control.

Interestingly, the catalyst prepared by the conventional impregnation has a comparable reaction profile to that observed for the reaction with $Mg(OH)_2$ and the reaction without a catalyst. The reaction with the catalyst does appear to yield a higher selectivity towards FA which suggests that the nanoparticles are functioning at a significantly reduced rate. It is likely that this is a result of a small proportion of the metal nanoparticles lying within the active size range.

4.8.   The Effect of the Au-Pd Ratio

It has already been shown in this work that the incorporation of Pd into Au supported catalysts can enhance catalytic performance for the catalytic oxidation of FF. For this reason, it was important to design a set of experiments in order to investigate the role of each metal. A series of $AuPd/Mg(OH)_2$ catalysts were prepared using the conventional sol-immobilisation technique with varied quantities of Au and Pd metal and with a targeted overall metal loading of 1 wt.%. MP-AES was used in order to precisely identify the metal loadings of Au and Pd for each of the catalyst. Table 4.1 contains the Au and Pd metal loadings of each of the catalysts confirmed by MP-AES.

It is clear that the overall metal weight loading fluctuates somewhat. This appears to be a consequence of higher quantities of Pd loaded onto the support than anticipated. This is likely a result of the palladium stock solution being higher in Pd concentration than previously thought. These catalysts were subsequently tested for oxidation of FF to FA. In order to assure a fair comparison between the catalysts, the mass of catalyst used was varied in order to satisfy a 500:1 molar substrate to metal ratio. Due to the discrepancies in metal

weight loadings, the FA yield was normalised to account for variations. The results of these tests are displayed in Figure 4.25.

Table 4.1. The metal loadings corresponding to a series of Au and Pd catalysts supported on $Mg(OH)_2$ are displayed. The Au and Pd metal loadings were confirmed by MP-AES.

Catalyst	Au (wt.%)	Pd (wt.%)	Total Metal Loading (wt.%)
$Pd/Mg(OH)_2$	0.00	1.32	1.32
$AuPd/Mg(OH)_2$ A	0.12	1.16	1.28
$AuPd/Mg(OH)_2$ B	0.26	0.86	1.13
$AuPd/Mg(OH)_2$ C	0.56	0.50	1.06
$AuPd/Mg(OH)_2$ D	0.54	0.42	0.96
$AuPd/Mg(OH)_2$ E	0.79	0.29	1.08
$Au/Mg(OH)_2$	1.01	0.00	1.01

It is evident from Figure 4.25 that the ratio of Au and Pd in the catalyst has a profound effect on the reaction profile. At 0.5 h, the highest FA yields appear to be obtained with the monometallic Au and Pd catalysts. Synergistic interactions between the two metals appear to be an exception to this, as comparable FA yields to the monometallic catalysts are observed with catalysts consisting of approximately a 1:1 Au:Pd weight ratio. Interestingly, the opposite is true for the FA yield observed after the 4 h reaction. A synergistic trend between the two metals is observed, with the highest FA yields observed with equimolar quantities of Au and Pd. By examining the quantity of FF converted by each of the catalysts (displayed in Table 4.2) with time, it is possible to derive an explanation for this trend.

The FF conversions at 0.5 h obtained from the monometallic catalysts are higher than the bimetallic catalysts with the only exception being the equimolar AuPd catalyst. It is likely that the high FA yields displayed by these three catalysts at 0.5 h is a result only of more substrate being converted. The monometallic catalysts appear to be more active and there appear to be some synergistic interactions between the bimetallic catalysts.
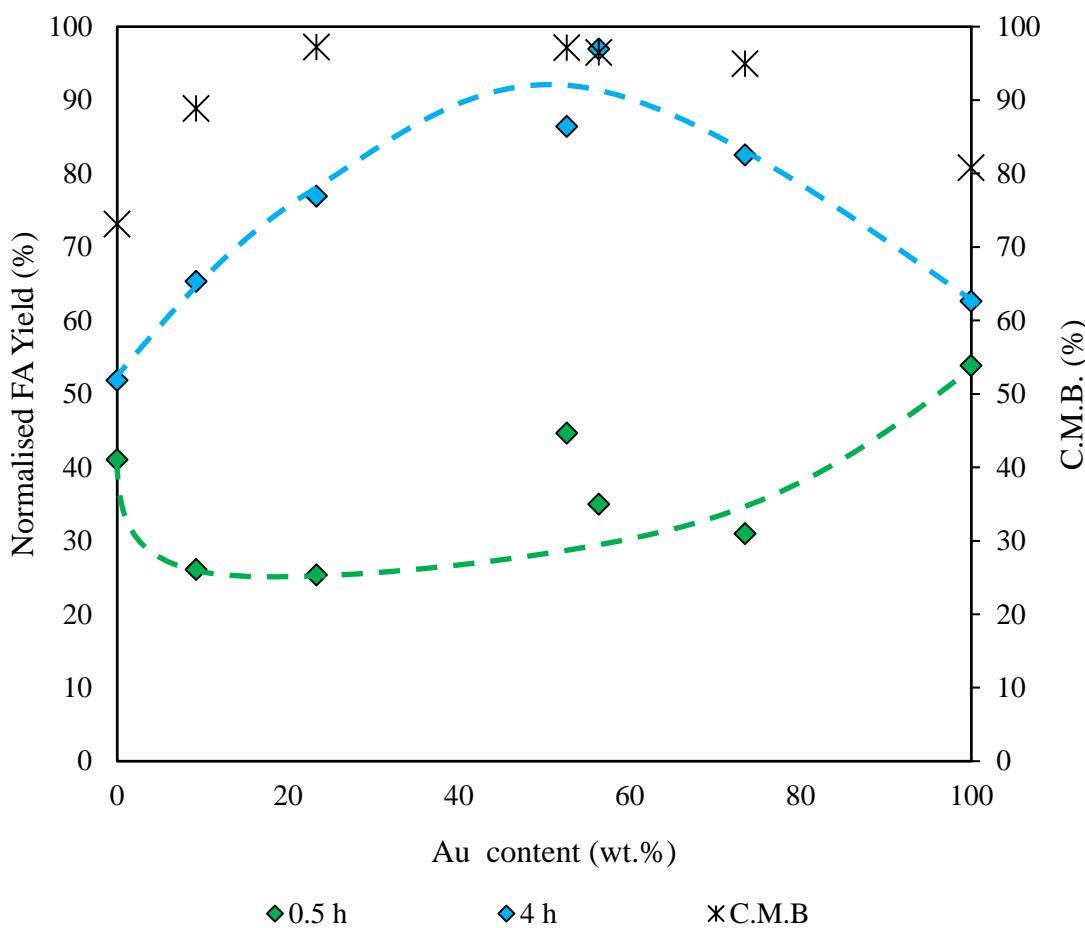
Figure 4.25. A series of catalysts containing varied quantities of Au and Pd supported on Mg(OH)$_2$ were tested for the oxidation of FF using the modified experimental procedure and under standard conditions. The normalised FA yield for each catalyst is displayed at 0.5 h and 4 h along with the C.M.B. at 4 h. **Reaction conditions:** 10 mL substrate (0.3 M), NaOH:substrate = 1, O$_2$ (3 bar), substrate:metal = 500, 30 °C, 4 h.

The FF conversions at 0.5 h obtained from the monometallic catalysts are higher than the bimetallic catalysts with the only exception being the equimolar AuPd catalyst. It is likely that the high FA yields displayed by these three catalysts at 0.5 h is a result only of more substrate being converted. What can be said is that the monometallic catalysts appear to be more active and there appear to be some synergistic interactions between the bimetallic catalysts.

Table 4.2. The FF conversions at 0.5 h for the corresponding catalysts are displayed.
Reaction conditions: 10 mL substrate (0.3 M), NaOH:substrate = 1, O_2 (3 bar), substrate:metal = 500, 30 ℃, 4 h.

Au (%)	Conversion (%)
0.0	54
9.2	40
23.3	35
52.6	52
56.4	35
73.5	45
100.0	77

There is a clear synergistic trend in the observed FA yield at 4 h. As the active metal content of the catalysts become more equimolar, the normalised FA yield is greater. A similar trend is observed for the carbon mass balance. It is possible that the high activity displayed by the monometallic catalysts is detrimental to their overall performance. The low CMBs associated with these catalysts suggest that a significant proportion of substrate is being lost to polymerisation. It is well known that chemical species formed in reaction can reduce catalytic activity through active site poisoning[54]

It can be postulated that short surface lifetimes of the substrate may be responsible for their formation. The low initial conversions associated with the equimolar catalysts may be a result of synergistic interactions which in turn lead to stronger adsorption of the substrate to the nanoparticles. Another possibility is that a higher population of desirable active sites are present in the equimolar catalysts which would lead to higher FA yields. It is difficult to suggest how plausible these theories are at this point but further work consisting of adsorption studies could shed more light on the reactivity of these catalysts.

4.9. Application of Kinetics to the Reaction System

Reaction kinetics are an incredibly useful tool in order to develop a greater understanding of a reaction system. Determination of the reaction rates and reaction orders can reveal useful information regarding the reaction mechanism and subsequently assist with catalyst design.

Due to the complexity of this reaction system, assigning reaction orders and rate constants is difficult. It has been determined that there are at least three reactions leading to the formation FA proceeding simultaneously. The first step in obtaining the rate constants for the three reactions was to determine the reaction orders with respect to each reactant. This was conducted using the initial rates methodology. Due to the sensitivity of the substrate to undergo polymerisation, the reaction rates were monitored in terms of FA produced rather than the traditional method of substrate consumption. In addition, the competitive nature of the catalytic aldehyde oxidation and the Cannizzaro reaction meant that it was difficult to derive accurate figures for the FA concentration produced by these pathways. In order to account for this, the concentration of FA produced from the Cannizzaro reaction was deducted from the concentration of FA produced in the presence of the catalyst. This is summarised in equation 1.

$$[FA]_{DO} = [FA]_{total} - [FA]_{CAN}$$

Equation 1. An expression used to determine rate in which FF is consumed through the direct catalytic oxidation to FA. DO - Direct catalytic oxidation, CAN – Cannizzaro reaction, total – standard reaction from FF in the presence of a catalyst.

Additionally, the oxidative dehydrogenation of alcohol was monitored by the total concentration of FF and FOH produced. This is summarised in equation 2.

$$[FOH]_{Consumed} = ([FF] + [FA])$$

Equation 2. An expression used to determine the rate in which FOH was consumed through catalytic oxidation.

155

Finally, the rate of the Cannizzaro reaction is determined by monitoring the concentration of FA produced in the absence of any catalyst.

This method of determining the rates of each reaction are reliant upon three assumptions.

1. FA is stable in the reaction system.

2. The supported metal nanoparticles do not actively promote the Cannizzaro reaction.

3. FA produced *via* the Cannizzaro pathway is minimal when monitoring the rate of the oxidative dehydrogenation pathway.

4.9.1. Determination of the Reaction Orders

The reaction order of each pathway was derived by monitoring the effect [substrate], [O_2] and [NaOH] had on the reaction rate. For each reaction, short term interval sampling was used to derive reaction rates using the initial rates methodology. Figure 4.26 demonstrates how the reaction rate of each pathway is affected when the substrate concentration is varied.

The catalytic oxidation of FF appears to follow first order kinetics with respect to the substrate concentration. Determining the reaction order of the oxidative dehydrogenation is more difficult. At low FOH concentrations, the reaction appears to follow first order kinetics. However, as the concentration reaches the standard reaction concentration (0.3 M), it appears to change to follow zero order reaction kinetics. It is likely that this is a result of active site saturation. As the concentration of the substrate is increased beyond 0.2 M, the catalytic turnover is limited by the surface lifetime of substrate. This suggests that the oxidative dehydrogenation reaction obeys zeroth order kinetics under standard reaction conditions. The Cannizzaro reaction appears to follow second order kinetic with respect to the substrate. This is expected as two substrate molecules are consumed in each reaction.
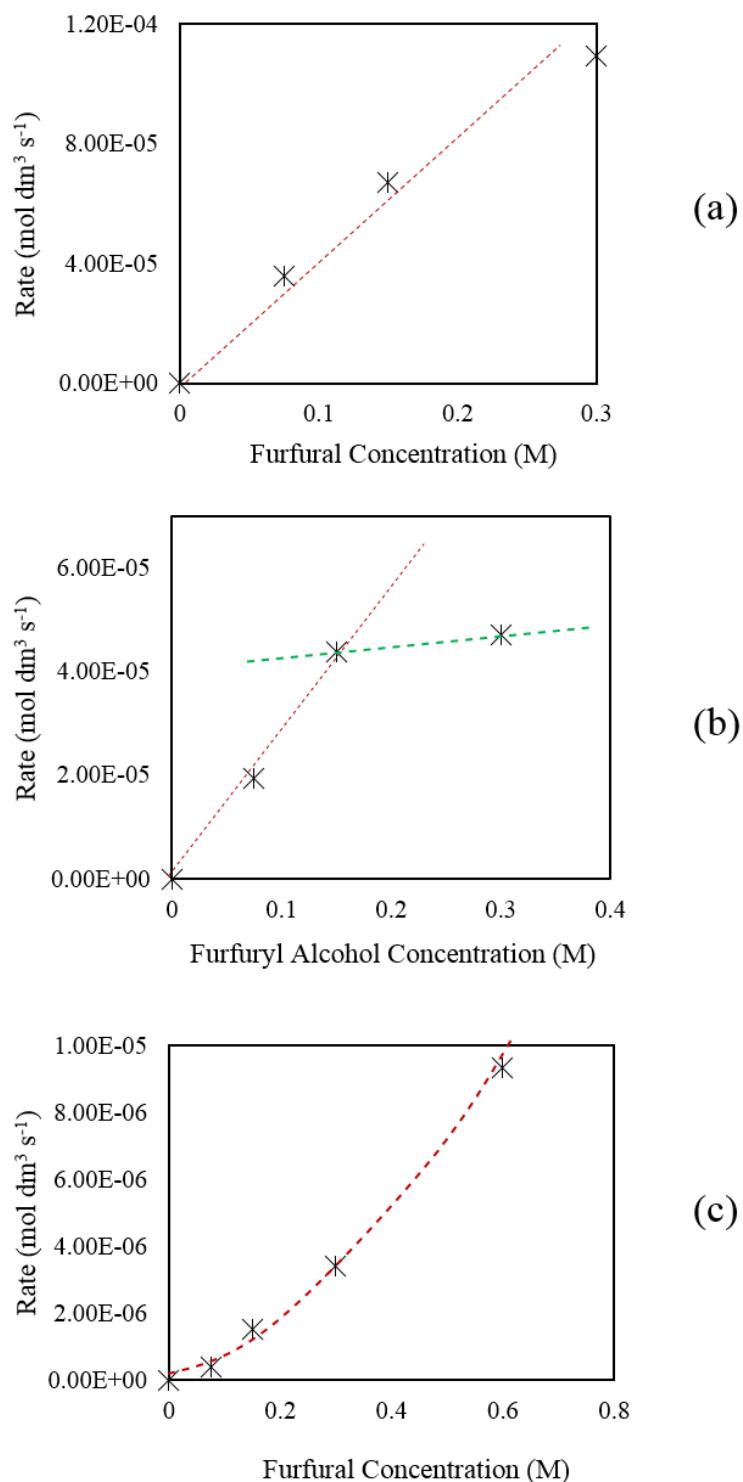
Figure 4.26. Graphical representations revealing how the rates of reaction are effected by substrate concentration in (a) catalytic aldehyde oxidation, (b) oxidative dehydrogenation of FOH and (c) the Cannizzaro reaction.
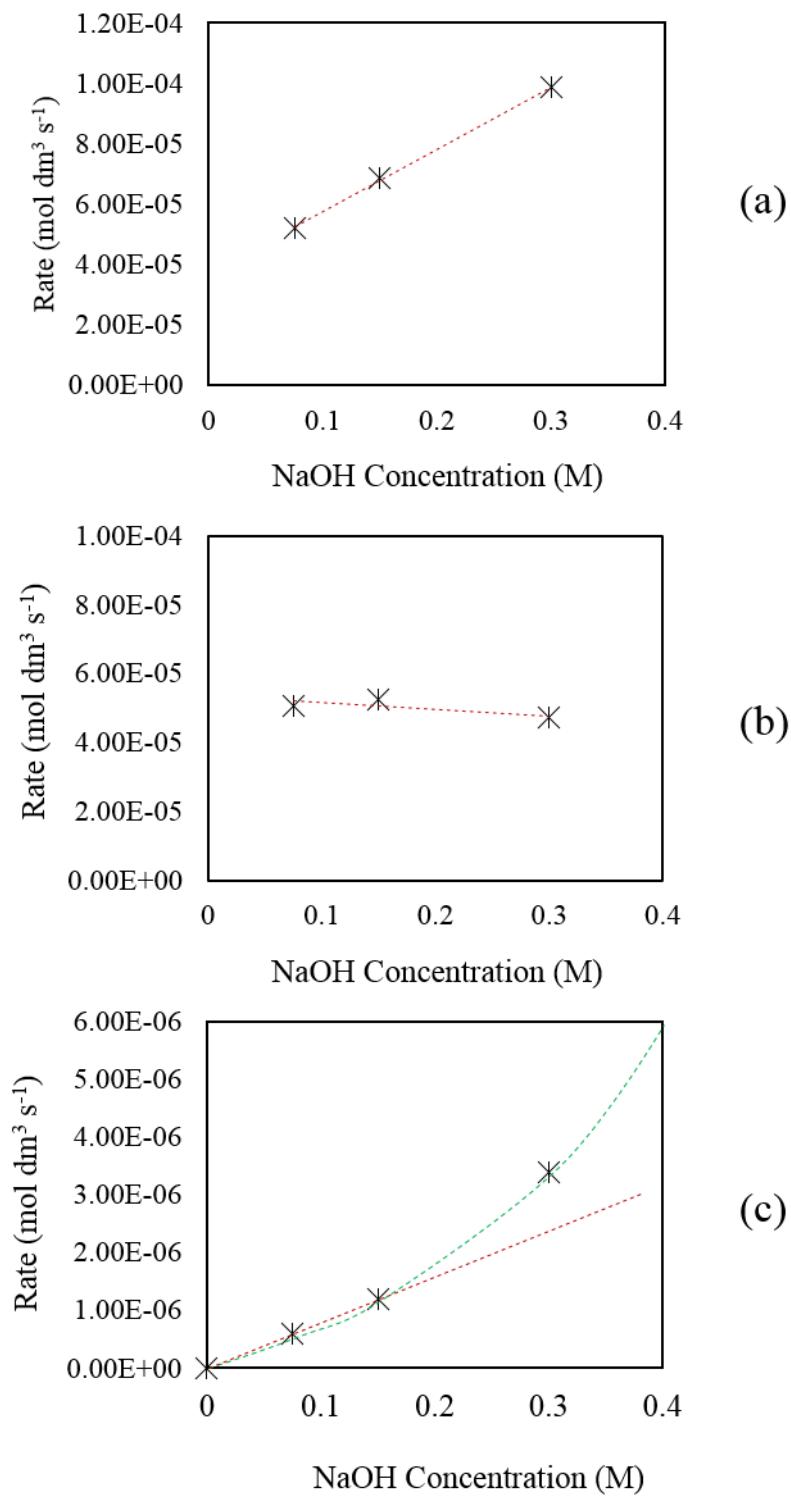
Figure 4.27. Graphical representations revealing how the rates of reaction are effected by NaOH concentration in (a) catalytic aldehyde oxidation, (b) oxidative dehydrogenation of FOH and (c) the Cannizzaro reaction.
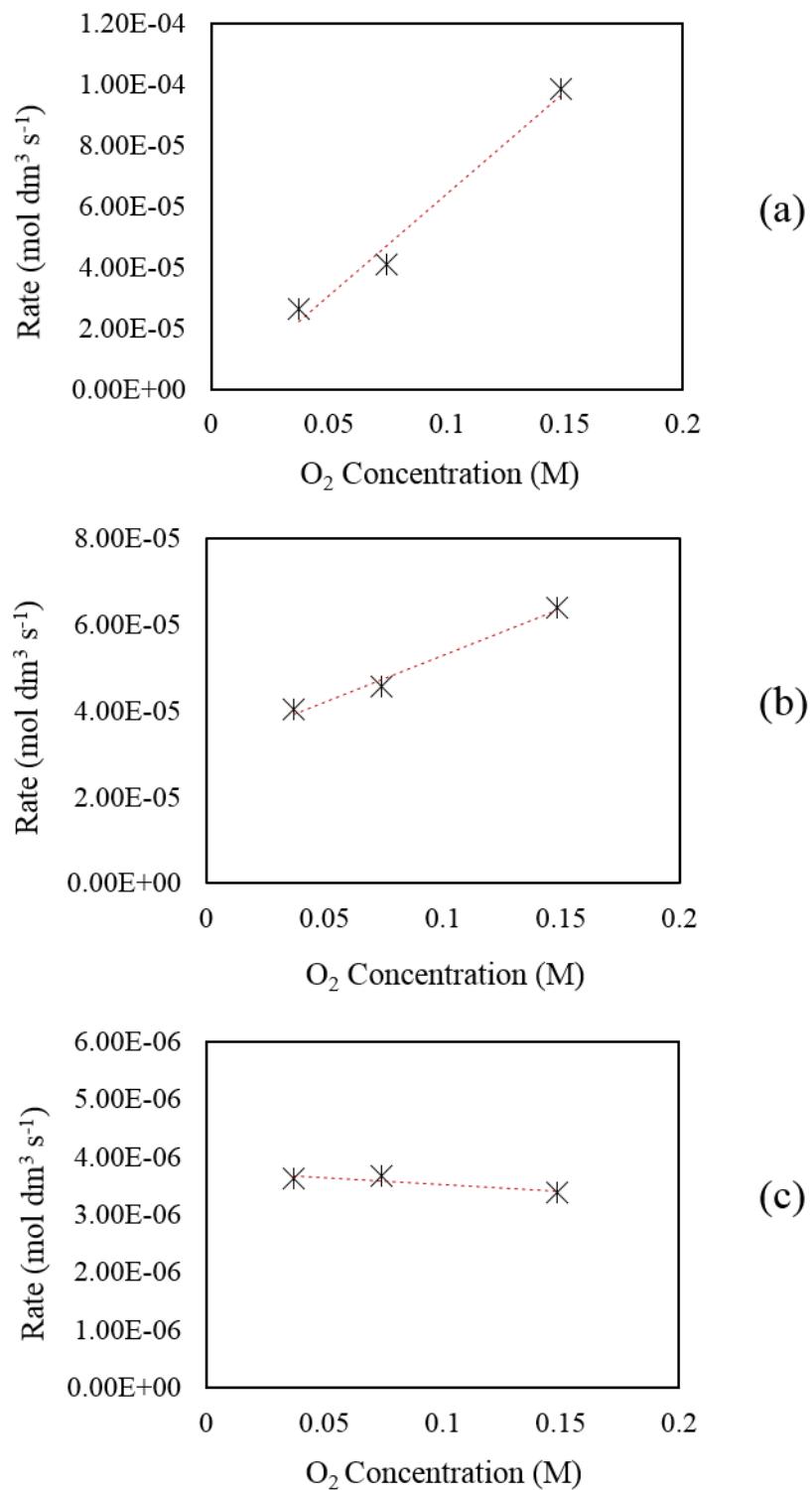
Figure 4.27 reveals how the rate of each reaction is affected by the concentration of NaOH.

Figure 4.28. Graphical representations revealing how the rates of reaction are effected by NaOH concentration in (a) catalytic aldehyde oxidation, (b) oxidative dehydrogenation of FOH and (c) the Cannizzaro reaction.

For the catalytic oxidation of FF, a first order trend is observed. This suggests that there is

a stoichiometric relationship between NaOH and this reaction pathway – one molecule of NaOH is consumed for each conversion of FF to FA. The catalyst offers an alternative reaction pathway which involves the nucleophilic attack of the aldehyde by the ⁻OH species. As this transformation does not appear to take place in the absence of the catalyst, it must be assumed that the substrate must be bound to the surface of the catalyst for this to occur. It was postulated previously in this chapter that the binding of the substrate may weaken the C-H bond of the targeted carbon centre, hereby facilitating the substitution of the H with the sacrificial OH species. The relationship between the reaction rate and NaOH strengthens this theory as a possible mechanistic solution.

Interestingly, the rate of the oxidative dehydrogenation pathway does not appear to be effected by NaOH concentration. This may suggest that NaOH plays no part in the oxidation of the alcohol species. This is unusual as it is known that hydroxyl groups often play an important in the activation of the substrate[49] in oxidation reactions involving Au catalysts. Another possible explanation for this result is that the catalyst is saturated with OH species prior to the first data point. It is likely that if additional reactions were conducted at lower concentrations of NaOH, a rate dependence on NaOH concentration would be observed. As it stands, under the standard reaction conditions the NaOH concentration has a zero order relationship with the reaction rate.

It is well known that the Cannizzaro reaction is initiated through an interaction between the substrate and base[55]. From this statement it is obvious that the rate of the Cannizzaro reaction would be dependent on the concentration of NaOH. Figure 4.27 shows that at low concentrations of base, the rate of the reaction appears to have a first order relationship with respect to NaOH concentration. As the NaOH concentration increases, the relationship appears to become more second order in nature. This observation is not unusual as previous publications investigating the kinetics of the Cannizzaro reaction have documented the same trend[55]. At high concentrations of base it is stated that an interaction between an $R.CHO_2^{2-}$ species and FF can occur. Two molecules of NaOH would be required for the formation of this doubly charged anion. It is unlikely that this secondary pathway is dominant at a concentration of 0.3 M. For the estimation of the rate constants, it must be assumed that the rate of the Cannizzaro reaction is first order with respect to NaOH under standard reaction conditions.

Figure 4.28 reveals how the rate of each reaction is affected by the concentration of O_2. In order to determine the molar concentration of O_2 in the system, pressures in bar were converted to molar concentration using the ideal gas law.

There is a clear first order relationship between the reaction rate and O_2 pressure for the catalytic oxidation of FF to FA. This suggests that O_2 must play a pivotal role in the reaction mechanism. As discussed in Chapter 3, H_2O has been found to reduce O_2 in other similar catalytic reactions[44], leading to the formation of *OH and *OOH species. It is likely that these species are responsible for the increase in reaction rate as oxygen concentration is increased. A first order relationship is also observed for the oxidative dehydrogenation reaction, which is likely a result of the same species being formed. Interestingly, there is no change in the rate of the Cannizzaro reaction when the concentration of O_2 is varied. This is expected as O_2 is not considered to play a part in previously published derivations of the Cannizzaro mechanism[55]. However, if *OH radical species are being produced through the reduction of O_2 by NaOH you may expect to see some dependence on O_2. The fact that no dependence is observed could suggest that *OH radicals are only generated in small quantities or rapidly decompose under the reaction conditions. If this is the case then it is likely that the rate of the catalytic oxidation of FF and oxidative dehydrogenation pathways are more dependent on the *OOH species being produced.

To summarise, under standard conditions the direct oxidation pathway has a first order rate dependence on substrate, NaOH and O_2 concentrations. The oxidative dehydrogenation has a first order rate dependence on substrate and O_2 concentration and a zero order rate dependence with respect to NaOH. The rate of the Cannizzaro reaction has a second order relationship with respect to substrate concentration, a first order relationship with respect to NaOH concentration and a zero order rate dependence with respect to O_2.

4.9.2. <u>Determination of Reactions Rate Constants</u>

The rate equations of each reaction were derived from the initial rates study. They are displayed in Figure 4.29.

$$K_{DO} = k.[FF]^1.[O_2]^1.[NaOH]^1$$

$$K_{OD} = k.[FF]^1.[O_2]^1.[NaOH]^0$$

$$K_{CAN} = k.[FF]^2.[O_2]^0 .[NaOH]^1$$

Figure 4.29 The rate equations derived from the initial rates experiments for; DO – Catalytic oxidation of FF to FA, OD – Catalytic oxidative dehydrogenation of FALC and CAN-intermolecular Cannizzaro reaction.

From the rate equations in 4.29, it is possible to derive rate constants for each reaction. In order for this to be possible, the rate (K) of each reaction must be determined. Figure 4.30 contains graphs corresponding to the initial rates measurements of each reaction. Again using the initial rates methodology, it is possible to extract the relative rates of each reaction. It was determined that K_{CAO}, K_{OD} and K_{CAN} is 0.0001096, 0.0000639 and 0.00000339 mol dm^{-3} s^{-1}. By taking these initial rates and inserting them into each rate equation along with the starting concentrations of each reactant, it is possible to determine the rate constant for each reaction.

Table 4.3. The rate equations and rate constants derived for each of the reaction pathways.

Pathway	Rate Equation	Rate constant (k)
Catalytic Aldehyde Oxidation (CAO)	$K = k.[FF]^1.[O_2]^1.[NaOH]^1$	5.89 x 10^{-3} mol^{-2} dm^6 s^{-1}
Oxidative Dehydrogenation (DO)	$K = k.[FF]^1.[O_2]^1.[NaOH]^0$	1.33 x 10^{-3} mol^{-1} dm^3 s^{-1}
Cannizzaro Reaction (CAN)	$K = k.[FF]^2.[O_2]^0.[NaOH]^1$	8.22 x 10^{-5} mol^{-2} dm^6 s^{-1}

y = 0.0001096 x

(a)

y = 0.00006390 x

(b)

y = 0.00000339 x

(c)
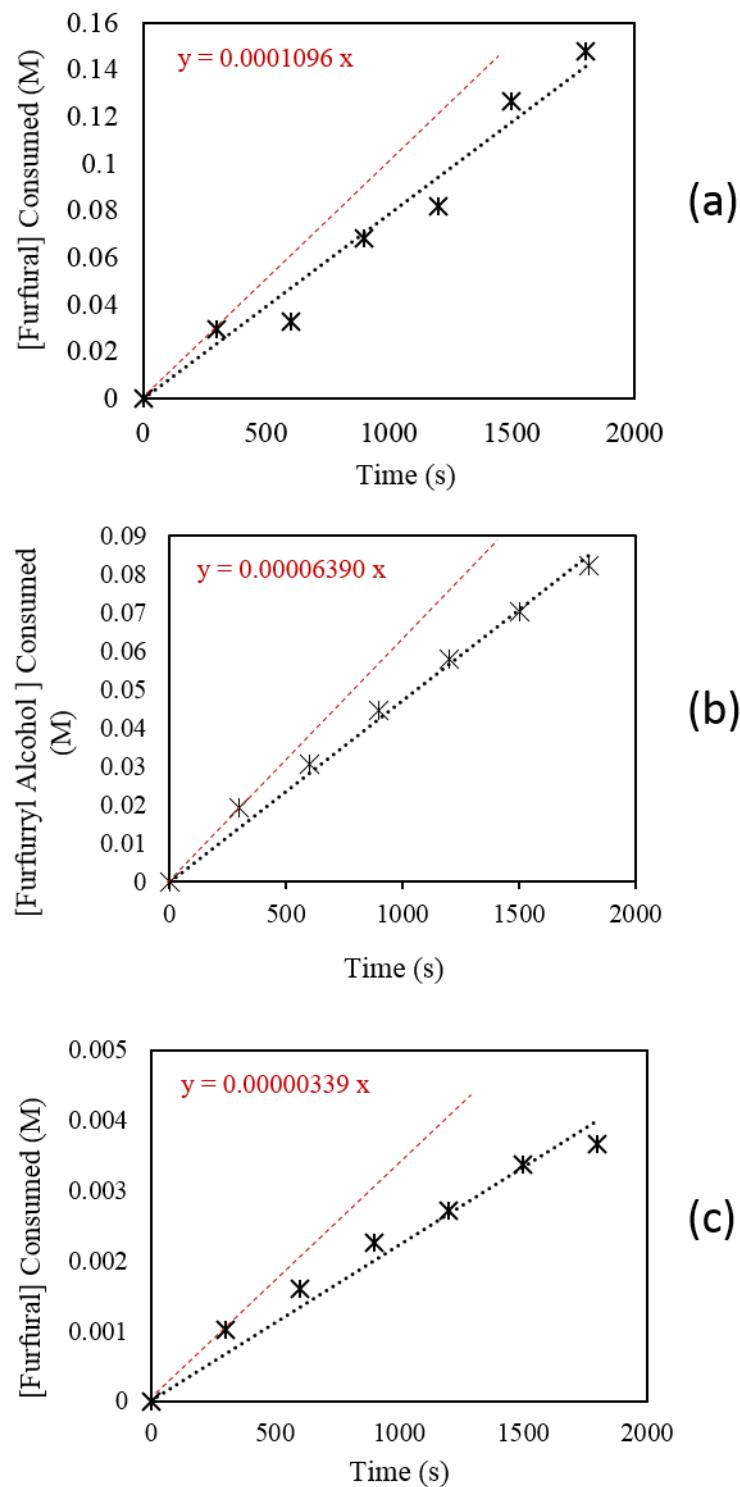
4.9.3. Determination of the Activation Energies (Ea)

Figure 4.30. Initial rates experiments for (a) catalytic aldehyde oxidation, (b) oxidative dehydrogenation and (c) the Cannizzaro reaction. All reactions were conducted under standard reaction conditions.

Having systematically determined the reaction orders and rate constants of each reaction pathway, it was then necessary to determine the activation energy (Ea) of each reaction pathway in order to give a more complete understanding of the reaction profile. In order to do this, additional initial rate experiments were conducted for each of the reactions at varied temperatures. Due to the problems associated with polymerisation experienced at elevated temperatures, initial rate experiments were conducted at lower temperatures than the standard reaction temperature. The rate constants were derived for each reaction at each temperature using the same method shown previously. Once derived, it was possible to use the rate constants to create Arrhenius plots for each of the reactions. These are displayed in Figure 4.31. From the Arrhenius plots it was possible to derive activation energies for each of the reactions.

Table 4.4. Derived data for the kinetics of each reaction pathway observed in the catalytic oxidation of FF.

Reaction	Cannizzaro	Oxidative Dehydrogenation	Catalytic Aldehyde Oxidation
Catalytic	NO	YES	YES
Rate Equation	$K = k \cdot [FF]^2 \cdot [O_2]^0 \cdot [NaOH]^1$	$K = k \cdot [FAlc]^1 \cdot [O_2]^1 \cdot [NaOH]^0$	$K = k \cdot [FF]^1 \cdot [O_2]^1 \cdot [NaOH]^1$
Reaction Order	Third	Second	Third
Activation Energy (Ea)	78.4 KJ mol^{-1}	32.9 KJ mol^{-1}	13.9 KJ mol^{-1}

Activation energies of 13.9 KJ mol^{-1}, 32.9 KJ mol^{-1} and 78.4 KJ mol^{-1} were determined for the catalytic aldehyde oxidation, oxidative dehydrogenation and the Cannizzaro reaction respectively. The significant increase in activation energy required for the substrate to form FA *via* the Cannizzaro pathway compared with the catalytic oxidation of FF. The observed conversion of substrate to FA *via* the Cannizzaro pathway is insignificant when compared to the reaction in the presence of the catalyst. The presence of the catalyst significantly reduces the activation barrier by offering an alternative reaction pathway. Additionally, the activation energy determined for FOH oxidation is higher than the aldehyde oxidation suggesting that the oxidative dehydrogenation to form the aldehyde is a more energy intensive transformation.
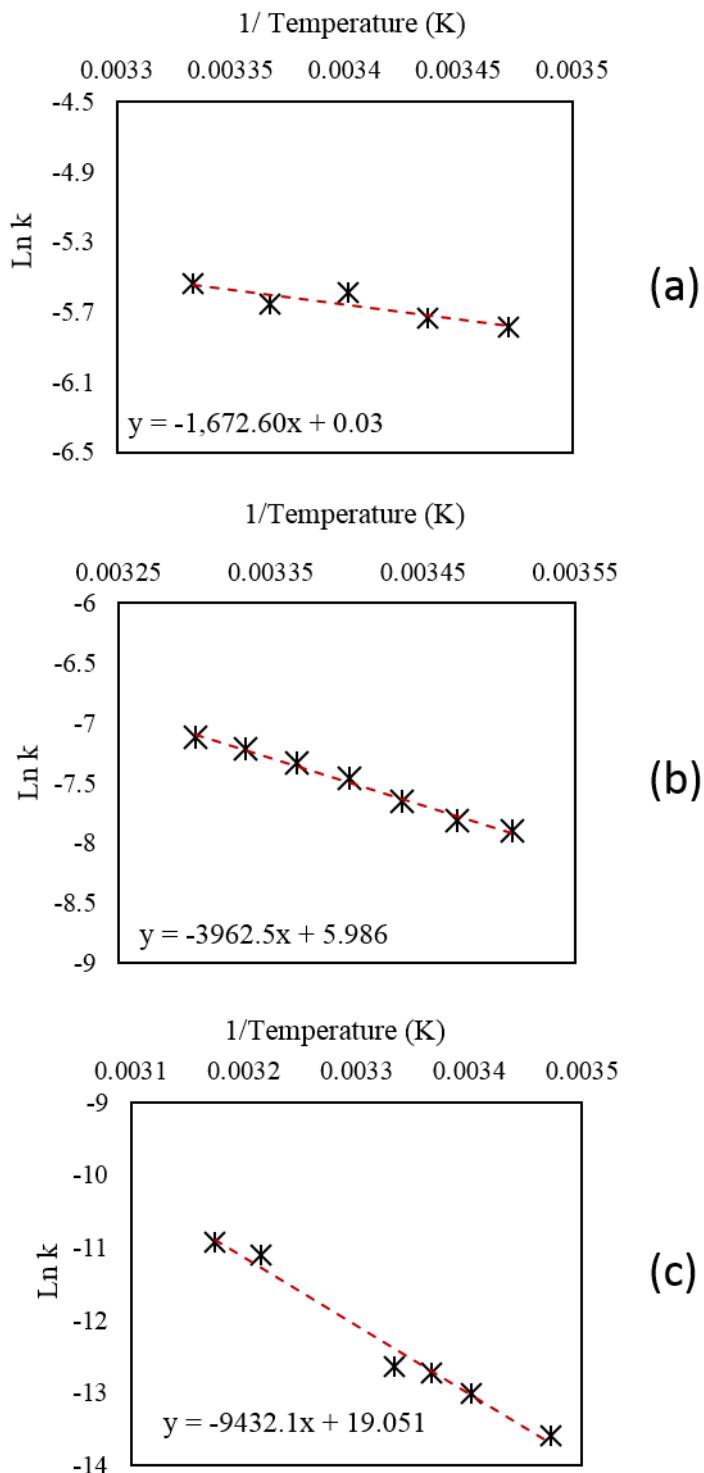
Figure 4.31. Arrhenius plots for (a) catalytic aldehyde oxidation, (b) the oxidative dehydrogenation of FOH and (c) the Cannizzaro reaction

4.10. Conclusions

The Primary objective of this area of work was to find a catalyst which could selectively oxide FF to FA efficiently, under mild reaction conditions. It was quickly determined that the presence of a sacrificial base complicated the system, as it led to the activation of competitive reaction pathways.

Initial investigations trialled the use of a 1 wt.% Au/TiO_2 catalyst for this reaction. Reasonable results were obtained but significant quantities of carbon were lost which was suggested to be a result of intermolecular polymerisation of FF in the solution. It was subsequently discovered that increasing the reaction temperature promoted this unfavourable polymerisation, which consequentially led to the reactions being conducted at 30 ℃. Catalyst deactivation appeared to be a problem. Product inhibition studies confirmed that FA had no effect on catalytic performance. As a result, it was hypothesised that the loss in catalytic performance over time was a result of the irreversible binding of resins to the active sites of the catalyst.

The catalyst was subsequently optimised in an attempt to reduce the polymerisation of FF through the promotion of the desired pathway. $Mg(OH)_2$ (confirmed by XRD) had previously be found to be a highly active support for Au nanoparticles in the oxidation of Alcohols[38]. For this reason, a 1 wt.% $Au/Mg(OH)_2$ catalyst was produced and tested under the standard reaction conditions. A significant improvement in the conversion of FF was observed, however, polymerisation still appeared to be a problem as the C.M.B. observed was comparable with that displayed by the 1 wt.% Au/TiO_2 catalyst. Incorporation of Pd into the $Au/Mg(OH)_2$ catalyst significantly reduced the polymerisation, which ultimately allowed for higher yields of FA to be generated. Interestingly, the rate of FF consumption decreased with the $AuPd/Mg(OH)_2$ system despite the reduction in polymerisation. It was speculated that the incorporation Pd may alter the electronic properties of the active site and ultimately effected the binding strength of the substrate to the site. This is however, purely speculation and more work would be required to confirm this hypothesis. The $AuPd/Mg(OH)_2$ catalyst was subsequently used as the standard catalyst for the remaining work and reuse tests determined that the catalyst did not appear to deactivate upon subsequent uses.

Tests conducted in the absence of any catalysed confirmed that a Cannizzaro reaction producing stoichiometric quantities of FOH and FA was also taking place. This confirmed

a hypothesis made earlier in the chapter as small quantities of FOH were consistently detected. In order to gain a further understanding of the reaction profile, a mechanistic study was conducted where the effect of NaOH and O_2 on each reaction pathway was assessed. It was determined that the oxidation rate of FF and FOH was significantly promoted by both NaOH and O_2. NaOH has previously been shown to significantly promote the oxidation of alcohols[36] and work in Chapter 3 revealed that carbonyls could undergo oxidation through interaction with NaOH in the absence of a catalyst. O_2 can be reduced by H_2O to produce surface bound hydroxyl species which are considered to be crucial in oxidation reactions involving Au nanoparticles[44, 49]. It was determined that the Cannizzaro reaction was significantly promoted by NaOH but did not appear to be effected by O_2. This was expected as O_2 is not believed to play a part in the Cannizzaro reaction mechanism[55]. It was determined that any alcohol produced *via* the Cannizzaro pathway was rapidly oxidised back to FF, which explained why only small quantities of FOH were observed in the standard reaction.

The size of the AuPd particles were found to have a significant effect on the performance of the catalyst. Additional $AuPd/Mg(OH)_2$ catalysts prepared by Mod-IMP and Con-IMP were tested. The Mod-IMP has comparable activity to the standard sol-immobilsed catalyst, whereas the catalyst prepared by Con-IMP has very little influence on the reaction. Each catalyst was characterised by TEM and it was determined that the catalyst prepared by Con-IMP consisted of significantly larger metal particles, hence the link between particle size and activity was derived. It is well known that the particle size of Au nanoparticles significantly influences catalytic activity in oxidation reactions[50, 56]. The relationship between Au and Pd was also addressed. A series of catalysts with varying Au:Pd ratios were prepared and tested for the oxidation of FF. It was clear that a synergistic relationship between Au and Pd existed. High activities but poor C.M.B's were observed when monometallic Au and Pd catalysts were tested. As the molar ratio between Au and Pd becomes more stoichiometric, slower reaction rates but higher yields of FA were observed. This increased reaction control supports the hypothesis made previously; incorporation of Pd into Au may alter the electronic properties of the nanoparticles, which could ultimately change to binding strength of the substrate to the active site.

Finally, kinetics was applied to the system in order to assess the efficiency of the catalytic reaction. The initial rates method was used in order to determine the rate equations for the oxidation of FF, the oxidation of FOH and the Cannizzaro reaction. These rate equations

were then used to calculate activation energies for each of the reactions which were derived through the use of Arrhenius plots. Activation energies of 13.9, 32.9 and 78.4 KJ mol^{-1} were derived for the oxidation of FF, oxidation of FOH and the Cannizzaro reaction respectively. It is important to mention that the kinetic study was dependent on a number of assumption and the figures acquired can only really be considered as estimates at this time. Significantly more data points must be included in the kinetic studies for the acquired figures to be consider accurate.

It is important to note that the Cannizzaro reaction is the current industrial method used for the preparation of FA from FF[26]. A substantially lower activation barrier was calculated for the oxidation of FF when compared to the Cannizzaro reaction, which clearly underlines the potential of using a catalyst for this process industrially.

4.11. References

1. C. M. Cai, T. Y. Zhang, R. Kumar and C. E. Wyman, *Journal of Chemical Technology and Biotechnology*, 2014, **89**, 2.

2. A. Bohre, S. Dutta, B. Saha and M. M. Abu-Omar, *ACS Sustainable Chemistry & Engineering*, 2015, **3**, 1263.

3. P. Gallezot, *Chemical Society Reviews*, 2012, **41**, 1538.

4. J.-P. Lange, E. van der Heide, J. van Buijtenen and R. Price, *Chemsuschem*, 2012, **5**, 150.

5. H. Y. Zheng, Y. L. Zhu, B. T. Teng, Z. Q. Bai, C. H. Zhang, H. W. Xiang and Y. W. Li, *Journal of Molecular Catalysis A-Chemical*, 2006, **246**, 18.

6. S. Sitthisa and D. E. Resasco, *Catalysis Letters*, 2011, **141**, 784.

7. L. R. Baker, G. Kennedy, M. Van Spronsen, A. Hervier, X. J. Cai, S. Y. Chen, L. W. Wang and G. A. Somorjai, *Journal of the American Chemical Society*, 2012, **134**, 14208.

8. S. G. Wang, V. Vorotnikov and D. G. Vlachos, *ACS Catalysis*, 2015, **5**, 104.

9. S. Iqbal, X. Liu, O. F. Aldosari, P. J. Miedziak, J. K. Edwards, G. L. Brett, A. Akram, G. M. King, T. E. Davies, D. J. Morgan, D. K. Knight and G. J. Hutchings, *Catalysis Science & Technology*, 2014, **4**, 2280.

10. J. G. Zeikus, M. K. Jain and P. Elankovan, *Applied Microbiology and Biotechnology*, 1999, **51**, 545.

11. A. Corma, S. Iborra and A. Velty, *Chemical Reviews*, 2007, **107**, 2411.

12. C. Delhomme, D. Weuster-Botz and F. E. Kuehn, *Green Chemistry*, 2009, **11**, 13.

13. S. Shi, H. Guo and G. Yin, *Catalysis Communications*, 2011, **12**, 731.

14. H. Guo and G. Yin, *Journal of Physical Chemistry C*, 2011, **115**, 17516.

15. J. H. Lan, Z. Q. Chen, J. C. Lin and G. C. Yin, *Green Chemistry*, 2014, **16**, 4351.

16. N. Alonso-Fagundez, I. Agirrezabal-Telleria, P. L. Arias, J. L. G. Fierro, R. Mariscal and M. L. Granados, *RSC Advances*, 2014, **4**, 54960.

17. Y. Tachibana, T. Masuda, M. Funabashi and M. Kunioka, *Biomacromolecules*, 2010, **11**, 2760.

18. H. Choudhary, S. Nishimura and K. Ebitani, *Chemistry Letters*, 2012, **41**, 409.

19. K. J. Zeitsch, in *The chemistry and technology of furfural and its many by-products*, Elsevier, 2000, vol. 13, pp. 225-228.

20. C. J. Tsai, W. C. Chang, C.-H. Chen, H. Y. Lu and M. Chen, *European Polymer Journal*, 2008, **44**, 2339.

21. E. Taarning, I. S. Nielsen, K. Egeblad, R. Madsen and C. H. Christensen, *Chemsuschem*, 2008, **1**, 75.

22. F. Boccuzzi, A. Chiorino, M. Manzoli, P. Lu, T. Akita, S. Ichikawa and M. Haruta, *Journal of Catalysis*, 2001, **202**, 256.

23. F. Menegazzo, M. Signoretto, F. Pinna, M. Manzoli, V. Aina, G. Cerrato and F. Boccuzzi, *Journal of Catalysis*, 2014, **309**, 241.

24. X. L. Tong, Z. H. Liu, L. H. Yu and Y. D. Li, *Chemical Communications*, 2015, **51**, 3674.

25. M. Signoretto, F. Menegazzo, L. Contessotto, F. Pinna, M. Manzoli and F. Boccuzzi, *Applied Catalysis B-Environmental*, 2013, **129**, 287.

26. K. J. Zeitsch, in *The chemistry and technology of furfural and its many by-products* Elsevier, 2000, vol. 13, pp. 159-163.

27. P. Parpot, A. P. Bettencourt, G. Chamoulaud, K. B. Kokoh and E. M. Beigsir, *Electrochimica Acta*, 2004, **49**, 397.

28. Q. Y. Tian, D. X. Shi and Y. W. Sha, *Molecules*, 2008, **13**, 948.

29. H. Choudhary, S. Nishimura and K. Ebitani, *Applied Catalysis A-General*, 2013, **458**, 55.

30. A. Gandini and M. N. Belgacem, *Actualite Chimique*, 2002, 56.

31.   K. Lamminpaa, J. Ahola and J. Tanskanen, *Industrial & Engineering Chemistry Research*, 2012, **51**, 6297.

32.   K. Lamminpaa, J. Ahola and J. Tanskanen, *RSC Advances*, 2014, **4**, 60243.

33.   H. J. Guo and G. C. Yin, *Journal of Physical Chemistry C*, 2011, **115**, 17516.

34.   X. Yang, X. Wang, C. Liang, W. Su, C. Wang, Z. Feng, C. Li and J. Qiu, *Catalysis Communications*, 2008, **9**, 2278.

35.   M. Haruta and M. Date, *Applied Catalysis A-General*, 2001, **222**, 427.

36.   W. C. Ketchie, M. Murayama and R. J. Davis, *Topics in Catalysis*, 2007, **44**, 307.

37.   V. V. Costa, M. Estrada, Y. Demidova, I. Prosvirin, V. Kriventsov, R. F. Cotta, S. Fuentes, A. Simakov and E. V. Gusevskaya, *Journal of Catalysis*, 2012, **292**, 148.

38.   G. L. Brett, Q. He, C. Hammond, P. J. Miedziak, N. Dimitratos, M. Sankar, A. A. Herzing, M. Conte, J. A. Lopez-Sanchez, C. J. Kiely, D. W. Knight, S. H. Taylor and G. J. Hutchings, *Angewandte Chemie-International Edition*, 2011, **50**, 10136.

39.   D. I. Enache, J. K. Edwards, P. Landon, B. Solsona-Espriu, A. F. Carley, A. A. Herzing, M. Watanabe, C. J. Kiely, D. W. Knight and G. J. Hutchings, *Science*, 2006, **311**, 362.

40.   W. B. Hou, N. A. Dehm and R. W. J. Scott, *Journal of Catalysis*, 2008, **253**, 22.

41.   S. Gil, M. Marchena, L. Sanchez-Silva, A. Romero, P. Sanchez and J. L. Valverde, *Chemical Engineering Journal*, 2011, **178**, 423.

42.   N. Dimitratos, A. Villa and L. Prati, *Catalysis Letters*, 2009, **133**, 334.

43.   E. Skupien, R. J. Berger, V. P. Santos, J. Gascon, M. Makkee, M. T. Kreutzer, P. J. Kooyman, J. A. Moulijn and F. Kapteijn, *Catalysts*, 2014, **4**, 89.

44.   B. N. Zope, D. D. Hibbitts, M. Neurock and R. J. Davis, *Science*, 2010, **330**, 74.

45.   B. N. Zope and R. J. Davis, *Green Chemistry*, 2011, **13**, 3484.

46.   M. Sankar, E. Nowicka, E. Carter, D. M. Murphy, D. W. Knight, D. Bethell and G. J. Hutchings, *Nature Communications*, 2014, **5**, 6.

47.   A. Villa, N. Janjic, P. Spontoni, D. Wang, D. S. Su and L. Prati, *Applied Catalysis A-General*, 2009, **364**, 221.

48.   B. N. Zope, S. E. Davis and R. J. Davis, *Topics in Catalysis*, 2012, **55**, 24.

49.   M. S. Ide and R. J. Davis, *Accounts of Chemical Research*, 2014, **47**, 825.

50.   W. C. Ketchie, Y.-L. Fang, M. S. Wong, M. Murayama and R. J. Davis, *Journal of Catalysis*, 2007, **250**, 94.

51.   N. Dimitratos, J. A. Lopez-Sanchez, D. Lennon, F. Porta, L. Prati and A. Villa, *Catalysis Letters*, 2006, **108**, 147.

52. N. Dimitratos, J. A. Lopez-Sanchez, J. M. Anthonykutty, G. Brett, A. F. Carley, R. C. Tiruvalam, A. A. Herzing, C. J. Kiely, D. W. Knight and G. J. Hutchings, *Physical Chemistry Chemical Physics*, 2009, **11**, 4952.

53. N. Dimitratos, J. A. Lopez-Sanchez, S. Meenakshisundaram, J. M. Anthonykutty, G. Brett, A. F. Carley, S. H. Taylor, D. W. Knight and G. J. Hutchings, *Green Chemistry*, 2009, **11**, 1209.

54. M. D. Argyle and C. H. Bartholomew, *Catalysts*, 2015, **5**, 145.

55. J. Clayden, N. Greeves, S. Warren and P. Wothers, Oxford University Press, New York, 2001, pp. 1081-1082.

56. W. H. Fang, J. S. Chen, Q. H. Zhang, W. P. Deng and Y. Wang, *Chemistry-A European Journal*, 2011, **17**, 1247.

Chapter 5

Conclusions and Future Work

In this thesis, a range of heterogeneous catalysts containing supported Au, Pd and Pt nanaoparticles were investigated for the selective oxidation of glycerol and the selective oxidation of furfural. The purpose of this final chapter is to reiterate the conclusions derived from each body of work and offer additional work which could be conducted to support the hypotheses drawn.

5.1. The Selective Oxidation of Glycerol

A AuPt/TiO$_2$ was used as a standard catalyst to investigate the effect the reaction conditions had on the rate and selectivity of the reaction. Increasing the oxygen pressure was found to promote selectivity to glyceric acid (GA) and tartonic acid (TA) at the expense of lactic acid (LA). It was suggested that O$_2$ plays a crucial role in this direct oxidation pathway. Regretably, increasing the pressure of O$_2$ was also found to increase C-C cleavage, which supports the theory made previously by Davis and co-workers[1, 2], that O$_2$ is involved in the production of H$_2$O$_2$. Perhaps more interestingly, increasing the reaction temperature and NaOH concentraton was found to siginifcantly promote the production of LA. The mechanism by which LA is produced from glycerol is somewhat debated in the literature[3, 4]. Nevertheless, it is agreed that the first two steps involve the oxidation of glycerol to glyceraldehyde (GD) which is followed by the dehydration of a terminal alcohol group to produce 2-hydroxyacrylaldehyde. It is possible, that increasing the reaction temperature is favouring both the oxidation and subsequent dehydration step. An isotopic labelling experiment involving the use of ^{18}O could be used to prove this, as shown in Figure 5.1.
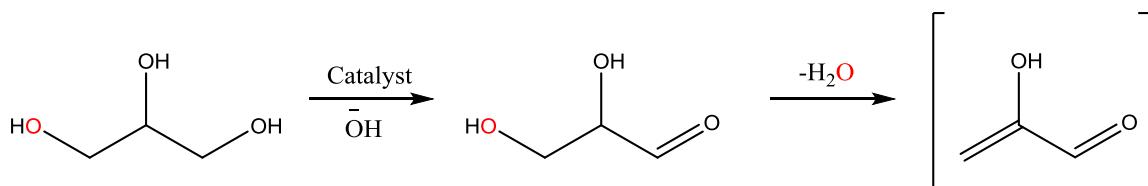
Figure 5.1. Proposed isotopic labelling experiment. ^{18}O is represented in red.

If the reaction was conducted where the substrate consisted of terminal alcohol groups containing ^{18}O, it would be possible to determine whether temperature promotes these two steps. If this is the case, increasing the reaction temperature would lead to higher quantities of $H_2^{18}O$ in solution. By running reactions at different temperatures and monitoring the quantity of $H_2^{18}O$ in the reaction solution it would theoretically be possible to confirm this hypothesis.

The next step in the mechanism is debated. It was initially suggested that 2-hydroxyacrylaldehyde undergoes a rearrangement to produce LA[3]. A recent publication by Crabtree and co-workers[4] offered a different explanation. They suggested that the 2-hydroxyacrylaldehyde is first oxidised to methylglyoxal and is subsequently followed by an intermolecular Cannizzaro reaction to produce LA. An additional isotopic labelling experiment could be used to confirm this, as shown in Figure 5.2.
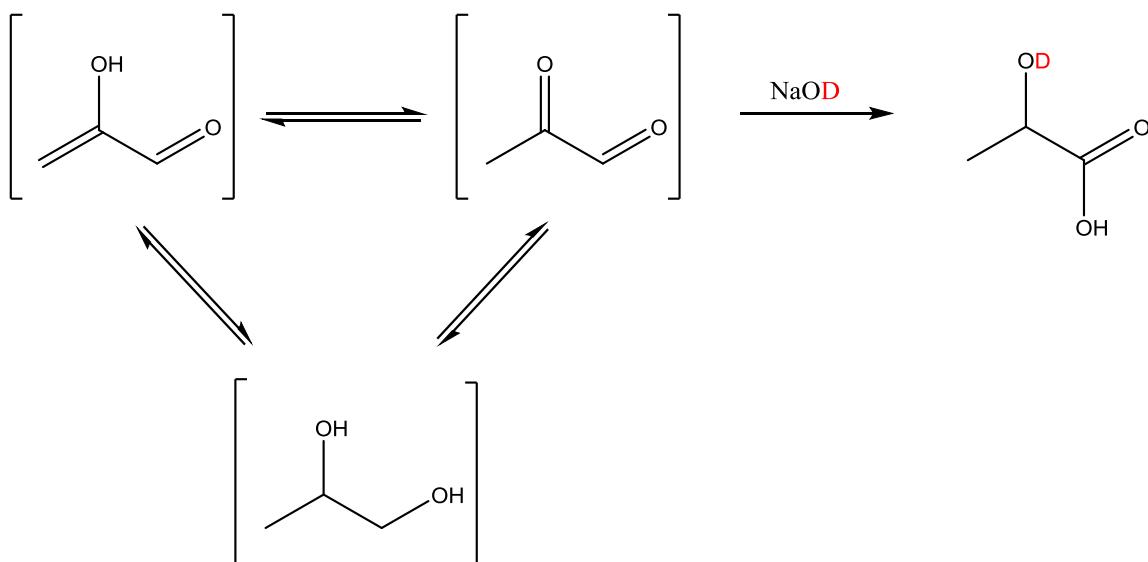
Figure 5.2. Isotopic labelling experiment to confirm Cannizzaro reaction. Deuterium is represented in red.

Starting the reaction from 2-hydroxyacrylaldehyde or methylglyoxal in the presence of deuterated base (NaOD) would prove that this is the case. This is typically the experimental method in which Cannizzaro reactions are confirmed[5]. It would be difficult to conduct this experiment from glycerol, as it is known that OH plays a crucial role in the activation of

C-H bonds, which could complicate things. An additional complication could arise from the H atoms in the water interconverting with the deuterated alcohol in LA.

Following this work, experiments were conducted in order to assess how the reaction products were affected by the catalyst and the reaction conditions. Reactions were conducted where reactions products such as GA, GD, LA etc. were used as the substrate. Considerably different reaction rates and product selectivity was observed than expected when compared to the product distribution and rate of glycerol oxidation. The oxidation of GA gave exceptionally low reaction rates and poor selectivity to TA was observed for the oxidation of GA, GD and dihydroxyacetone (DHA). From these results it was suggested that GA and TA are primary reaction products which would explain why mesoxalic acid is never observed in the reaction. This observation has been recognised previously, as Davis and co-workers reported poor activities when oxidising GA in the presence of a 1 wt.% Au/TiO$_2$ catalyst[6]. It was suggested that this was a result of the external hydroxyl group (NaOH) favouring interaction with the carboxylic acid group of the substrate rather than partaking in the activation of the C-H bond. Confirmation that GA and TA are primary products is exceptionally difficult to prove experimentally. Operando studies using IR, MS and even the temporal analysis of products (TAP) could be used to assess the identity of the species and the method in which they bind to the surface of the catalyst.

A lot of emphasis in this thesis was placed on determining the source and mechanism by which the unfavourable C-C scission occurs. A study was conducted where varied quantities of H$_2$O$_2$ were added at the beginning of the reaction. Increasing quantities of H$_2$O$_2$ was found to increase C-C bond cleavage in the initial stages of the reaction. It was subsequently suggested that H$_2$O$_2$ is directly responsible for the cleavage that occurs in this reaction which has previously been hypothesised by Davis and co-workers[1]. The mechanism by which this occurs however is still unclear. It was proposed in Chapter 3 that Dakin oxidation was responsible for this cleavage. Dakin oxidation typically involves the reaction of a hydroxylated phenyl carbonyl with H$_2$O$_2$ in base to produce a benzenediol and a carboxylate. The high electron density of the hydroxylated phenyl is considered to have a crucial impact on the kinetics of the reaction and as a result, this reaction is only really observed when the carbonyl is attached to an ortho- or para- functionalised hydroxylated phenyl. It was postulated that the high electron density of the nanoparticles may be able to imitate the hydroxylated phenyl when the substrate is bound to a nanoparticle. To my knowledge this has never been hypothesised previously. In order to

confirm whether this occurs, isotopic labelling experiments could once again be used. For proof of concept, it would first be suitable to use a substrate which is known to partake in Dakin oxidation such as 4-hydroxybenzaldehyde. By conducting a reaction with this substrate in the presence of a Au supported catalyst and $^{18}O_2$, it would be possible to determine whether:

(i) O_2 is reduced by H_2O to produce H_2O_2

(ii)   Whether H_2O_2 produced in this way partakes in Dakin Oxidation.

If Dakin oxidation is occurring, you would expect to see a labelled oxygen in the benzenediol product. A diagrammatic representation of this experiment is displayed in Figures 5.3 and 5.4.

$$O_2\text{*} + H_2O\text{*} \rightarrow OOH\text{*} + HO\text{*}$$

$$OOH\text{*} + H_2O\text{*} \rightarrow H_2O_2\text{*} + HO\text{*}$$

$$HO\text{*} + e^- \leftrightarrow HO^- + \text{*}$$
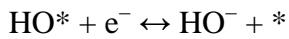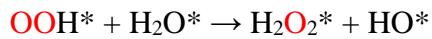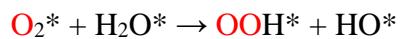
Figure 5.3. Formation of H_2O_2 through the reduction of O_2 by H_2O as proposed by Davis and co-workers[1]. ^{18}O is represented in red.
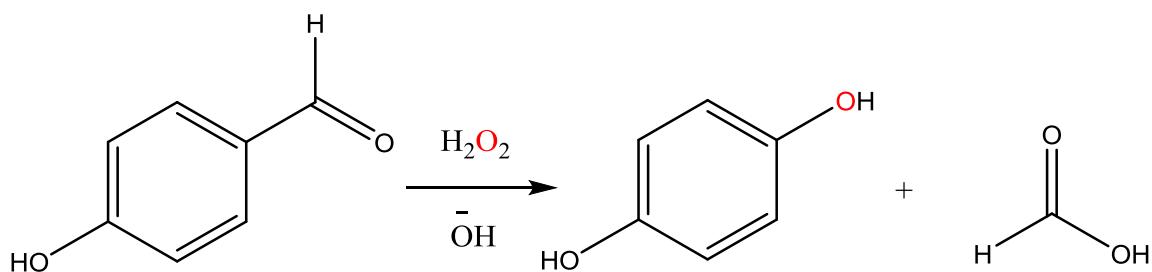
Figure 5.4. Possible interaction of the labelled H_2O_2 with the 4-hydroxybenzaldehyde leading to the formation of the labelled benzene diol. ^{18}O is represented in red.

If this was successful, the next step would be to prove that this is occurring in the selective oxidation of glycerol. The proposed mechanism for this is displayed in Figure 5.5. This experiment would again be done in the presence of NaOH, $^{18}O_2$ and a supported Au catalyst.
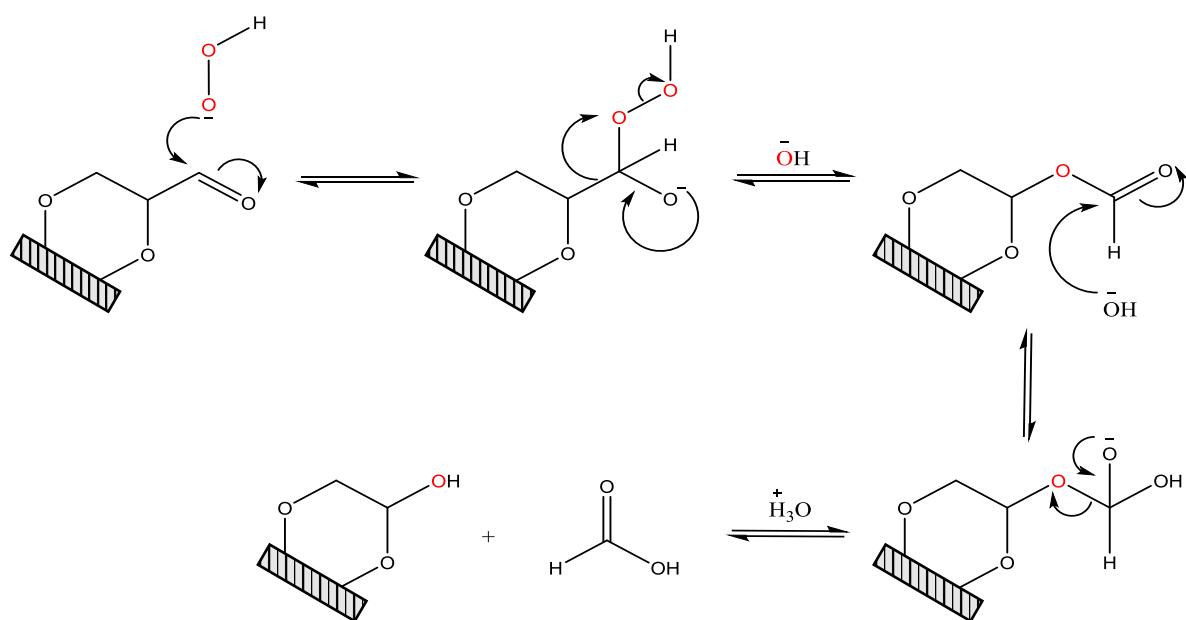
Figure 5.5. Proposed mechanism for the C-C cleavage observed in the selective oxidation of glycerol. OOH species is produced by reduction of O_2 with H_2O. O_2 atoms are labelled (^{18}O) and are represented in red.

If this is proven to be the mechanism by which the C-C cleavage occurs, strategies to reduce this interaction could then be invoked to try and improve the C_3 reaction selectivity. The work in Chapter 3 supports the suggestion that the use of hydrophobic supports can reduce this cleavage[7, 8]. This suggests that the H_2O_2 forms on the surface of the support rather than on the nanoparticle itself.

The catalytic oxidation of glycerol under base free conditions was not as successful as the reaction rates observed were not as high as those already reported in literature[9]. Nevertheless, trimetallic AuPdPt nanoparticles supported on TiO_2 were found to be more active than the corresponding bimetallic counterparts. A support study with the trimetallic

system revealed that the support can significantly influence the reaction rate. With this in mind, it was postulated that the design and synthesis of base functionalised materials for use as supports may be a way of promoting the reaction rate further. It has previously been suggested that hydroxyl species play a crucial role in the activation of C-H bonds which are required for the initial alcohol oxidations. Wilson and co-workers have recently shown that Mg-Al solid bases can significantly promote catalytic performance for the base free oxidation of HMF[10]. Perhaps materials such as these should be trialled as potential catalysts supports for this reaction.

Mesoxalic acid has a range of potnetial applications including use as a complexing agent as well as a precursor to produce 4-chlorophenylhydrazoned mesoxalic acid (MOA), which has shown to be a promising anti-HIV agent[11]. For this reason, an efficient method for the preparation of MOA from glycerol would be desirable. Early work by Gallezot and co-workers showed that glycerol could be selectively oxidised to MOA over Pt-Bi catalysts[12, 13]. However, since then there has been very few indications that MOA is produced from the oxidation of glycerol. As stated earlier in this chapter, this may be a result of hydroxyl species favouring interaction with the carboxylic acid groups on TA rather than participating the C-H activation of the remaining alcohol group. It was also suggested previously that TA may be a primary oxidation product. Using a basic mesoporous material as the catalyst support could increase the contact time between the substrate and the catalyst and could allow for the activation of the secondary alcohol group.

5.2. The Selective Oxidation of Furfural

The fundamental objective of this work was to find a catalyst which could selectively oxidise furfural (FF) to furoic acid (FA). A Au/TiO$_2$ catalyst was initially trialled and was found to produce adequate yields of FA. Despite this, large quantities of carbon were lost through the intramolecular polymerisation of FF. The suceptibility of FF to partake in intramolecular polymerisation reactions had been reported previously[14, 15]. Time online reactions revealed that the catalyst appeared to be deactivated over time. Product inhibition studies involving FA confirmed that it was not the source of the deactivation. It was postluated that the deactivation was attibuted to the irreversible binding of the polymers to the catalyst. In order to confirm whether this was the case further work is required. Identification of the polymer and the spiking of reactions with varying quantities of the

polymeric species could confirm whether this hypothesis is correct. Previous studies revealed that the use of a biphasic reaction system reduced the extent of the polymerisation[16]. It was suggested that this was due to reduced concentration of FF in the active phase, limiting the interactions between the compounds. For this reason, the application of this process in a flow reactor or even spinning disk reactors[17] could further improve the selectivity of this process. It would also be interesting to determine whether the polymerisation is decreased if lower concentrations of FF are used in the reactions.

The use of $Mg(OH)_2$ as a support was found to significantly increase the rate of the reaction. $Mg(OH)_2$ had previously been shown to be a highly active support for the liquid phase oxidation of alcohols over gold catalysts[9]. The enhanced catalytic performance was attributed to the increased population of hydroxyl groups in close proximity to the active site. Previous work by Davis and co-workers has highlighted the importance of hydroxyl species in oxidation reactions involving Au nanoparticles[2]. Despite the improved reaction rate, it was evident that polymerisation remained a problem. Pd was subsequently added to the catalyst in an attempt to reduce the polymerisation through the promotion of the competative oxidation pathway. Synergistic interactions between Au and Pd have be found to significantly enhance the reaction rate in the catalytic oxidation of alcohols[18, 19]. Interestingly and unexpectedly, a decrease in the reaction rate was observed but an increase in the FA yield and mass balance was also reported. In order to investigate this further, a series of $AuPd/Mg(OH)_2$ catalysts were produced with varing metal ratios, and were tested for the oxidation of FF.

The monometallic Au and Pd catalysts were found to produce the highest reaction rates but gave the poorest FA yields and a significant quantity of carbon was lost through polymerisation. Interestingly, as the Au and Pd loading became more stoichiometric, so too did the reaction rates but signicantly larger yields of FA and higher mass balances were observed. This trend was suggested to be the result of a synergistic interaction between the Au and Pd, ultimately leading to a change in the electronic properties of the nanoparticles. It was hypothesised that this change in the electronic properties of the nanoparticles led to the formation of higher energy active sites, which in turn, increased the sticking propability of the substrate and ultimately the binding energy, ultimately leading to a more controled interaction of the catlyst with the substrate. In order to confirm this theory, further work investigating the adsorption of FF to the series of the catalysts would be required. One possible way of doing this would be conduct an isothermic study using temperature

programmed desorption (TPD). This would involve adsorbing a monolayer of FF to the surface of each catalyst, gradually increasing the temperature and monitoring the temeprature of desorption. If a trend materialises between the initial rate and the desorption temperatures of the catalysts, it would provide compelling evidence in support of this theory.

From an industrial perspective, a catalyst must be able to maintain a high level performance for extended periods without deactivation. In order to assess the industrial viability of the AuPd/Mg(OH)$_2$ catalyst, a reusability study was conducted. Three reuse tests were conducted, where the catalyst was filtered, dried and restestest. There did not appear to be any reduction in the performance of the catalyst from the experimental data, however, TEM indicated that the mean particle size of the AuPd clusters did appear to increase very slightly after each use. A more comprehensive study involving significantly more reuse tests would be required in order to truly assess the stability of this catalyst.

Mechanistic studies were used to derive a reaction profle for the system and a complex reaction profile involving competative reaction pathways emerged (Figure 5.6.)
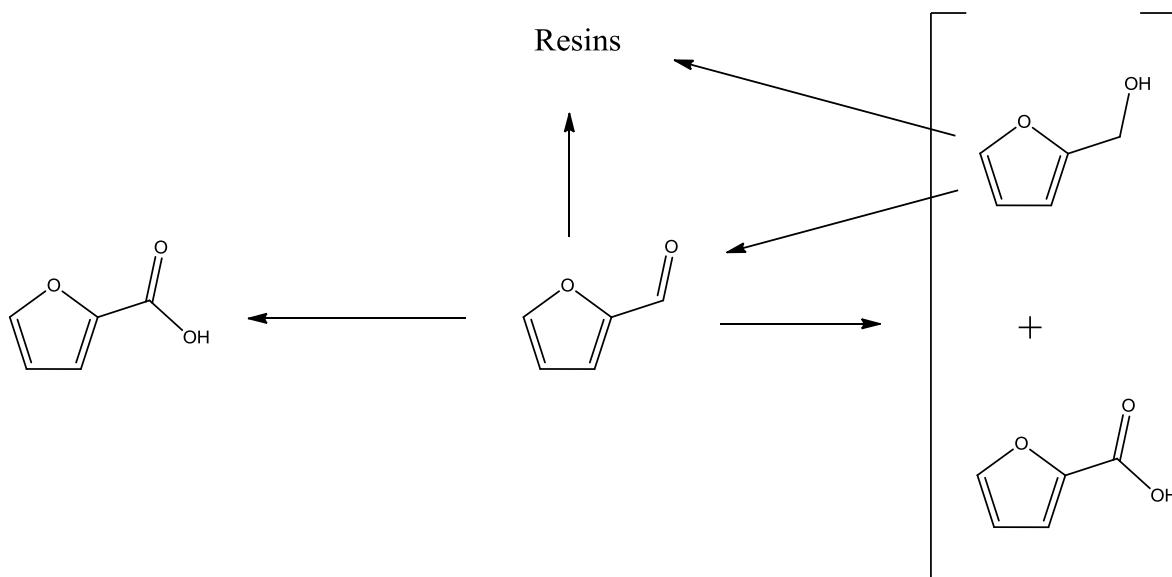
Figure 5.6. Reaction profile derived for the aerobic oxidation of furfural over a 1 wt.% AuPd/Mg(OH)$_2$ under basic conditions.

A reaction conducted in the absence of any catalyst produced stoichiometric quantities of furfuryl alcohol (FOH) and FA which strongly suggested that a NaOH initated Cannizzaro reaction was taking place. Even in the presence of a catalyst small quantities of FOH were observed, which suggested that the Cannizzaro reacton was taking place even under exceptionally oxidising conditions. A deuterated experiment could be conducted to confirm that the Cannizzaro reaction is operational under these reaction conditions, although, the experimental results observed in Chapter 4 strongly suggest that the Cannizzaro reaction is operational in this system. Increasing the concentration of NaOH and O_2 pressure in the reaction was found to significantly promote the catalytic oxidation of FOH and FF. Various labelling experiments could be used to investigate the role of these reactants in both the oxidation of FOH and FF. It is likely that NaOH promotes the activation of C-H bonds, as reported by Davis and co-workers[2]. The role of O_2 is less clear, but it is likely involved in the formation surface bound OH bonds and the freeing up of active sites on the metal nanoparticle.

FA is currently produced industrially by the Cannizzaro reaction of FF. This involves the post reaction seperation of FA from FOH which is both costly and time consuming. It had previously been stated that the use of a catalyst for this transformation was not viable on an industrial scale, due to the formation of unfavourable bi-products through competitive side reactions[20]. This work has shown that with a highly active heterogeneous catalyst, these unfavourable side reactions can be suppressed through the promotion of a direct oxidation pathway. A kinetics study subsequently conducted, primarily to assess how much more efficient the catalytic process is than the conventional industrial method. Initial rates tests were conducted in order to determine the rate equations for the oxidative dehydrogenation of FOH to FF, oxidation of FF to FA and the Cannizzaro reaction. These rate equations were subsequently used to determine the activation energies of each reaction. The activation energy for the catalytic oxidation of FF was found to be substantially lower than that of the Cannizzaro reaction under this set of conditions, which ultimately highlights the potnetial benefits of using a catalyst for this reaction on an industrial scale. It is important to mention that this kinetic study was dependent on a number of different assumptions regarding the reaction profile and significantly more data points would be required to increase the reliability of this statement. Nevertheless, these results are exceptionally promising moving forward.

Further optimisation of the catalyst and/or the reaction conditions could completely irradicate the requirement of an extraction step as no unfavourble by-products are formed. The next target would be to develop a system capable of yielding 100 % FA yield. It would also be interesting to see whether this system would work for the oxidation of other similar substrates such as functionalised pyrroles or thiophenes which are also notoriously difficult to handle.

5.3. <u>References</u>

1. B. N. Zope, D. D. Hibbitts, M. Neurock and R. J. Davis, *Science*, 2010, **330**, 74.
2. M. S. Ide and R. J. Davis, *Accounts of Chemical Research*, 2014, **47**, 825.
3. P. A. Shaffer and T. E. Friedemann, *Journal of Biological Chemistry*, 1930, **86**, 345.
4. L. S. Sharninghausen, J. Campos, M. G. Manas and R. H. Crabtree, *Nature Communications*, 2014, **5**.
5. J. Clayden, N. Greeves, S. Warren and P. Wothers, Oxford University Press, New York, 2001, pp. 1081-1082.
6. W. C. Ketchie, M. Murayama and R. J. Davis, *Topics in Catalysis*, 2007, **44**, 307.
7. L. Prati, A. Villa, C. E. Chan-Thaw, R. Arrigo, D. Wang and D. S. Su, *Faraday Discussions*, 2011, **152**, 353.
8. A. Villa, N. Dimitratos, C. E. Chan-Thaw, C. Hammond, L. Prati and G. J. Hutchings, *Accounts of Chemical Research*, 2015, **48**, 1403.
9. G. L. Brett, Q. He, C. Hammond, P. J. Miedziak, N. Dimitratos, M. Sankar, A. A. Herzing, M. Conte, J. A. Lopez-Sanchez, C. J. Kiely, D. W. Knight, S. H. Taylor and G. J. Hutchings, *Angewandte Chemie-International Edition*, 2011, **50**, 10136.
10. L. Ardemani, G. Cibin, A. J. Dent, M. A. Isaacs, G. Kyriakou, A. F. Lee, C. M. A. Parlett, S. A. Parry and K. Wilson, *Chemical Science*, 2015, **6**, 4940.
11. L. Xin, Z. Y. Zhang, Z. C. Wang and W. Z. Li, *Chemcatchem*, 2012, **4**, 1105.
12. P. Fordham, M. Besson and P. Gallezot, *Catalysis Letters*, 1997, **46**, 195.
13. P. Fordham, R. Garcia, M. Besson and P. Gallezot, *11th International Congress on Catalysis - 40th Anniversary, Pts a and B*, 1996, **101**, 161.
14. J. H. Lan, Z. Q. Chen, J. C. Lin and G. C. Yin, *Green Chemistry*, 2014, **16**, 4351.
15. H. Guo and G. Yin, *Journal of Physical Chemistry C*, 2011, **115**, 17516.

16. H. J. Guo and G. C. Yin, *Journal of Physical Chemistry C*, 2011, **115**, 17516.

17. X. Feng, D. A. Patterson, M. Balaban and E. A. C. Emanuelsson, *Chemical Engineering Journal*, 2014, **255**, 356.

18. W. C. Ketchie, M. Murayama and R. J. Davis, *Journal of Catalysis*, 2007, **250**, 264.

19. W. B. Hou, N. A. Dehm and R. W. J. Scott, *Journal of Catalysis*, 2008, **253**, 22.

20. K. J. Zeitsch, in *The chemistry and technology of furfural and its many by-products* Elsevier, 2000, vol. 13, pp. 159-163.

Chapter 6

Appendix

This chapter includes the calibration graphs for each compounds analysed in Chapter 3 and 4. In addition to these, the graphs from the initial rates experiments in Chapter 4 are displayed.

## 6.1. Calibrations for the Selective Oxidation of Glycerol
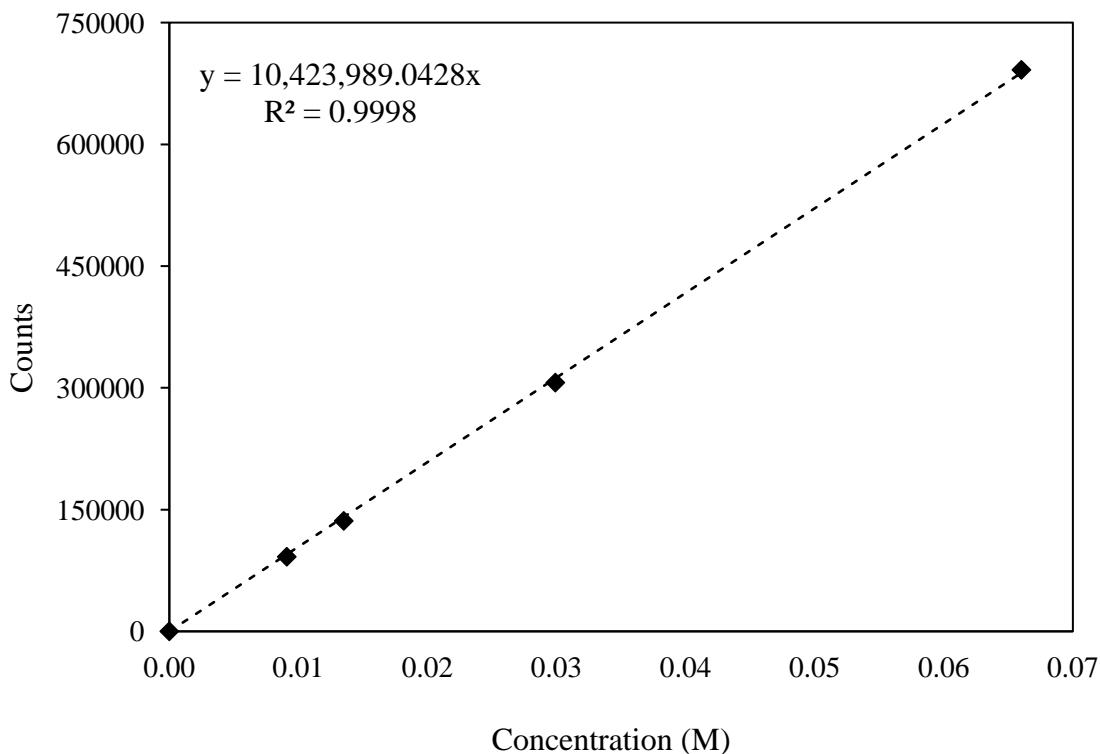
Figure 6.1.1. HPLC calibration curve for glycerol. Analysis was conducted using a refractive index detector.
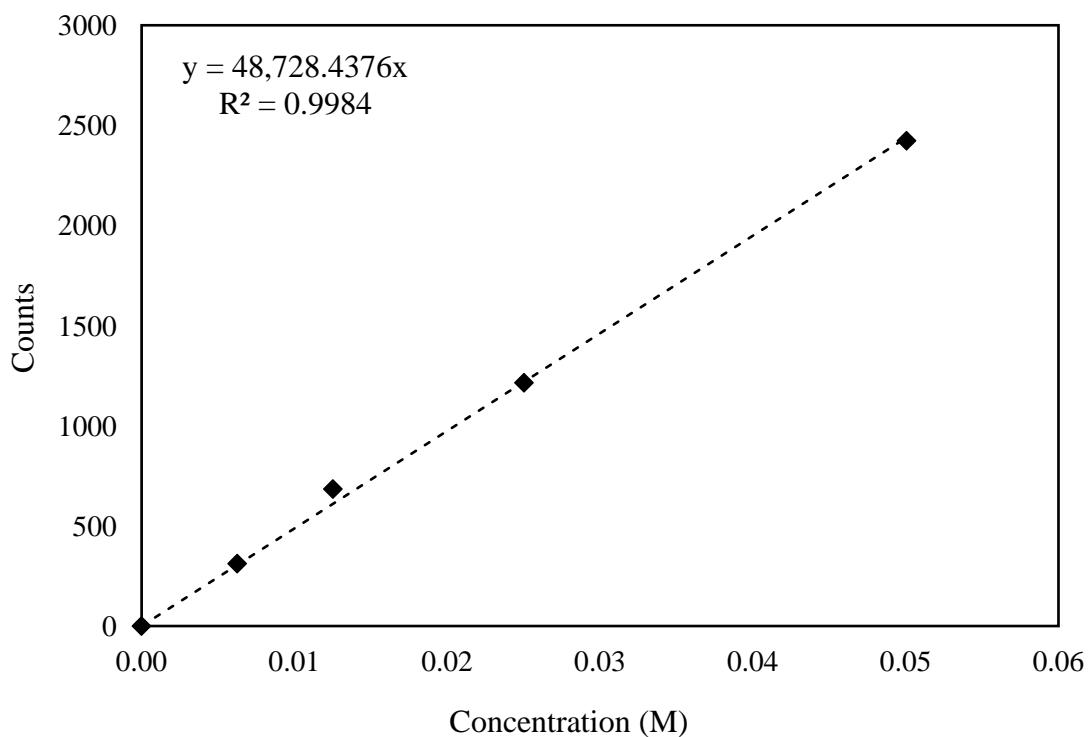
Figure 6.1.2. HPLC calibration curve for glyceric acid. Analysis was conducted using a diode array detector.
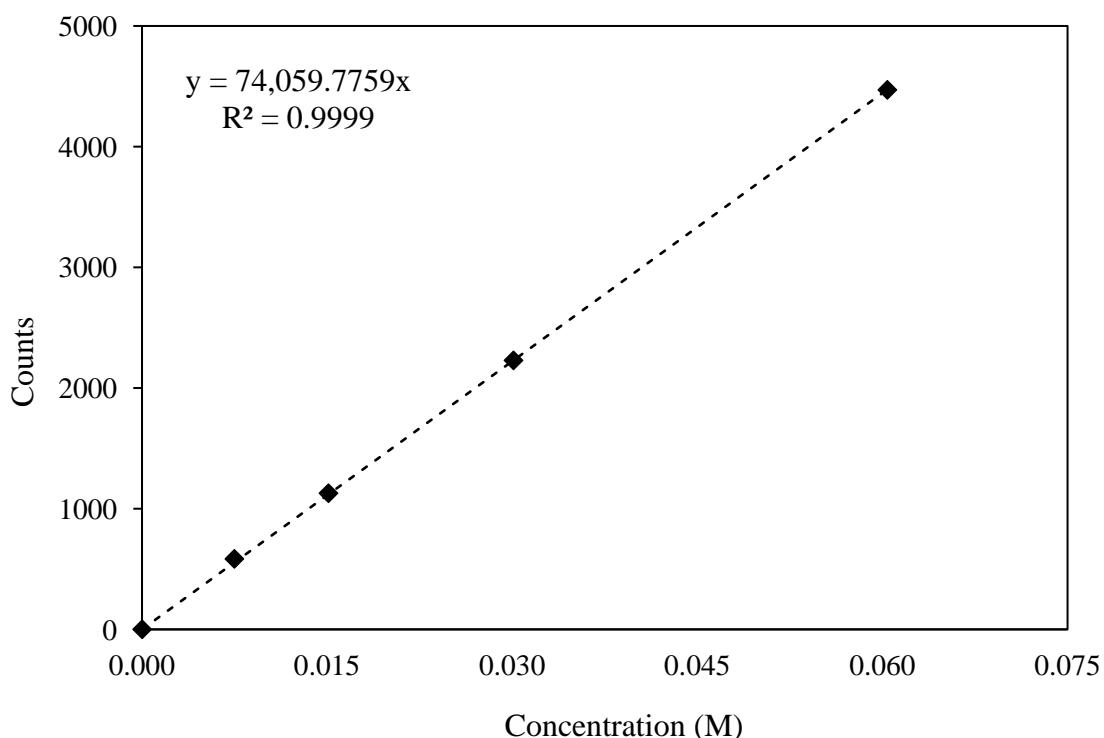
Figure 6.1.3. HPLC calibration curve for dihydroxyacetone. Analysis was conducted using a diode array detector.
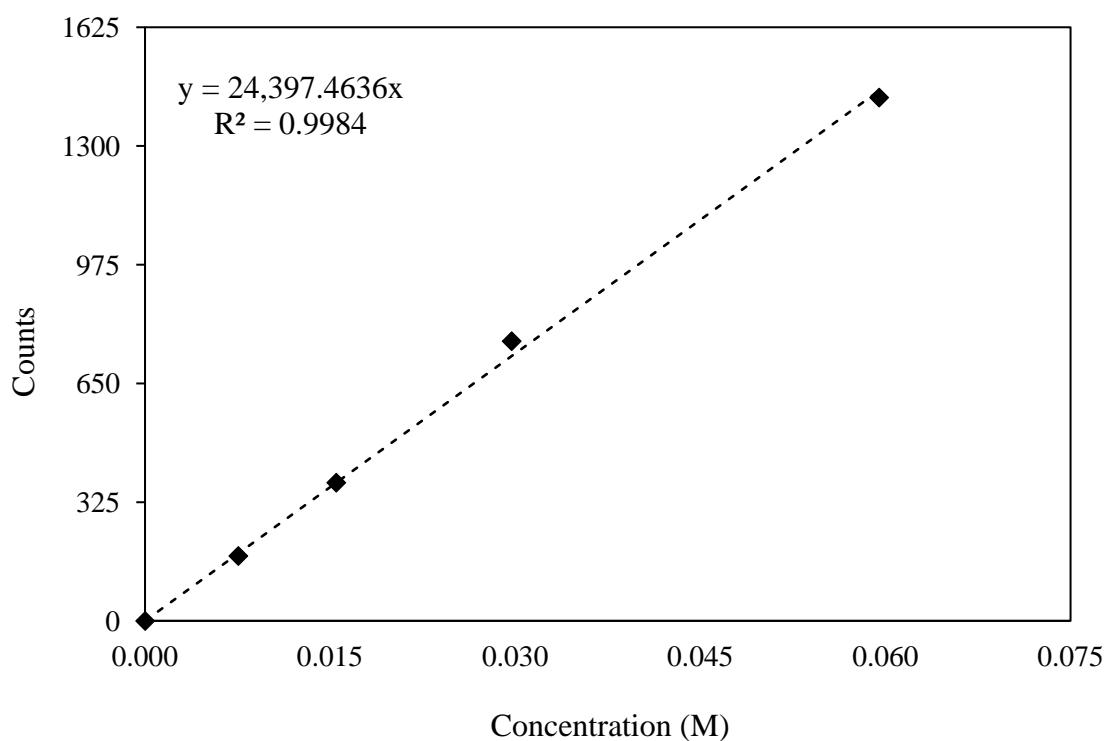
Figure 6.1.4. HPLC calibration curve for glyceraldehyde. Analysis was conducted using a diode array detector.
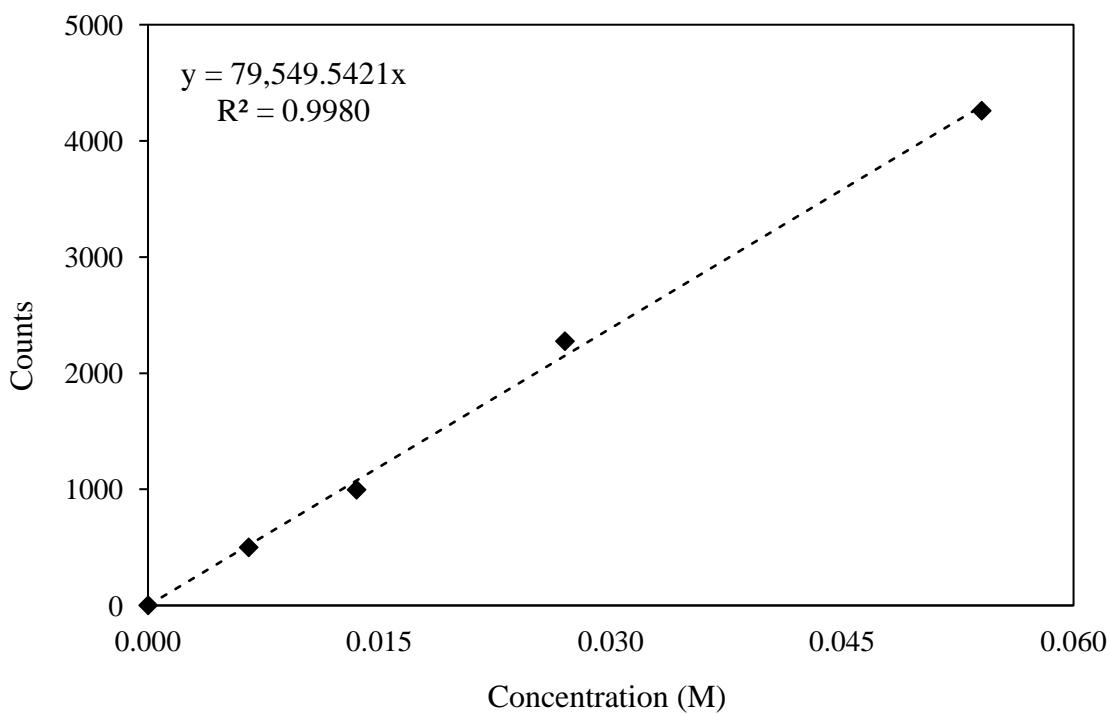
Figure 6.1.5. HPLC calibration curve for lactic acid. Analysis was conducted using a diode array detector.
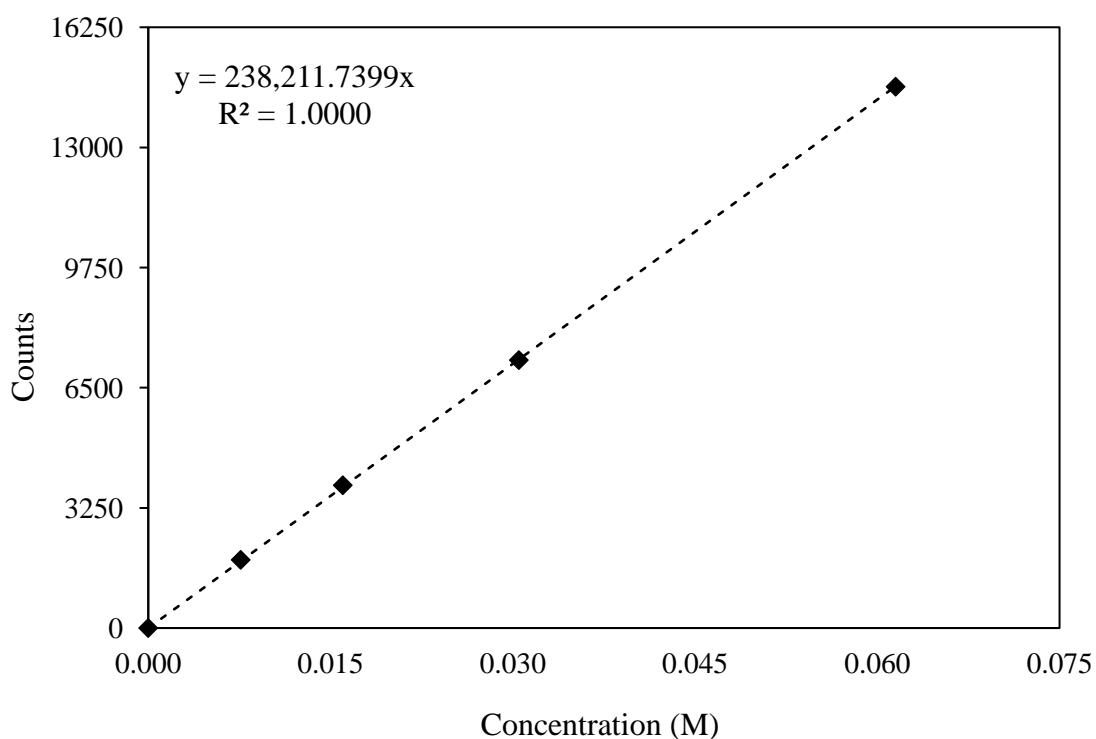
Figure 6.1.6. HPLC calibration curve for tartronic acid. Analysis was conducted using a diode array detector.
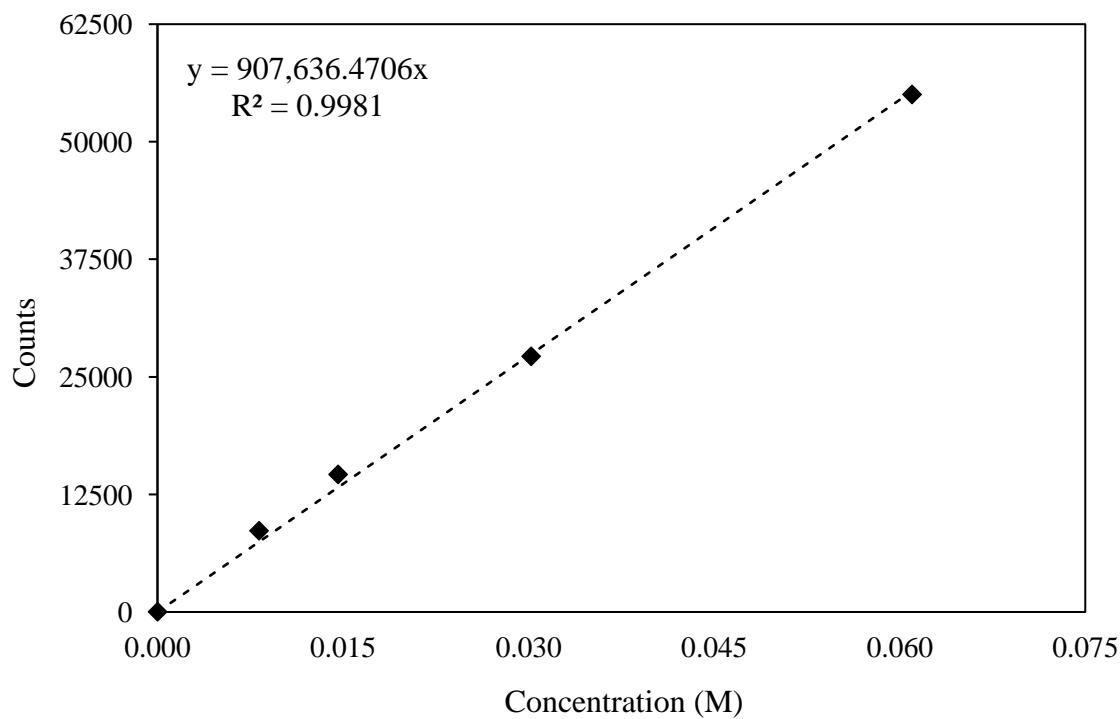
Figure 6.1.7. HPLC calibration curve for oxalic acid Analysis was conducted using a diode array detector.

186

$y = 36{,}426.7835x$

$R^2 = 0.9940$
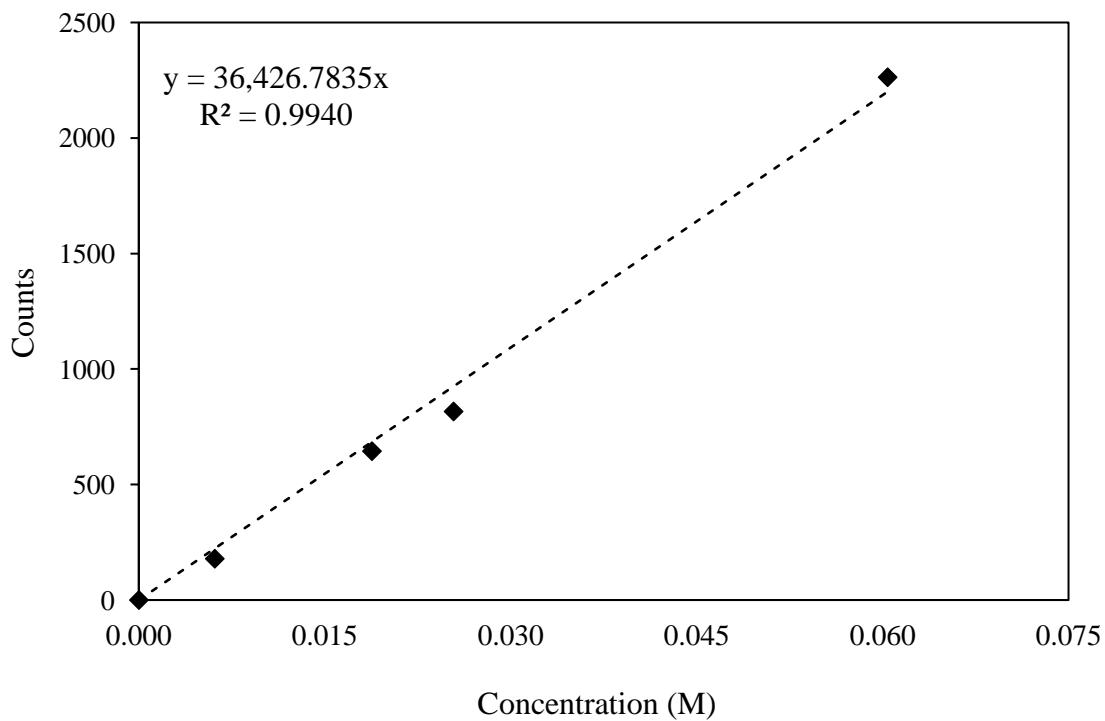
Figure 6.1.8. HPLC calibration curve for formic acid Analysis was conducted using a diode array detector.

$y = 256{,}518.8246x$

$R^2 = 0.9998$
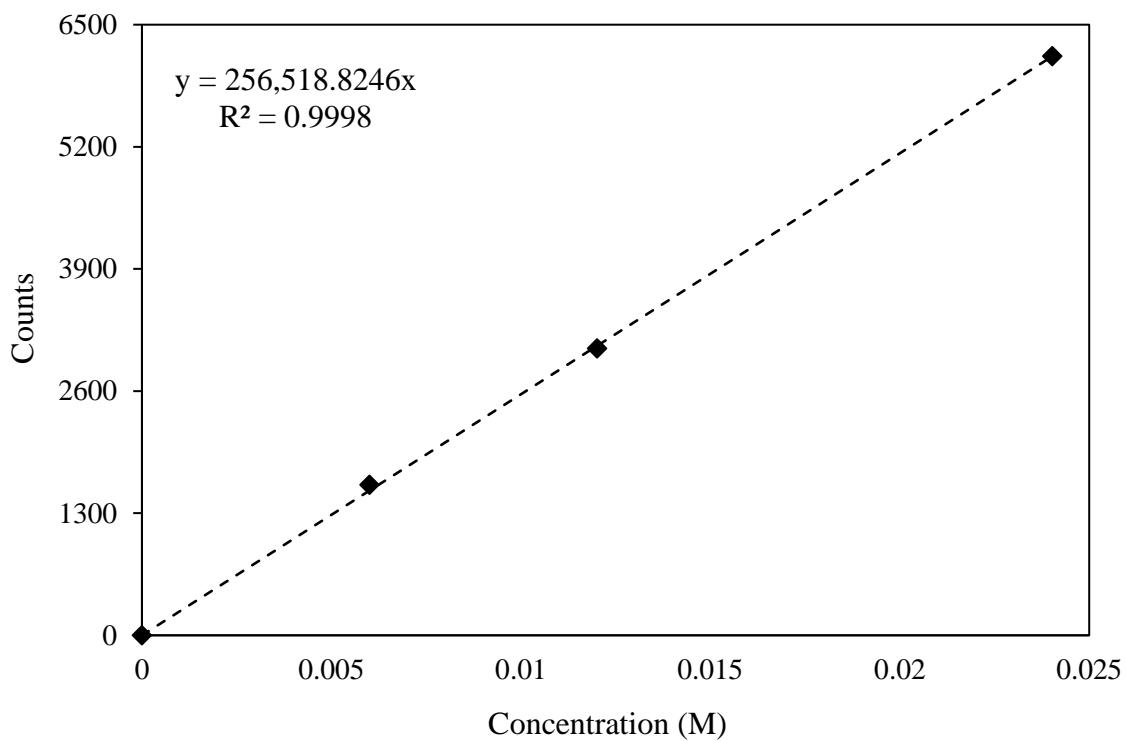
Figure 6.1.9. HPLC calibration curve for β-hydroxypyruvic acid. Analysis was conducted using a diode array detector.
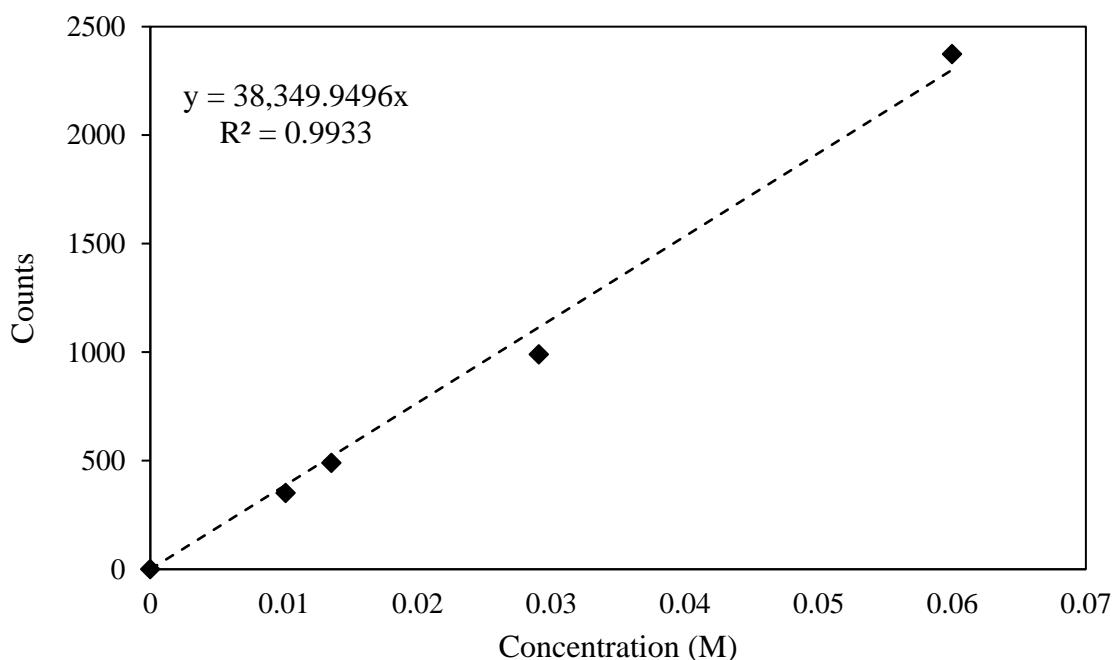
Figure 6.1.10. HPLC calibration curve for glycolic acid. Analysis was conducted using a diode array detector.

6.2. Calibrations for the Selective Oxidation of Furfural
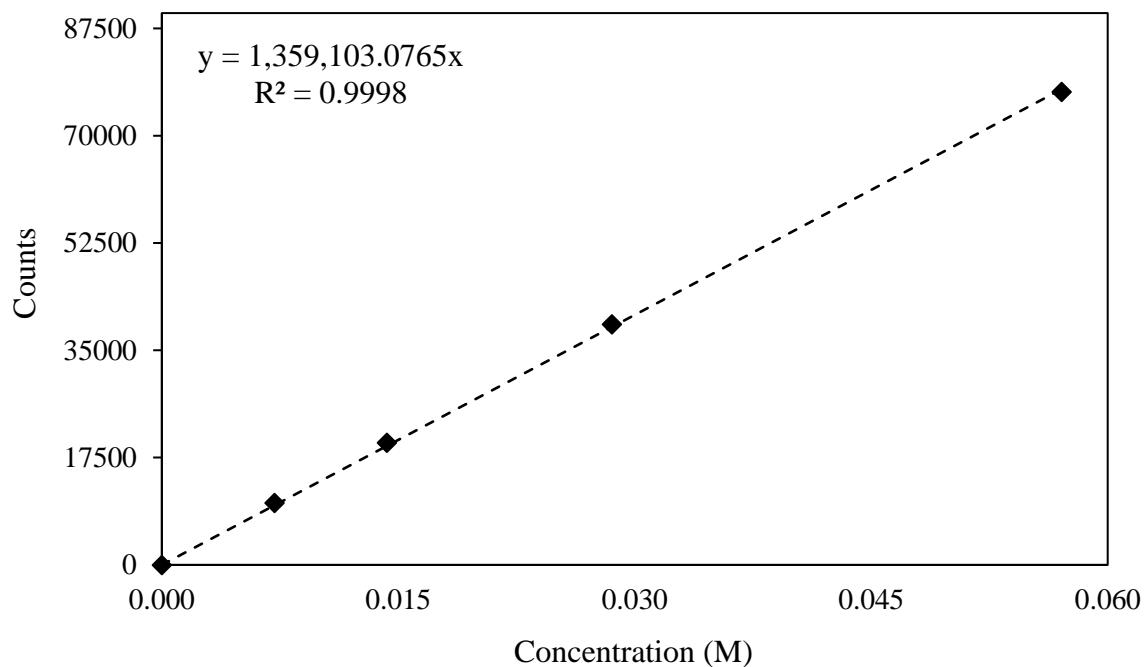
Figure 6.2.1. HPLC calibration curve for furfural. Analysis was conducted using a diode array detector

188
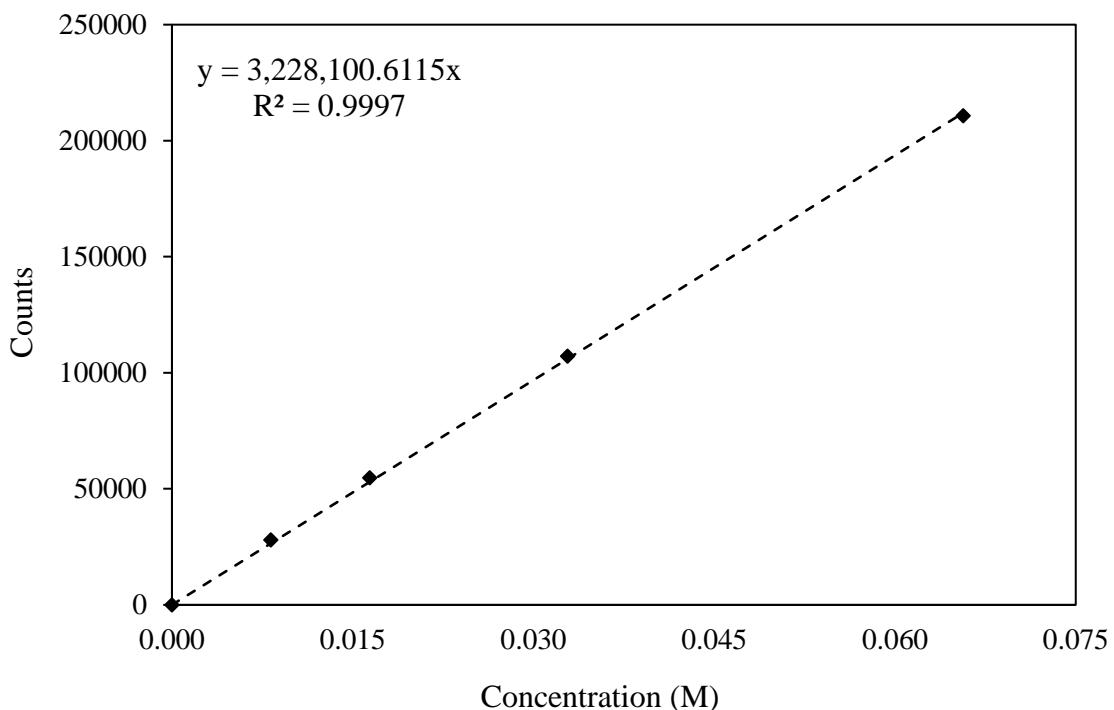
Figure 6.2.2. HPLC calibration curve for furoic acid. Analysis was conducted using a diode array detector
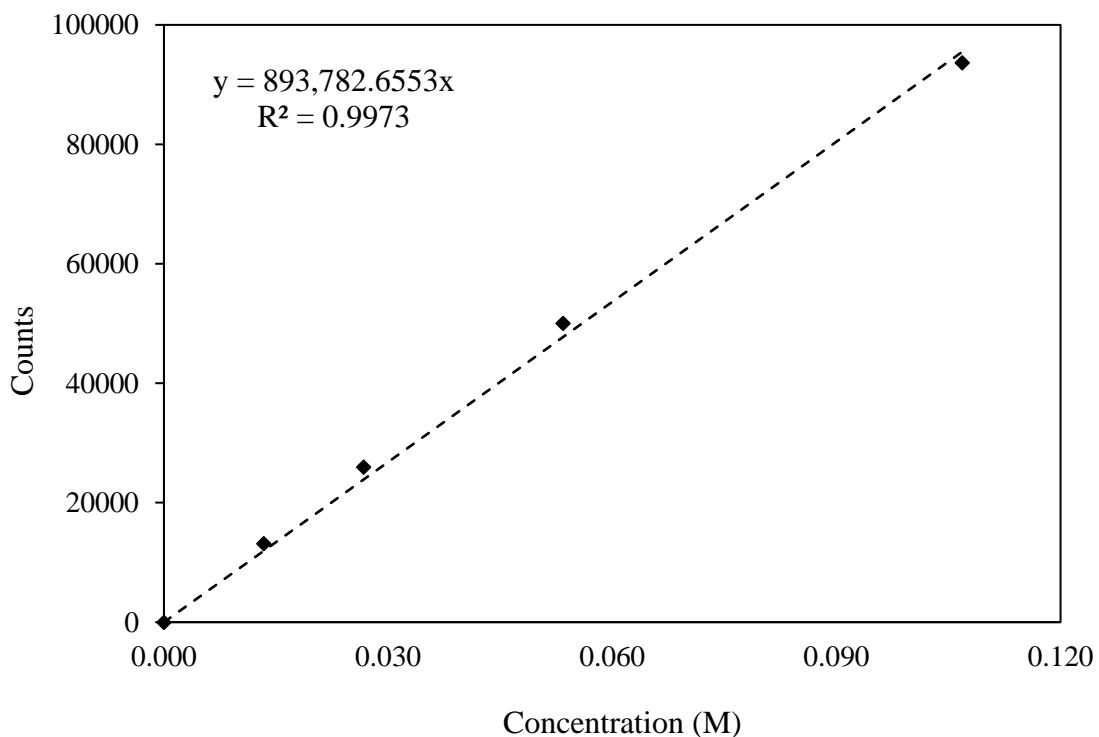

Figure 6.2.3. HPLC calibration curve for furfuryl alcohol. Analysis was conducted using a diode array detector